N92-15432

509409

124 p

GLOBAL TRENDS

Coordinator

G. Mégie (France)

Principal Authors

M.-L. Chanin (France)	J. C. Gille (USA)
D. Ehhalt (FRG)	M. P. McCormick (USA)
P. Fraser (Australia)	G. Mégie (France)
J. F. Frederick (USA)	M. Schoeberl (USA)

Other Contributors

L. Bishop (USA)	J. B. Kerr (Canada)
R. D. Bojkov (Switzerland)	W. D. Komhyr (USA)
W. Chu (USA)	K. Kunzi (FRG)
J. J. DeLuisi (USA)	K. Labitzke (FRG)
M. Geller (USA)	C. Mateer (Canada)
S. Godin (France)	R. D. McPeters (USA)
N. R. P. Harris (USA)	A. J. Miller (USA)
W. J. Hill (USA)	R. M. Nagatani (USA)
R. D. Hudson (USA)	G. C. Reinsel (USA)
	G. C. Tiao (USA)

CHAPTER 2

GLOBAL TRENDS

TABLE OF CONTENTS

2.0 INTRODUCTION

Measuring trends in ozone, and most other geophysical variables, requires that a small systematic change with time be determined from signals that have large periodic and aperiodic variations. Their time scales range from the day-to-day changes due to atmospheric motions through seasonal and annual variations to 11-year cycles resulting from changes in the sun ultraviolet output. Aperiodic variations include the irregular quasi-biennial oscillation, with a period of roughly 26–28 months, approximately 4-year variations, and other sources of interannual differences.

Because the magnitude of all of these variations is not well known and highly variable, it is necessary to measure over more than one period of the variations to remove their effects. This means at least 2 or more times the 11-year sunspot cycle. Thus, the first requirement is for a long-term data record. The second related requirement is that the record be consistent; a small effect is being sought, and changes in instrumentation or data analysis method will obscure changes in the atmosphere. A third requirement is for reasonable global sampling, to ensure that the effects are representative of the entire Earth. Therefore, the various observational methods relevant to trend detection are reviewed in Section 2.1 to characterize their quality and time and space coverage. Available data are then examined for long-term trends or recent changes in ozone total content (Section 2.2) and vertical distribution (2.3), as well as in related parameters such as stratospheric temperature (2.4), source gases and tropospheric ozone (2.5), and aerosols (2.6). The relation between trends in total column ozone and variations observed in the solar ultraviolet radiation at the ground are discussed in Section 2.7, and outstanding issues in trends detection are emphasized in Section 2.8.

2.1 OBSERVATIONAL METHODS RELEVANT TO TREND DETECTION

2.1.1 Introduction

This section briefly describes the measurement techniques that have been used in the past or are expected to be used in the future to quantitatively measure trends in total ozone or the ozone vertical distribution. More detailed descriptions of these techniques have been presented elsewhere, in the Ozone Trends Panel Report (WMO, 1989, hereafter denoted OTP) and in previous reports (WMO, 1986; NASA, 1988), earlier ozone assessments, and in scientific journals and reports. The purpose of this section is to describe these observations briefly and to characterize their quality, as well as their time and space coverage.

For the individual measurements, the most critical quantity is stability, or the absence of time-dependent systematic errors. A systematic error, i.e., an error that is consistently present, is the amount by which the mean of a large number of individual observations of the same ozone value could differ from the "true" value. This is also referred to as the accuracy. The relevance of the accuracy to trend determination is further discussed in Section 2.1.6.

In the following sections, the term precision is used to refer to the random variations or spread of values that an instrument would report when observing a constant ozone value. It is sometimes referred to as repeatability, and depends on the random errors of the measuring system. This is important for many studies of atmospheric processes, and could be important for trend studies when only a few observations of a particular kind are available. However, most quantities compared in trend studies involve averaging a large amount of data, reducing the spread, so precision is often not of primary importance.

The section is organized as follows: Section 2.1.2 describes the measurements that have resulted in the data that have been used to derive trends, or closely related observations. The techniques that are expected to add to the trend data for future analyses are presented in Section 2.1.3. Both of these sections are divided into ground-based observations (including balloons or rockets launched from the ground) and satellite observations. Intercomparisons of different types of data, and what they indicate about the capabilities of the different techniques, are described in 2.1.4, which is divided into sections on present and future trend data. This portion of the chapter concludes with brief discussions of the sampling requirements in time and space (2.1.5) and an overview of trend-measuring capabilities (2.1.6).

2.1.2 Measurements Used in Current Trend Analyses

Measurements of ozone in the atmosphere have been made for many years. However, most of the data that have the length of record, accuracy, and stability to allow a search for trends only go back to about the time of the IGY (International Geophysical Year) in 1957. Figure 2.1-1 gives a time-line for the types of measurement that have been used for trend analyses, and the periods involved. These measurements are outlined below.

2.1.2.1 Total Ozone Measurements

Ground-based Measurements

Absorption spectroscopy affords a sensitive means for monitoring the column abundance of ozone from the ground. The attenuation of monochromatic radiation is related to the number of absorbing
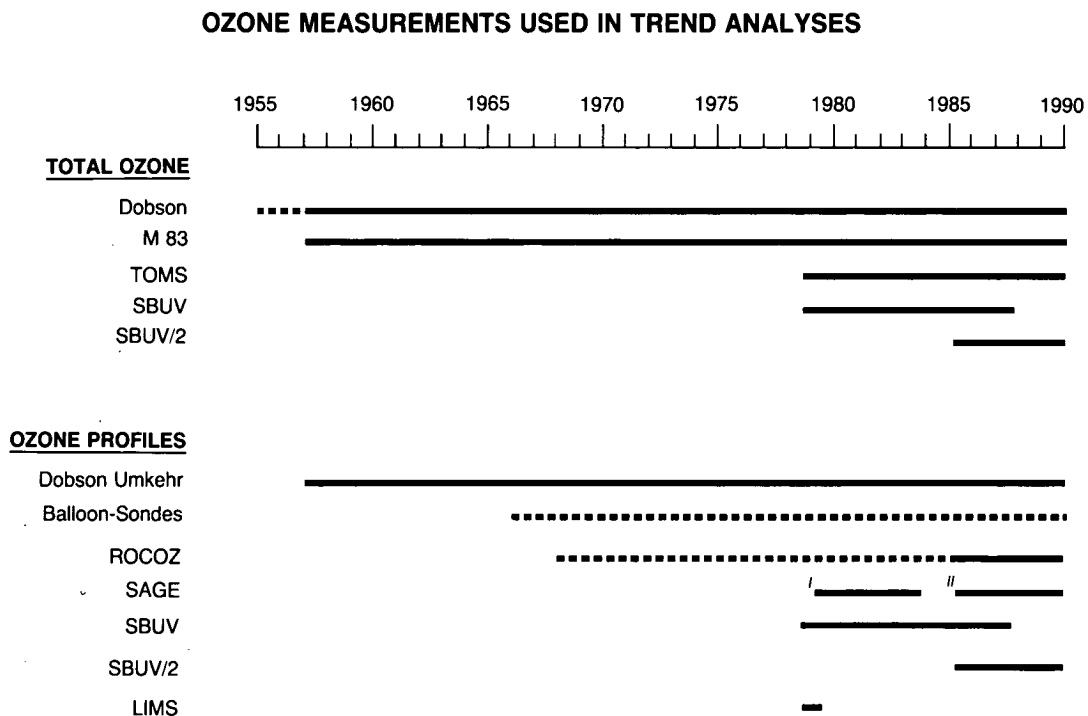
OZONE MEASUREMENTS USED IN TREND ANALYSES

Figure 2.1-1. Time lines of measurements available for use in ozone trend analyses at the present time.

molecules in the optical path as they undergo state transitions that absorb incoming radiation. Absorption features in the ultraviolet and visible regions of the spectrum mainly involve electronic transitions and hence are generally relatively insensitive to temperature and pressure, which is a feature that considerably simplifies the reduction of the data to slant-column abundances.

The source of incoming light may be a celestial body, usually the sun, but also the moon, or a star, or it may be the light scattered from the sunlit zenith sky. Direct-light absorption measurements can be carried out only during clear periods from the ground, since an unobstructed view of the light source is required. Scattered light measurements can be obtained in cloudy weather by some absorption systems.

Dobson Spectrophotometer

The standard instrument in the Global Ozone Observing System is the Dobson spectrophotometer (Dobson, 1957). The instrument is a quartz double monochromator which measures the relative intensities of pair wavelengths in the Huggins ozone absorption band (300–350 nm) from which total ozone in a vertical column of the atmosphere can be deduced. Most precise observations are made on direct sunlight and standard double-pair wavelengths designated AD (305.5/325.4 and 317.6/339.8 nm). Less precise observations are made on clear or cloudy zenith skylight or, infrequently, moonlight. (For a more detailed description of the Dobson spectrophotometer and its operation, see OTP.) Direct sun AD observations generally provide the most precise measurements if the secant of the zenith angle, μ, is less than 3.

Long-term ozone measurement precision for the Dobson spectrophotometer, for annual means, is estimated to be 1% (at the 2 σ level), based on the standard deviation σ from analyses of mean data from individual stations (WMO, 1980, 1981, 1982). Attainment of this precision requires that observations at all times be made on correct wavelengths; that changes in spectral characteristics of the instrument be accounted for using data derived from periodic standard lamp tests; that recalibration of the wedge be performed, if evidence suggests it is needed; that periodic recalibrations of the instrument be performed by the Langley method (Dobson and Normand, 1962) or through intercalibration with a primary standard Dobson instrument (Komhyr et al., 1989); that observational errors be minimized; that the temperature dependence of the ozone absorption coefficients be taken into account; and that relations derived empirically between direct sun and clear or cloudy zenith sky observations be adequately quantified. For use of the total ozone data in global trend analyses, it is necessary, furthermore, that observations be made on a sufficient number of days each month in order to obtain representative monthly mean data (see Section 2.1.5), and that the observations not be unduly influenced by local interfering absorbing species, such as sulfur dioxide and nitrogen dioxide or ozone produced photochemically in locally polluted air.

Until 1968, Dobson instrument calibrations at different stations were generally conducted randomly and independently. From 1974 onwards, increasing numbers of instruments have been modernized, refurbished, and calibrated by direct intercomparison with the WMO designated World Primary Standard Dobson Spectrophotometer No. 83, maintained at the World Dobson Spectrophotometer Central Laboratory in Boulder, Colorado. In subsequent intercomparisons, these instruments have shown typical calibration changes of 0–2% for direct sun observations on AD wavelengths. The long-term (1962–1987) ozone measurement stability of Primary Standard Dobson Instrument No. 83 is reported to have been maintained at ±0.5% (Komhyr et al., 1989). Since the mid-1970s, virtually all (90) Dobson instruments of the global Dobson instrument station network have been calibrated several times either directly with instrument No. 83 or indirectly through intercalibrations with Secondary Standard Dobson spectrophotometers calibrated in Boulder in 1977.

The uneven geographical distribution of the existing Dobson spectrophotometer network (Figure 2.1-2) gives rise to a spatial sampling error when attempts are made to determine global ozone content and trends. At most, the Dobson instruments can provide trend information for specific regions of the globe. An important utility of the Dobson instruments is their ability to provide correlative data for satellite instruments that measure ozone on a global scale (Fleig et al., 1986; 1989a; 1989b; Bojkov et al., 1988; McPeters and Komhyr, 1989), but that are subject to calibration drifts and are not highly sensitive to tropospheric ozone.

Filter Ozonometers M-83 and M-124

Since 1957, routine ground-based total column ozone measurements have been made at more than 40 stations in the USSR using a filter ozonometer instrument designated as type M-83 (not to be confused with the Standard Dobson ozone spectrophotometer, which was the 83rd instrument manufactured of the Dobson type). The filter-type instrument is based upon the same principle as the Dobson spectrophotometer in using differential absorption of ultraviolet radiation in the 300–350 nm Huggins band of ozone. The M-83 instrument, however, uses two broadband filters and measures the relative attenuation of the solar ultraviolet radiances either directly from the sun or indirectly from the zenith sky (Gustin, 1963).

Direct intercomparisons between M-83 filter instruments and Dobson spectrophotometers prior to 1971 (Bojkov, 1969) revealed that the M-83 records show 6% less ozone when the observations are restricted to an air mass μ <1.5, and 20% to 30% more ozone when data are taken for μ > 2.0. A strong dependence
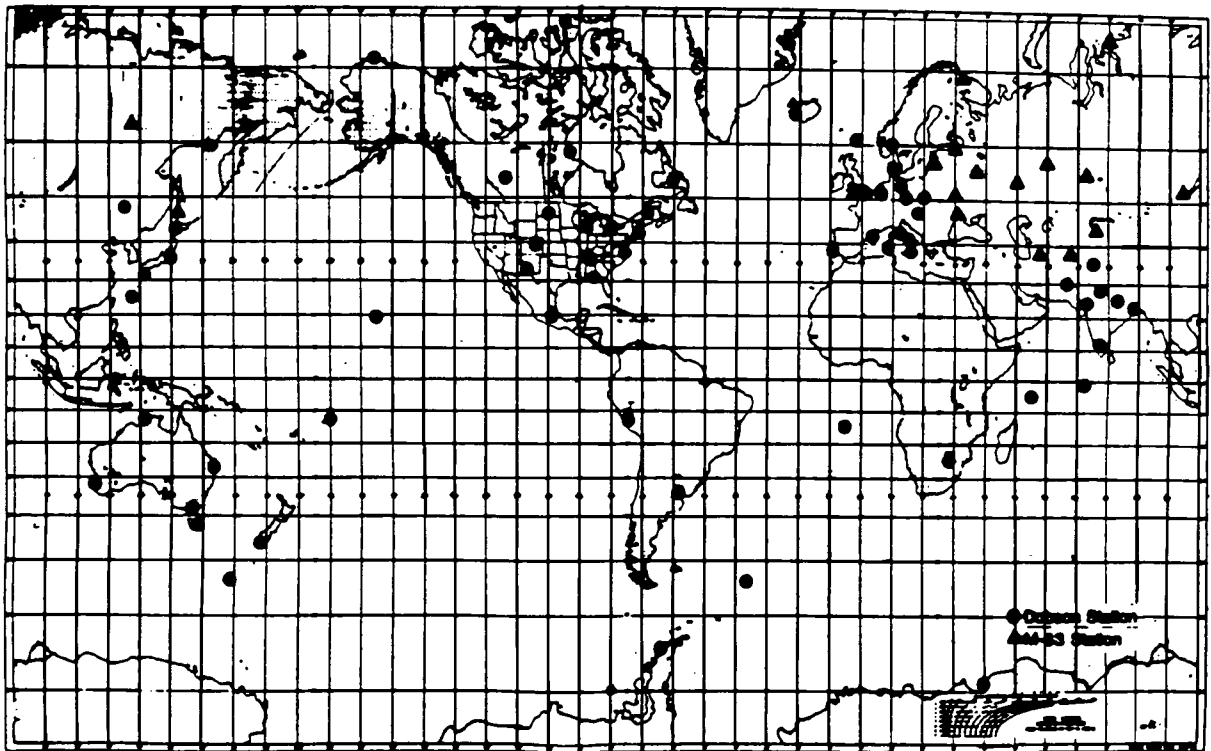

Figure 2.1-2. Location of Dobson (●) and M-83 (▲) stations.

on turbidity was also detected, with 9% to 14% higher ozone readings when the surface visibility was less than 5 km. These strong deviations for $\mu > 2.0$ make many of the high-latitude measurements in the USSR very uncertain, especially for measurements prior to 1972, as described below.

Improved filters were introduced into the M-83 instrument starting in 1972–1973 (Gustin, 1978). The new filters have maximum transmittance at 301 nm and 326 nm, and their band passes are less than those in the earlier version: 22 nm (291–312 nm) and 15 nm (319–334 nm). Comparison of Nimbus-4 BUV satellite overpasses over M-83 stations in the USSR demonstrated a standard deviation of about 50 Dobson Units before 1973, and about 25 DU afterward (WMO, 1980, 1983). The Nimbus-4 BUV overpasses of Dobson stations maintained a standard deviation of about 17 DU during the 1970–1977 lifetime of the satellite.

A much newer, reportedly improved instrument designated as M-124 has been installed in many stations since 1986 (Gustin and Sokolenko, 1985), but no ozone data have been reported yet for this instrument. No trend data with the M-124 can be expected for about a decade unless the data can be satisfactorily cross-calibrated with the M-83 data from the same location.

Satellite observations

Total Ozone Monitoring Spectrometer (TOMS)

The TOMS, launched on the Nimbus-7 spacecraft in 1978, is an instrument (Heath et al., 1975) whose primary measurement goal is to obtain contiguous mapping of the total column ozone amount over the globe (Bowman and Krueger, 1985; Schoeberl et al., 1986). To achieve this, TOMS step scans across the sub-orbital track, sampling radiation backscattered from the underlying surface and atmosphere. Ozone column amounts are inferred by utilizing the wavelength dependence of the Earth's ultraviolet albedo in the Huggins band of the ozone absorption spectrum. The TOMS raw data are measurements of the direct and backscattered solar UV radiation at six fixed wavelength channels (312.5, 317.5, 331.2, 339.8, 360, and 380 nm). Data from the first four channels are used in pairs to provide three estimates of the total column ozone amount by the differential absorption method. The remaining two channels, which are free of ozone absorption, are used to determine the effective background albedo.

It was recognized from the outset that this technique was intrinsically capable of very high accuracy and stability, since the requirement was for a relative measurement of the ratio of Earth's backscattered UV radiance to the solar UV irradiance at the same wavelength. Because both measurements could in principle be made with the same instrument, the determination of albedo as a function of wavelength should not depend on either the absolute calibration of the instrument nor on long-term variations in the sensitivity of the instrument. However, a serious uncertainty is introduced by the use of the diffuser plate, which is not common to both measurements but only used to transform the solar irradiance into a radiance that is comparable in magnitude to the backscattered Earth radiance, and can be measured in the same manner. Observations of the solar irradiance indicated that the diffuser plate was degrading and becoming less reflective with time. Cebula et al. (1988) developed a model of the diffuser and instrument degradation, which was adopted by the Ozone Processing Team (OPT). Application of this model in the reduction of the TOMS data led to a downward drift of the TOMS results compared to those of the ground-based Dobson network (see above) reported by Fleig et al. (1986, 1989a), Bojkov et al. (1988).

Extensive analysis reported by the Trends Panel indicated that the OPT model had large uncertainties and had almost certainly underestimated the true diffuser plate degradation. The errors were large enough to allow agreement with the Dobson data. Subsequently, some results for trends in total ozone in the

167

Trends Report were based on normalizing the TOMS data to the Dobson values. This allows extension to global coverage, but is at best only an approximation and provides no independent information from TOMS on the trends.

Subsequently, a major advance in the analysis of the TOMS data has been made. Bhartia et al. (1989) pointed out that, for the related Solar Backscatter Ultraviolet (SBUV) experiment, there was a wavelength at 305.8 nm whose data could be used with those from the SBUV 312.5 nm channel to form a new "D pair." Results from this pair are less sensitive to diffuser degradation for two reasons. First, the degradation varies with wavelength, but the D pair wavelengths are only 6.7 nm apart, compared to the 18.7 for the A pair. In addition, because the difference in ozone absorption coefficients is larger for the D pair than for the other pairs, results are estimated to be only 0.22 times as sensitive to diffuser drift than the archived values, which are based on a latitude-dependent weighted sum of the A, B, and C pairs. Because of the large absorption coefficients, D pair values can only be obtained in the tropics, where the total column amount is small, but a comparison showed that they follow the Dobson values much more closely than the archived values do. This provides confirmation that the archived data are in error, as well as strong corroboration that the error mechanism has been identified (Bhartia et al., 1989; Hudson et al., 1989, private communication).

Generalizing from these insights, McPeters et al. (1989, private communication) have developed the "pair justification" method. The basis is that different pairs have different sensitivity to diffuser degradation errors, resulting in a drift between pairs than can be measured accurately. By requiring that all pairs obtain the same total ozone result, and assuming that the uncorrected diffuser degradation is approximately linearly dependent on wavelength, a unique determination of the total ozone is obtained that is independent of diffuser degradation. The implementation makes use of pairs denoted A, B, and C (312.5/331.2; 317.5/ 339.8; 331.2/339.8 nm). There appears to be a fundamental limit of 0.5–1.0% per decade to the stability that can be obtained. Test results are described in Section 2.1.4.

Solar Backscatter Ultraviolet Spectrometer

The Solar Backscatter Ultraviolet (SBUV) spectrometer (described below in Section 2.1.2.2) also measures the solar ultraviolet radiation that is backscattered by the Earth and atmosphere. Data from four of its wavelength channels, which are the same as four of the TOMS channels, are used in the same way to determine total ozone amounts, but only in the nadir directly below the spacecraft. SBUV ozone values are systematically slightly lower than those from TOMS, but they vary with time in the same way. Because SBUV also relies on the same diffuser plate, its total ozone values have also decreased with time due to diffuser degradation.

2.1.2.2 Profile Measurements

Ground-based Measurements

Standard Dobson Umkehr

The Dobson instrument can also be used to obtain information on the vertical distribution of ozone. Measurements of the downward scattered radiation at two wavelengths are made for solar zenith angles Z from 60–86.5 degrees. From the ratio of these radiances as a function of Z, which reverses for Z near 90 degrees, the vertical profile can be inferred. (The method takes its name from the German word for a reversal.) The solution is usually given in terms of the layer mean ozone partial pressure (nb) of ozone in layers about 5-km thick, but with layer 1, the troposphere, about 10-km thick.

Although the retrieval provides data for Umkehr layers 1 through 9 (0–48 km), the averaging kernels for the present standard algorithm indicate that only data for layers 4 to 8 (19–43 km) should be used for trend analysis, while other layers should be used with caution. The vertical resolution of the retrieval for these layers is from 11 to 14 km. The systematic uncertainty or bias is estimated to be 15–20% in the OTP, and 5–12% by DeLuisi et al. (1989a). Random errors, due to the dependence of the ozone absorption coefficients on the varying temperature, tropospheric and stratospheric aerosols, thin clouds invisible from the surface, and instrumental effects, are of the order of 5–10%, some of which could be reduced by monitoring the clarity of the zenith sky. Neither the systematic nor random errors should seriously affect estimation of long-term trends. Trend estimation will be affected by instrument drifts, by changes in calibration, by stratospheric aerosols, and by real atmospheric temperature trends. Calculations indicate that realistic temperature trends ($< 2°C$/decade) will induce errors $< 0.2\%$/decade in ozone trends for layers 4 through 8 (Figure 3-12, Chapter 3, OTP). Serious errors from stratospheric aerosols are easily recognized in the data and such contaminated data may be edited out before trend estimation. Moderate and smaller errors may be adequately corrected by the methods of DeLuisi et al. (1989a) or by statistical methods using proxy data (Reinsel et al., 1989). Finally, instrumental factors may be handled by statistical methods (e.g., sudden calibration changes as by Reinsel et al., 1989) or by re-evaluation of the observations using new calibration data.

To reduce the time required for an Umkehr measurement, the Short method was developed and tested by Mateer and DeLuisi (1984). This method uses the A-C-D Dobson wavelength pairs in place of the C pair that is used for the Standard Umkehr method. By using the triple pair, ozone profile information is obtained when measurements are made during a solar zenith angle change of 80 to 89 degrees. In contrast, the C pair Standard Umkehr method that has provided most of the past data requires a solar zenith angle change of 60 to 90 degrees. An exploratory ozone profile retrieval algorithm for the Short Umkehr has been developed for testing. An operational algorithm will be developed after the present Standard Umkehr algorithm (Mateer and Duetsch, 1964) has been updated.

Although Umkehr observations date back to the 1930s, the current Umkehr profile archive at the World Ozone Data Centre (viz., retrievals using the present standard C-Umkehr algorithm) begins about the time of the IGY (ca. July 1957). The archive comprises over 35,000 ozone profile retrievals for some 68 stations, uniformly processed using the standard retrieval algorithm (Mateer and Duetsch, 1964). For 26 of these stations, the entire station record consists of fewer than 100 profiles. Reinsel et al. (1984), found only 13 stations with a sufficient number of observations and length of record for use in their trend analyses, while Reinsel et al. (1989) only used 10. One of the stations, Mont Louis, no longer makes observations. The record of Aspendale (the only Southern Hemisphere station in the trend set) ends in 1982. From 1983 onward the record is being continued at Melbourne, 25 km away. The remaining trend stations cover the latitude range from 24 to 53° North.

It appears that additional stations, especially those in the Automated Dobson Network (Komhyr et al., 1985), will have a sufficient number of observations and length of record to be used for trend estimation within the next 5 years. There are presently seven automated Dobson instruments that routinely obtain Standard and Short Umkehr measurements. These instruments were developed by NOAA/GMCC (Komhyr et al., 1985) and are located at Perth (Australia); Lauder (New Zealand); Huancayo (Peru); Mauna Loa (Hawaii); Boulder, Colorado (United States); Haute Provence (France); and Fairbanks, Alaska (United States). The frequency of Umkehr measurements is significantly increased by the automated Dobson because observers are not required, and a shorter observing time (for the Short Umkehr) decreases the chance of cloud interference. Ancillary measurements of sky conditions are also made at the automated Dobson sites. These measurements consist of zenith-sky clouds and turbidity. In addition, lidar measure-

ments of stratospheric aerosols for correcting errors to the Umkehr profiles (DeLuisi et al., 1989a) are routinely made at Mauna Loa, Boulder, and Haute Provence.

Balloon Ozonesondes

Balloon ozonesondes are compact, lightweight, balloon-borne instruments flown with standard meteorological radiosondes for measurement of ozone, air pressure, and air temperature up to altitudes of about 30 km. Regener (1960, 1964) developed a very fast response chemiluminescent ozonesonde, but these instruments often exhibited considerable variations in sensitivity to ozone (which was later corrected). Thus, while an early measurement program provided a great deal of useful information on the ozone climatology over the North American continent, the variable response characteristics associated with the measurements and the relative shortness of the record render the data unsuitable for ozone trend studies in the troposphere and stratosphere.

Brewer and Milford (1960) described an electrochemical ozone detector employing the well-known oxidation of potassium iodide (KI) by ozone as the basic reaction. Subsequently, Griggs (1961) investigated the physical and chemical aspects of a similar balloon-borne instrument commonly referred to as the Brewer "bubbler" ozonesonde. Versions of the instrument are manufactured in the United States, G.D.R., and India. Because the air pumps of the Brewer ozonesondes are lubricated with a thin film of oil that may destroy ozone, they must be conditioned with ozone prior to flight time to minimize the ozone destruction. With proper conditioning, ozone losses can be kept to a few percent, as has been the case at Hohenpeissenberg Observatory (F.R.G.). A few soundings from routine ozone measurement programs conducted in past years, however, have exhibited ozone losses, in extreme cases of up to 50%. Improvement in data quality is achieved through normalization of all soundings to Dobson spectrophotometer total ozone. The normalization factor for any sounding is a constant by which ozone values at all altitudes are multiplied. Use of a constant multiplication factor for normalization may, however, not be justified for soundings that exhibit large ozone losses within the instrument (Hilsenrath et al., 1986). Brewer ozonesonde data having normalization factors that range from 0.95–1.25 are generally acceptable; in an analysis later in this chapter the range 0.9–1.2 is used. The average correction factor for more than 1,000 ozonesondes flown over 20 years at Hohenpeissenberg is 1.07. Other uncertainties associated with ozone measurements with Brewer ozonesondes stem from variations in pump air flow rates above 10 mb, particularly for lightly lubricated pumps that become "dry" after several hours of operation . Build-up of AgI on the platinum anode during operation may also affect sensor performance. The significance of errors due to these effects has not been adequately assessed.

A considerable amount of useful atmospheric ozone vertical distribution data has nevertheless been obtained with the Brewer ozonesondes. The data are suitable for ozone trend analyses, particularly from stations that have maintained unchanged instrument preflight conditioning and test procedures throughout the entire measurement program.

Komhyr (1969) developed an electrochemical concentration cell (ECC) ozonesonde utilizing the reaction of ozone with KI, but with platinum cathode and anode electrodes contained in separate sensor chambers connected by an ion bridge. This sensor evolved from a carbon-iodine (CI) ozonesonde (Komhyr, 1964) that is no longer in use in the United States, but continues to be used in Japan. Because the chemical composition of the electrodes of the ECC sensor remain unchanged during operation, the sensor can be used indefinitely without deterioration of performance. The ECC sonde incorporates a miniature air pump fabricated from Teflon reinforced with glass fibers. The pump is not lubricated, so that minimal conditioning with ozone is required to prevent ozone loss within it. Early versions (type 3A) of the ECC ozonesonde

employed a pump of rectangular cross section. Because of non-uniformity of manufacture, some of the pumps exhibited excessive leakage at pressure altitudes above 15 mb, which in extreme cases have been underestimating the ozone by more than 15%. A newer instrument version (type 4A) employs a Teflon pump of circular cross section with external O-ring seals that is claimed to render the pumps and instruments suitable for use at higher altitudes.

ECC ozonesondes using a 1% KI cathode electrolyte yield measured total ozone amounts that agree closely with Dobson spectrophotometer total ozone. For example, for 525 soundings made by NOAA since 1984 over a wide range of operating conditions, from the tropics to the polar regions, the mean ECC sonde-Dobson spectrophotometer total ozone normalization factor was 1.01 ± 0.05 (1σ) (Komhyr et al., 1989). ECC ozonesondes are, therefore, suitable for use at stations where independent measurements of total ozone are not available, e.g., in polar regions during the polar night.

Ozone measurement uncertainty for ECC sondes is estimated to be $\pm 10\%$ in the troposphere, $\pm 5\%$ in the stratosphere up to 10 mb, with the uncertainty increasing to $20 \pm 5\%$ at 3 mb (Hilsenrath et al., 1986). Two ECC ozonesondes flown with an ozone UV-photometer during the MAP-GLOBUS campaign of 1983 (Aimedieu et al. 1987) gave ozone values that differed from the photometer values by $2.1 \pm 1.1\%$ at 8.1 ± 1.1 mb, and by $-0.6 \pm 3.0\%$ at 3.9 ± 0.4 mb. The low ozone values measured above 10 mb, if real, may stem from application during data processing of inadequate pump efficiency corrections. Variability in the data at these altitudes is attributable at least in part to variations in manufacture of the pump components. It must be pointed out that small, continuing improvements over the years have led to more accurate measurements, but they may also result in spurious indications of trends.

Rocket ozonesondes

Over the last 2 to 3 decades, several groups in various countries have developed and used rocket-sondes. In the USSR, rocket optical ozonesondes (Brezgin et al. 1977) and chemiluminescent sondes (Konkov and Perov, 1976; Perov and Khrgian, 1980; Perov and Tishin, 1985) have been introduced. A solar photometer (Subbaraya and Lal, 1981) and another optical sonde (Somayajulu et al., 1981) have been developed in India. However, the longest data record has been collected in the United States by the ROCOZ and ROCOZ-A systems, which are described here.

The ROCOZ-A ozonesonde is a four-filter, sequential-sampling, ultraviolet radiometer. The instrument was originally developed for stratospheric soundings aboard an ARCAS rocket (Kreuger and McBride, 1968a,b). This instrument was subsequently modified for launch aboard a smaller diameter Super-Loki launch vehicle. In 1982, an instrument improvement program was initiated at NASA's Goddard Space Flight Center/Wallops Flight Facility (WFF). Changes were made to the center wavelengths and spectral shapes of the ultraviolet filters. An integrated calibration facility was established (Holland et al., 1985), and new data reduction procedures were designed (Barnes et al., 1986). A description of the present design of the radiometer has been published by Barnes and Simeth (1986). Because of the short data record of the present instrument, these data are not directly applicable to trend studies at this time.

The ROCOZ-A ozonesonde is propelled aloft by a Super-Loki booster rocket. At rocket burnout, the instrument and its carrier coast to a nominal apogee of 70 km, where the payload is ejected for deployment on a parachute. The radiometer measures the solar ultraviolet irradiance over its filter wavelengths as it descends through the atmosphere. The amount of ozone in the path between the radiometer and the sun is then calculated from the attenuation of solar flux as the instrument falls. In addition, radar from the launch site measures the height of the payload throughout its descent. Finally, knowledge of the solar zenith angle

allows calculation of the fundamental ozone value measured by the radiometer; that is, ozone column amount as a function of geometric altitude. Ozone number density is the derivative of ozone column amount versus altitude. Combined with auxiliary atmospheric soundings for pressure and temperature, ROCOZ-A can duplicate the fundamental ozone values of backscatter ultraviolet (Barnes, 1988) and solar occultation measurements (Cunnold et al., 1989) from satellites. ROCOZ-A comparisons have also been made with the ultraviolet spectrometer on the SME satellite (Barnes et al., 1987b).

Details of the measurements of the precision of ROCOZ-A ozone column amounts and ozone number densities have been published (Holland et al., 1985; Barnes et al., 1986). In addition, there are published results from an equatorial ozone measurement campaign (Barnes et al., 1987a) that found very low variability in stratospheric ozone, temperature, and pressure. From the results of this campaign, it is possible to estimate the precision of the remaining measurements in the ROCOZ-A data set. The full set of precision estimates for ROCOZ-A is given in Barnes et al. (1989). For ozone number densities and mixing ratios, the profile-to-profile repeatability of ROCOZ-A measurements is estimated at 3 to 4%.

The estimates of the accuracy of the ROCOZ-A profiles are also given in Barnes et al. (1989). For ROCOZ-A ozone amount, the accuracy estimates come from an internal, unpublished error analysis. The analysis is based on errors of the effective ozone absorption coefficients used to convert the radiometer readings into ozone profiles, plus the differences between the ozone values at altitudes where two ROCOZ-A channels give simultaneous readings (Barnes et al., 1986). A laboratory flight simulator, based on long pathlength photometry (DeMore and Patapoff, 1976; Torres and Bandy, 1978), has been constructed to measure the accuracy of ROCOZ-A ozone readings. Publication of a detailed error analysis will follow the conclusion of experiments with the simulator. It will complete the primary characterization of the ROCOZ-A ozonesonde. ROCOZ-A ozone number densities and ozone mixing ratios are estimated to be accurate to 5 to 7% and 6 to 8%, respectively.

The vertical resolution of ROCOZ-A ozone profiles is 4 km (Barnes et al., 1986). This resolution comes from the data reduction algorithm for the profiles, since measurements from the instrument are less than 100 meters apart during flight. ROCOZ-A ozone column amounts are smoothed before differentiation for ozone density. The vertical resolution of the smoothed profiles has been adjusted to roughly match the 8-km resolution quoted for the two limb scanning instruments on the Solar Mesospheric Explorer (Rusch et al., 1984), and the 1- to 5-km vertical resolution for SAGE II (Mauldin et al., 1985b).

Satellite Observations

The Stratospheric Aerosol and Gas Experiment (SAGE I and II)

SAGE I and SAGE II are both satellite-borne multi-wavelength radiometers employing solar extinction (occultation) techniques to measure stratospheric aerosols and gases. Ozone profiles are determined from measurements of attenuation of solar radiation by ozone in the most intensely absorbing portion of the Chappuis band, at 600 nm. SAGE I was launched aboard the dedicated Applications Explorer Mission-2 in February 1979 and operated for 34 months until November 1981, when the spacecraft electrical system failed. SAGE II was launched on the Earth Radiation Budget Satellite in October 1984, and has operated continuously since then. Both SAGE I and SAGE II are in approximately 600 km circular orbits with inclination angles of 56 and 57 degrees, respectively, such that the latitudinal coverage is almost identical. Detailed descriptions of the instruments are given by McCormick et al. (1979), and Mauldin et al. (1985a,b).

172

The capabilities of the two instruments are not identical because of small differences in the instrument configurations and data processing algorithms.

In the solar occultation technique, measurements are made of the solar radiation transmitted through the atmosphere as the sun sets (or rises) behind it relative to the spacecraft. The transmission for a given ray path is the ratio of the signal strength for that ray path to the signal when the sun is above the atmosphere. The vertical distribution of ozone is determined from the changes in the transmission. Other wavelengths allow the concentrations of other gases and aerosols to be determined; the aerosol effects on the ozone transmittance may then be corrected. The retrieval algorithms are described in the OTP, Ch. 3, or in Chu and McCormick (1979), Mauldin and Chu (1982), and by Chu (1986). Because of the high signal-to-noise ratio, a vertical resolution of 1 km is achieved in the stratosphere.

It is important to note that the measurements performed by the SAGE instruments are self-calibrating, in that only relative radiance measurements are required to determine the transmission and, therefore, the distribution of atmospheric species such as ozone. Consequently, no absolute radiance calibration is necessary. The only requirement is that the instrument retain constant responsivity for the duration of each spacecraft sunrise or sunset, usually about 100 seconds. However, the position of the line of sight must be accurately known, which requires very accurate data on the position of the spacecraft during the observing events and a reasonably stable spacecraft. The OTP analysis indicates that absolute accuracy of the ozone values determined by SAGE I and SAGE II is about 6 to 9%, depending on altitude. However, the stability, or ability to detect changes, was 2 to 7% for SAGE I, and 1.3 to 4% for SAGE II. The uncertainty in the difference between SAGE I and SAGE II ozone values allow changes of 2% over the several years between their observing periods to be detected from 25 to 45 km.

A limitation of the occultation technique is the relatively small amount of data obtained, two vertical profiles per orbit, and the changing location of the observed latitudes, rendering comparisons between occultation instruments difficult. The ozone trends detection uncertainty estimated above for the SAGE I and II ozone data do not include errors caused by the undersampling of the natural variability of the ozone distribution in both the spatial and temporal domains.

Ozone data from SAGE II between November 1984 to November 1988 have been archived at the National Space Science Data Center (NSSDC). The SAGE I ozone data have also been archived at NSSDC. Reprocessing of the SAGE I ozone data using the updated temperature correction information from NOAA-NMC has been performed for the ozone trends study, and the data are currently being rearchived at NSSDC. The new temperature data introduce only small differences at high altitudes in the low-latitude regions.

Solar Backscatter Ultraviolet Spectrometer (SBUV)

The SBUV is a downward viewing double monochromator that was launched on the Nimbus-7 spacecraft in 1978 to measure the UV albedo of the atmosphere and surface for the purpose of determining the vertical profile of ozone, in addition to total ozone. Singer and Wentworth (1957) suggested that observations from above the atmosphere, in which the fraction of sunlight reflected back to space (the planetary albedo) is measured as a function of wavelength, could be used to deduce the concentration of ozone as a function of pressure (i.e., altitude). Other experiments utilizing the same principle have flown on Kosmos-65, OGO-4, Nimbus-4, Atmospheric Explorer D, and most recently, NOAA-9 and the Japanese OHZORA satellite.

173

The SBUV made measurements in 12 wavelength channels, located at (in nm) 255.5, 273.5, 283.0, 287.6, 292.2, 297.5, 301.9, 305.8, 312.5, 317.5, 331.2, and 339.8. Measurements in the channel at 255.5 nm were not used because they were contaminated by NO fluorescence; the next seven were used for extracting profile information, while the last four (which are common with TOMS) are used to determine the total ozone. The solutions are given in terms of ozone amounts within the Umkehr layers. The analysis presented in the OTP shows that only data in layers 6 to 9 (approximately 28 to 48 km) are independent and reliable for trend studies. The vertical resolution of the solutions is 8 to 10 km.

Again, in principle, this technique requires only the measurement of the ratio of the backscattered Earth radiance to the solar irradiance, with the attendant insensitivity to calibration accuracy and stability, but the use of a diffuser plate involves another optical element in the measurement of the solar irradiance which eliminates this advantage. On Nimbus-7, SBUV and TOMS shared the same diffuser plate. SBUV observations of the solar irradiance also showed that the diffuser plate was degrading with time, most rapidly at the shortest wavelengths. The diffuser model of Cebula et al. (1988) was developed from the SBUV observations and used by the OPT for the SBUV data reduction also. The archived results showed very large (25%) downward ozone changes in the upper stratosphere over 8 years, which was the reason for the original appointment of the Ozone Trends Panel. In this case also, it was found that the uncertainties in the diffuser model were much larger than expected, and that the changes in the stratosphere were probably smaller than indicated by the archived data and could even be slightly positive. In this case, the D pair again supports the assertion that the degradation is larger than predicted by the model, but there has been no method developed to date for finding an independent determination of the diffuser degradation at the shorter wavelengths. Thus, at the moment the SBUV data can provide no independent information on long-term trends in the ozone profile (see OTP).

Limb Infrared Monitor of the Stratosphere

The Limb Infrared Monitor of the Stratosphere (LIMS) is a six-channel limb scanning infrared radiometer that also was launched on Nimbus-7 in 1978 (Gille and Russell, 1984; OTP). This type of instrument measures the infrared radiation emitted by atmospheric molecules as the instrument scans across the limb. Because of the geometry, this technique has an inherently high vertical resolution and the ability to sound to high altitudes. Because it measures infrared emission, it can obtain measurements at all local times, resulting in very dense coverage. LIMS obtained ozone data from 15 to 64 km altitude, with a vertical resolution of 2.5 km. The absolute accuracy was about 10%, and the precision a few percent.

Because of the small signals involved, it is necessary to cool the detectors. LIMS life was limited by the technology of that period, which dictated the use of a solid cryogen cooler. This resulted in a 7-month lifetime. Otherwise, it should be useful for trend measurements, especially since it provides a 1978/79 determination. LIMS data were used in the OTP to help evaluate other data.

2.1.3 Measurements for Future Trend Analyses

Many of the methods described previously will continue to be used to obtain data for trend studies. Where these methods are reasonably accurate and stable with time, this is essential, because it extends the length of the data record. However, as technology advances, improvements to old techniques are continually being introduced and new measuring systems are being developed. A number of these are shown in the timelines on Figure 2.1-3, and are described below.

PROJECTED OZONE MEASURING SYSTEMS
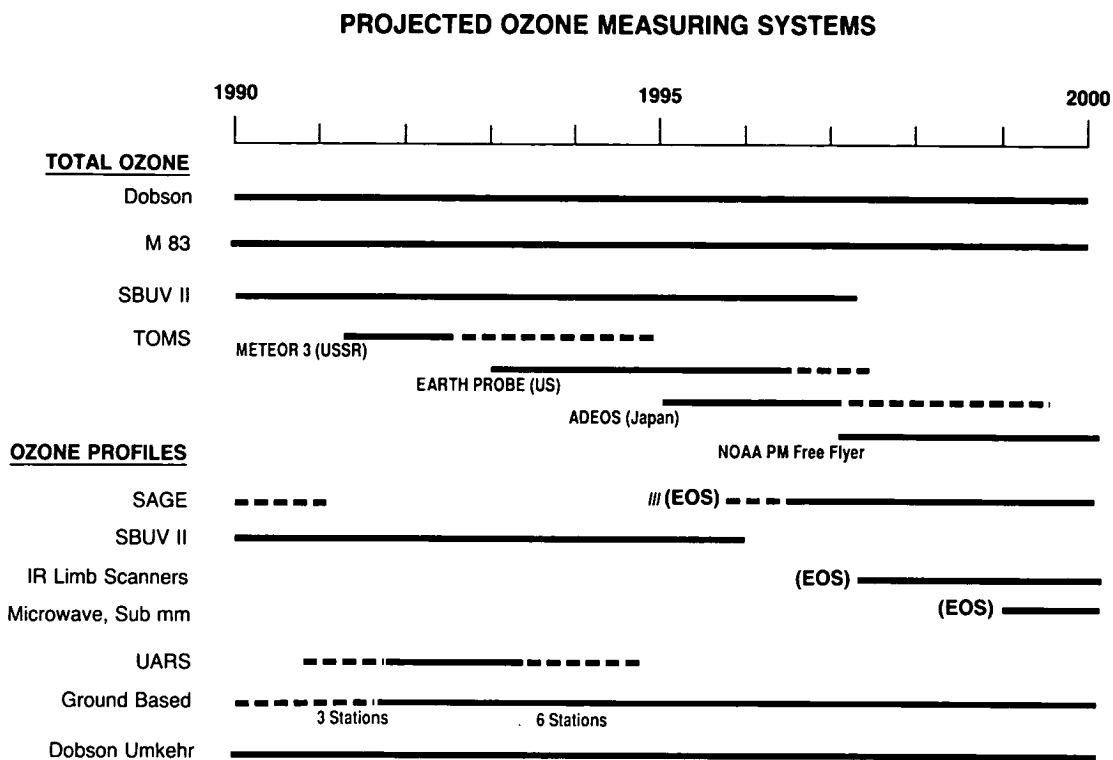
Figure 2.1-3.   Time lines for ozone measuring systems that are projected to be operating over the next decade.

2.1.3.1   Total Ozone Measurements

Ground-based Measurements

The Brewer Spectrophotometer

The Atmospheric Environment Service of Canada developed the fully automated Brewer ozone spectrophotometer in the early 1980s. Development of the Brewer instrument was based, in part, on earlier work by Wardle et al. (1963) and Brewer (1973) and was carried out with the goal to replace or supplement the Dobson instrument in the world network. There are presently about 30 instruments operating in 15 countries, including the seven Canadian stations (Kerr et al., 1988). At present, five stations are reporting data to the WODC. The record of routine measurements of total ozone made with the Brewer spectrophotometer started in 1982. These records are presently not of sufficient length to carry out a proper independent trend analysis.

The spectrophotometer is a modified Ebert type with a 1,800-lines/mm holographic grating used in the second order. It simultaneously measures the intensity of light at 5 wavelengths in the ultraviolet absorption spectrum of ozone with a resolution of 0.6 nm. The operational wavelengths are 306.3 nm, 310.0 nm, 313.5 nm, 316.8 nm, and 320.0 nm. Measurements at these wavelengths allow correction for the effects of sulfur dioxide, a potential interferent for Dobson ozone measurements in polluted air. A more complete

description of the automated instrument is given by Kerr et al. (1985). The Brewer instrument has been calibrated on an absolute scale using the ozone absorption coefficients of Bass and Paur (1985). Intercomparison with the Dobson instrument has shown that the Dobson AD direct sun total ozone measurement is about 3% larger than the Brewer measurement. When this bias is removed, the long-term agreement between field Brewer and Dobson instruments at Toronto and Edmonton has been within 1% (Kerr et al., 1988; 1989a).

Although the method to measure total ozone with the Brewer instrument is similar to that for the Dobson instrument, there are differences in sampling and reporting daily data. These differences arise primarily because the Brewer instrument is fully automatic and thereby capable of sampling continuously throughout the day. Measurements are screened and only those of good quality are used to determine the daily mean total ozone value that is reported. In general, good quality direct sun measurements can be made on about 75% of the days at a typical mid-latitude station.

High Resolution Visible/Ultraviolet Absorption Spectroscopy

Absorption spectroscopy affords a sensitive means for monitoring the column abundance of several stratospheric species (e.g., Noxon et al, 1979; McKenzie and Johnston, 1982; Pommereau et al., 1988a, 1988b). A useful approach is to measure the absorption of light scattered by the sunlit zenith sky. An important feature of such measurements is that they can be carried out on cloudy as well as clear days. The optical paths (or air mass factors) relevant to a species in a stratospheric layer become very large at solar zenith angles greater than about 88 degrees, maximizing the slant-column abundance of absorber and hence the observed percent absorption.

Modern optics, electronics, computers, and detectors allow atmospheric absorption spectroscopy to be done with very high precision, typically 0.05% absorption. Multichannel detectors eliminate the uncertainties that scanning optics introduce. Least-squares fitting of the observed spectra to those recorded in the laboratory with the same instrument for several atmospheric gases allows the abundance of more than one atmospheric species to be determined simultaneously. Under favorable spectral conditions, the sensitivity stated above can be enhanced a factor of 50 by such fitting. The stratospheric species that are most amenable to observing with ultraviolet/visible absorption spectroscopy have proven to be O_3, NO_2, NO_3, and OClO. The characteristics of one instrument that has been applied to these species is used here as an example of the type that is achievable today.

The example (Mount et al, 1987) is a crossed Czerny-Turner spectrometer, with a grating chosen so that the appropriate color filters provide second-order light in the red region of the spectrum, approximately 605–685 nm (for NO_3 observations) and third-order light in the blue region, approximately 400 to 450 nm (for O_3, NO_2, and OClO observations). The instrument is used at approximately 0.5-nm spectral resolution. The detection system is a Reticon diode array cooled by a refrigerator to about $-70°C$; the array contains 1,024 independent silicon diodes that simultaneously measure the spectrum over the indicated wavelengths. Eleven diodes cover the full width at half maximum of the instrumental spectral profile. Thus, spectral lines are highly oversampled.

An important advantage of simultaneous measurement of the desired spectral interval (as opposed to scanning) is the elimination of time-dependent changes during the course of a measurement (particularly atmospheric scintillation effects). These can be quite important when the measured species absorb only a few tenths of a percent of the incoming light, as is the case for ozone and OClO in general and for NO_2 at small zenith angles. After least squares fitting the observed sky data to the reference absorption spectra

measured in the laboratory, the one-sigma standard errors of the fitted column abundances are typically 2–5% for large solar zenith angles for NO_2. Ozone columns can be determined to 10–15% accuracy using the Chappuis bands. Future development is expected to improve this considerably. While most efforts with this technique have been on the measurement of other gases, the technology presumably could be applied to ozone measurements as well.

The largest source of systematic error in the measurements is the evaluation of the air mass factors for scattered light that are used to convert measured slant column abundances to vertical column abundances. These errors largely affect the accuracy but not the precision of the data. Estimated error limits in air mass factors are no more than 10% for solar zenith angles near 90 degrees, and they are substantially less for smaller angles.

Satellite Observations

Future Flights of TOMS Instruments

TOMS data have proven of great value in observing and studying the polar ozone depletions, as well as in providing information on the global decrease of total ozone. With the development of independent techniques for determining the diffuser reflectivity, TOMS data should be able to provide a determination of total ozone decrease over all areas of the globe that is independent of the ground-based Dobson network, although it should agree with the latter in areas where both obtain measurements. For these reasons, it is extremely important to continue TOMS-type measurements. The TOMS instrument on Nimbus-7 is now over 10 years old, and efforts have been made for future flights of TOMS-type instruments on several spacecraft.

First flight of a new, technically upgraded instrument is scheduled for the fall of 1991 on board the Soviet Union's Meteor-3 spacecraft. Unlike the sun-synchronous orbit of Nimbus-7, the Meteor-3 orbit will precess with a period of 225 days. Thus, the coverage will not be as uniform as that obtained with previous data, and adjustments will have to be made for diurnal variations. TOMS has also been selected to fly on a small U.S. Explorer-class satellite in 1993, and on the Japanese ADEOS satellite, scheduled for launch in February 1995. In these cases the orbit will again be sun-synchronous.

An upgraded TOMS will also be part of the Global Ozone Monitoring Radiometer (GOMR), an operational instrument to make long-term ozone measurements. The GOMR, discussed further below, will be included in the complement of operational instruments on the NOAA afternoon free-flier, beginning in about 1997.

2.1.3.2 Profile Measurements

Ground-based Measurements

Brewer Umkehr

Although Umkehr observations have been made with the Brewer Ozone Spectrophotometer for several years (Mateer et al., 1985, Kerr et al., 1989b), this has been a developmental period during which the observational technique and the algorithm have changed. The present body of data is insufficient for trend analysis.

177

A Brewer Umkehr observation consists of zenith sky intensity ratio measurements for three wavelength pairs over the solar zenith angle range from 60 to 90 degrees. The profile retrieval data cover the altitude range of layers 1 to 10 (0–53 km). The averaging kernels for the present algorithm show that the retrievals for layers 4 to 8 (19–43 km) and marginally layer 9 (43–48 km) are suitable for trend estimation. Until a complete error analysis has been carried out for the Brewer Umkehr system, those for the standard Dobson Umkehr may be considered as only approximately applicable. Results of an intercomparison of Brewer Umkehr, Dobson Umkehr, and ozonesonde data have indicated that the quality of the Brewer Umkehr technique is comparable to that of the Dobson "short" Umkehr method (McElroy et al., 1989).

Lidar

The lidar measurements of the ozone vertical distribution are based on the Differential Absorption Laser technique (DIAL), which requires the simultaneous emission of two laser wavelengths characterized by a different ozone absorption cross section. Part of the laser radiation is scattered back to the surface, where it is collected by a telescope, detected by a photomultiplier and time-sampled to retrieve the altitude resolution of the measurement. The derivative of the logarithm of each signal is computed and the ozone number density is obtained from the difference of the derivatives, divided by the differential ozone cross section. The lidar technique has been described by Mégie et al. (1977), Uchino et al. (1978), Pelon and Mégie (1982), Werner et al. (1983), Pelon et al. (1986), Ancellet et al. (1988), Godin et al. (1989), and McDermid and Godin (1989).

In principle the technique is self-calibrating, and thus particularly suited for the detection of trends. Two types of error affect the ozone lidar measurement. The random or statistical error is related to the signal-to-noise ratio. The systematic error is related on one hand to errors in the value of the ozone absorption cross sections used and their dependence on temperature, and on the other to uncertainties in the different physical processes, such as the Rayleigh and Mie scattering or the absorption by other species (NO_2, SO_2). The systematic error can be reduced by additional measurements of temperature and aerosol vertical profiles or use of empirical models. The random error which results from this correction is less than 3% in the whole altitude range. The choice of the two wavelengths used in the experiment depends directly on the altitude range monitored. In the troposphere, the limiting factor is the systematic error, which becomes smaller as the difference in wavelength is reduced. A wavelength separation of less than 10 nm is used, and the time necessary to obtain a tropospheric ozone profile is about 10 min for an altitude resolution superior to 1 km and an overall uncertainty less than 5%. In the stratosphere, the separation of the wavelengths needs to be larger (~50 nm) in order to limit the statistical error. Furthermore, the range solution has to be degraded in the upper range of the measurement (above 30 km) to account for the rapid decrease of the signal-to-noise ratio with altitude. With the present systems, obtaining an ozone profile in the 15–50 km altitude range requires an integration time of 2 to 3 hours for an altitude resolution of 0.5–8 km and a corresponding uncertainty of 2% to 10%.

Microwave Radiometry

Microwave radiometers (MR) are being used increasingly to investigate the middle atmosphere. An MR measures the thermal emission from rotational transitions of the molecule under investigation. The frequency employed is typically below 300 GHz (1 mm wavelength) to reduce the effects of tropospheric opacity (e.g., clouds or aerosols) and local thermodynamic equilibrium (LTE) conditions apply to ~80 km altitude. The sensor operates on the superheterodyne principle that provides a very high spectral resolution, allowing the determination of the exact shape of the emission line. Since the shape of the emission lines are dominated by pressure broadening to 80 km altitude, profiles can be retrieved from an exact measure-

ment of the emission line shape. At low altitudes (~ 15 km) the emission line widths become very large, and this, together with instrumental problems (base line and non-linearities) makes low-altitude retrievals very difficult. The altitude range over which high-quality ozone profiles can be determined from MR measurements is typically 15 to 70 km (Zommerfeld and Kunzi, 1989) with an altitude resolution of ~10 km. The accuracy claimed for this sensor is 1 part per million by volume, and the statistical error is of the order of 15%. The measuring time required for a complete profile is approximately 1 hour. Another instrument, developed by De la Noe et al. (1988) has obtained measurements of the ozone distribution with reported random errors from 1 to 5% at 40 km. Connor et al. (1987) present an error analysis for data obtained in Antarctica during 1986; they show measurement accuracies of 15–19% (depending on altitude), supported by intercomparisons with other observations. A detailed study performed recently by Bevilacqua and Olivero (1988) showed that the best vertical resolution attainable is 6 or 7 km.

It should be noted that the accuracy can be improved by using observing sites at high altitudes, thus reducing the attenuation by tropospheric water vapor. For a mid-latitude site at 500 m above sea level (Bern, Switzerland), the observing statistics for favorable conditions are >80% of the time during fall, winter, and spring, and ~50% of the time for summer. Model calculations (Kunzi and Rubin, 1988) indicate that for >90% of available observing time the sensor has to be at ~3,000 m altitude for the tropics, whereas in polar regions the site can be at any altitude.

MR instruments seem particularly well suited to perform long-term trend measurements of total stratospheric and mesospheric ozone and its vertical distribution, since an MR is easily calibrated with black body radiators and thereby has a response that can be made stable over long periods. Furthermore, the operation and data retrieval of an MR can be fully automated and require only little maintenance by skilled operators. However, at present, only little experience is available with MRs in ozone research and more intercomparisons and experience with sites in different climatic regions is needed.

Satellite Observations

Solar Backscatter Ultraviolet Radiometer—Version 2 (SBUV/2)

NOAA is currently flying the Solar Backscatter Ultraviolet Radiometer—Version 2 (SBUV/2) as an operational instrument for measurement of both total ozone and vertical profiles. The first SBUV/2 was launched on NOAA-9 in 1984 and continues to operate in overlap with the instrument launched on NOAA-11 in 1988. This series of instruments is planned to be in orbit through the lifetime of the present afternoon series of NOAA polar orbiting satellites (ca 1996). These satellites sound the atmosphere. Unfortunately, an onboard check of the diffuser plate incorporated in the NOAA-9 SBUV/2 failed to function properly. At the same time, the processed ozone data from this instrument indicate a time-dependent bias with respect to the ground-based information as well as the Nimbus-7 SBUV data that is opposite in sign to our general understanding of diffuser plate degradation. No data from either instrument are now available. This time-dependent bias is still under examination; if the cause for this disparity is discovered, the data will be reprocessed accordingly. An attempt has been made to correct the onboard diffuser plate check on the SBUV/2 follow-on units.

The failure to obtain data from the NOAA-9 SBUV/2 is especially damaging, since the first 2 years overlapped with the last 2 years of the SBUV. The SBUV/2 data could have been used to correct the SBUV diffuser model, allowing a reliable profile trend to be obtained over the 8-year life of SBUV. Alternatively, the differences between the first 2 years of SBUV and SBUV/2 could have been used to get a direct difference, as was done for data from SAGE I and SAGE II.

Upper Atmosphere Research Satellite

The Upper Atmosphere Research Satellite (UARS) is scheduled for launch by the U.S. National Aeronautics and Space Administration (NASA) in late 1991. The instruments have been designed for research purposes and the study of dynamical, chemical, and physical processes in the stratosphere, mesosphere, and lower thermosphere. Although it is not designed to measure ozone trends, a few of the instruments may provide data useful for trend studies.

Ideally, each of the ozone measurements will be sufficiently accurate that it can be compared with the existing body of previous data. However, because of the small trends and the often larger systematic biases between different types of instruments, the clearest indications are likely to occur when similar instruments are used. Some possibilities are: comparisons of ozone measurements among infrared limb-scanners such as UARS IR limb scanners (CLAES and ISAMS) as compared to LIMS and to future EOS instruments (see following); comparisons between measurements made by the UARS Microwave Limb Sounder (MLS) and the future EOS MLS; comparisons between measurements made by the infrared occultation instruments (UARS HALOE, and the later ILAS [see following]); and perhaps also comparisons among the visible occultation observations performed by the successive SAGE instruments.

Infrared Limb Atmospheric Spectrometer (ILAS)

The ILAS is under definition study by the Japanese Environmental Agency for possible launch on the ADEOS satellite, now scheduled for February 1995. It is a solar occultation spectrometer, baselined to use three monochromators in the middle infrared. In addition to the measurement of ozone (9–10 micrometer bands), several other trace species and aerosols will be measured over the 10–60 km altitude range.

Earth Observing System (EOS)

The U.S. National Aeronautics and Space Administration (NASA), the European Space Agency (ESA), and the Japanese Space Agency (NASDA) are developing a co-ordinated international system of polar platforms for remote sensing of the atmosphere, oceans, land surface, biosphere, and solid Earth. The goals are to begin or continue a set of baseline observations of key variables that indicate the state of the entire Earth system, and continue them for at least 15 years. At this time, instrument selection is still underway.

NASA has selected instruments for the definition phase for NASA's polar orbiting platforms (NPOP-1 and -2). It includes, for NPOP-1, an infrared limb sounder and SAGE III occultation instruments that should provide observations of ozone with high vertical resolution, high accuracy, and precision from cloud tops to 80 km. The limb sounder will also be capable of high horizontal resolution. Launch is scheduled for late 1996. In addition, a SAGE III instrument is planned as an attached payload for the Space Station to provide profiles at low to mid-latitudes to complement the NPOP-1 high latitude coverage. The Space Station is scheduled for launch in 1995. For NPOP-2, definition studies are being carried out for limb sounders operating in the infrared, sub-millimeter, and microwave portions of the spectrum, which will make additional measurements of ozone profiles.

The Global Ozone Monitoring Radiometer (GOMR) is planned to be the next in the series of NOAA operational satellite ozone monitoring systems. It is to fly on the satellite series subsequent to the current Advanced TIROS-N with launch about the mid-1990s. The GOMR will supplant the SBUV/2. The GOMR is

currently envisioned as two subsystems: an ultraviolet nadir and side-scan sounder based on Nimbus-7 TOMS technology, as noted above, and an infrared limb sounder based on EOS limb sounding instruments. The nadir sounder will provide total ozone in the sunlit portion of the Earth while the limb sounder will provide stratospheric profiles of ozone and other minor constituents important to ozone photochemistry and climate. The final configuration of the satellite ozone monitoring system is undergoing evaluation.

Three instruments providing ozone measurements in the stratosphere have been selected by the European Space Agency for flight on the first ESA Polar Platform (EPOP-1). GOMOS (Global Ozone Monitoring by Occultation of Stars) is an instrument intended to monitor ozone by stellar occultation, observing the full UV/visible/near-infrared spectrum of stars using a double grating spectrometer. SCIA-MACHY (Scanning Imaging Absorption Spectrometer) is a combination of two spectrometers operating also in the UV/visible/near-infrared part of the spectrum to observe transmitted, reflected, and scattered light. It is designed to be used for both nadir and limb sounding plus solar occultation and will provide measurements of tropospheric ozone. MIPAS (Michelson Interferometer for Passive Atmospheric Sounding) is a limb sounder operating in the mid-infrared region of the spectrum. All these instruments are presently in Phase A studies.

2.1.4   Comparisons of Errors/Capabilities

2.1.4.1   Intercomparisons Relevant to Present Data

Total Ozone—Dobson-TOMS-SBUV

TOMS values for total ozone are in good agreement with those from SBUV, being systematically about 1% higher for reasons that are not completely understood. Fleig et al. (1989b), Reinsel et al. (1988), Bojkov et al. (1988), and OTP examined the drift of SBUV relative to an ensemble of 41 Dobson stations and found that there was a roughly linear drift between SBUV and Dobson of -0.38% per year over 6 years. The intercomparison of TOMS data with the network of Dobson stations was also discussed as a function of time in OTP. This shows that TOMS total ozone declined slowly relative to the 41-station ensemble between 1979 and mid-1982—about -0.25% per year—and declined rapidly thereafter, at a rate of about -0.53% per year through October 1986, the end of the period studied. The decline for SBUV was similar. These results are confirmed by a recent study performed by McPeters et al. (private communication, 1989) using a network of 39 stations as shown in Figure 2.1-4a.

While total ozone measured by SBUV/TOMS clearly declined relative to that measured by the Dobson network, further tests were necessary to determine whether the problem is due to degradation of the satellite instruments or to changes in individual Dobson instruments. One such test involved satellite overpass of Mauna Loa, Hawaii, on those days during which the World Primary Standard Dobson instrument, instrument No. 83, was undergoing its regular recalibration at that location. Komhyr et al. (1989) report that the stability of this instrument has been maintained to 0.5-1% since 1962. The trend of TOMS relative to this instrument, also shown in Figure 2.1-4a, is very similar to that obtained relative to the 39-station ensemble—little change from launch through mid-1982 followed by a rapid decline thereafter amounting to approximately -0.7% per year through 1988.

As described above, a purely internal check for instrument degradation is possible for SBUV. The "D" wavelength pair, consisting of wavelengths 305.8-312.5 nm is sensitive to ozone because of its large ozone cross section and is very insensitive to wavelength-dependent degradation errors because of the small wavelength separation. The drift of normal SBUV ozone relative to D pair ozone exhibits the same
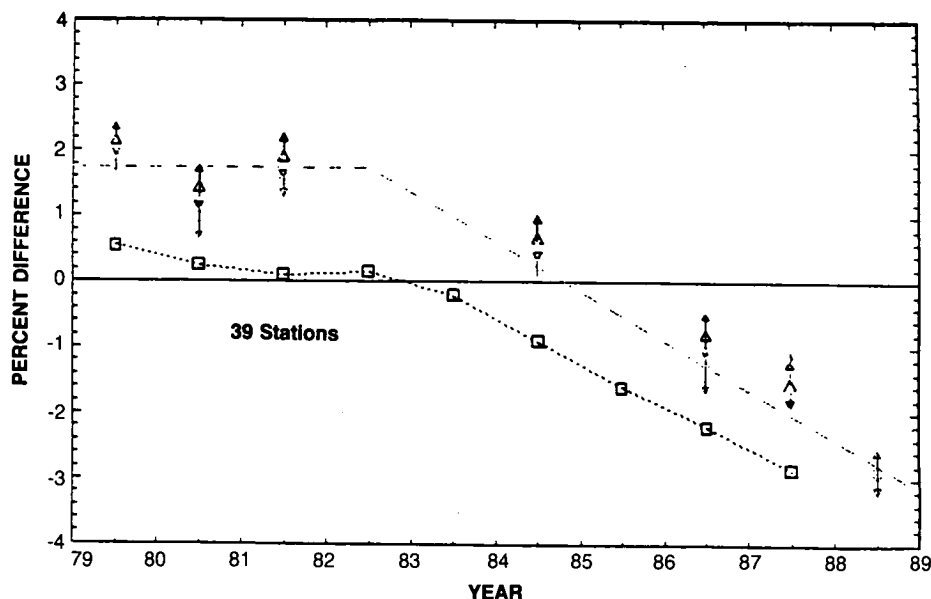
Figure 2.1-4a. Comparison between archived TOMS total ozone data and Dobson data. These TOMS measurements have been corrected for diffuser plate degradation by the method described by Cebula, Park, and Heath (1988) and the Ozone Processing Team (1989). Triangles show the difference between TOMS and the World Primary Dobson Instrument No. 83. (There are reasons to think the 1980 Dobson data are of lower quality than those for other years.) Squares show differences between TOMS and a network of 39 Dobson stations. Both comparisons show a sharp drop of TOMS relative to Dobson ozone, especially since 1982.

pattern as that observed for SBUV/TOMS relative to Dobson and for TOMS relative to instrument No. 83—little change before 1982 followed by rapid change thereafter.

The conclusion that there was about 3.4% drift between SBUV/TOMS and the Dobson network between 1979 and 1987, with much of the drift occurring after 1982, seems inescapable. The fact that the same pattern of relative stability in the TOMS-Dobson comparisons before 1982, followed by a sharp decline between 1982 and 1986, was repeated for so many of the ensemble of 41 independent Dobson stations was strong evidence for SBUV/TOMS instrument degradation, and insufficient correction. The complete confirmation by comparison with the World Standard Dobson instrument and by internal evidence of relative pair drift furnish compelling additional evidence that this trend relative to Dobson is a robust result. As pointed out previously, this drift of SBUV/TOMS is believed to result from degradation of the diffuser plate used to measure solar flux, with incomplete correction.

TOMS data for the ground station overpasses have been reprocessed using the "pair justification" calibration. The comparison of them to the data obtained by Dobson 83 during its calibration at Mauna Loa are shown by the triangles in Figure 2.1-4b, from which it can be seen that there is no large, systematic drift between them greater than a few tenths of a percent over 9 years. Because the techniques are so different, this agreement between the Dobson and TOMS support the conclusion that both are correct. Further confirmation is provided by the squares in Figure 2.1-4b, which presents comparison data between TOMS and a network of 39 stations. They suggest a drift of 0.5% over 8 years, close to the level of calibration stability achievable for this technique (it could also be explained by about a 1%/year increase in tropospheric ozone).
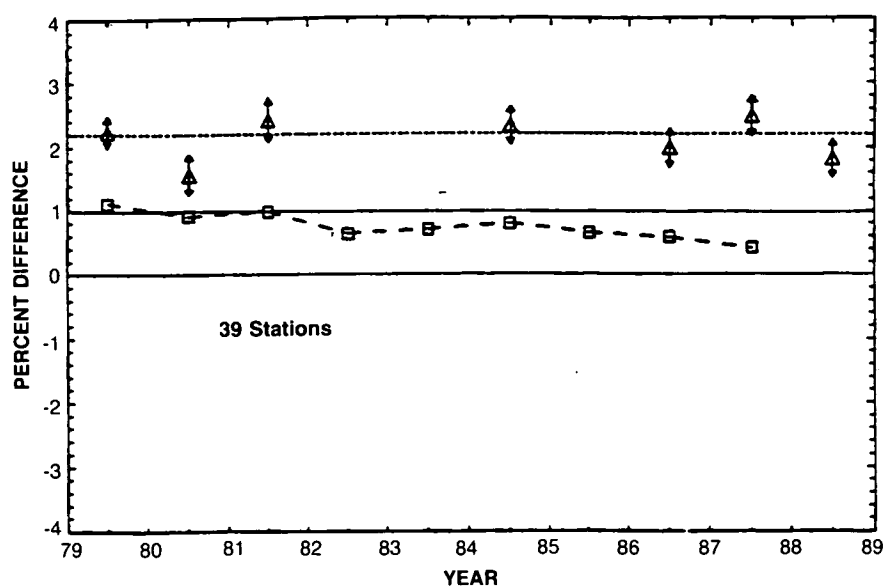
Figure 2.1-4b. Comparison between TOMS total ozone data, where diffuser plate degradation was corrected by the "pair justification" method, and Dobson data. Triangles show the difference between the World Primary Dobson Instrument No. 83 calibration measurements. (There are reasons to think the 1980 Dobson data are of lower quality than those for other years.) The squares show the differences with the network of 39 stations used for Figure 2.1-4a. These results show that once corrected, TOMS has not drifted relative to instrument 83 between 1979 and 1988, and has only changed by about 0.5% relative to the 39 station network between 1979-1987. This may be a real effect (see text).

Vertical Profiles

SAGE I / SAGE II

The accuracy of estimating ozone trends using SAGE I and SAGE II ozone data is discussed in OTP, Chapter 2. It is limited by the systematic errors between the two instruments. These errors range from 5.8% below 25 km to 1.5% at 30 km, 1.6% at 40 km, and 3.0% at 50 km height (see Figure 2.1-3c). This assessment does not include any spatial or temporal sampling error associated with these two data sets.

SAGE I / SAGE II and SBUV

An intercomparison of SAGE I/II and SBUV ozone measurements was performed for the periods February 1979 through November 1981 and October 1984 through December 1986. It is described in detail in OTP. For this comparison, the SAGE I/II profiles were integrated, from concentration as a function of geometric altitude, the primary SAGE product, into Umkehr-layer amounts. In Umkehr layers 7, 8, and 9, SAGE I ozone layer amounts were consistently lower than SBUV in 1979–1981 by 4 or 5%, but SAGE II ozone layer amounts were consistently higher than SBUV in 1984–1986 by 10±2%. The results in Umkehr layer 6 consistently showed SAGE I about 4% higher than SBUV in 1979–1981 and SAGE II about 10% higher than SBUV in 1984–1986. The 1980–1985 offset between SAGE and SBUV increased

183

monotonically with altitude between Umkehr layers 6 and 9. Coupled with the other information on degradation of the SBUV diffuser plate and the self-calibrating nature of the SAGE instruments, this comparison supports the conclusion that the large ozone changes reported by SBUV at high altitudes are due to larger diffuser degradation at the shorter wavelengths that allowed in the SBUV data reduction.

SBUV, SAGE I, and LIMS Ozone Intercomparisons

In OTP (Chapter 5) the ozone observations during March and April 1979 from three simultaneous satellite instruments, namely the SBUV, SAGE I, and LIMS, were examined. (For a discussion of LIMS, see OTP or Gille and Russell, 1984 and Remsberg et al., 1984.) The analysis is an intercomparison of the ozone data from these instruments in terms of ozone column abundance in four Umkehr layers (layers 6 to 9). In the case of SAGE I and LIMS, it was necessary to convert their primary measured ozone quantities to ozone Umkehr layer amounts for comparison purposes. Since the sampling locations of the SAGE instrument are distributed in a narrow latitudinal belt for a 24-hour period, as opposed to the nearly global observations of the SBUV and LIMS for the same period, the comparison analysis is carried out by following the SAGE I latitudinal sampling progression. Because the three satellite instruments never sampled at the same locations and times, the comparison was made in terms of the zonally averaged ozone layer amount in these Umkehr layers.

For the case of April 1979 and SAGE I sunset, the standard deviation of the SAGE I instrument about its zonal means is less than 10% except at high latitudes. The standard deviation for LIMS about its zonal mean is about 4%, and that for SBUV is about 2%. All three satellite systems show the same pattern with latitude. The results show that SBUV data are about 3% systematically lower than the mean of the three instruments in layer 6 but not systematically different from the other instruments in layers 7, 8, and 9. For each of the three satellites, for each of the four Umkehr layers, and for each of the four times, the root-mean-square deviation from the average of the three instruments is given in Table 2.1-1. For 15 out of 48 entries in Table 2.1-1, the deviations are less than 3%; for 23 out of 48 entries the deviations are between 3 and 5%; and for 10 out of 48 entries the deviations are greater than 5% but less than 10%. This set of data

Table 2.1-1. Estimated overall percentage differences of the calculated zonal mean ozone layer amount of SBUV, SAGE, and LIMS with respect to the average of these three instruments

		UMKEHR LAYER					
		Layer 6			Layer 7		
		SBUV	SAGE	LIMS	SBUV	SAGE	LIMS
1	Sunrise (March 79)	4.5	6.3	2.6	2.4	4.2	4.6
2	Sunrise (March 79)	2.8	3.1	1.6	3.8	2.8	4.0
3	Sunrise (April 79)	5.1	3.7	1.3	2.9	1.5	3.7
4	Sunrise (April 79)	3.8	3.6	2.1	2.8	1.4	3.4
		Layer 8			Layer 9		
		SBUV	SAGE	LIMS	SBUV	SAGE	LIMS
1	Sunrise (March 79)	1.6	3.6	4.4	4.2	6.1	8.9
2	Sunrise (March 79)	3.0	4.1	4.2	3.3	7.7	8.6
3	Sunrise (April 79)	1.6	3.2	3.9	3.0	7.3	9.5
4	Sunrise (April 79)	2.6	1.7	3.3	6.2	1.8	6.9

shows that three totally different satellite systems agree with each other to about 4% in measuring zonal mean ozone amounts in the four Umkehr layers in the middle to upper stratosphere in April, 1979. The conclusion is that this is the level of agreement that has been demonstrated between different measuring techniques as of this time. The differences are probably due in part to differences in systematic errors, such as the absorption coefficients, as well as to effects of the individual techniques. A further inference is that when one is looking for small changes, at this time it is probably necessary to use instruments of the same or closely related types, with the same systematic errors.

SAGE I and SAGE II Comparisons with Ozonesondes

As a further step in understanding data quality, electrochemical concentration cell (ECC) and Mast ozonesonde profiles from the World Ozone Data Center (WODC) data base have been compared with SAGE I and SAGE II ozone profiles, and discussed in OTP (Chapter 5). SAGE I and SAGE II data sets, composed of six profile pairs each, were chosen for comparison at the following six stations: Edmonton (53N,113W), Churchill (58N,94W), Hohenpeissenberg (47N,11E), Wallops Island (38N,75W), Lindenberg (52N,14E) and Praha (50N,14E).

SAGE I and SAGE II measurements over these stations occurred at regular intervals as either of these instruments sampled the latitude band containing any particular station. The six profile pairs representing the SAGE I period are shown in the top six panels of Figure 2.1-5. The WODC profiles were converted to ozone number density, the fundamental unit of ozone measured by both SAGE I and SAGE II. The ozone number density profiles are plotted as a function of pressure from approximately 250 to 5 mb. The SAGE I profiles are plotted as the thin curve bounded by two dashed curves, the dashed curves representing 1σ uncertainties on the SAGE I measurement. The dates of each measurement, the SAGE I event type (sunrise or sunset measurement), the spatial and temporal separation of the station-to-SAGE measurement tangent point, and the correction factor for the ozonesonde are provided on each graph. Typically, SAGE averages over a cylinder of diameter 1 km and length 200 km. The ozonesonde correction factor represents the ratio between the total ozone as measured by the Dobson instrument at the station and the total ozone derived by integration of the ozonesonde profile. Correction factors deviating greatly from unity are indicative, generally, of ozonesonde profiles of questionable reliability. In the analysis done here, ozonesonde profiles were not selectively screened out by rejecting those with correction factors outside of the intervals mentioned above.

The WODC and SAGE I profile pairs in Figure 2.1-5 had a maximum spatial separation of 481 km at Praha and a minimum separation of 71 km at Lindenberg. The maximum and minimum temporal separation between the profile pairs occurred at Hohenpeissenberg and at Lindenberg, respectively. Thus the profile pair at Lindenberg is the closest coincidence between the *in situ* ozone measurement and the remote sensing ozone measurement. This ozonesonde profile is almost entirely contained within the uncertainties of the SAGE I measurement. The precision of an ozonesonde measurement, which is not provided by WODC, has been estimated at 5–10% from ground to tropopause, and at 5% from tropopause to 25 km (Barnes et al., 1985; Hilsenrath et al., 1986). Similar results are shown on Figure 2.1-6 for the SAGE II instrument.

Estimates of the differences between the ozonesonde and satellite ozone measurements are given in the lower panels of Figures 2.1-5 and 2.1.6 over the altitude range from 15.5 to 30.5 km. Each difference profile was calculated by first interpolating the six ozonesonde profiles to the altitudes at which SAGE I and SAGE II measure ozone. For each altitude, the six ozonesonde values were averaged as were the six SAGE I or SAGE II values. The mean values were used to compute the percentage difference between the ozonesonde and the satellite measurements relative to the mean of the ozonesondes. The mean

Figure 2.1-5. Samples of profile pairs measured by ozonesondes and the SAGE I instrument appear in the upper six panels. The lower panel is the mean percentage difference between the ozonesondes and the SAGE I ozone. Ozonesonde profiles were interpolated to the altitudes 15.5, 16.5, ..., 30.5 km. The dashed curves represent one standard error.

EDMONTON

WODC   8/ 2/86
SAGE II 8/ 3/86
Sunrise

Δ Distance 190 km
Δ Time   0.5 Days
Correction 0.997

CHURCHILL

WODC   6/ 5/85
SAGE II 6/ 6/85
Sunrise

Δ Distance 277 km
Δ Time   0.7 Days
Correction 0.933

HOHENPEISSENBERG

WODC   2/ 4/87
SAGE II 2/ 3/87
Sunset

Δ Distance 386 km
Δ Time   0.6 Days
Correction 1.124

PRESSURE (mb)

WALLOPS

WODC   11/12/85
SAGE II 11/10/85
Sunset

Δ Distance 344 km
Δ Time   1.1 Days
Correction   0

LINDENBERG

WODC   7/ 2/86
SAGE II 7/ 1/86
Sunset

Δ Distance 226 km
Δ Time   0.7 Days
Correction 1.048

PRAHA

WODC   2/ 2/87
SAGE II 2/ 2/87
Sunset

Δ Distance 324 km
Δ Time   0.3 Days
Correction 1.286

$O_3 (cm^{-3})$

$O_3 (cm^{-3})$

100 (SAGE II/WODC-1)

ALTITUDE (km)
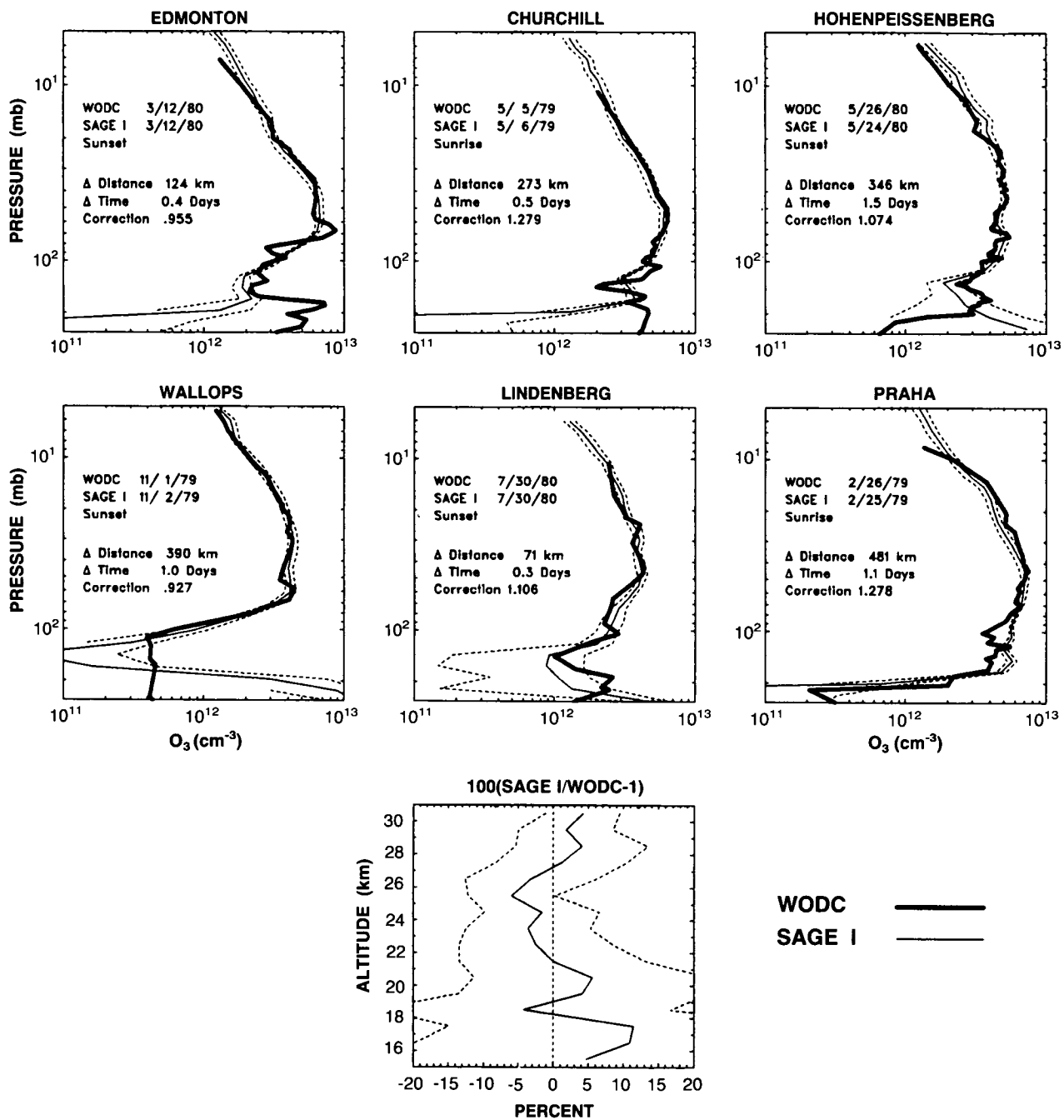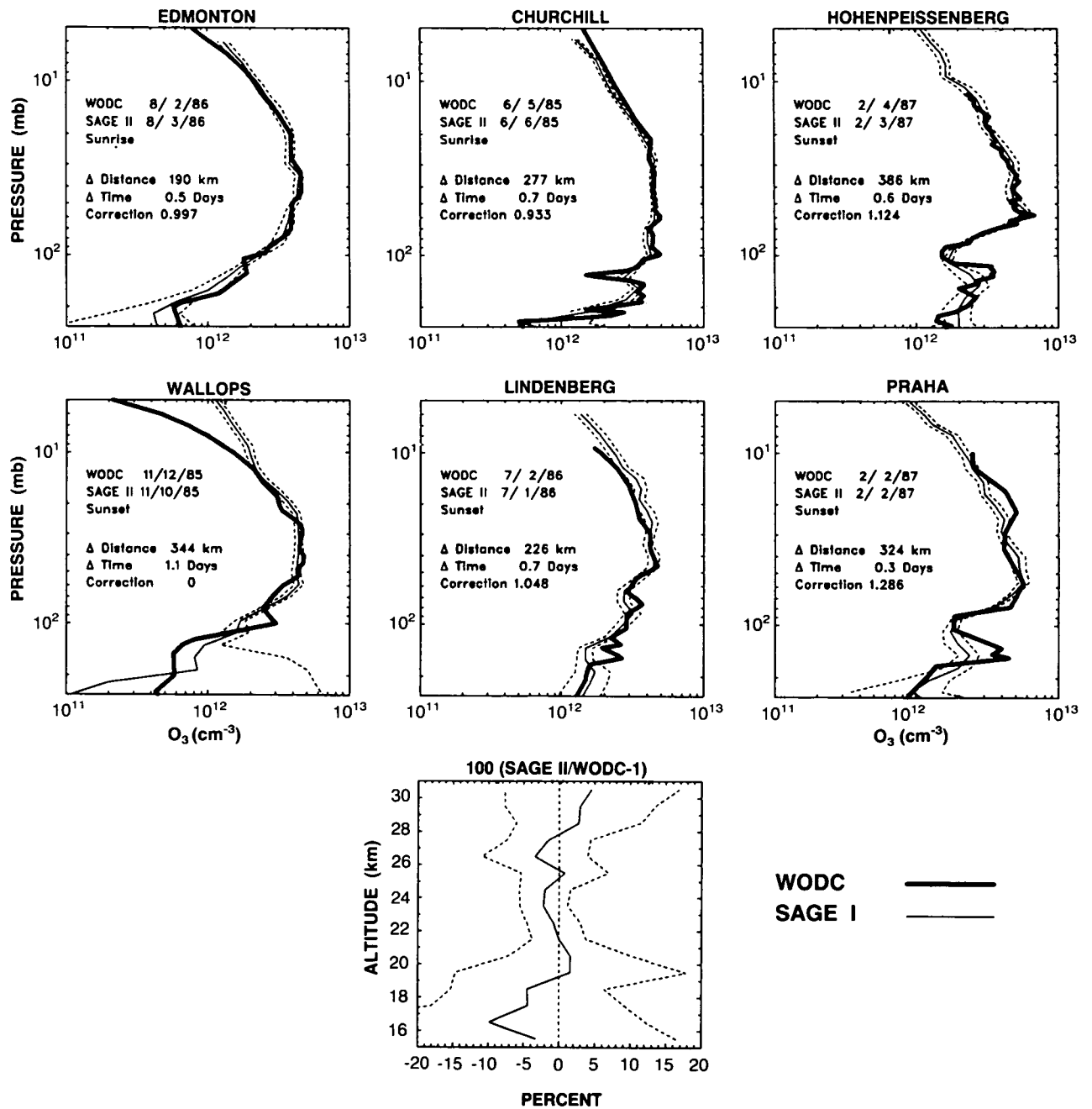
PERCENT

WODC ───────

SAGE I ───────

Figure 2.1-6. Samples of profile pairs measured by ozonesondes and the SAGE II instrument appear in the upper six panels. The lower panel is the mean percentage difference between the ozonesondes and the SAGE II ozone. Ozonesonde profiles were interpolated to the altitudes 15.5, 16.5, ..., 30.5 km. The dashed curves represent one standard error.

percentage difference is plotted as the solid curve in the lower panels of Figures 2.1-5 and 2.1-6 with the dashed curves representing the standard error of the mean percentage difference. Using these relatively small samples, the differences between the satellite and the ozonesonde measurements are on the order of 5–10%.

A similar analysis to that described above was performed on a larger sample of ozonesonde and satellite pairs from the same set of stations listed above. An ozonesonde profile and a satellite profile were considered a pair if the satellite measurement location was within 1,000 km of the sonde launch station and within 5 days of the launch time. This criterion yielded 2,306 SAGE I-WODC pairs and 1,474 SAGE II-WODC profile pairs. These sets of pairs had a mean temporal separation of 2.4 ± 1.4 days and a mean spatial separation of 700 ± 200 km. The results of averaging, to form the percentage differences relative to the ozonesondes, are shown in Figure 2.1-7, with the horizontal bars representing the 95% confidence interval of the mean percentage difference. Between 20.5 and 27.5 km, the differences are mostly negative and centered at approximately −6%. Above 27.5 km, the differences computed using both SAGE I and SAGE II ozone are consistently tending toward higher values, a possible indication of ozonesonde pump inefficiency at high altitudes. Below 20.5 km, the SAGE II comparisons with the ozonesondes show an essentially constant difference with magnitude less than 5%, but with increasing uncertainties owing to the spatial and temporal ozone gradients below the ozone concentration peak.

The conclusion is that comparisons of SAGE I and SAGE II profiles, colocated in time and space with ozonesonde profiles archived in the WODC data base, reveal that both the SAGE I and SAGE II satellite measurements consistently agree to within ±7% above approximately 20.5 km.

SAGE-Umkehr

The results of the trends analysis performed on the SAGE I/II data and Umkehr are discussed in Chapter 5 of OTP. At present, a direct comparison between the two data sets, as far as ozone trend is
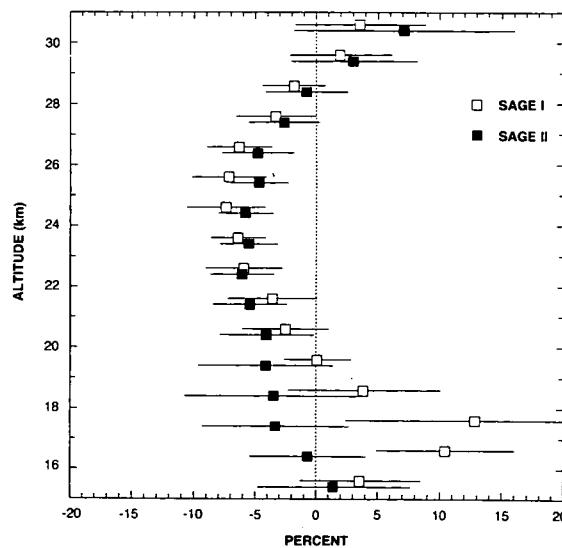

Figure 2.1-7. Mean differences between SAGE I and ozonesondes (open squares) and SAGE II (solid squares) and ozonesondes. Error bars are the 95% confidence interval on the mean ($\pm 2\sigma$).

concerned, has not been performed. The reprocessed SAGE I data that were used for the ozone trends study are being archived at NSSDC. Comparisons between Umkehr data and the previously archived version of the SAGE I ozone data showed some biases between the two data sets within the time period from 1979 to 1981 (Newchurch et al., 1987). An updated comparison with the revised SAGE I ozone data has not been performed. No comparison between the SAGE II ozone data and the Umkehr data has been performed. The changes derived from SAGE I-SAGE II differences and the Umkehr data are discussed in Section 2.3.

2.1.4.2 Intercomparisons Relevant to Future Trend Analyses

Total Ozone—Dobson Versus Brewer and TOMS

The Brewer data have been used in a number of intercomparisons which are of importance to present trend analyses and will be relevant to future trend studies. A number of sites, including five stations in Canada, have been making ground-based total ozone measurements on a routine basis with both the Brewer and Dobson instruments. These data, plus the TOMS measurements, provide three independent sets of routine field measurements of the same atmospheric constituent over a time period of a few years. Intercomparison between these data sets has been useful in evaluating monitoring performance and capabilities. Results of comparisons between Brewer and Dobson data at Toronto and Edmonton have shown an agreement within 1% and a statistically insignificant long-term drift (Kerr et al., 1989a; 1989b). Comparison between TOMS data and Brewer data has shown that the TOMS total ozone has been decreasing relative to that of the Brewer at a rate of 0.6% per year at Toronto between 1983 and 1987, and 0.61% per year at Edmonton between 1984 and 1987 (Evans and Kerr, 1989). These values are similar to the 0.64% per year decrease of TOMS data relative to the ensemble of Dobson data for the same time period (Figure 2.1-4).

Vertical Profiles

Microwave-Umkehr

Only one long-term (greater than 1 year) intercomparison of ozone profiles obtained from Umkehr observations and microwave measurements has been published (Lobsiger, 1987). From April 1984 to April 1985, 334 daytime ozone profiles were obtained with a microwave sensor operated at the University of Bern, Switzerland. For Umkehr layers 6 through 9, simultaneous data were available for 211 days from the Arosa Umkehr station at a distance of approximately 200 km. The seasonal variations observed by both instruments are very similar and the corresponding correlation coefficients for layers 6–8 are 0.87, 0.87, and 0.74, respectively.

SBUV—Microwave

A comparison was carried out between ozone profiles derived from microwave data obtained at the University of Bern, Switzerland and SBUV data. For the latter, archived data (i.e., with no allowance for SBUV instrument drift) were mapped using the Kalman filter technique and evaluated at Bern. Daily data were calculated at pressure levels between 30 and 0.7 mb; when plotted as time series they showed regular variations with season. The Bern data were available for four periods between December 1981 and June 1987. All data were smoothed with a gaussian filter 10-days wide, to reduce short-term fluctuations.

In all periods, there were appreciable biases. Averaged over altitude, the mean differences ranged from 30% to − 15%. The level showing the least bias was at 7 mb, where differences ranged from − 3% to − 13%. The standard deviations around these biases between 10 and 1 mb are 7–10% in the last three periods, with correlations of about 0.5. Because there were changes in the instrument, observational method, and data reduction, it is likely that the changes between the first and second periods, and between the third and fourth, are due to instrumental effects. (During these observational periods, differences between SBUV and the Arosa Umkehr observations showed differences of 0 to −6%, with standard deviations of about 7% and correlations of about 0.5.) The results are not appreciably changed if the comparisons are carried out for ozone amounts integrated over Umkehr layers. The shapes of the vertical profiles were also compared. There were occasions when the agreement was reasonably good, but other situations when there were large differences. There was no obvious correlation of these differences with season.

In conclusion, these microwave observations, while somewhat noisy, and the SBUV observations appear to follow ozone variations and obtain roughly similar results for the day-to-day changes. However, there are large biases which are not entirely understood, and which appear to be rather sensitive to the details of the observations. In order to look for trends, the observing and data reduction will need to be standardized and held constant. As absorption by tropospheric water vapor is a major interference, observing from high, dry sites should reduce some of the observational problems, as noted previously.

De la Noe et al. (1988) reported an intercomparison between microwave ozone profiles and profiles obtained by the BUV instrument on the OHZORA satellite during September 1985. Over the altitude range 37–55 km, they found an average rms difference of less than 10% for distances between satellite and microwave soundings below 1,500 km, and in general less than 20% for larger distances. They also report comparisons with SAGE II, and find average rms differences of 18% during 1985. Connor et al. (1987) report approximately 10% agreement in microwave-ozonosonde comparisons.

LIDAR—Umkehr—Satellite

Recently, the capability to make lidar measurements of the ozone number density has been demonstrated in France, the Federal Republic of Germany, Japan, and the United States. Two systems are presently operational for systematic stratospheric measurements. The first one is located at the Observatoire de Haute-Provence (OHP), France and has been operating since October 1986. The second one, located at Table Mountain Observatory (TMO), California, USA began systematic measurements in February 1988. Comparisons have been performed with other instruments such as the Umkehr, SBUV, and SAGE II. Concerning the short Umkehr method, a comparison based on 43 profiles at OHP indicated that lidar was about 3% higher than Umkehr in layers 5 and 6, but with the Umkehr values larger than the lidar values by about 7% in layer 7. Concerning SBUV, the comparisons have involved 12 measurements performed in July 1985 and 1986. The lidar values are generally higher than SBUV, with an average difference of about 10%. The comparison with SAGE is more direct in that it does not require conversion to mixing ratios and pressure coordinates, but there are fewer matchups. In general, the difference is less than 15% for each profile. Finally, a comparison of the ozone seasonal variation at different altitudes as determined by the lidar, SBUV, and Umkehr instruments has also been performed at OHP and shows that the shapes are very similar, but that the lidar data show a significantly larger amplitude (Godin et al., 1989).

An intercomparison campaign involving the TMO lidar, the mobile lidar station recently developed by the Goddard Space Flight Center, SAGE II, rocket- and balloon-borne instruments (i. e., ROCOZ-A and ECC sondes) was organized at Table Mountain Observatory in October-November 1988. The com-

parison between the two lidars, which could not be operated at the same time because of interferences between the two systems (located 600 meters apart), shows a day-to-day agreement within 10% in the 20 km–40 km altitude range. This is somewhat greater than the error bars of the two systems, but it can be explained by the fact that the instruments didn't observe exactly the same air masses at a period when the day-to-day variability of ozone was quite high. The comparison with the other instruments involved in the campaign is based on 3 days of observation. The results show an agreement within the instruments' error bars in most cases. However, it is clear that the agreement depends strongly on local meteorological conditions, because the different measurements are not simultaneous. In particular, the agreement was less satisfactory during the passage of an airmass of tropical origin characterized by a lower ozone content.

2.1.5 Temporal Sampling Requirements for Total Ozone Trend Detection

Total ozone measurements are made on a routine basis at many stations around the world. The data are then reported to the WMO World Ozone Data Center in Toronto, Canada and printed regularly in a series of publications entitled *Ozone Data for the World*. Ideally a station takes several readings each day, with the times at which these readings are taken centered around local noon. These measurements are combined to form daily means which are then reported to *Ozone Data for the World* for publication. The daily means are averaged to form monthly means, and it is the monthly means that have been used in all statistical trend analyses. In practice, however, problems such as local weather, funding, and operator availability ensure that total ozone readings are not made every day. Understanding the effects of such missing data on the calculated trends is important in assessing the results of trend analyses and in designing future monitoring networks. A recent study by Tiao et al. (1989) examined the consequences of a reduction in the daily sampling frequency on trend estimates using data from *Ozone Data for the World*. The stations with the most complete daily records were chosen and year-round trends were estimated from data sets where the monthly total ozone means were calculated by using first all the data (1/1), then every other daily value (1/2), next one in four daily values (1/4), and so on down to one in sixteen daily values (1/16): in the last case just two daily values were thus used to calculate each monthly mean. The results are shown in Table 2.1.2. The trend estimates and their standard errors do not vary very much as the sampling rate is reduced to the 1/4 rate, although some differences are found at Mauna Loa and Hohenpeissenberg. These results seem to indicate that for the period 1970–1985 the precision of the long-term trend estimates will not be appreciably different at stations that sampled every other day than they would have been if that station had sampled every day. The reason for this insensitivity is the high day-to-day autocorrelation found in total ozone readings: the larger the day-to-day autocorrelation, the less sensitive the monthly mean (and hence the trend estimate) is to missing daily values. It should be noted that Tiao et al. eliminated the daily values *systematically* and spaced the remaining daily observations evenly through the month. These results are in agreement with the observation that for any particular calendar month, at a particular station, the ratio of the standard deviation of the daily total ozone measurements within the month to the

Table 2.1-2 Summary of Ozone Trend Estimates (in % per year) in total ozone and associated standard error

Sampling rate	Tateno	Hohenpeissenberg	Mauna Loa
1/1	− .002 ± .082	− .078 ± .061	− .382 ± .090
1/2	− .022 ± .082	− .099 ± .066	− .370 ± .091
1/4	− .010 ± .080	− .136 ± .080	− .300 ± .095
1/8	− .046 ± .073	− .103 ± .083	− .348 ± .092
1/16	− .009 ± .082	− .187 ± .084	− .322 ± .093

standard deviation of the monthly means from year to year is typically found to be about 2, indicating that there are about 4 truly independent observations each month.

Tiao et al. (1989) addressed a related issue which concerns estimating relationship between variables in two neighboring locations. Employing total ozone data from two European stations (Arosa and Hohenpeissenberg) and those from three Japanese stations (Sapporo, Tateno, and Kagoshima), they have found that the correlation estimates based on monthly averages of daily measurements are insensitive to temporal sampling rate when the measurements are taken on the same days across the locations. On the other hand, the estimates deteriorate as the time lag between measurements taken at the two locations is increased. The main reason for this phenomenon is likely to be that relations on a monthly scale are primarily due to short-term contemporaneous correlations on a daily basis. Although their empirical findings are based on the same variable (total ozone) at two different locations, similar phenomenon is likely to occur between different atmospheric parameters at the same location. Thus, in designing a measurement program when relations between variables are of interest, it is important to exercise care in arranging the timings of different measurements both across and within stations.

Tiao et al. (1989) also investigated how different lengths of record and differing degrees of month-to-month autocorrelation within the data record affect the trend estimate and its standard error, and concluded that the precision of the trend estimates depends critically on the degree of the month-to-month autocorrelation in the measurements. If the month-to-month autocorrelation is large, it is indicative of unexplained medium to long-term variations in the data, and the standard error of the trend estimate is consequently large. It will be most difficult to provide early warning of a trend in total ozone in an area where the month-to-month autocorrelation is naturally high. In practice this means the tropics, and unfortunately there are not many long-term series of measurements in this region.

2.1.6 Concluding Remarks

In the previous sections, numerous past and emerging techniques for the measurement of ozone have been described. Where possible their accuracies and precisions have been presented. A few further remarks on the application of these techniques to the detection of trends are in order.

Following the definitions given in the introduction, if the systematic errors are truly consistent (as, for example, if they are dependent on a poorly known absorption coefficient), the changes or trends that can be detected may be smaller than the absolute error of a system's measurements. This is often the case; applicability then depends on how stable the system or instrument remains over time.

Ground-based instruments can be checked and recalibrated as necessary. These are generally regarded as being capable of long-term stable operation. This is technically true; actual results may depend on funding, the importance attached to the measurements, the skill of the observer, and other non-technical factors. An advantage is that the same instrument is used repeatedly for the observations, so instrument-to-instrument variations do not come into play at a single location.

Balloon and rocket measurements may be calibrated immediately before flight, but only rarely afterward. In addition, the conditions under which observations are made are generally different from those in which the calibrations are carried out. Perhaps most seriously, small instrument-to-instrument variations add an additional source of noise to attempts to look for trends. Because there is usually a relatively limited number of such observations, they have been of limited use for trend studies to date.

The features of satellite instruments are in some ways the converse of ground-based instruments. They cannot be checked in orbit, although they usually have a capability for in-flight calibration of at least some of the critical features of their designs. However, again it is the same instrument used at all locations as well as all times, so gradients and changes may be detected, depending on instrument stability. There is probably not enough experience to say much about instrument-to-instrument differences; the experience with SAGE I and II is encouraging that these effects can be small, but the SBUV-SBUV/2 problems are a cause for concern. Comparisons between different techniques are often illuminating. In principle the differences could be large, but the differences less than ~4% found among SAGE, SBUV, and LIMS in 1979 is an indication of the present level of agreement between different techniques that can be achieved. As noted above, these differences are probably due in part to differences in systematic errors, implying that at the present time, when one is looking for small changes, it is necessary to use very similar if not identical techniques, including instruments and data reduction algorithms, to keep the systematic errors constant. In future it may be possible, with a great deal of care, to reduce the systematic errors to the point that data from different instruments can be combined in trend analyses. This will require further laboratory measurements of the ozone absorption coefficients and their temperature and pressure dependences, comparisons of the retrieval algorithms, and field intercomparisons under as many conditions as possible.

A large amount of data has been collected over many years by instruments whose characteristics are known reasonably well. Initially, few of these measurements were made for the purpose of determining long-term changes. Fortunately, some of these data have the requisite accuracy and stability to provide a reasonable data base for efforts to detect and quantitatively measure changes in the ozone overburden and its vertical distribution, such as those reported by the OTP and later in this chapter.

Looking to the future, the measurement situation for total ozone is moderately satisfactory. The present network of Dobson stations is continuing for the most part, and provides a reasonable network for detecting regional and probably zonal trends in the middle latitudes of the Northern Hemisphere. New ground-based instrumentation appears to provide compatible data, allowing a continuation of the measurement series.

For global observations, the TOMS instrument continues to operate, having already provided almost one solar cycle (11 years) of data. A new technique for internal calibration appears to allow the TOMS to provide an entirely separate data record for total ozone that can be compared and checked against the ground-based network. Additional TOMS instruments are planned for flight on a variety of spacecraft during the 1990s, eventually reaching operational status late in the century. In the interim, if the problems with the instrument and data reduction are solved, the operational SBUV/2 could potentially provide another very valuable data record from the mid-1980s until the operational TOMS is launched.

The situation for the measurement of trends in vertical profiles is somewhat less satisfactory. In the past the ground-based Umkehr techniques were subject to interference by aerosols. It is believed that these may now be corrected, using new techniques and independent measurements of aerosol distributions, but further testing and validation is necessary. The new lidar and microwave methods also require further work to fully understand and characterize them. In addition there are sampling problems; the number of stations taking regular Umkehr observations is limited, and most of them are in the mid-latitudes of the Northern Hemisphere. At present, there are very few stations employing the new technology.

For the present, only data from the SAGE instruments appear to have the long-term stability to allow trend detection. SAGE II (and its spacecraft) are already over 5 years old, and there is not a planned successor until 1996. A failure could result in a lengthy gap. In addition, these data are subject to the

193

limitations of the sampling of the occultation technique and the attendant uncertainties in comparing different years (see OTP, Chapter 5). Again, if the problems with the SBUV/2 can be successfully resolved, they could potentially make an extremely valuable contribution. Other profile measurements will be obtained by research instruments on UARS, but it is unclear how well they will be able to extend the previous data records. An infrared limb scanner is scheduled to become available in 1996.

Present planning for ozone trend measurements suggests a systems approach, based on complementary ground-based and satellite observations. In this, satellite measurements can be checked for unexpected drifts through comparison with a network of carefully calibrated, maintained, and operated ground-based instruments. In turn, the satellite instruments act as transfer standards, indicating whether any of the ground instruments are drifting relative to the others. This will be especially challenging with respect to the measurement of vertical profiles. The stations in the Network for the Detection of Stratospheric Change (NDSC), which will include new instruments (lidar, UV, IR, and microwave spectrometers), are being planned with this function in mind.

2.2   TRENDS IN TOTAL OZONE

2.2.1   Introduction

This section summarizes the current understanding of trends in total column ozone. The objective of the analyses reported here are: (1) to re-examine the data set used by the Ozone Trends Panel (OTP) using several different statistical models which make varying assumptions in their treatment of the measurements, (2) to update trends derived from the Dobson network using the most recent data available, and (3) to examine the regional behavior of changes in total ozone using both ground-based and satellite-based measurements.

It is essential to recognize the merits and limitations of both the Dobson network and orbiting remote sensors. The Dobson network provides a long-term data record whose duration is suitable for detailed statistical analysis. The deficiency is a limited geographic coverage, with a bias toward middle latitudes of the Northern Hemisphere. The data record obtained by satellites has global coverage, although at present the length of record is inadequate for derivation of long-term trends. In addition, the trends that exist in data sets obtained by satellites contain drifts of instrumental origin. A correction is therefore required, and at present this must be done in an approximate way by comparison with the Dobson network. However, new approaches to data processing may minimize this problem in the future. Nonetheless, satellite measurements are useful in identifying geographic variations in ozone change.

A major effort in the Ozone Trends Panel Report centered on developing a provisionally revised Dobson data set. This made use of ozone measurements from nearby stations, temperatures measured at 50 mb, and detailed studies of the records from each instrument to identify problems in the Dobson data set. In addition, comparison of co-located ozone measurements made by the Nimbus-7 TOMS instrument and the Dobson network allowed identification and correction of inconsistencies in the latter data base. Further information appears in Chapter 4 of the Ozone Trends Panel Report. The updated trend analyses reported here adopt the provisionally revised data base for each Dobson station through December 1986, the latest information available to the Ozone Trends Panel in early 1988. As of this writing, available data after 1986 have received a screening similar to that performed for the provisionally revised Dobson data set, and a number of adjustments have been made to data from 1987 and 1988 to smooth erratic variations.

2.2.2 Trend Analysis of Dobson Total Ozone Data

2.2.2.1 Result of the 1988 Ozone Trends Panel and Comparison with Other Studies

In 1988, the Ozone Trends Panel completed a statistical analysis of Dobson data from a network of stations, most of which were located between 30 and 64 degrees North latitude. The Panel focused on data over the period 1965–1986 for three reasons: It contained two complete solar cycles; effects of the atmospheric nuclear bomb tests should have subsided by 1965; and many more Dobson stations were operating in 1965 than in 1957–1958, thereby providing a more substantial data base than was available in earlier years. The percent changes in total ozone over the 17-year period 1970–1986 were reported by season and latitude zone. These results appear in the first column of Table 2.2-1, labeled as OTP. This work built on statistical studies of ozone performed over the last decade (e.g., Bloomfield et al., 1983; Hill et al., 1986; St John et al., 1981; Reinsel et al., 1987b). Over the Northern Hemispheric latitude band 30–64 degrees North, there was a wintertime change of about -4% for this period (ranging from -2% to -6%

Table 2.2-1. Comparison of trend results by season and latitude (17 years % change between 1970 and 1986 with one standard error in parentheses)

Zone/ Latitude	OTP	AS1	UW&C1	UW&C2	AS2
Year Round					
53–64°N/55°N	−2.3(0.7)	−1.6(0.8)	−2.1(0.7)	−2.0(0.7)	−1.8(1.0)
40–52°N/45°N	−3.0(0.8)	−2.6(0.7)	−1.9(0.6)	−1.6(0.6)	−1.9(0.8)
30–39°N/35°N	−1.7(0.7)	−0.8(0.8)	−1.0(0.7)	−1.3(0.6)	−1.9(0.9)
Average	−2.3(0.5)	−1.7(0.5)	−1.7(0.5)	−1.6(0.6)	−1.9(0.8)
Winter					
53–64°N/55°N	−6.2(1.5)	−4.2(1.6)	−4.7(0.8)	−5.1(0.8)	−5.1(1.0)
40–52°N/45°N	−4.7(1.5)	−5.1(1.4)	−3.4(0.7)	−3.6(0.6)	−4.0(0.7)
30–39°N/35°N	−2.3(1.3)	−1.7(1.3)	−1.5(0.8)	−2.1(0.7)	−2.8(0.8)
Average	−4.4(1.0)	−3.7(1.0)	−3.2(0.6)	−3.6(0.6)	−4.0(0.7)
Summer					
53–64°N/55°N	−0.2(0.8)	−1.1(0.8)	−0.7(0.7)	−0.9(0.7)	−0.6(1.0)
40–52°N/45°N	−1.9(0.7)	−1.2(0.7)	−1.5(0.7)	−1.1(0.5)	−1.2(0.8)
30–39°N/35°N	−1.9(0.8)	−0.6(0.8)	−1.2(0.8)	−1.2(0.6)	−1.2(0.9)
Average	−1.3(0.5)	−1.0(0.5)	−1.1(0.5)	−1.1(0.5)	−1.2(0.8)

Notes:
OTP = Ozone Trends Panel result based on zonal series.
AS1 = Allied-Signal results using zonal series.
UW&C1 = Universities of Wisconsin and Chicago results using regional/latitudinal analysis where the same trend is assumed to apply to all stations in a single region.
UW&C2 = Universities of Wisconsin and Chicago results using regional/latitudinal analysis with a linear trend in latitude.
AS2 = Allied-Signal results using regional/latitudinal analysis of individual stations including a nuclear weapons correction. The text describes additional differences between the AS2 and UW&C1 and UW&C2 models.

with increasing latitude), a summertime change of about -1%, and a year-round change of about -2%. The statistical model included terms to account for changes in ozone related to the quasi-biennial oscillation (QBO) cycle in winds and the 11-year solar cycle. The long-term trends that remained, as reported in Table 2.2-1, could not be explained by these known natural variations.

Recent analyses by scientists at Allied-Signal, Inc. and the Universities of Wisconsin and Chicago have subsequently verified the findings of the Ozone Trends Panel, including a new analysis of the sensitivity of derived trends to (1) the length of data records, (2) regional differences, and (3) the statistical techniques applied. Of particular interest were the major perturbations in ozone before 1965 and after 1982 and their effects on derived trends, as well as the differences observed among different geographical regions (e.g., North America, Europe, and Japan). The nuclear weapons tests in the early 1960s and natural phenomena, such as the El Chichon volcanic eruption and El Niño events in the 1980s, may be related to these ozone fluctuations. Figure 2.2-1 is a time history of residual zonal mean total ozone in Dobson Units (DU) with most known natural and man-made variations subtracted out. This shows some large perturbations in the post-1982 period following, but not necessarily related to, the El Chichon volcanic eruption. With respect to regional differences, Figure 2.2-2 (a)-(c) shows larger decreases over North America and Europe than over Japan after allowing for known variability. The nonrandom fluctuations that remain in Figure 2.2-2 arise from sources of variation not included in the statistical model, for example the El Niño oscillation, and an incomplete subtraction of known sources such as the QBO. However, these nonrandom fluctuations are removed by the autoregressive filter. The European wintertime dip in 1982–1983 is particularly noticeable.

Table 2.2-1 presents a comparison of five separate sets of trend results, including the Ozone Trends Panel findings, over the 17-year period 1970 through 1986. In these and all subsequent Dobson analyses, the statistical models account for variations in ozone related to the solar cycle, the QBO, and, where applicable, nuclear weapons tests during the 1960s. The derived long-term trends cannot be explained by any of these mechanisms. The time dependence of ozone changes related to nuclear weapons tests is based on calculations by the Lawrence Livermore Laboratory chemical-transport model (Wuebbles and Kinnison, 1989). However, the magnitude of the ozone change is determined from the statistical analysis and is allowed to vary with latitude.

The choice of the period 1970–1986 for the trend assessment corresponds to the period during which theory predicts the onset of effects on the ozone layer related to chlorofluorocarbon (CFC) release. The trend is assumed to start in January 1970 and be zero prior to this time. Sensitivity to the starting date is discussed later. The form of the trend model used in all of the studies is described in Appendix 2.A.

The results in the second column of Table 2.2-1, labeled AS1, were developed by Allied-Signal researchers with the same zonal mean series of total ozone data used by the Ozone Trends Panel for latitude belts 30–39°N, 40–52°N and 53–64°N. Results in the third and fourth columns were obtained by researchers from the Universities of Wisconsin and Chicago (designated UW&C). Unlike the first two sets of results, which analyzed the data after it was pooled into the zonal mean series shown in Figure 2.2-3, the UW&C studies derived a separate trend of each of the 25 stations within the 26–60°N latitude band (see Table 2.2-2, excluding Reykjavik and Uccle). The trends were then fitted (or regressed) against latitude using two different methods. In the first method, labeled UW&C1, all stations within each of three different latitude zones, 30–39°N, 39–50°N and 50–64°N, were assumed to have a common average trend. In the second method, labeled UW&C2, the trends were regressed as a linear function of latitude (Bojkov et al., 1989). Both UW&C methods allow for apparent regional differences over North America, Europe, Japan, and the Middle East. The first method more closely corresponds to the OTP and AS1 analyses based on the
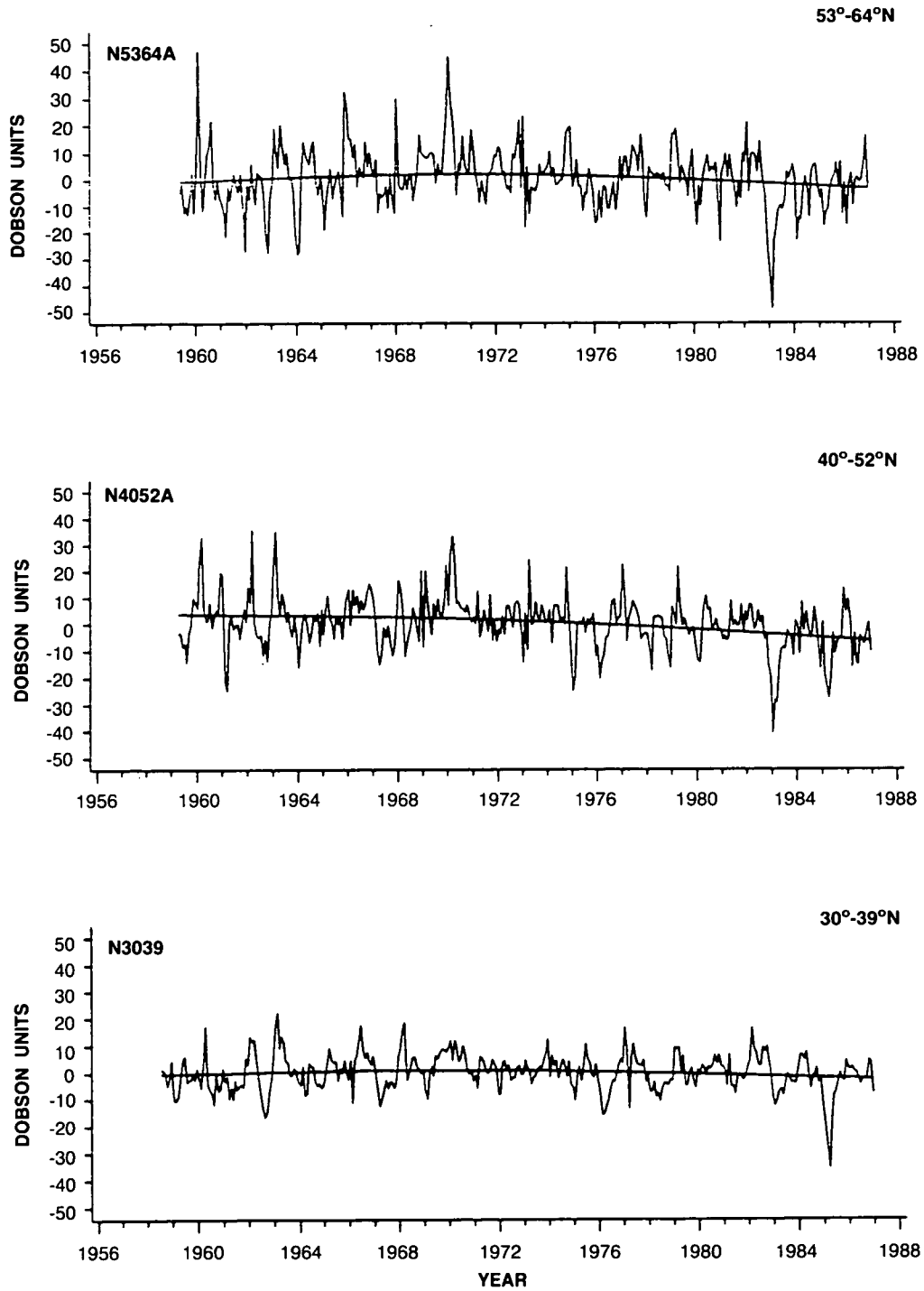
196

Figure 2.2-1. Monthly and zonally averaged Dobson total ozone values versus time after removal of seasonal, quasi-biennial oscillation (QBO), solar cycle, and nuclear test effects. A smooth line is shown for each of the three latitude zones 53-64°N, 40-52°N, and 30-39° N.
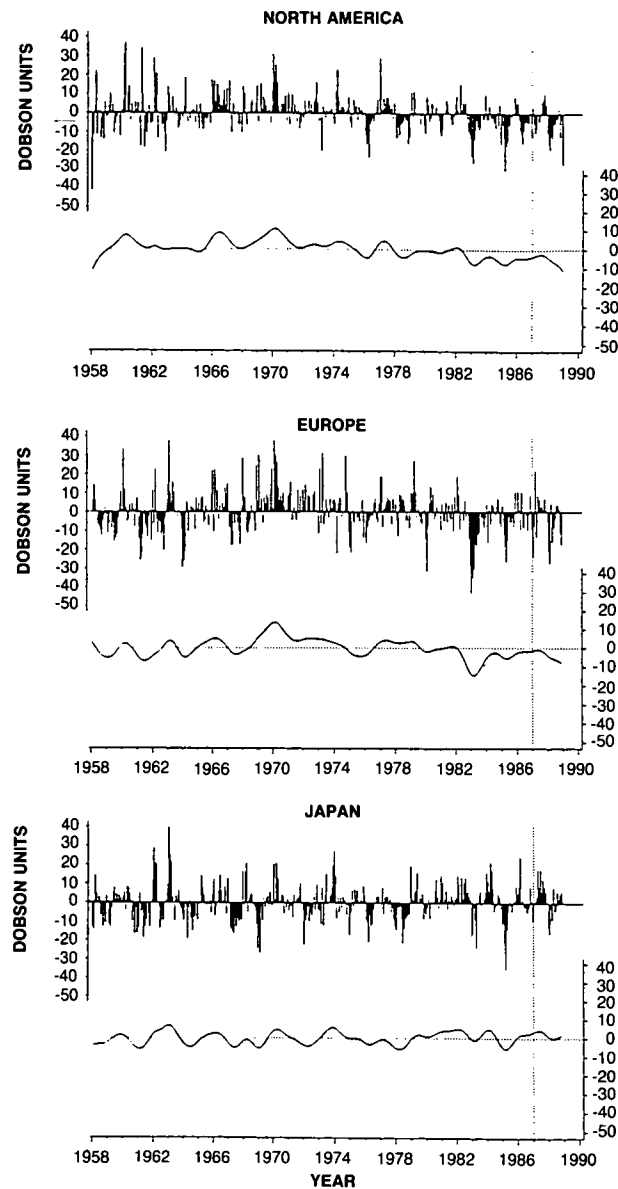
Figure 2.2-2a. Regional plots of Dobson total ozone after removal of seasonal, solar, QBO, and nuclear test effects for North America (top), Europe (center), and Japan (bottom), all months. The deviations are plotted in Dobson units where the upper panels give monthly values and the lower panels are smoothed. Nonrandom fluctuations are removed from the trend analysis by an autoregressive filter. Vertical lines at the end of 1986 denote the end of the data set available to the Ozone Trends Panel.

zonal mean series, while the second method provides a capability for estimating trends as a function of latitude. Overall the second method uses more information contained in the data than does analysis of a zonal series, but it also makes a stronger assumption concerning the relationship of trends to latitude, namely that they are linear. In Table 2.2-1 the trend estimates are given for three latitude zones based on UW&C method 1, and the predicted changes are given for latitudes 55°N, 45°N, and 35°N based on UW&C

WINTER
NORTH AMERICA

WINTER
EUROPE
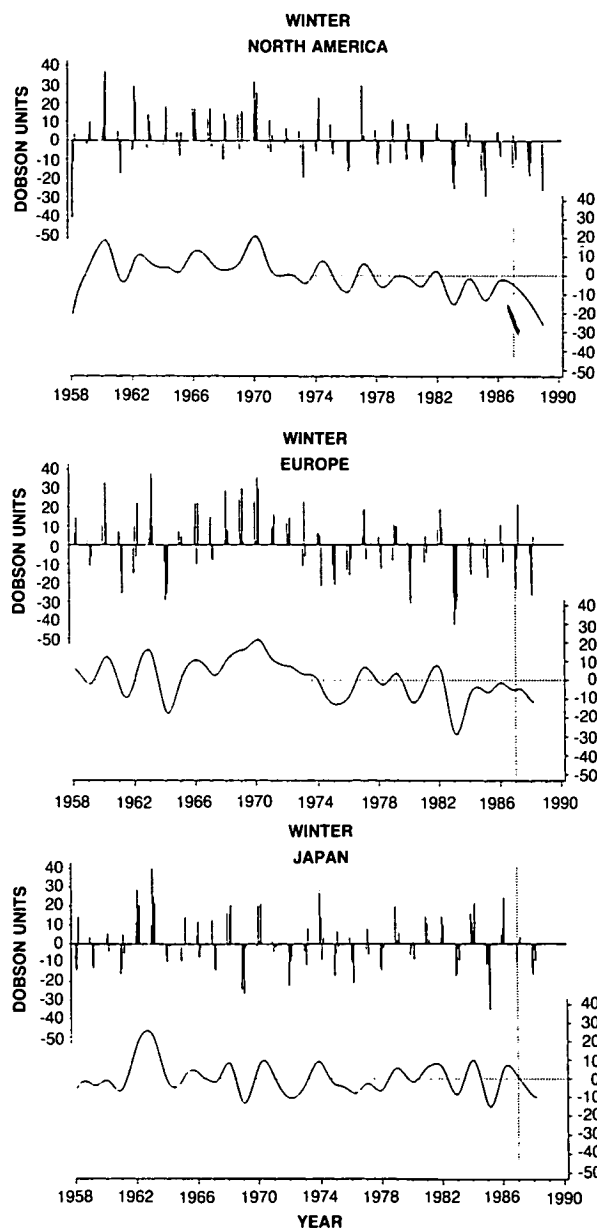
WINTER
JAPAN

YEAR

Figure 2.2-2b. Same as 2.2-2a for winter months (December-March).

method 2. Separate trends are derived for year-round, winter (December-March), and summer (May-August), respectively.

The last column in Table 2.2-1, labeled AS2, presents results obtained by Allied-Signal researchers using a technique similar to method 2 in the UW&C study but which includes adjustments for nuclear weapons tests in the 1960s. Results are based on only the 25 stations located at latitudes between 26°N and 64°N (Table 2.2-2). The AS2 results do not use the two stations from Egypt and Pakistan to form a separate
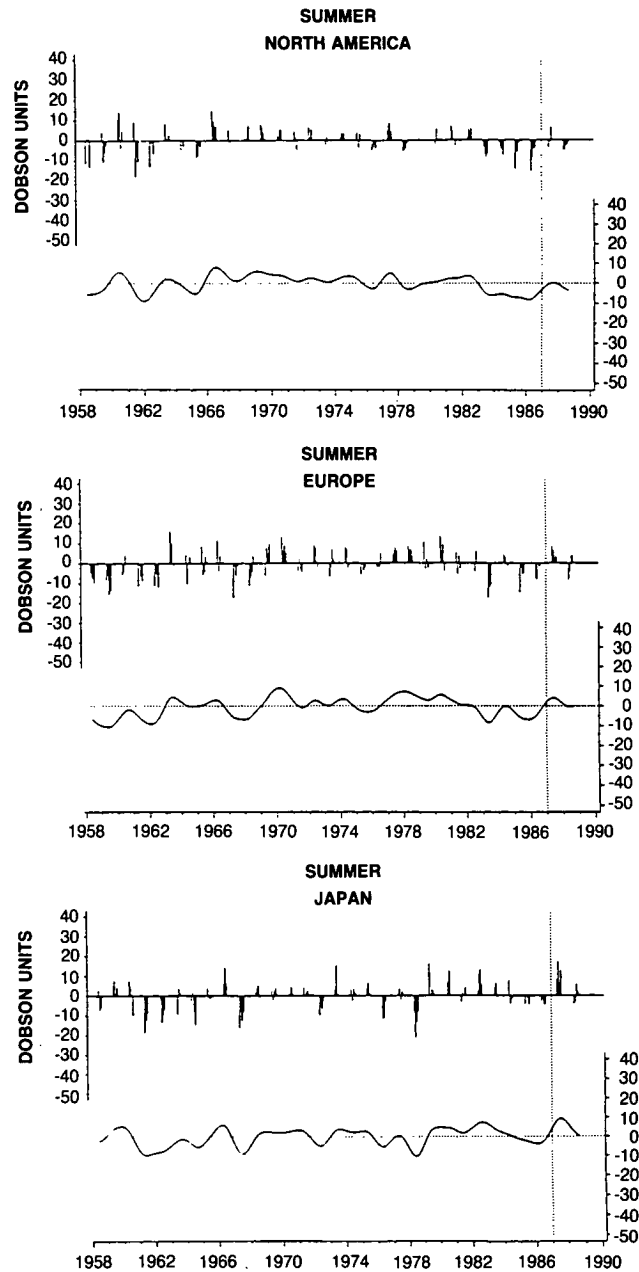
Figure 2.2-2c. Same as 2.2-2a for summer months (May-August).

Mid-East region because of the disproportionate influence these two stations can have on the summary results.

Overall, the five sets of results show a consistent pattern. They indicate a wintertime (December-March) change ranging from −2% to −6% between 1970 and 1986 which correlates with latitude, that is, the wintertime trends become more negative with increasing latitude. The value derived by the Ozone Trends Panel for winter near 55°N latitude tends to be 1–2% more negative than found in the other studies. Also, standard errors associated with the wintertime trends are smaller in those studies that accounted for the additional regional and latitudinal information.

ZONAL AVERAGE SERIES

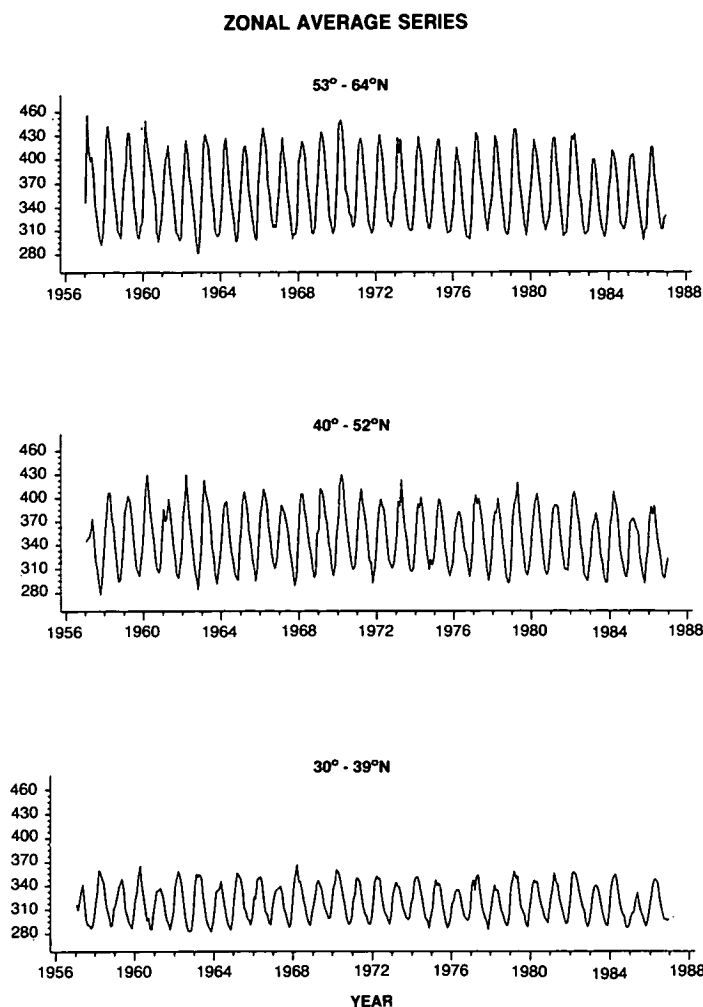**Figure 2.2-3.** Plots of Dobson total ozone monthly averages combined into time series for each latitudinal zone 53-64°N, 40-52°N, and 30-39°N. The vertical scale is in Dobson units.

Although for a given latitude, the five sets of summertime trend estimates may differ by as much as about 1%, the change in summertime averaged over all latitudes was about −1% in each study. No significant latitudinal pattern appears in the summertime trends. Similarly, in the year-round trends, no significant latitudinal pattern appears. The concept of "significance" here refers to the statistical sense of exceeding two standard errors. For each study, the average year-round change is approximately −2% over 17 years.

The difference between the two studies which used zonal series (labeled OTP and AS1 in Table 2.2-1) arise mostly from the differing lengths of record. For example, if the pre-1965 data and nuclear test adjustment are excluded from the AS1 analysis, as was done in the Ozone Trends Panel study, then the revised AS1 results would be close to the OTP trends. Other differences among the groups of results in Table 2.2-1 can be ascribed to the inclusion of a nuclear weapons adjustment, which was used in the columns marked AS1 and AS2, the use of four versus three regions and slightly different groups of stations

201

Table 2.2-2. List of Dobson total ozone stations at latitudes between 26°N and 64°N (data from these stations were revised by the Ozone Trends Panel through 1986)

Region	Station	Latitude	Start Date	End Date	Now available
N. America	Churchill	59°N	1/65	12/86	9/88
	Edmonton	54°N	1/58	11/86	3/88
	Goose	53°N	1/62	11/86	9/88
	Caribou	47°N	5/58	12/86	10/88
	Bismarck	47°N	1/58	12/86	10/87
	Toronto	44°N	1/60	11/86	9/88
	Boulder	40°N	1/64	12/86	10/88
	Wallops Island	38°N	1/70	12/86	10/88
	Nashville	36°N	1/63	12/86	10/88
	Tallahassee	30°N	5/64	11/86	4/88
Europe	Reykjavik	64°N	1/58	10/86	10/88
	Lerwick	60°N	1/58	11/86	10/88
	Leningrad	60°N	8/68	12/85	12/85
	Belsk	52°N	1/63	12/86	8/88
	Bracknell	51°N	1/69	12/86	10/88
	Hradec Kralove	50°N	1/62	6/86	10/88
	Uccle	50°N	7/71	12/86	8/88
	Hohenpeissenberg	48°N	1/67	12/86	11/88
	Arosa	47°N	1/58	12/86	10/88
	Vigna DiValle	42°N	1/58	12/86	11/87
	Cagliari	39°N	1/58	12/86	6/88
Japan	Sapporo	43°N	1/58	12/86	10/88
	Tateno	36°N	1/58	12/86	10/88
	Kagoshima	32°N	1/58	12/86	10/88
	Naha	26°N	4/74	12/86	10/88
Mid East	Cairo	30°N	11/74	10/86	10/88
	Quetta	30°N	1/58	12/86	10/88

(UW&C1 and UW&C2 versus AS2), the analysis of averaged zonal data versus the analysis of individual stations (OTP and AS1 versus UW&C2 and AS2), and small effects due to the choice of solar cycle and QBO adjustments. The essential information in Table 2.2-1 is that all of the analysis techniques produce similar latitudinal and seasonal patterns.

Trends derived from the AS2 model are shown on a station-by-station basis in Figures 2.2-4(a)-(c). Throughout the remainder of this section, trends will be expressed in percent per decade. This allows for easy comparison of trends derived from data records of differing lengths. For the year-round case, all the North American (N) trends are negative, all the European (E) trends are negative except Reykjavik at 64°N, and the four Japanese (J) trends are balanced on either side of zero change. The most northerly Japanese station, Sapporo, lies at 43°N. For the wintertime period, a strong latitudinal pattern emerges with the most negative trends appearing at the most northern latitudes. Only the Japanese stations show little or no wintertime change. In the summertime, the trends, although tending toward the negative side, show no latitudinal gradient.
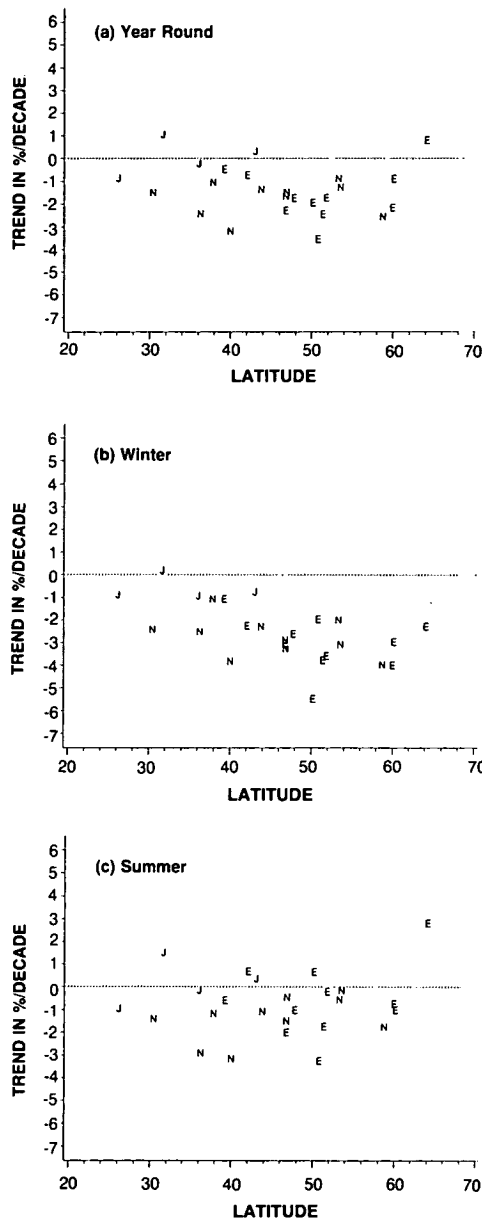
Figure 2.2-4. Individual trend estimates for the period 1970-1986 using the AS2 model of Allied-Signal, Inc. Trends appear versus latitude and are expressed in % per decade for (a) year-round, (b) winter (December-March), and (c) summer (May-August) periods. The plotting symbol is E = Europe, N = North America, and J = Japan.

Fisletov (1989) performed an independent trend analysis of the provisionally revised data from 30 Dobson stations and, in addition, examined the effect of including measurements from the 22 most reliable M-83 instruments in the USSR network. Trends based only on the Dobson record through 1986 lie in the range defined in Table 2.2-1 and show the same latitudinal and seasonal pattern.

2.2.2.2 Sensitivity Analysis

To quantify the dependence of the derived trends on factors such as data length, nuclear weapons adjustment, type of solar adjustment, inclusion of data from Soviet instruments, and nonseasonal versus seasonal trend models, a sensitivity analysis was done. The effects on the trends are summarized in Table 2.2-3 using the Allied-Signal models as baselines. The sensitivities are expressed as the change in trend, in % per decade, due to the factors considered. The results are similar to those obtained by the Ozone Trends Panel.

The exclusion of post-1982 data has a large effect as shown by item 1 in Table 2.2-3 and Figure 2.2-5 (a)-(c). The trends are noticeably less negative or more positive when only data through October 1982 are used. This date corresponds approximately to the arrival of the El Chichon aerosol at middle latitude. Interestingly, the effect on the trends from eliminating post-October 1982 data is larger in summer than in the winter. This is particularly evident when the data are analyzed using a regional/latitudinal model where the effect of dropping post-October 1982 data is to produce a summertime trend 0.8% per decade less negative and a wintertime trend 0.3% per decade less negative. The effects in summer and winter are both about 1% per decade using the zonal analysis. After 1982, summertime ozone in all three regions (North America, Europe, and Japan) went down and stayed down until 1987, whereas wintertime ozone showed some degree of recovery in all three regions (see Figure 2.2-2). Comparison of Figure 2.2-5(a)-(c) with Figure 2.2-4 (a)-(c) shows how the trend patterns change when the post-October 1982 data are dropped. This behavior may be a chemical response to volcanic aerosol from the El Chichon eruption or to a true change in the nature of the long-term trend in ozone. Since derived trends are highly influenced by extreme values or sustained dips at or near the end of the record, the addition of extra data from 1987 and 1988 is important to see if this nonlinear pattern is continuing (see Sections 2.2.2.3 and 2.2.3.2.).

Table 2.2-3. Summary of sensitivity analysis (% per decade effect on trends)

Sensitivity Scenario	Zonal Analysis[a]			Regional/Latitudinal Analysis[b]		
	Year-Round	Winter	Summer	Year-Round	Winter	Summer
1. Exclude Post 10/82 Data	+0.8	+0.9	+1.0	+0.3	+0.3	+0.8
2. Uniform Model	+0.6	—	—	+0.4	—	—
3. Exclude Pre-1965 Data	−0.6	−0.6	−0.5	−0.3	−0.1	−0.4
4. Exclude Nuclear Term	+0.2	+0.2	+0.1	+0.1	0.0	0.0
5. Add Russian Stations	−0.1	+0.4	−0.6	NA	NA	NA
6. Smooth Solar Term	0.0	0.0	0.0	0.0	0.0	0.0
7. Remove Solar Term	−0.1	−0.1	−0.1	−0.1	−0.2	−0.1
8. Remove QBO	+0.1	0.0	+0.1	0.0	−0.1	+0.1
9. Start Trend in 1/65 vs. 1/70	+0.4	+0.7	+0.3	+0.2	+0.5	+0.2
10. Start Trend in 1/75 vs. 1/70	−0.5	−0.9	−0.4	−0.4	−0.6	−0.4
11. Add 1987 and 1988 Data	NA	NA	NA	+0.2	+0.1	+0.3

[a]Sensitivity effect averaged across three zones 30–39°N, 40–52°N, 53–64°N using AS1 model.
[b]Sensitivity effect predicted at 45°N using AS2 model.
Note: Rounding is to nearest 0.1% decade.
The table entry indicates the amount (in % decade) to *add* to the trend from the standard scenario to obtain the trend for the sensitivity scenario.
Example: if data after 10/82 are omitted from the AS1 standard calculation, the zonal year-round trend increases in a positive direction by +0.8% decade; i.e., from −1.0 (standard) to −0.2 (sensitivity calculation).
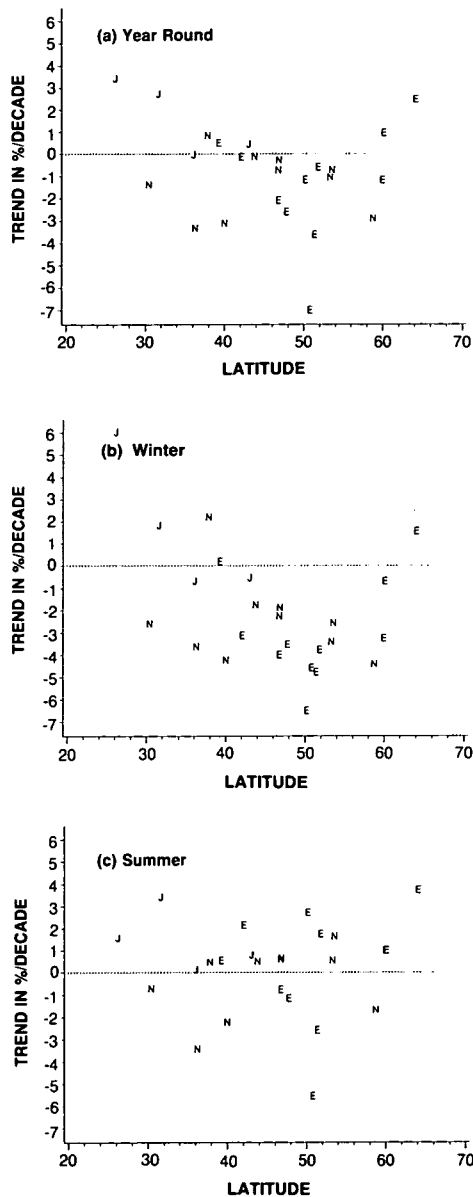Winter = December–March; Summer = May–August.

Figure 2.2-5. Individual trend estimates for the period 1970-1986 using the AS2 model of Allied-Signal, Inc. Same as Figure 2.2-4 except trends are fitted only through October 1982. Trends appear versus latitude and are expressed in % per decade for (a) year-round, (b) winter (December-March), and (c) summer (May-August) periods. The plotting symbol is E = Europe, N = North America, and J = Japan.

If the statistical model assumes that trends are the same for all months (i.e., a uniform trend), then the trends are closer to zero by about 0.5% per decade. Analyses suggest that the uniform trend model is not appropriate for use on data poleward of 40°N, since there are statistically significant winter versus summer differences in the trends.

As mentioned earlier, exclusion of pre-1965 data because of possible nuclear effects and the paucity of data leads to more negative trends. In a regional latitudinal analysis, the effect on the winter trends is small. However, in a zonal analysis like that done by the Ozone Trends Panel, the wintertime change is made more negative by about 0.6% per decade when the pre-1965 data are excluded. So, depending on the formulation of the model and the way data are handled, the wintertime trend can be quite sensitive to the re-1965 data.

An analysis by Allied-Signal researchers shows that inclusion of data from Soviet instruments in the zones poleward of 40°N makes the winter trend less negative or more positive by about 0.4% per decade when averaged across the latitude belt 30–64°N, but enhances the summer reduction, with little effect on the year-round trend.

Exclusion of the nuclear adjustment makes the trends less negative by about 0.2% per decade. The treatment of the solar cycle and the QBO in winds has little or no effect on the trends.

The sensitivity of the derived trend to the start date has interest because of issues related to (1) the trends being larger after October 1982 than in the earlier period, and (2) the trend start point being at or near extremes of the solar cycle. As pointed out above, the trend estimates are relatively insensitive to the solar cycle. However, as seen in Table 2.2-3, the trend estimates are sensitive to the start date. For example, in the zonal analysis, the derived winter trend is less negative by 0.7% per decade when the trend is started 5 years earlier (i.e., January 1965) and more negative by 0.9% per decade when the trend is started 5 years later (i.e., January 1975). This could be due in large part to influence of the post-October 1982 data. That is, the influence of the post-October 1982 data becomes larger when the trend period is taken to be shorter relative to the baseline period.

In the sensitivity analysis shown in Table 2.2-3, it should be noted that, in most cases, the regional/latitudinal analysis is less sensitive to the factors considered than is the zonal series analysis. Hence, the former approach is more robust and is currently the analysis of choice for the Allied-Signal and Wisconsin-Chicago research groups. Another reason for its preference is that variability within and across regions can be taken into account along with the latitudinal relationship.

In a separate regional sensitivity analysis (Table 2.2-4) using the Wisconsin-Chicago model, a comparison of trends was made using both the "provisionally revised" Dobson data set and the Dobson data as originally published. This showed that over Europe the "provisionally revised" data gave trends that were about 1% per decade more negative in all seasons than did the original data. Much smaller differences between trends in the two data sets resulted over North America and Japan. The differences in trends caused by the data revisions and especially by the seasonal versus uniform trend model explain why earlier published studies (Hill et al., 1986; Reinsel and Tiao, 1987a) show no significant trends, since the previous

Table 2.2-4. Regional sensitivity analysis comparing trends from the "Provisionally Revised" Dobson data set with the original published data

	Trend Difference = (Revised − Original) in % per Decade		
	Japan (26°N–43°N)	North America (30°–59°N)	Europe (39°N–60°N)
Year-Round	0.2	0.0	−1.0
Winter	0.2	0.4	−1.2
Summer	0.2	−0.2	−0.8

studies used a uniform trend model on the original Dobson data. Additional discussion of this issue appears in Chapter 4 of the Ozone Trends Panel Report.

In summary, the choice of model (seasonal versus uniform, and zonal versus regional/latitudinal), timing of the trend starting date, and the record length have the largest effects on the derived trends. However, the general pattern of significant wintertime changes at the middle and higher latitudes remains intact under different scenarios.

2.2.2.3 Update of Trends into 1988

As of this writing, data were available into 1987–1988 from all but one of the Dobson stations in Table 2.2-2 (Leningrad). In most cases, data were available through August 1988 or later (see last column of Table 2.2-2). When these data were included in the trend analysis, most of the year-round, winter, and summer trends became slightly less negative. The effects of the additional data are shown in Table 2.2-3 based on the AS2 model, and the individual station trends appear in Figure 2.2-6 (a)-(c) for year-round, winter, and summer, respectively. At 45°N, the winter trends are less negative by 0.1% per decade. At 55°N (not listed in Table 2.2-3), the winter trend is less negative by 0.2%. The biggest change was seen in the summer, where the trend at 35°N is calculated to be 0.5% per decade less negative.

Trends in total ozone tend to be less negative in all seasons when the 1987 and 1988 data are added. Table 2.2-5 summarizes the trend estimates updated into 1988 by latitude alongside the estimates through December 1986, using the AS2 model. Figures 2.2-7(a) through (c) show the differences between trends estimated into 1988 versus those through December 1986 at each station. Notice that at most sites the trend differences are positive with the addition of the new data. Overall, the year-round trend estimates predicted at 35°N and 45°N are no longer statistically significant. The winter trend estimates updated into 1988 at the latitudes 45°N and 55°N are significant but closer to zero than those through December 1986, while the trend at 35°N is slightly more negative. Table 2.2-5 shows that the addition of data into 1988 does not alter the general conclusions of the Ozone Trends Panel, although differences in detail exist.

Table 2.2-6 summarizes the regional effects of including the 1987 and 1988 data by tabulating the AS2 model trends using data through 1986, together with the results using all data available into 1988. In both situations, the Japanese region shows no significant trend year-round, winter or summer. In both cases the year-round and winter trends are significant over North America and Europe, and the summer change is significant over North America. In most cases the changes are slightly smaller when the data set is updated into 1988 as compared to changes derived through 1986.

Although including or excluding the solar cycle term in the statistical model has little effect on the estimated linear trend in ozone (see Table 2.2-3), there appears to be a measurable solar effect on ozone itself. This effect has no apparent relationship to latitude as demonstrated in Figure 2.2-8. The average solar coefficient over the 25 Northern Hemisphere stations is 0.03 Dobson units per unit of 10.7 cm flux (standard error 0.005). This corresponds to a change in ozone of approximately 1.2% from a typical solar maximum to solar minimum, a range taken of 140 units as measured by the 10.7 cm flux.

2.2.2.4 Summary of Dobson Analyses and Comparison with Theory

Recent studies have both verified the findings of the Ozone Trends Panel regarding changes in Northern Hemisphere total ozone over the period 1970 through 1986 and extended the analyses using data through
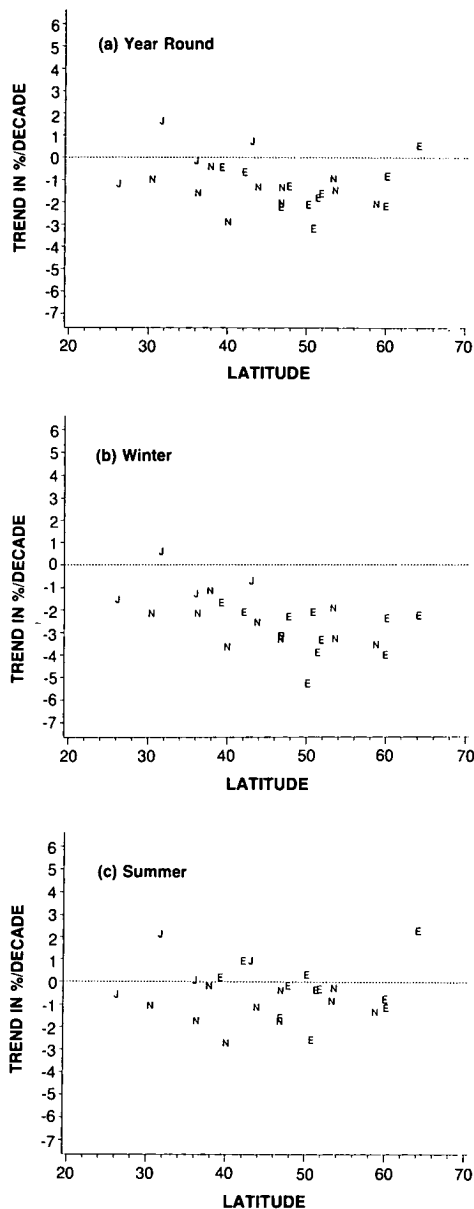
Figure 2.2-6. Individual trend estimates for the period 1970-1988 using the AS2 model of Allied-Signal, Inc. Same as Figure 2.2-4 except trends are fitted using updated data into 1988. Trends appear versus latitude and are expressed in % per decade for (a) year-round, (b) winter (December-March), and (c) summer (May-August) periods. The plotting symbol is E = Europe, N = North America, and J = Japan.

late 1988. Over the latitude band 26–64°N, the new analyses (see Table 2.2-6) found a wintertime trend averaging about −2.2% per decade for the period 1970–1986, with summertime and year-round trends averaging about −0.7% and −1.1% per decade, respectively. These results are slightly less negative than those of the Ozone Trends Panel. The winter reductions become larger with increasing latitude, varying from −1.7% per decade near 35°N to −3.0% per decade near 55°N.

208

Table 2.2-5. Trends in total ozone derived from Dobson data updated into 1988 compared with trends derived through 1986 (trends are in % per decade with one standard error in parentheses). Winter = December–March; Summer = May–August

	Year Round		
Latitude	1986	1988	Diff.
55°N	−1.08(.56)	−.99(.58)	.1
45°N	−1.10(.49)	−.94(.50)	.2
35°N	−1.11(.53)	−.88(.54)	.2
	Winter		
Latitude	1986	1988	Diff.
55°N	−3.02(.59)	−2.70(.58)	.3
45°N	−2.34(.41)	−2.26(.47)	.1
35°N	−1.66(.48)	−1.81(.53)	.2
	Summer		
Latitude	1986	1988	Diff.
55°N	−.35(.60)	−.21(.59)	.1
45°N	−.68(.45)	−.34(.48)	.3
35°N	−1.01(.51)	−.47(.54)	.5

A variety of sensitivity studies were performed to determine which features of the ozone data and the analysis techniques most affected the derived trends. The choice of model (seasonal versus uniform and zonal versus regional/latitudinal), timing of the trend starting date, and the record length have the largest influences on the derived trends. However, regardless of the model or the particular treatment of the data, significant negative trends appear in winter at middle to high latitudes.

At the time of this writing, total ozone data are available through late 1988 at many stations. Year-round and winter trends computed using the most recent data (middle to late 1988) are slightly less negative than the trends derived through 1986, while summer trends were noticeably less negative at latitude 35°N. Winter trends based on the updated data continue to show an increase with latitude, from about −1.0% per decade near 35°N to −2.7% per decade near 55°N.

The executive summary of the OTP report presented predicted change in total column ozone based on two-dimensional models for summer (May-August) and winter (December-March). Results appeared as the difference between computed column ozone averaged over the 11-year period 1976–86 and that for 1965–75. For summer the computed difference imply a trend of −0.4 to −0.6% per decade over the latitude range 35°N to 55°N. These values lie within one standard error of the derived summer trends in Table 2.2-5. Predicted trends during winter are more negative than those in summer, being approximately −0.5, −0.8, and −1.1% per decade at 35°N, 45°N, and 55°N, respectively. The corresponding observed trends in Table 2.2-5 are −1.8 ± 1.0, −2.3 ±1.0, and −2.7 ±1.2% per decade, where the error bars are 2 σ, 95% confidence limits. Theory and observation both yield trends which become more negative as one moves poleward. However, in all cases the models produce trends that are less negative than the observations and lie outside of the 2 σ error bars.
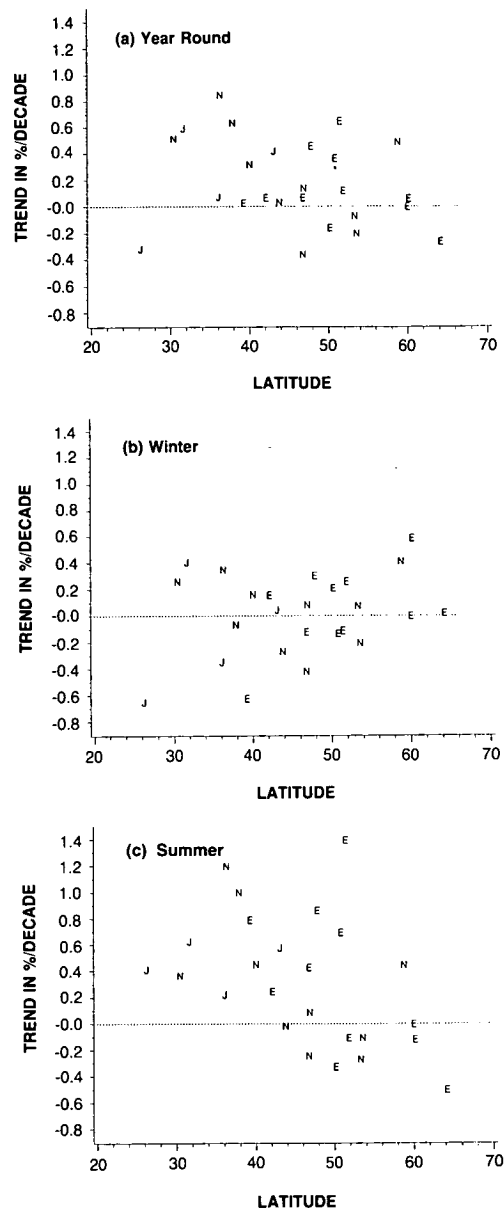
Figure 2.2-7. Differences between estimated trends into 1988 versus trends through 1986. The difference is calculated as the trend including data into 1988 minus the trend through 1986, expressed in % per decade at each Dobson station between 26°N and 64°N (a) year-round, (b) winter (December-March), and (c) summer (May-August).

2.2.3 Analysis of Satellite-Based Data from SBUV and TOMS Beginning in November 1978

2.2.3.1 Data Base and Analysis Procedure

The SBUV and TOMS sensors on the Nimbus-7 satellite began operation in November 1978. Given the short length of these data bases and other problems discussed below, it is not feasible to derive true

Table 2.2-6. Trends in total ozone derived by region based on data through 1986 and data updated through October 1988 (trends are in % per decade with one standard error in parentheses). Winter = December–March, Summer = May–August

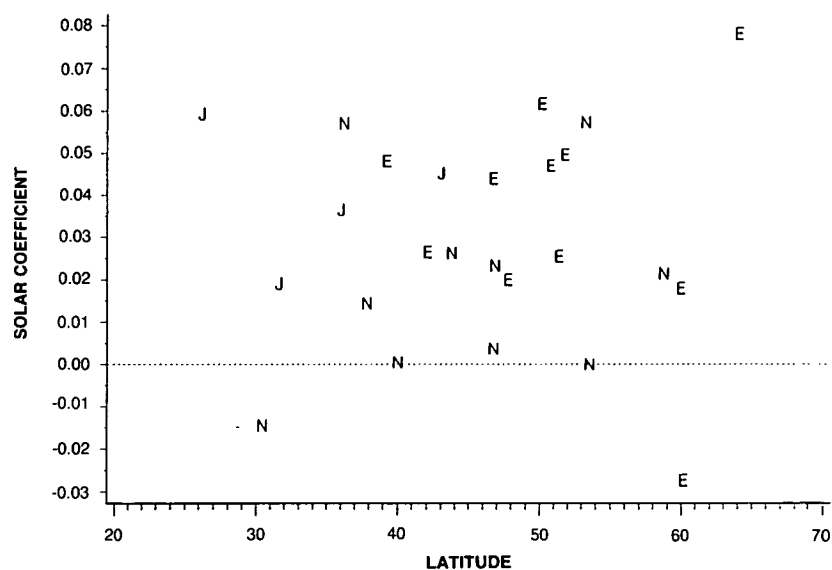| Region	Number of Stations	Year Round 1986	1988	Winter 1986	1988	Summer 1986	1988
N. America	10	−1.7(.3)	−1.6(.3)	−2.8(.4)	−2.9(.3)	−1.4(.4)	−1.2(.4)
Europe	11	−1.5(.3)	−1.4(.3)	−3.0(.4)	−2.9(.4)	−0.6(.4)	−0.3(.3)
Japan	4	+0.2(.5)	+0.5(.5)	−0.5(.6)	−0.6(.5)	+0.3(.7)	+0.8(.6)
26–64°N	25	−1.1(.5)	−0.9(.5)	−2.2(.6)	−2.2(.6)	−0.7(.4)	−0.3(.5)

Figure 2.2-8. Solar coefficient (Dobson units per unit of 10.7 cm flux) computed for 25 Northern Hemisphere stations from the AS2 model of Allied-Signal, Inc. The plotting symbol is E = Europe, N = North America, and J = Japan. The average solar coefficient is 0.030, with a standard error of 0.005.

long-term trends from the satellite record. However, satellite data cover the entire sunlit portion of the globe and, subject to the constraint of a short duration, provide valuable information on the geographic patterns of ozone change. Here the satellite data complement the Dobson record, which indicates regional variability in ozone trends but has insufficient geographic coverage to allow detailed analysis of this structure. Figure 2.2-9 (a)-(b) illustrates the geographic variation in ozone changes based on TOMS results normalized to the Dobson network to remove instrument drifts. The plots give the percent differences between annual mean ozone over the period 1987–88 and over 1979–80. Decreases appear in almost all regions. On the Northern Hemisphere (Figure 2.2-9a) the largest ozone decreases, −4.5 to −7.5%, appear at mid-latitudes, especially over the Pacific Ocean. The most prominent feature in the Southern Hemisphere is the ozone decrease which becomes more pronounced as one moves toward the polar region.

The remainder of this section examines the spectral variability of changes in ozone over an 8-year period beginning in 1978 based on SBUV, TOMS, and the Dobson network. The results should be used

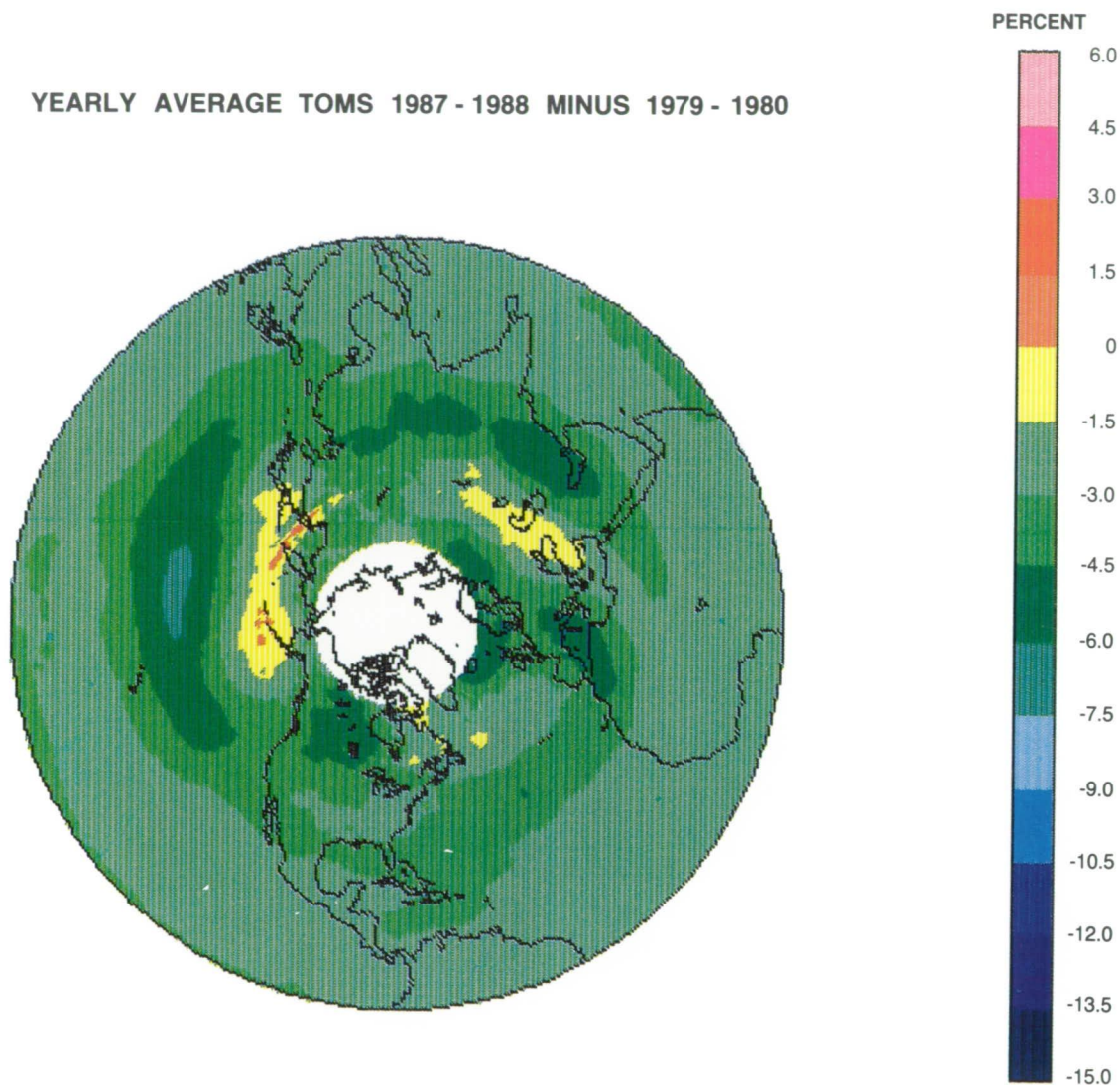YEARLY AVERAGE TOMS 1987 - 1988 MINUS 1979 - 1980

Figure 2.2-9a. Geographic structure in total ozone changes based on TOMS. Results are percent difference in annual mean ozone for 1987-1988 and 1979-1980 for Northern Hemisphere.

only as a measure of geographic structure in ozone changes, not as trends in the same sense derived from the entire long-term Dobson record.

Instrument degradation is a major issue in the analysis of satellite data sets over multi-year periods. Fleig et al. (1986), McPeters and Komhyr (1989b), and Bojkov et al. (1988) have performed a similar analysis for TOMS. Although drifts in the satellite data sets have been removed by comparison to the Dobson network, the correction involves a degree of uncertainty. For this analysis, the SBUV data were normalized to the Dobson record by fitting a single linear trend to all coincident measurements over the 8-year observing period. The TOMS data were normalized to Dobson by comparing coincident measurements during single
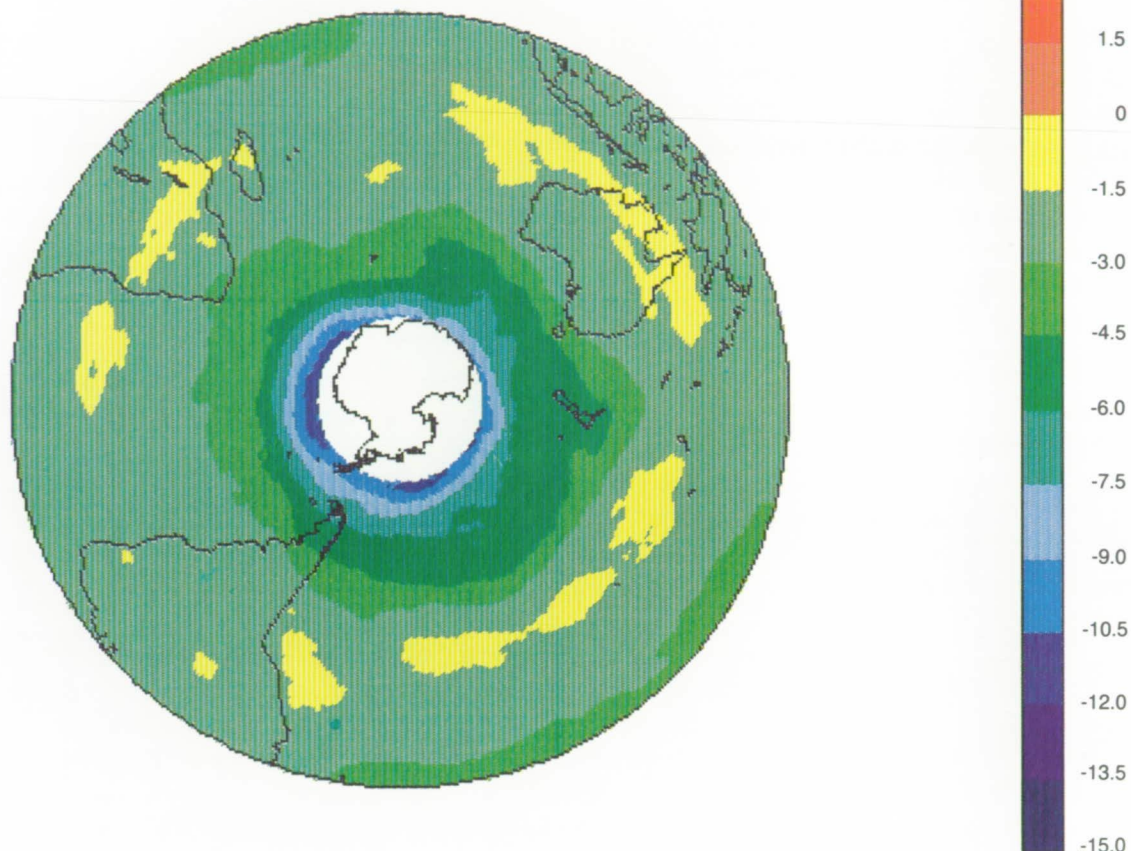
YEARLY AVERAGE TOMS 1987 - 1988 MINUS 1979 - 1980

PERCENT

6.0
4.5
3.0
1.5
0
-1.5
-3.0
-4.5
-6.0
-7.5
-9.0
-10.5
-12.0
-13.5
-15.0

Figure 2.2-9b. Same as Figure 2.2-9a for Southern Hemisphere.

months and deriving a linear trend for each month of the year (R.S. Stolarski, private communication, 1989).

The information of interest is the geographic pattern of changes in total ozone over 8 or 10 years, corrected for solar cycle dependence. A problem arises here in that the data records are less than one solar cycle in length. In particular, the 10.7 cm flux ($F_{10.7}$) decreases markedly during the period 1978 through 1986. As a result, initial test calculations showed unacceptably high correlations between total ozone and $F_{10.7}$. To circumvent this situation, the long-term Dobson record was used to determine the historical relationship between $F_{10.7}$ and total ozone (see Figure 2.2-8). This correlation provided a basis for removing the solar cycle effect from the SBUV and TOMS data sets. The changes in ozone over 8 years, corrected in this way, were compared to those in which the $F_{10.7}$ correlation was removed from the satellite time

213

series directly. The geographic pattern of ozone change was the same in both cases. This arises from the absence of a clear latitudinal dependence in the solar cycle effect, as shown in Figure 2.2-8. The absolute values of the changes in total ozone, however, depend on the treatment of the solar cycle correlation. This result again demonstrates that the available satellite data are most useful for examining geographic patterns of ozone change. As the data base grows to span more than one solar cycle, studies of true long-term trends will become feasible.

For analysis of the SBUV and TOMS data, the statistical model described in Appendix 2.A was revised so that total ozone, adjusted for the solar cycle, was the dependent variable. In addition, the analysis omitted autoregressive structure in the noise and the term related to the QBO. To account for different variances in a given month of different years, the model was fitted by a weighted estimation procedure with weights for each month inversely proportional to the monthly variances. Finally, the monthly trends were combined into seasonal values by taking the simple averages of December through March as winter and May through August as summer.

2.2.3.2 Geographic Patterns of Ozone Change and Comparison with the Dobson Network

As part of the NOAA/National Weather Service (NWS) continuing Stratospheric Monitoring Program, the Climate Analysis Center has produced monthly global analyses of the SBUV total ozone data (Nagatani et al., 1988). These use the NWS standard rectangular grid array on a polar stereographic projection where the grid size is approximately 3 degrees latitude by 3 degrees longitude at middle latitudes. For each hemisphere the grid is composed of 4,225 points total.

Analyses of total ozone from SBUV were done utilizing the statistical model outlined above for each grid point in each hemisphere. The monthly ozone changes, corrected for solar cycle dependence, were then combined into four winter/summer categories. Results for the Northern Hemisphere appear in Figure 2.2-10 (a)-(b). All contours have the units of percent change per decade, although the data base encompasses only an 8-year period. Note that the analysis ceases at 60°N. This is because the SBUV sensor can acquire data only in daylight. Since the solar terminator moves in latitude with the seasons, 60°N is generally the highest latitude at which data are available during all months.

Figure 2.2-10 (a) and (b) show that changes in ozone deduced in winter tend to be more pronounced and have more regional variability than those in summer, although substantial variations in space exist in both seasons. During winter in the Northern Hemisphere, the changes vary from about −4% per decade over northwest U.S.S.R. to +4% per decade over northeastern North America, with positive changes over the northwest Pacific Ocean and eastern Asia. Note also, the substantial negative changes in the mid-latitude ocean areas where no ground-based observations exist. Summertime values also show a variance around the hemisphere, but with a reduced range. A problem that arises with a short data set is that the derived patterns can be influenced significantly by movement of wave structure in ozone. Derived changes may represent a geographic redistribution of ozone, rather than a net increase or decrease.

Results for the Southern Hemisphere appear in Figure 2.2-11 (a)-(b). While spatial variability around latitude circles is reduced compared to the Northern Hemisphere, many of the statements for the north apply to the Southern Hemisphere as well. One item of particular note is that the largest changes in ozone are over the ocean areas. This demonstrates the value of the extensive coverage obtained by a satellite-borne instrument.
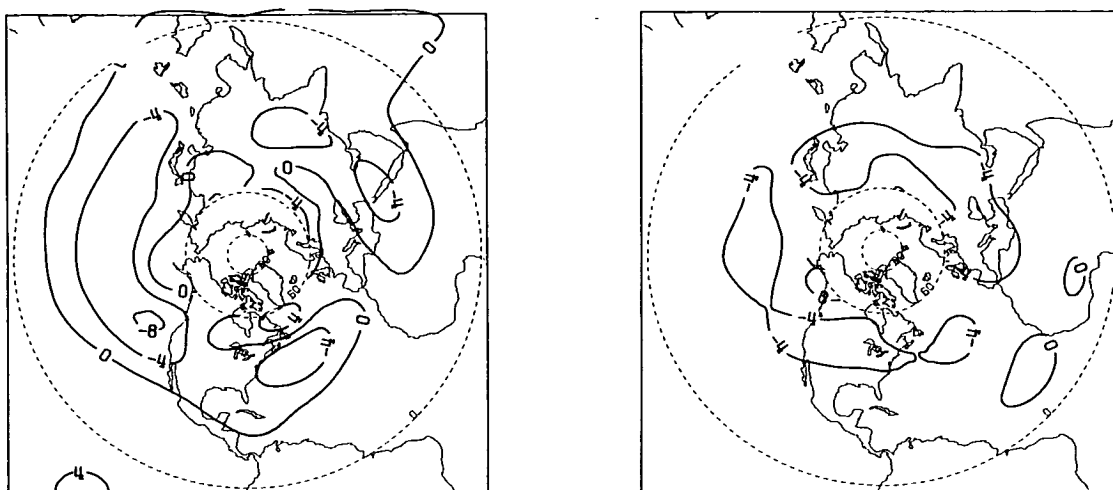
Figure 2.2-10. Geographic pattern of change in total ozone derived from SBUV for the Northern Hemisphere, November 1978-October 1986 for (a) winter (December-March) and (b) summer (May-August). Results are expressed in percent per decade, although the data set covers only an eight-year period. The SBUV ozone values have been adjusted by comparison to the Dobson network to remove instrument artifacts and correlation to the solar cycle.

Figure 2.2-11. Geographic pattern of change in total ozone derived from SBUV for the Southern Hemisphere, November 1978-October 1986 for (a) winter (December-March) and (b) summer (May-August). Results are expressed in percent per decade, although the data set covers only an eight-year period. The SBUV ozone values have been adjusted by comparison to the Dobson network to remove instrument artifacts and correlation to the solar cycle.
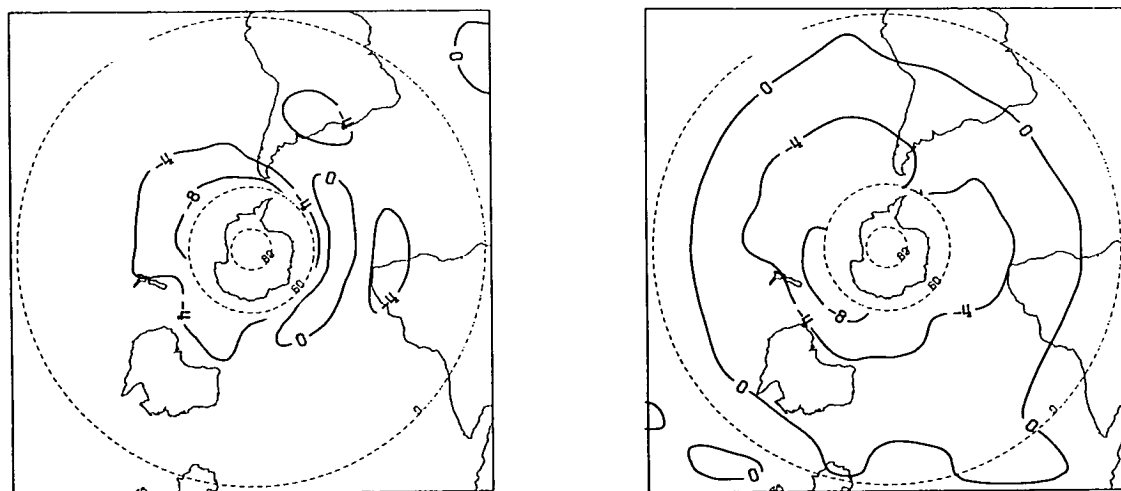
215

The geographic structure in Figures 2.2-10 and 2.2-11 implies that zonal mean changes in ozone can represent small differences between larger positive and negative quantities. The zonal mean results based on 8 years of SBUV measurements indicate decreases in summertime ozone over the Northern Hemisphere which exceed those in winter. This result, which appears contrary to the trends in Table 2.2-5, arises from the short duration of the data set. Reference to Figure 2.2-2 (c) reveals a dip in ozone beginning in 1982, which lasts into 1986 over North America and Japan. This period coincides with the final 4 years of the SBUV data set. A recovery in summertime ozone occurs in all regions after the end of the SBUV record.

An analysis similar to that presented above is possible using data from the TOMS instrument. However, for the purpose of this section it is sufficient to show that both SBUV and TOMS detect consistent changes in ozone at selected points on the globe. The TOMS data used in this analysis were provided by R.S. Stolarski and R.D. Hudson (1989, private communication) and have been adjusted by reference to the Dobson network as mentioned previously. These data were placed on a two degree latitude by five degree longitude grid. Comparisons between ozone changes deduced from SBUV and TOMS were done at 14 geographic locations, eight in the Northern Hemisphere and six in the Southern Hemisphere, as listed in Table 2.2-7. For each of the 14 grid points the regression model was applied as for SBUV.

Figure 2.2-12 presents the results derived from both SBUV and TOMS at each of the 14 locations over the 8-year period November 1978 through October 1986. The two sets of results track each other very well, with the largest difference being about 3% per decade at point number 9 (latitude 60°S, longitude 150°E). This discrepancy may arise from the better horizontal resolution and coverage of TOMS in cases where tight gradients exist. The similarity between curves in Figure 2.2-12 supports the reality of the global patterns in column ozone change derived from SBUV. The TOMS data set extends later in time than that from SBUV. An analysis of the 10-year TOMS record, through October 1988, produced a pattern which is generally consistent with that in Figure 2.2-12.

Although both the SBUV and TOMS data sets have been adjusted to conform in a general sense with the Dobson network, this procedure does not force agreement by individual region. It is therefore of interest

Table 2.2-7. Latitudes and longitudes of the 14 grid points selected for comparison of changes in ozone derived from SBUV and TOMS

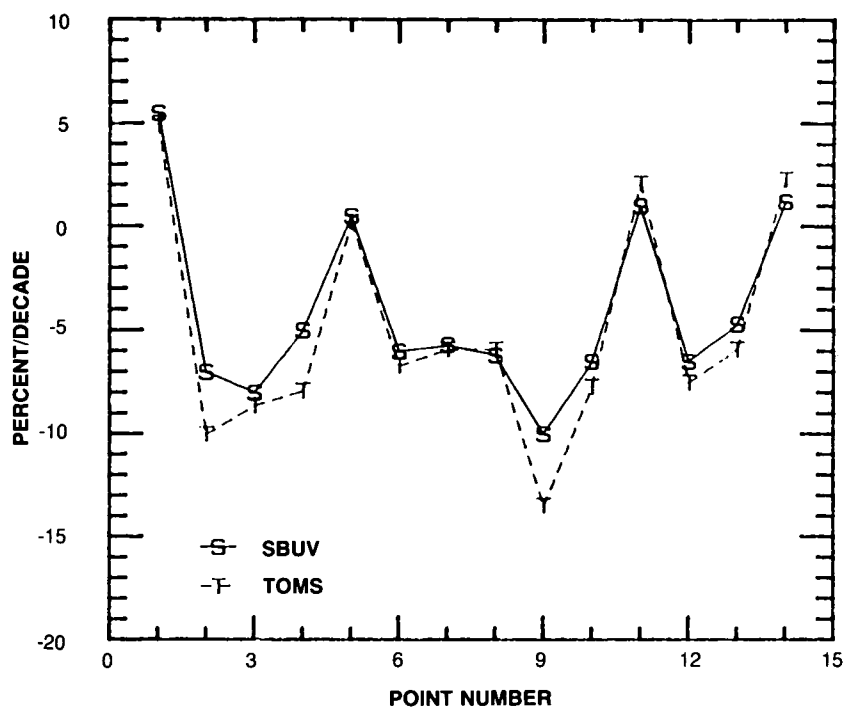| Point Number	Latitude	Longitude	Season
1	54°N	50°W	winter
2	34°N	55°W	winter
3	34°N	130°W	winter
4	34°N	80°E	winter
5	14°N	25°W	summer
6	40°N	120°E	summer
7	44°N	100°W	summer
8	40°N	20°E	summer
9	60°S	150°E	summer
10	44°S	100°W	summer
11	10°S	40°W	summer
12	44°S	120°W	winter
13	24°S	50°W	winter
14	44°S	20°W	winter

Figure 2.2-12. Changes in total ozone based on eight-year data sets from the SBUV and TOMS instruments. Values refer to the 14 sites listed in Table 2.2-7 and are expressed in percent per decade, although the data sets cover only the eight-year period November 1978 through October 1986.

to examine the compatibility of the ground-based and satellite results over the short time period encompassed by the latter data set. The investigation uses Dobson ozone measurements only over an 8-year period (November 1978-October 1986). As such, the concept of a long-term trend should not be applied. The focus here is on the consistency of geographic patterns in ozone change derived from independent measurement systems. This analysis applies a statistical regression model described in Appendix 2.A to the 25 Dobson stations listed in Table 2.2-2 which are located in Japan (J), Europe (E), and North America (N).

Figure 2.2-13 (a)-(b) presents results for winter and summer over the 8-year period, where the change in percent per decade for each station appears at the appropriate latitude. Comparison of the winter map of Figure 2.2-10 (a) with its Dobson counterpart shows several interesting features. The Japanese stations indicate a change which becomes less negative with increasing latitude. This corresponds well with the latitudinal variation derived from SBUV over this region, with an increase in ozone appearing northwest of Japan. European Dobson data generally indicate the reverse, with a strong negative change with increasing latitude. Changes derived from the Dobson instruments are somewhat larger in magnitude, but reveal a latitudinal pattern in agreement with SBUV. Finally, over North America ozone changes derived from Dobson instruments show no obvious pattern. Based on the map from SBUV, this may arise from the fact that this region is divided into a positive northeast sector and a negative western region.

For the summer season, Figure 2.2-13 (b) shows ozone changes over Japan which are virtually independent of latitude. The result from SBUV in Figure 2.2-9 (b) shows the −4% per decade contour
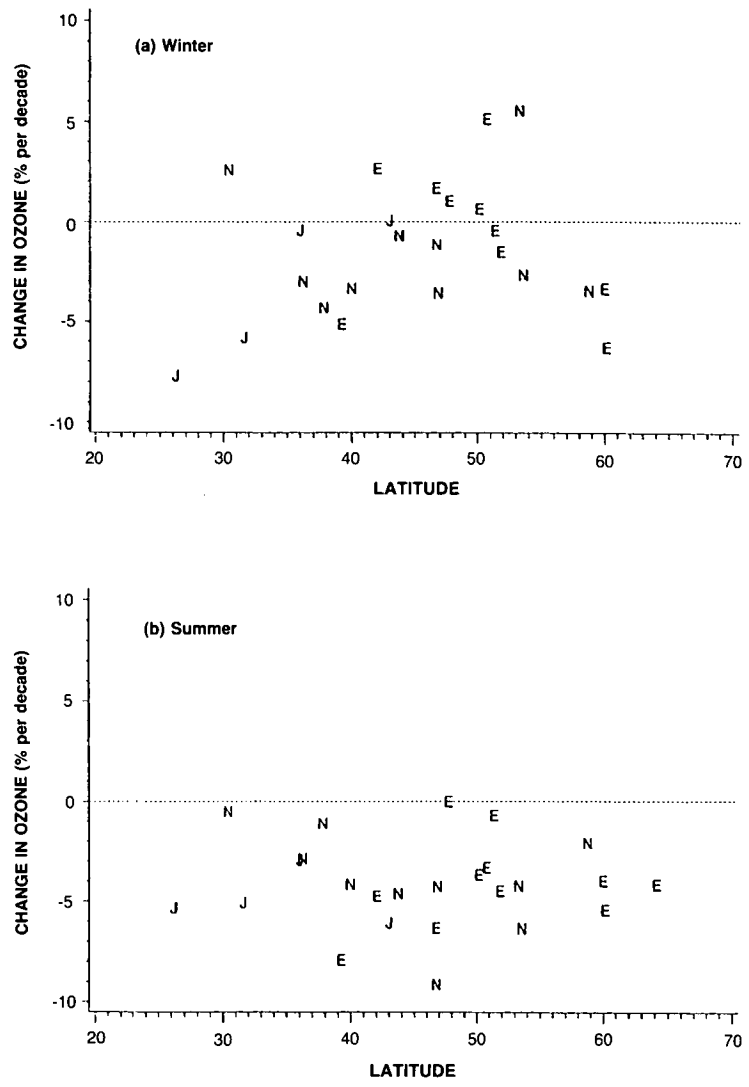
Figure 2.2-13. Changes in total ozone derived from Dobson data for the eight-year period over which SBUV measurements are available, November 1978-October 1986 for (a) winter and (b) summer. The plotting symbol is E = Europe, N = North America, and J = Japan. Results are expressed in percent per decade.

running parallel to the country. Europe also shows a much flatter gradient in summer than in winter, and this is substantiated by SBUV which gives a uniform change of about -4% per decade over this region. Over North America SBUV indicates a very weak gradient, and Figure 2.2-13 (b) reveals ozone changes which depend on the specific location with no obvious latitudinal pattern.

In view of the behavior shown in Figure 2.2-2 and in the SBUV data set, it is of interest to compute the changes in ozone after November 1978 contained in the Dobson record. Table 2.2-8 presents results from the AS2 model, expressed in percent per decade, based only on 8- and 10-year periods beginning in November 1978. Values appear for winter and summer at latitudes 55°N, 45°N, and 35°N and should be

Table 2.2.8. Changes in total ozone derived from the Dobson Network for periods coincident with the SBUV and TOMS data sets (changes in the 8 and 10 years data sets are expressed in equivalent % per decade to facilitate comparisons; one standard error appears in parentheses)

Latitude	Winter[a]		Summer[a]	
	8 Years	10 Years	8 Years	10 Years
55 N	−1.8 (1.5)	−2.2 (1.1)	−4.0 (0.8)	−2.4 (0.7)
45 N	−2.0 (1.0)	−2.7 (0.7)	−4.0 (0.8)	−1.6 (0.5)
35 N	−2.2 (1.5)	−3.3 (1.0)	−3.9 (0.8)	−0.8 (0.7)

[a]The 8 and 10 year records cover November 1978–October 1986 and November 1978–October 1988, respectively. Due to the short duration of these data sets, the derived changes should not be interpreted as long-term trends in the sense presented in previous tables. Winter = December–March, Summer = May–August.

compared with results in Table 2.2-5. As expected, standard errors derived for the shorter data set are larger than those in Table 2.2-5, but the trends still remain significant at the one sigma level. With an adopted uncertainty of one standard error, the wintertime changes derived from the short and long-term Dobson data sets agree. However, a very different picture emerges in summer. Here the ozone changes expressed in percent per decade derived over a 10-year period are very different from those based on 8 years of data. Furthermore, both sets of summer results in Table 2.2-8 imply larger changes in ozone per unit time than does Table 2.2-5. The difference between the 8 and 10-year results arises from the upturn in summetime ozone after 1986 as shown in Figure 2.2-2 (c). The results in Table 2.2-8 should not be interpreted as long-term trends, but they are nonetheless important. In particular, they show that after statistical correction for known sources of variability, atmospheric ozone still displays a temporal behavior which is more complex than a long-term linear trend. This underscores the difficulty in interpreting derived trends in terms of cause and effect.

2.2.3.3 Conclusion of Satellite Data Analyses

The analyses described above yield the following conclusions. (1) For an 8-year record beginning in November 1978 the patterns of ozone change derived from SBUV and TOMS at the 14 selected sites are generally consistent. This suggests that SBUV and TOMS are compatible for detecting geographic patterns in ozone change. In specific regions of very tight gradients, however, the high horizontal resolution of TOMS may provide a more realistic result. (2) Maps of changes in total ozone based on SBUV show significant variability around latitude circles, and a zonal average ozone change can represent the small difference between highly variable quantities. (3) Seasonal changes in total ozone observed by SBUV from November 1978 through October 1986 differ from expectations based solely on the long-term Dobson record. A separate analysis of Dobson measurements beginning in November 1978 supports this conclusion. However, the rate of change of summertime ozone derived from the short Dobson data set is very sensitive to the addition of measurements made after 1986.

2.3 TRENDS IN VERTICAL OZONE DISTRIBUTION

2.3.1 Introduction

This section summarizes present understanding of trends in the vertical ozone distribution. Emphasis is given to the altitude range in the upper stratosphere where the percentage change in ozone concentration

219

at mid-latitude due to anthropogenic chlorine perturbation is expected to be the largest. The major problem in such an analysis is the scarcity in space and time of the data available from both satellite and ground-based measurements.

As the Ozone Trends Panel (OTP) evaluation has shown that measurements performed by the SBUV instrument on the Nimbus-7 satellite cannot be used for trend analysis, the satellite section (2.3.2) is based only on the measurements of the SAGE I (February 1979–November 1981) and SAGE II (October 1984–December 1988) instruments. As far as ground-based measurements are concerned, only 10 stations in the Northern Hemisphere have a long and reliable enough record of Dobson spectrophotometer Umkehr measurements to be used for trend analysis. In addition, such data are affected by the very high aerosol load in the stratosphere from 1982 to 1984 following the major eruption of the El Chichon volcano. Finally, when considering the available stations performing regular balloon-borne ozonesonde measurements, the situation is even worse with regard to data reliability, especially at the uppermost level.

Therefore, the same merits and limitations of both orbiting remote sensors and the ground-based network, as emphasized in Section 2.2.1 for total column ozone trends analysis, are also relevant in this section. The limitations are even more stringent here, because the biases due to the limited geographic coverage and length of record may be larger due to the restricted data base which can be used. The objectives of the present analysis are thus limited. They are: (1) to update the SAGE II data set through 1988 as compared to the 1986 limitation of the Ozone Trends Panel Report, (2) to perform a detailed statistical analysis of both Umkehr and balloonsonde measurements to evaluate the usefulness of the available ground-based data for the detection of trends in the vertical ozone distribution throughout the stratosphere. As for the total column ozone study performed in the Ozone Trends Panel Report, a trend analysis has been made for each station in order to derive on a station-by-station basis the various natural (solar cycle, aerosols) and man-made variations in the ozone concentration at various altitude levels. It thus constitutes a completely new data evaluation.

2.3.2   Comparison of SAGE I and SAGE II Stratospheric Ozone Measurements

SAGE I and II use the solar occultation technique to measure aerosol extinction and trace gas concentration in the atmosphere (McCormick et al., 1979; Mauldin et al., 1985 a,b, see Section 2.1.1.2). The retrieved ozone profiles have a vertical resolution of 1 km, and their range extends from cloud top up to an altitude limited by the signal-to-noise ratio; for SAGE I the upper limit is about 55 km, and for SAGE II it is approximately 65 km. Profiles are smoothed over a 5-km layer at heights above approximately 48 km to increase signal-to-noise ratio at these altitudes. SAGE I and II instruments utilize essentially the same design with similar optical components. Differences between the two instruments include the number of spectral channels (7 for SAGE II and 4 for SAGE I), the use of narrower spectral bandwidths on SAGE II, and the use of a rectangular field-of-view on SAGE II versus a circular one on SAGE I. These differences do not introduce any significant systematic errors between SAGE I and II ozone measurements as will be discussed below.

The principal sources of error in the measurement of an individual ozone profile are radiometric imprecision, digitizer truncation, and scan mirror pointing errors. These random errors are approximately uncorrelated vertically, and their combined effect on an individual retrieved ozone profile is estimated at each point on the profile from the variance of the measurements from approximately 4–5 scans of the SAGE mirror across the viewing altitude. Each SAGE profile, however, also possesses an uncertainty in reference altitude of approximately 0.25 km which contributes to uncertainties in profile repeatability (Cunnold et al., 1989).The principal systematic errors between SAGE I and SAGE II arise from instrument

scan mirror calibration and the uncertainty in our knowledge of the absorption cross-section of ozone at 600 nm convolved with instrument bandpass and solar spectrum. Aerosols can also produce biases in the ozone retrievals, but only at those altitudes where aerosol concentrations are large (i.e., mostly below 25 km altitude). The relative systematic error between the SAGE instruments is estimated to be approximately 2% (Cunnold et al., 1989). The random error components for both instruments are less than 10% for a vertical resolution of 1 km.

2.3.2.1 Zonal Means

SAGE I and II scan the atmosphere over the Earth's limb at the terminator twice on each of 15 daily orbits. The orbital inclination causes the observation latitude to periodically vary from approximately 75°S to 75°N dependent on season. The latitudes of the SAGE I and SAGE II measurement locations for February 1979 to November 1981, and October 1984 to November 1987, respectively, are displayed for sunset measurements in Figure 2.3-1. Due to the SAGE I orbital elements, the coverage does not repeat from one year to the next as it does for the SAGE II measurement location latitudes. Any gaps in the curves of Figure 2.3-1 are periods of time during which no satellite occultations occurred. Because of power problems on the spacecraft, only sunset data were taken by SAGE I after July 1979, and additional gaps are observed in the SAGE I curves due to this problem. A complete set of sunrise measurements for SAGE II, however, is available.

For analysis purposes, the SAGE I and II data were spatially grouped into 11 latitude bands. The equatorial latitude band was 15°S to 15°N, and the midlatitude bands were 10° wide centered at 20°, 30°, 40°, 50°, and 60° north and south. As the SAGE I or SAGE II observations passed into and subsequently out of one of the latitude bands above, the ozone measurements were averaged to form a zonal mean. In addition, the temporal duration defining a zonal mean was limited to a maximum of 1 week. Thus, a given latitude band contains more than one zonal mean if SAGE I or SAGE II sampled the latitude band for a continuous period of greater than 1 week duration. These typically occur when the measurement location latitude changes from increasing with time to decreasing with time.

Time series of SAGE I and II ozone zonal means at 30 km altitude are shown in Figure 2.3-2a for selected latitude bands. For comparison purposes, they have been time shifted to a common origin. Each time series was analyzed with a three-component linear regression model containing semiannual, annual, and 27-month period terms. The 27-month period term was chosen to model a quasi-biennial oscillation (QBO) in the ozone. The model fits to the data, which are intended as a visual aid, are shown as the continuous curves. At 30 km these time series display the expected features of seasonal ozone variability, namely the strong annual variation in the midlatitudes and the semiannual oscillation in the equatorial region. From Figure 2.3-2a, it is observed in the midlatitudes that both instruments agree in amplitude and phase with no apparent consistent bias. The largest differences occur at the Equator and are due to the fact that the QBO terms in the model are not in phase between the two data sets.

The vertical distribution of the annual and semiannual component amplitudes between 25 km and 50 km were computed and are shown in Figure 2.3-2b. The continuous curves on the plots represent the amplitudes in percentage from the model mean. Squares, either filled-in or open, mark those amplitudes which are statistically significant at the $\pm 2\ \sigma$ confidence level. A comparison between the SAGE I and SAGE II annual and semiannual component amplitudes shows the similarity in the vertical distribution of amplitude. Both instruments agree on the altitudes at which the midlatitude annual amplitudes effectively vanish, i.e., at 25 km in both hemispheres and at 38 km in the Southern Hemisphere. At 25 km, a phase change occurs between the zonal mean time series below and above this altitude (Wang et al., 1989).
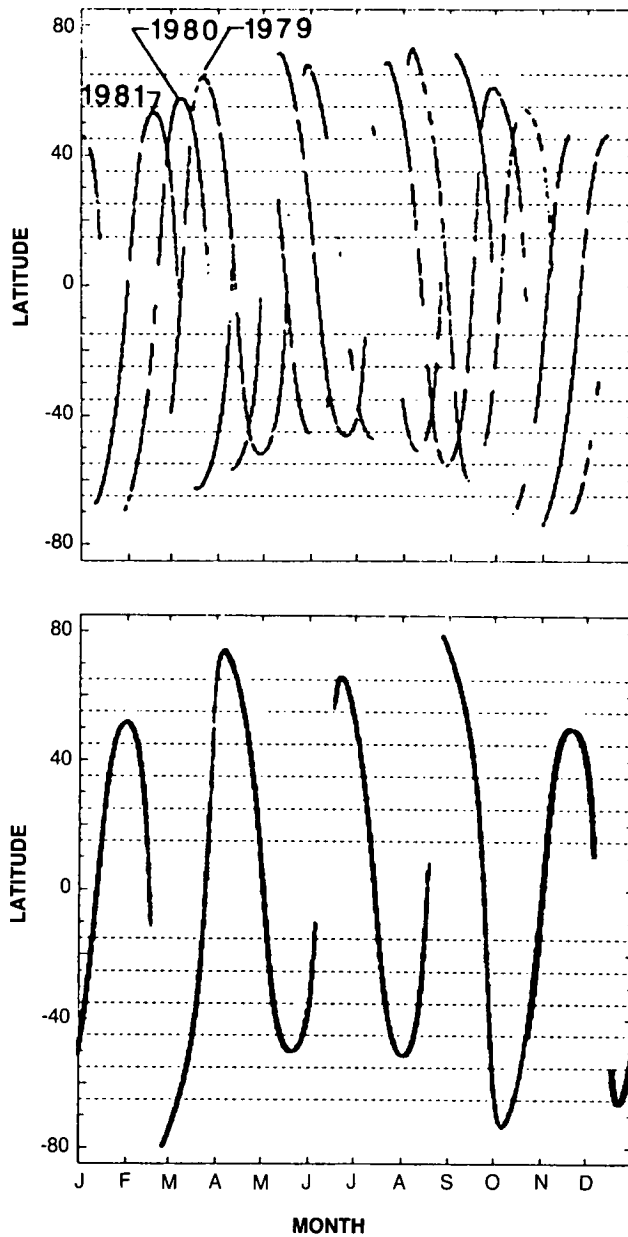
221

Figure 2.3-1. (a) Latitudes of the SAGE I sampling locations for sunset. (b) Latitudes of the SAGE II sampling locations for sunset. Because of the SAGE II orbital characteristics, the latitude coverage appears as a single curve even though 3 years are plotted.

As of this writing, SAGE II has been in operation for over 4 years. The daily averages of ozone concentration sampled within 10°-wide latitude bands symmetrically placed about the equator were modeled using the analysis previously described. The results for 35 km are shown in Figure 2.3-3. The regressions adequately represent the seasonal and semiannual variability observed in the ozone time series. In addition, near the Equator, the QBO in ozone becomes clearly defined. The high vertical resolution of the SAGE II ozone measurements significantly improves our knowledge of vertical structure of the ozone QBO. Also evident in Figure 2.3-3, the semiannual oscillation appears as a significant component in the ozone vari-
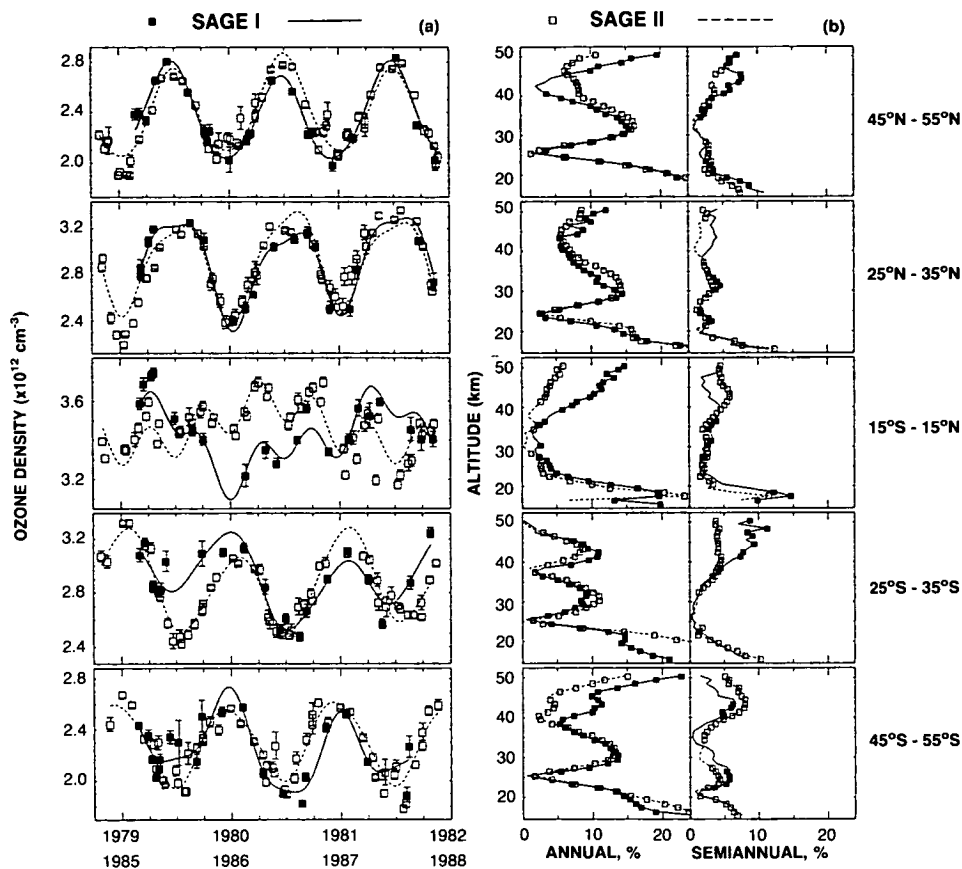
222

Figure 2.3-2. (a) Zonal mean ozone number density at 30 km for SAGE I during the period February 1979 - November 1981 and SAGE II during the period October 1984 - November 1987 for the five latitude bands of 45°S-55°S, 25°S-35°S, 15°S-15°N, 25°N-35°N, and 45°N-55°N. The vertical bars are the 95% confidence interval on the zonal mean. Smooth curves are the regression estimates. The data have been time shifted for comparison as indicated on the abscissa. (b) Amplitudes of the seasonal and semiannual components of the SAGE I and SAGE II zonal mean time series as derived from the regression coefficients. Units are in percent relative to the model mean.

ability, especially at 5°S. Marching poleward of the Equator, it is observed that the seasonal oscillation gains in amplitude with the semiannual oscillation decreasing in strength.

2.3.2.2 Change in SAGE I and SAGE II Ozone Concentrations

The change in stratospheric ozone concentration that occurred between the 33-month lifetime of SAGE I and the first 4 years of SAGE II was estimated in three ways over an altitude range from 25 to 50 km, the region of the atmosphere essentially free of aerosols that could have any effect on the SAGE II ozone retrieval.

The first method of estimating the ozone change, which minimizes the effects of seasonal and spatial sampling biases, is to select sets of profiles where SAGE I and II sampled the same month of the year within the same latitude band. Such a period of time is defined as an intersection and corresponds to a
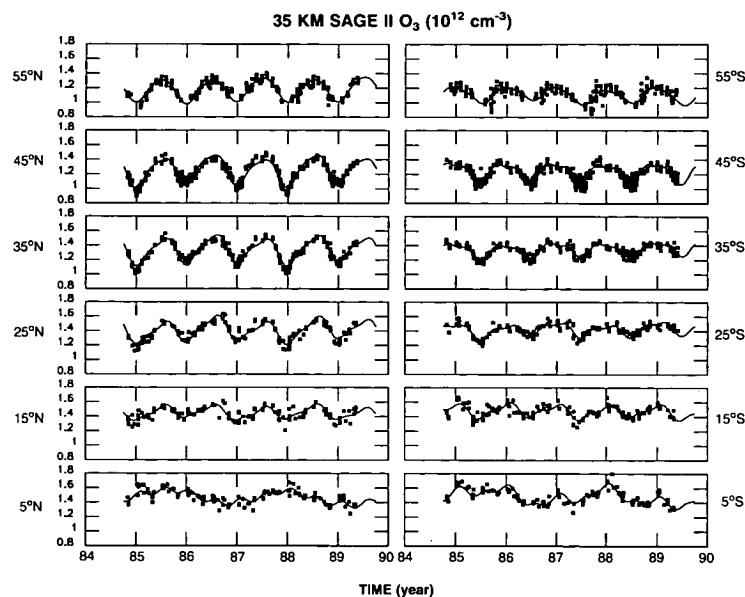
223

Figure 2.3-3. Daily mean ozone number density at 35 km for SAGE II for twelve latitude bands, each 10° wide-centered on the latitudes listed. The continuous curves represent regressions using a model containing components with periods of 30 months, 12 months, and 6 months.

period of time in the year, of approximate duration 1 month, during which both SAGE I and II sampled the same latitude band. Note that an intersection is independent of the actual year during which measurements were made. The intersection is defined strictly in terms of the month within the year. Within the 11 latitude bands considered, 105 intersections were isolated containing a total of approximately 7,300 SAGE I profiles and 25,000 SAGE II profiles. For each intersection, the SAGE I and II profiles were averaged separately.

The second method of estimating the ozone change is to simply compute the zonal mean time series averages and form the percentage difference. This method has the possible disadvantage that seasonal sampling biases may be introduced.

The third method of estimating the ozone change is to use the regression coefficients derived from the zonal mean time series and compute the mean value of the series over the time period of the data. This method's disadvantage is the empirical nature of the model.

Using all three methods described above, the percentage difference between the SAGE II mean and the SAGE I mean was computed at each altitude using the SAGE I mean as the reference. The intersection (method 1) percentage differences and their corresponding standard errors are displayed in the upper six panels of Figure 2.3-4. For all latitude bands, excluding 60°N and 60°S, methods 2 and 3 gave very similar results to those of method 1. Throughout the 11 latitude bands considered, except for 60°S, the ozone changes from SAGE I to SAGE II are within the range of − 4% to + 4%. The larger decreases observed in the Southern Hemisphere near 60°S are heavily driven by the intersection in the austral springtime and are likely due to vortex dynamics.

Identical analysis (method 1) was performed using two wider latitude bands: 20°N to 50°N and 20°S to 50°S, areas over which there is relatively dense sampling by both instruments. The mean percentage

224
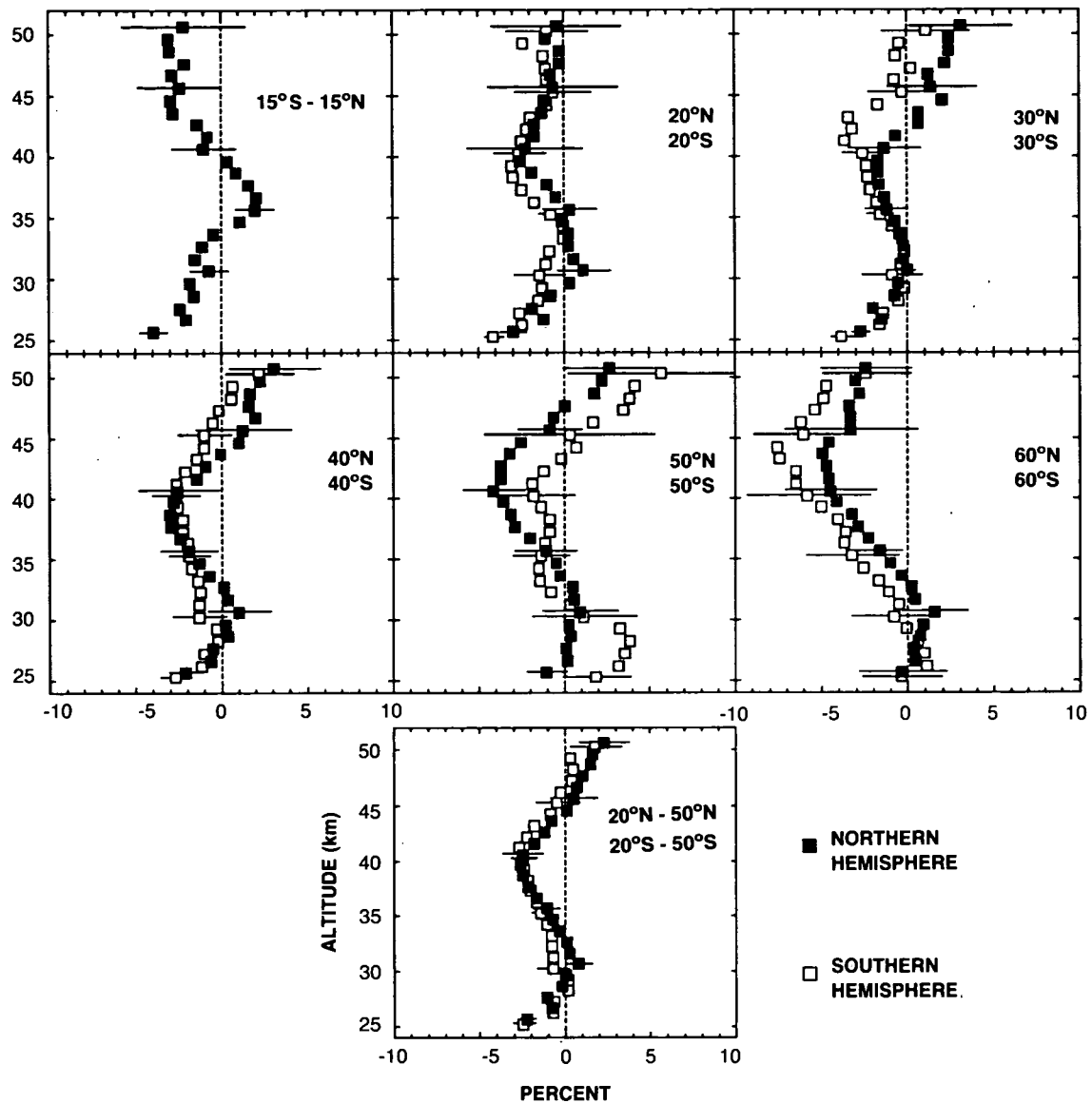
Figure 2.3-4. Mean percentage difference between SAGE II and SAGE I versus altitude computed from the intersection of SAGE I and SAGE II. All intersections occurring between 15°N to 55°N or 15°S to 55°S were combined into one sample to produce the results in the lower panel. The horizontal bars, placed at 5 km intervals, represent the standard error of the mean percentage difference. SAGE I is the reference in all percentage calculations.

differences appear in the lower panel of Figure 2.3-4. The agreement between the two hemispheres is apparent, and indicate for the 6-year period between 1980 (SAGE I) and 1986 (SAGE II):

—an ozone decrease between 35 and 44 km with the maximum ozone change of -3% $\pm 2\%$ occurring at 40 km,

—an ozone decrease of -3% $\pm 2\%$ at 25 km and an essentially zero ozone change at 28–33 km and 45–48 km.

These values represent the changes that occur over this time period and no attempt has been made to separate out natural and man-induced variability.

2.3.3   Analysis of Umkehr Data

A trend analysis of stratospheric Umkehr profiles of ozone from 10 stations in the Northern Hemisphere is considered over the period 1977–1987. It constitutes an update of the analysis by Reinsel et al. (1987). The stations are Belsk, Arosa, Lisbon, Sapporo, Tateno, Kagoshima, Boulder, Edmonton, New Delhi, and Poona. Umkehr profile ozone data in the highest 5 Umkehr layers (4–9) are considered in the trend study, which covers an altitude range of approximately 19–45 km. A detailed analysis of the interdependence of the various Umkehr layers and resulting vertical resolution has been performed in the Ozone Trends Panel Report. It shows that ozone retrievals for Umkehr layers 4 to 8 are suitable for trend studies and that the effective vertical resolution for these layers varies from 15 to 11 km. Trends derived in layer 9, where the retrieval is more sensitive to real ozone changes in layer 8—and has greater sensitivity to such changes than the layer 8 retrieval—are of limited interest.

One of the major problems in Umkehr measurements is related to the impact of stratospheric aerosols from volcanic activities. This problem has become even more acute during the period following the eruption of the El Chichon volcano. A comprehensive theoretical examination of aerosol effects on Umkehr measurements was presented by Dave et al. (1979) and DeLuisi (1979) and the problem has been addressed by Reinsel et al. (1984) and DeLuisi et al. (1989a,b). The results of these studies indicate that accounting for the effects of aerosols on the Umkehr data measurements is critical in any trend analysis of these data. The major volcanic eruption of El Chichon in April of 1982 produced significantly larger amounts of atmospheric aerosols than at any time in the previous 25 years. This, in turn, has produced a much more severe impact on Umkehr measurements from stratospheric aerosols from El Chichon than earlier periods. For illustration, deseasonalized monthly averages of Umkehr data in layers 4 through 9 at Arosa are plotted for the period 1977–1987 in Figure 2.3-5. The effects of aerosols on the Umkehr data, starting towards the end of 1982, are apparent. We note that low Umkehr values occur during 1982–1983 not only in the upper layers 7–8 but also in layers 4, 5, and 6. This is in contrast to the earlier theoretical calculations of Dave et al. (1979), which indicate that little error in Umkehr measurements should occur in the middle layers 4, 5, and 6 due to volcanic aerosols. This, in turn, suggests the possibility that real decreases in ozone occurred in these middle layers during 1982–1983 as a result of El Chichon and other natural events of that time period. Hence, large empirical adjustments of these data in layers 4, 5, and 6 for aerosol error effects during this period may not be appropriate.

Because of this severe impact on the Umkehr data, considerable caution needs to be exercised when performing a trend analysis using Umkehr data over the period 1982–1987. In particular, the techniques of the previous analysis (Reinsel and Tiao, 1987) need to be modified to account for the possibility of differences in the aerosols' effects on Umkehr data during the El Chichon period relative to earlier effects—especially any possible nonlinearity in the effects on Umkehr data as a function of optical thickness because of the much larger range of observed optical thickness values during El Chichon than in earlier periods. Because of this, in present trend analysis of both empirically corrected and theoretical model-corrected Umkehr data, two different procedures were considered to treat Umkehr data during a portion of 1982–1983. In the first one (i), all available Umkehr data were used. In the second one (ii), Umkehr data during the portions of 1982–1983 most affected by aerosols were omitted from the analysis. This resulted in the omission of, at most, 8 months of data at each station, generally for the period from November 1982 through June 1983. Procedure (ii) is motivated by the fact that errors in Umkehr data appeared to follow a somewhat different relation to optical thickness for these extreme cases. Also in an empirical adjustment approach, these
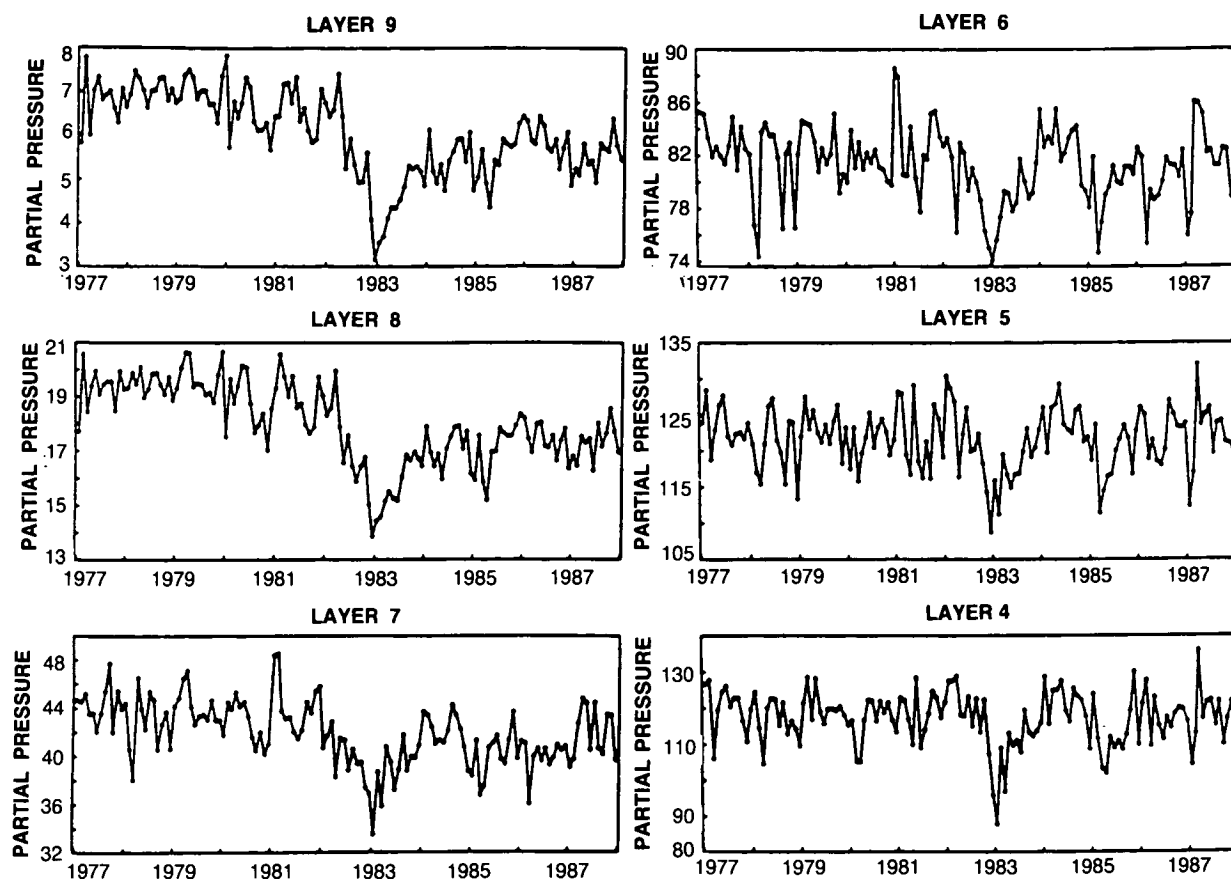
Figure 2.3-5. Deseasonalized Umkehr data at Arosa for layers 4-9, unadjusted for aerosols, for the period January 1977 through December 1987.

extreme cases might exert a substantial influence on the overall estimation results for the aerosol effects, and hence on estimation results for other parameters. In addition, it is rather clear that Umkehr data during this period would be the most sensitive and most difficult to accurately correct in the theoretical model calculations.

The trend analysis has been performed for each of the 10 stations using two statistical models which differ in the approaches of the aerosol effects. These models are described in Appendix 2.A. They include an $F_{10.7}$ solar flux term to account for solar cycle variations, although large uncertainties remain in this evaluation due to the shortness—10 years—of the period analyzed relative to the 11-year solar cycle. The empirical adjustments for the effects of aerosols on the Umkehr data have previously involved the use of monthly averages of measurements on atmospheric transmission of solar radiation available at Mauna Loa, Hawaii (Reinsel et al., 1984, 1987). More recently, lidar aerosol data from several locations in the north temperate latitudes, including Hampton, USA, Garmish, FRG, and Observatoire de Haute-Provence, France, became also available for the last several years since around 1977. It is expected that these data will be more representative of aerosols at the Umkehr station locations than the Mauna Loa data. These lidar data have been used in a detailed study by DeLuisi et al. (1989a) to obtain stratospheric aerosol optical thickness derived from the lidar data for the period 1977–1987 as shown in Figure 2.3-6. DeLuisi et al.

GLOBAL TRENDS
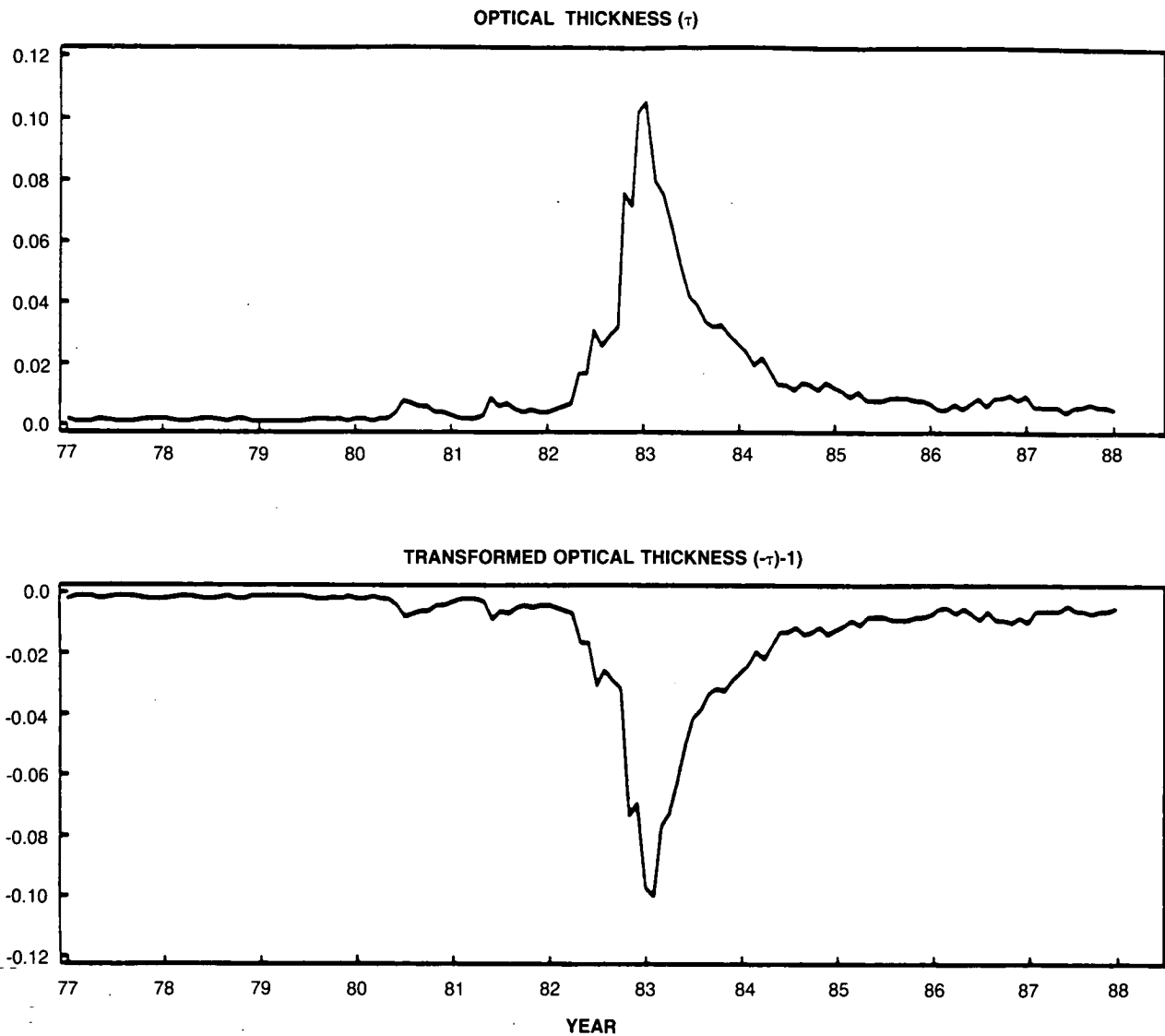
Figure 2.3-6. Stratospheric aerosol optical thickness derived from lidar data (Hampton, Va; Garmish, FRG; Observatoire de Haute-Provence, France) for the period 1977-1987.

(1989a) also used the lidar data in a radiative transfer model to calculate theoretical model estimates of the errors in Umkehr data due to volcanic aerosols, and thus provide theoretical corrections for the Umkehr data during 1978–1986. A detailed description of the correction methods are given by De Luisi et al. (1989a).

Parameter values for both time series models (1) and (2) were estimated for each of the 10 Umkehr stations and each of the five Umkehr layers, 4 through 8, using both procedures (i) and (ii) mentioned previously. (For comparison, a model of the form (2), which does not include any empirical aerosol adjustment, was also estimated for the uncorrected Umkehr data.) Therefore, two distinct sets of estimation results have been obtained for both the empirical aerosol adjustment model (1) and the model (2), where Umkehr data have been corrected for aerosol errors using theoretical model-based calculations (DeLuisi et al., 1989a). The results will be referred to as "empirical corrections" (model 1) and "theoretical

228

A. EMPIRICAL CORRECTIONS MODEL
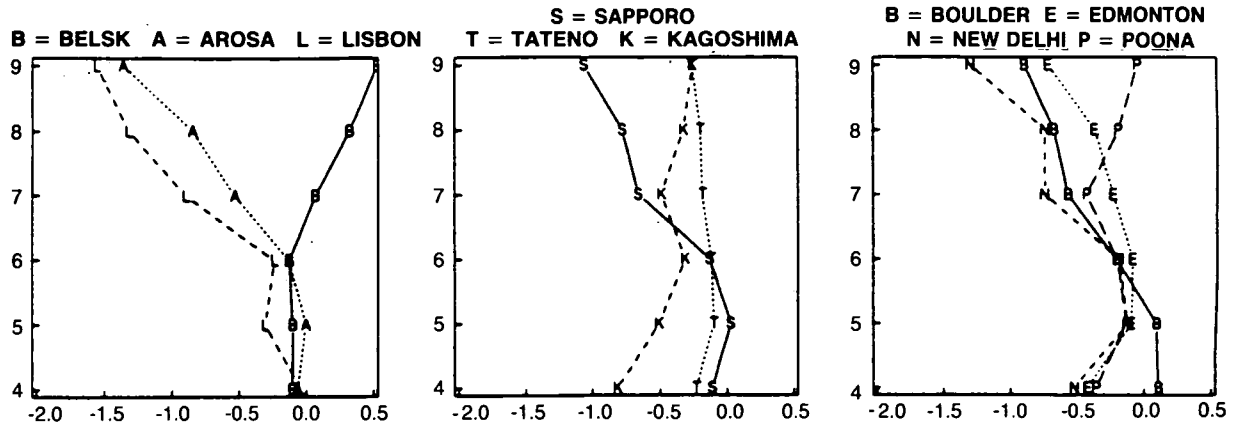
B. THEORETICAL CORRECTIONS MODEL
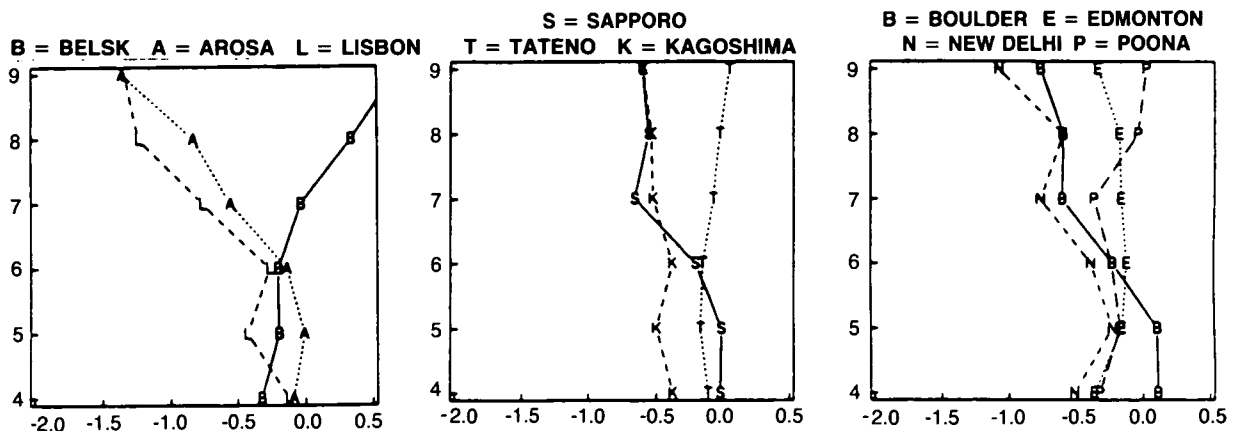
Figure 2.3-7. Umkehr data trend estimates (% per year) from 10 individual Umkehr stations for layers 4-9, for the period January 1977 through December 1987. (Portions of the data, approximately from November 1982 to June 1982 were deleted in the analysis.) (a) Trend estimates based on empirical aerosol corrections model, (b) Trend estimates based on theoretical aerosol corrections model.

corrections" (model 2), and for the two procedures as "no deletions" (method i) and "with deletions" (method ii). The individual station estimates of trend and solar cycle coefficients from both models are plotted in Figure 2.3-7 a-b for each Umkehr layer, for the method (ii), when data were deleted during a portion of 1982–1983.

Estimates of the overall trend in ozone for each layer, as well as reasonable estimates of the uncertainty in the overall estimates, have also been computed by using random-effects models for individual station estimates as in Reinsel et al. (1987). The resultant $\pm 2\ \sigma$ confidence interval estimates of trends during 1977–1987 from both the empirical and the theoretical adjustment models (1) and (2) for both procedures are given in Table 2.3-1, together with the solar flux coefficient estimates in % per 100 $F_{10.7}$ solar flux units.

The results of the above analysis indicate statistically significant decreases in ozone during 1977–1987 in Umkehr layers 7 and 8 using either method of correction for aerosol errors, and using either procedure (i) or (ii) for the treatment of data during a portion of 1982–1983. The deletion procedure yields slightly less negative trend estimates in layer 8 for the empirical adjustment technique, and has little effect in this layer

229

Table 2.3.1. Overall trend estimates (in % per year) from 10 Umkehr Stations for the period 1977–1987 with associated standard errors ($\pm 2\,\sigma$)

Layer	Empirical Correction Model (1)		Theoretical Correction Model (2)	
	No Deletions	Deletions in 1982–83	No Deletions	Deletions in 1982–83
8	$(-0.59 \pm .27)$	$(-0.51 \pm .26)$	$(-0.43 \pm .28)$	$(-0.42 \pm .27)$
7	$(-0.45 \pm .17)$	$(-0.45 \pm .16)$	$(-0.43 \pm .19)$	$(-0.43 \pm .18)$
6	$(-0.16 \pm .11)$	$(-0.17 \pm .11)$	$(-0.26 \pm .13)$	$(-0.22 \pm .11)$
5	$(-0.08 \pm .11)$	$(-0.10 \pm .11)$	$(-0.21 \pm .12)$	$(-0.14 \pm .11)$
4	$(-0.08 \pm .20)$	$(-0.18 \pm .20)$	$(-0.21 \pm .20)$	$(-0.15 \pm .20)$

Overall Solar flux estimates (in % per 100 units of $F_{10.7}$ flux) from the period 1977–1987

Layer				
8	(1.41 ± 0.81)	(1.48 ± 0.81)	(1.47 ± 0.94)	(1.61 ± 0.85)
7	(1.25 ± 0.89)	(1.28 ± 0.97)	(1.20 ± 0.93)	(1.38 ± 0.97)
6	(0.71 ± 0.63)	(0.81 ± 0.68)	(0.38 ± 0.74)	(0.72 ± 0.66)
5	(0.73 ± 0.61)	(0.90 ± 0.62)	(0.47 ± 0.68)	(0.79 ± 0.61)
4	(2.66 ± 1.15)	(2.87 ± 1.20)	(2.49 ± 1.18)	(2.82 ± 1.15)

for the theoretical model adjustment technique. The trend results for layer 7 are essentially the same for all methods. In the middle layers (4 and 5), the deletion procedure has more effect in the theoretical adjustment model, with less negative trend estimates occurring when data are deleted, but the reverse is true for the empirical model. For the most part, when the deletion procedure is used, the two correction methods yield fairly similar trend results overall. By contrast, the corresponding trend estimates obtained from a model such as (2) but with uncorrected Umkehr data are -0.87 ± 0.28, -0.71 ± 0.19, -0.31 ± 0.14, -0.23 ± 0.14, and $-0.26 \pm 0.22\%$ per year, respectively, for layers 8 through 4. Hence it is seen that failure to incorporate corrections for aerosol errors in the Umkehr data leads to highly distorted trend results, especially for layers 8 and 7.

The trend estimates obtained in this analysis for the period 1977–1987 are generally more negative in layers 7 and 8 than previous trend estimates obtained using data for the period 1970–1981 (Reinsel et al., 1987). Note also, that these estimates are substantially less negative than those obtained by DeLuisi et al. (1989a), which were based on a composite series of five Umkehr stations over the shorter period of 1979–1986 and which did not include an effect for solar flux variations. These trend results must be interpreted cautiously because of the shortness of the time period considered and because of the partial confounding between estimates of trend and solar flux effects over this relatively short period. As an illustration of the dependence of the trend results on the particular time period considered and on the effects of solar variations, a similar trend analysis for data over the period 1978–1987 was also performed. It yielded trend estimates in layers 4–6 that were generally positive and approximately 0.2% per year more positive than the trend estimates in Table 2.3-1 for those layers.

Finally one should note that the trends reported here take into account the effects of the solar cycle. They thus lead to an average decrease in ozone of about $-4.8 \pm 3.1\%$ at 40 km for the 10-year period between 1977 and 1987. When compared to the changes observed by the SAGE instruments, and within the uncertainty limits of SAGE and Umkehr trend results near 40 km, these two independent results are not inconsistent.

2.3.4 Analysis of Ozonesonde Data

A trend analysis using ozonesonde data collected at 13 stations over the period June 1965 through December 1982 has been previously reported (Tiao et al., 1986). This study has been updated for 9 of the 13 stations (Table 2.3-2) using all available data through December 1986. Individual ozonesonde readings in units of partial pressure at various pressure levels were first integrated into ozone amounts in 15 "fractional" Umkehr layers, shown in Table 2.3-3. The readings were screened to meet the following criteria: (1) the correction factor was between 0.9 and 1.2 for the Brewer-Mast (BM) sondes and between 0.9 and 1.15 for the ECC sondes, (2) the burst level was above the top of Umkehr layer 5B, (3) the corresponding daily total column ozone reading was available, and (4) readings with zero partial pressure were removed. In the earlier study, the correction factor in the screening procedure was set between 0.8 and 1.4 for the BM method and between 0.8 and 1.3 for the ECC method. The regression model used in the analysis is described in the appendix.

Employing available data through 1986, Table 2.3-4 gives the trend estimates and their associated estimated standard errors for each of the 15 layers of each of the 9 stations. The estimates are given in percent change per year. Figure 2.3-8 shows profiles of the trend estimates against the layers for each station. Broadly speaking over the majority of the stations, the noticeable features are a positive trend in the lower layers 1A-1D, a negative trend in the middle layers from 2A to 4B, and little or no trend for the layers 5A and above. An overall trend profile across the nine stations can be constructed by considering

Table 2.3.2. Ozonesonde stations, data spans, and measurement methods

Station	Latitude	Data Span	Method of Measurement
Kagoshima	32N	1/70–10/86	Japan
Tateno	36N	3/68–11/86	Japan
Sapporo	43N	3/68–4/86	Japan
Payerne	47N	9/68–12/85	Brewer-Mast
Hohenpeissenberg	48N	1/70–12/85	Brewer-Mast
Goose	53N	6/69–8/80	Brewer-Mast
		9/80–12/86	ECC
Edmonton	54N	10/70–8/79	Brewer-Mast
		9/79–11/86	ECC
Churchill	59N	10/73–8/79	Brewer-Mast
		9/79–10/86	ECC
Resolute	75N	3/66–11/79	Brewer-Mast
		12/79–10/86	ECC

Table 2.3.3. Fractional Umkehr Layers

Layer	1A	1B	1C	1D	2A	2B	3A	3B
Upper Boundary (km)	2.9	5.5	8.0	10.3	12.5	14.7	16.9	19.1

Layer	4A	4B	5A	5B	6A	6B	7	
Upper Boundary (km)	21.3	23.6	25.8	28.1	30.5	32.8	35.1	

Table 2.3-4. Trend estimates for nine stations (in % per year; data through December 1986 when available)

Layer	Kagoshima 32°N Trend	S.E.	Tateno 36°N Trend	S.E.	Sapporo 43°N Trend	S.E.
7	−0.0949	0.2570	−0.0288	0.2271	−0.2936	0.3331
6B	0.1168	0.2442	0.0820	0.2188	−0.3130	0.3102
6A	0.4450	0.2336	−0.0172	0.1501	−0.1553	0.2239
5B	0.1386	0.1486	0.0939	0.1213	0.0103	0.1554
5A	0.2157	0.1678	−0.0913	0.1057	0.2996	0.1272
4B	−0.0326	0.2033	0.0892	0.1281	0.0902	0.1821
4A	−0.9895	0.1871	−0.3791	0.1656	0.2923	0.2171
3B	−0.5869	0.4582	0.0672	0.1659	0.8617	0.3700
3A	−0.6076	0.5495	0.3598	0.3561	0.7556	0.5651
2B	−0.7148	0.6638	0.3021	0.3872	1.5540	0.6151
2A	1.5634	0.6002	0.4971	0.4650	2.0444	0.6631
1D	0.3251	0.6275	0.6034	0.4874	3.0894	0.6804
1C	0.8453	0.3820	0.3247	0.2446	−0.2249	0.2728
1B	1.1980	0.4418	0.5309	0.1842	0.2234	0.2888
1A	2.5065	0.4815	1.2485	0.2877	0.9364	0.5446

Layer	Payerne 47°N Trend	S.E.	Hohenpeissenberg 48°N Trend	S.E.	Goose Bay 53°N Trend	S.E.
7	−0.3927	0.1189	−0.4774	0.1266	1.1010	0.3989
6B	−0.2419	0.1011	−0.4549	0.1129	1.3753	0.3700
6A	0.0246	0.0872	−0.2564	0.0898	1.1855	0.2995
5B	−0.1226	0.0708	0.0377	0.0671	0.4013	0.2530
5A	−0.2046	0.0691	−0.0928	0.0731	0.0728	0.2075
4B	−0.4088	0.0680	−0.2457	0.0749	−0.0806	0.2150
4A	−0.5021	0.0831	−0.6372	0.0832	−0.6877	0.2600
3B	−0.8211	0.1518	−0.5486	0.1399	−0.9480	0.3735
3A	−0.6697	0.2427	−0.3854	0.1817	−0.8932	0.5202
2B	−0.9774	0.2857	−0.4241	0.2292	−1.5639	0.4874
2A	−0.2042	0.4118	0.0130	0.3712	−1.5020	0.8146
1D	0.3671	0.8308	2.3613	0.3648	−3.1778	0.9368
1C	1.6038	0.4287	2.6830	0.2150	−1.6966	0.5074
1B	2.1197	0.3390	2.2850	0.1762	−0.9935	0.4527
1A	2.4457	0.4170	2.3078	0.2487	−1.0987	0.4945

| Layer	Edmonton 54°N Trend	S.E.	Churchill 59°N Trend	S.E.	Resolute 75°N Trend	S.E.
7	3.0180	0.3989	3.3806	0.7391	−0.2466	0.3452
6B	2.9733	0.3887	2.7236	0.6748	−0.3685	0.3263
6A	2.2304	0.3403	1.0688	0.4455	−0.3610	0.1761
5B	1.0258	0.2485	−0.1247	0.3595	−0.0532	0.2658
5A	0.2672	0.2021	−0.9767	0.3092	−0.1598	0.0977
4B	−0.3388	0.2735	−1.4080	0.2847	−0.2328	0.0769
4A	−0.2767	0.2503	−1.9890	0.0995	−0.6220	0.0658
3B	−0.9817	0.3416	−0.9869	0.4493	−0.8826	0.1834
3A	−0.4881	0.5318	−1.1097	0.5889	−0.4674	0.1976
2B	−0.5528	0.7432	0.0407	0.3122	−0.3612	0.2293
2A	−2.1986	1.1197	−0.8426	0.8610	−0.5911	0.4114
1D	−1.6091	1.2641	−0.3072	1.4824	1.7975	0.0067
1C	−1.6674	0.4212	−1.0678	0.6925	1.4531	0.6260
1B	−0.7987	0.5065	−1.3955	0.5185	0.6997	0.4748
1A	−0.0882	0.6898	−0.7152	0.6638	−0.0624	0.0204
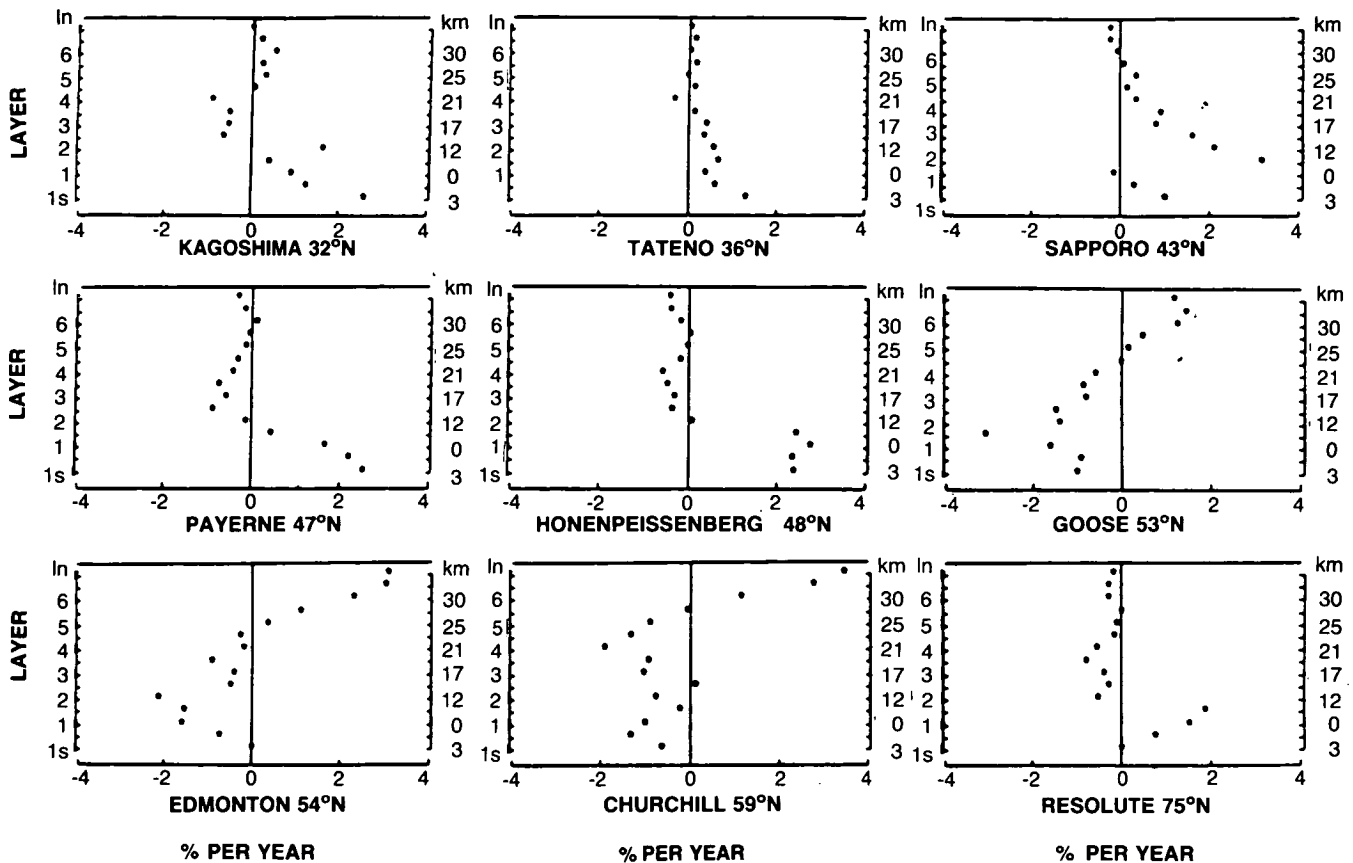
Figure 2.3-8. Trend estimates derived from ozonesondes measurements at 9 stations for 15 fractional Umkehr layers (% per year).

the nine estimates for each layer as a random sample from a normal population and compute the sample average and its estimated standard error. The results are given in Table 2.3-5. Statistically significant trend is observed in layers 3 and 4 (17–24 km). It corresponds to an average ozone concentration decrease of 0.46% per year.

One should be extremely cautious to draw conclusions on a global scale based on the analysis of the ozonesonde data. Figure 2.3-8 shows that considerable differences exist in the trend profiles across the stations, especially in the lower (1 and 2) and the upper (6 and 7) layers. This is also reflected by the width of the confidence intervals in Table 2.3-5. For example, the tropospheric trends derived for Payerne are probably too high because of an improvement in pre-launch procedure beginning in late 1983, not reflected by a level shift term in the statistical analysis. Otherwise, the two European mid-latitude stations do show a rather coherent behavior with similar trends in the lower stratosphere. The situation is rather confusing in the troposphere: although the three Japanese stations have generally positive trends, the three mid-latitude Canadian stations have negative trends, and large positive trends are observed at Resolute (75°N). In addition, while statistically significant ozone decreases are observed in layers 3 and 4, consideration of Table 2.3-4 shows that the decrease in layer 4 is mainly due to the period 1982–1986, as no significant trend is observed when the data through 1982 only are considered (see Table 2.3-5b). Such a picture is rather

233

Table 2.3-5. Summary of averages of trend estimates (% per year) and standard errors (S.E. $\pm 2\sigma$)

Layer	(a) Data thru 12/86		(b) Data thru 12/82	
	Average	S.E.	Average	S.E.
7	0.6620	0.5041	0.7875	0.6482
6B	0.6547	0.4536	0.6712	0.4933
6A	0.4627	0.2890	0.3669	0.4490
5B	0.1480	0.1224	0.1368	0.2132
5A	−0.0744	0.1292	0.0208	0.1331
4B	−0.2853	0.1523	0.0164	0.0973
4A	−0.6434	0.2052	0.1989	0.5425
3B	−0.5363	0.2073	−0.1615	0.1851
3A	−0.3895	0.1967	−0.4970	0.1998
2B	−0.2997	0.2941	−0.3090	0.4330
2A	−0.1356	0.4549	−0.0158	0.6358
1D	0.3833	0.6499	0.3940	1.1613
1C	0.2504	0.5135	0.1978	0.4633
1B	0.4301	0.4391	0.5121	0.2638
1A	0.8312	0.4646	0.6670	0.4538

consistent with the SAGE observations as it might expand the ozone decrease observed between 28 and 25 km towards lower altitude. However, in the SAGE data the maximum effect is observed at low latitudes in contrast with the sonde data where, except for Kagoshima, the decrease occurred at a number of mid-latitude stations. Thus, apart from the decrease in layer 3 observed consistently over most of the stations, it seems rather difficult to draw any definitive conclusion on a semi-global scale from this data set.

2.3.5 Comparisons with Model Calculations

Adding 15 months of new SAGE data to the analysis performed in the Ozone Trends Panel Report has not changed appreciably the observed change of −3 ±2% in ozone concentration near 40 km over the 6-year period 1980–1986. The more thorough analysis of data from 10 Umkehr stations in the Northern Hemisphere for the period 1977 to 1987 reports also a statistically significant decrease in ozone between 30 and 43 km, the decrease near 40 km being 4.8 ±3.1% after allowing for seasonal and solar-cycle effects and correcting the data for aerosol interferences. The mean values of the observed decreases at 40 km are less than the mean values predicted by theoretical calculations performed in the OTP and taking into account both chlorine and solar influences. These are in the range of −6 to −8% over the period 1979–1985. However the large experimental uncertainties prevent a critical test of the theory.

The SAGE change of −3 ±2% at 25 km over 6 years when considered together with the negative Umkehr trend in this height range and the statistically significant, but not globally representative trend of nearly −0.5% per year observed by ozonesondes between 17 and 24 km, seems to suggest that the stratosphere below 25 km is the prime contributor to the total ozone loss at mid-latitude. Changes below 25 km are not predicted by global models based only on gas phase processes. It is not clear whether this points to missing processes in the models of the lower stratosphere or that the sparse measurements are not representative of the global atmosphere.

2.4 TRENDS IN STRATOSPHERIC TEMPERATURE

2.4.1 Introduction

The purpose of this section is to reiterate and update the Ozone Trends Panel Report (OTP) temperature trend analysis. The objective of the OTP analysis was threefold: (1) to establish the quality of a variety of stratospheric temperature data sets; (2) to discuss temperature trend mechanisms, and (3) to determine the consistency of temperature changes with observed ozone changes. This last objective is particularly difficult to reach, since it requires data analyses that minimize the influences of other processes contributing to temperature trends.

Global temperature data sets for the region above 30 hPa (~22 km) are only available after late 1978. For trend analysis, any data set covering such a relatively short period can be strongly influenced by short period anomalies and multi-year cycles such as the Quasi-Biennial Oscillation (QBO), the solar cycle, and even significant interannual variability. In particular, the OTP noted the strong thermal perturbation associated with the El Chichon eruption which occurred near the middle of the analysis period (1979–1986). Thus, rather than trying to estimate a trend, the differences between annual averages at the beginning and the end of the data period were calculated in the OTP. The annual averaging minimizes the QBO effect, and the calculation of changes minimizes the thermal perturbation associated with El Chichon, since it avoids using explicitly the years 1981 through 1984. The effect of the change in the solar flux over this period was estimated using model simulations. Finally, the OTP tried to minimize interannual variability associated with extratropical dynamics by focusing on temperature trends near the tropics to estimate the consistency of ozone and temperature changes.

The update of the previous temperature analysis performed in the OTP report, is based on the temperature data set already available and updated when possible, and the recently available data from Rayleigh lidar observations. The possible implication for trend determination of the recent finding of a statistical relationship between the stratospheric temperature, the QBO, and the 11-year solar cycle is also discussed.

2.4.2 Stratospheric Temperature Data Sets

The stratospheric temperature data sets used in the OTP report were obtained from radiosondes, rocketsondes and satellite radiances. Recently lidar temperature data have become available. In this section, the three data sets used in OTP are briefly summarized and the new lidar data are discussed.

2.4.2.1 Radiosondes

Radiosondes are balloon-borne instruments launched frequently at regular intervals. The density of radiosonde sites is relatively high over most continental regions. However, few measurements are available over the oceans, particularly in the Southern Hemisphere. Radiosondes can measure temperatures above 10 hPa (30 km), but due primarily to the inaccuracy in the pressure measuring, the uncertainty in the temperature measurement above 30 hPa is large. Additional uncertainties arise from the lack of a radiosonde standard, and the variety of instrument types in use worldwide from different manufacturers. Also, for trend analysis, problems arise from the lack of documentation on instrumentation changes which have been introduced over the years, and application of corrections for solar short wave and long wave radiation errors. Although a number of authors report radiosonde temperature trends above 30 hPa, the OTP felt that the uncertainties of the measurements were too large above 30 hPa for trend determination.

235

2.4.2.2 Rocketsondes

Rocketsondes are rocket-borne instruments, usually thermistors, which can be carried into the mesosphere and lower thermosphere. Due to their larger cost and complex ground station requirements, rocketsonde stations are rather few and the number of sites has significantly decreased in the last few years. Temperature trends obtained from rocketsondes are also influenced by changes in instrument design in the early 1970s, nonstandard data recording procedures prior to 1969, and the estimate of aerodynamic and radiation corrections. The OTP used only high quality rocketsonde data subset accounting for problems, and eliminated rocketsonde measurements that presented temperature differences of 3 K or more with simultaneously launched radiosondes.

2.4.2.3 Satellites

Beginning with the launch of the TOVS (TIROS-N Operational Vertical Sounder) instrument aboard the NOAA polar orbiter series in late 1978, regular temperature soundings of the stratosphere became available on an operational basis (the Stratospheric Sounding Unit [SSU] and Microwave Sounding Unit [MSU] instruments). Satellite temperature measurements prior to this period lack sufficient accuracy or record length.

Trend determination from radiance measurements from the TOVS series is complicated by calibration drift and differences between the performance of instruments in the series. Two approaches for the determination of satellite temperature trends were discussed by OTP. National Meteorological Center [NMC] analyses use temperature retrievals from TOVS radiances and Gelman et al. (1986, 1988) estimated corrections to the operational analysis temperatures for trends calculations. These corrections were derived from comparison with rocketsonde temperatures. Nash and Forrester (1986) also estimated temperature trends from TOVS radiances by intercalibrating the different TOVS instruments using the operational overlap of NOAA-6's SSU and MSU. Thus they were able to estimate the change in the measured radiances in the subsequent SSU and MSU instruments and establish the stability of the measurements over the 1980–1986 period.

2.4.2.4 Lidar

Rayleigh lidars provide density, and therefore, temperature information in the stratosphere and mesosphere. The Rayleigh lidar operates by detecting the Rayleigh backscattered signal from ground-based laser (for a description of the method see Hauchecorne and Chanin [1981] and Chanin and Hauchecorne [1984]). Due to the recent development of the lidar technique and the limited number of operational sites, data from this source were not used in the previous OTP report. To this date, two Rayleigh lidars located in France have been used on an operational basis: Observatoire de Haute-Provence (OHP) (44 N, 6 E) since 1981 and Biscarosse (44 N, 1W) since 1986. The total number of profiles averaged over a nighttime period and defined hereafter as a sequence, exceeds 1000, with an average of two sequences a week. Since the lidar profile is determined by averaging several hours of data, the variability due to gravity waves, which appears in the instantaneous soundings, is reduced.

The Rayleigh lidar temperature precision is height dependent and better than 1 K below 50 Km. However the accuracy of the temperature measurement may be affected by a number of factors: the presence of aerosols, the saturation of the pulse counters from low-altitude returns, and parallax effects between the emission and reception axis. These uncertainties can however be partly corrected. Aerosols

236

can be determined by simultaneous measurements at different wavelengths and a second channel with reduced efficiency can be used for the low-altitudes returns. Parallax effects can be avoided by using a co-axial system. To estimate the accuracy of the Rayleigh lidar, intercomparisons have been performed with rocketsondes. In 1986, rocketsonde and lidar measurements showed temperature differences between 1 K and 2 K from 30 to 70 km. This difference was smaller than the difference between the two thermistors on the same payload. Furthermore, intercomparison of the OHP and Biscarosse systems (located within 500 km) over 66 simultaneous profiles showed a difference between the two systems of less than 2 K below 80 km.

2.4.3 Intercomparison of Stratospheric Temperature Data Sets

2.4.3.1 Radiosonde, Rocketsonde, and Satellite Data

The temperatures determined independently by Nash and Forrester (1986), NMC, radiosondes (Labitzke et al., 1985), and rocketsondes (Angell and Korshover, 1983) were compared in the OTP report. Generally the analyses agreed, although there were periods of significant disagreement especially in 1982–1983. Figure 2.4-1 (a,b,c,d) from OTP shows the results of these comparisons in the 100–30 hPa (16–22 km), 30–10 hPa (22–30 km), 5–1 hPa (36–48 km), and 2 hPa level (40 km).

2.4.3.2 Comparison of Lidar Data with SSU and NMC

A comparison was performed for the period 1981–1987 between the temperature obtained by lidar and the SSU and the NMC data. The data have been selected to be within 5 degrees of latitude and 10 degrees of longitude of the OHP lidar site. It is however also important to note that both the SSU and NMC data used here are different from those used in the OTP report. The SSU data used in the OTP report were zonal means corrected for instrument changes as described in OTP Section 6.2.2.1 (see Nash, 1988). The SSU data used here are the standard gridded radiances provided by the British Meteorological Office and have not been corrected, and the NMC data used have been adjusted as described by Gelman et al. (1986).

Figure 2.4-2 shows the brightness temperature for the SSU channel 27 (approximately 1.5 hPa) and the lidar temperature convolved with the SSU weighting function given in Barnett and Corney (1984). Figure 2.4-3 shows over the same period the NMC data at 42 km (2.0 hPa) and the lidar data. The average lidar-SSU difference is of 4 K, with a maximum difference of 6.5 K. The average lidar-NMC difference is 3 K at 42 km and varies from −5 K to 7 K.

The lidar-SSU and lidar-NMC differences are generally similar. They can be divided into four periods, which correspond to changes in the biases between the data sets. The first period beginning in 1981 and extending to early 1982 is characterized by larger values of the lidar temperatures. The second period, from early 1982 to mid-1983, is characterized by a close match up of the lidar SSU and NMC data. The third period, from mid-1983 to mid-1985, is characterized again by larger values of the lidar temperatures. The last period, extending from mid-1985 onward, shows smaller differences. Although the reasons for these differences are not readily apparent, it seems that the September 1983 satellite change from NOAA-7 to NOAA-8 resulted in the introduction of large bias between the lidar and SSU/NMC data sets. This
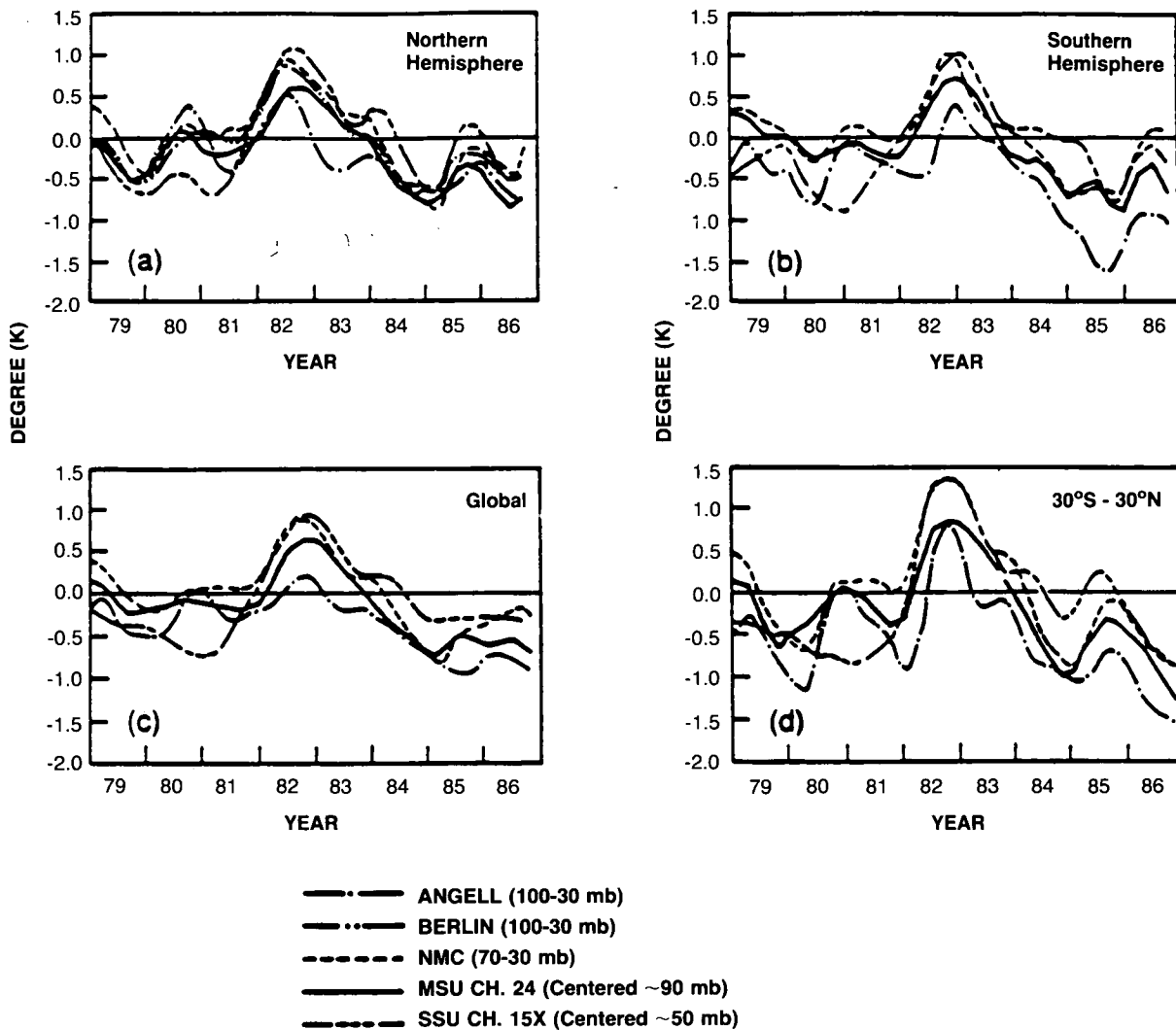
237

Figure 2.4-1a. Seasonal temperatures with the long-term seasonal averages removed and smoothed 1-2-1 in time: Angell 100-30 mb radiosonde thickness (solid dot); Berlin 100-30 mb thickness (long dash); NMC 70-30 mb thickness (short dash); MSU channel 24 centered at approximately 90 mb (solid); and SSU channel 15X centered at approximately 50 mb (solid dot) for (a) Northern Hemisphere average, (b) Southern Hemisphere average, (c) global average, and (d) 30°S-30°N average. Berlin data were available only for the Northern Hemisphere. Tick marks on the abscissa correspond to the D-J-F seasons.

effect is illustrated by the unadjusted data in OTP Figures 6.2.2.3 and 6.2.2.4, where the change from NOAA-7 to NOAA-8 is approximately accompanied by a 4-K cooling.

Comparisons were also performed between the lidar at 36 km and the SSU channel 26, and the lidar with NMC temperatures at 30 km (10 hPa), 36 km (5hPa), 48 km (1 hPa) and 55km (0.4 hPa) although this comparison relies on the downward extension of the lidar data by radiosondes, and is less germane to lidar-satellite comparisons. The best agreement between the lidar and NMC is obtained at 48 km with a maximum difference of 3 K. The causes of these differences will have to be studied further.
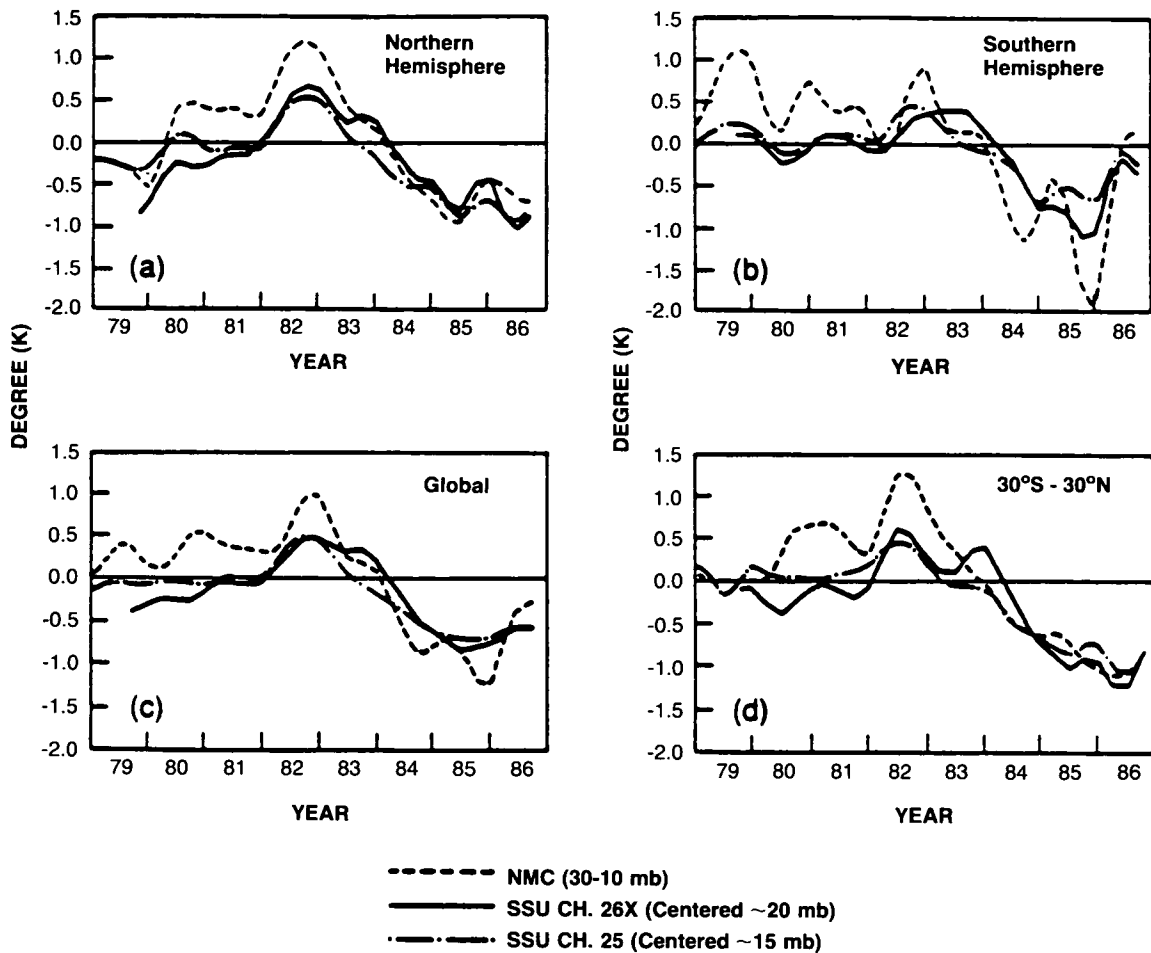
Figure 2.4-1b. Seasonal temperatures with the long-term seasonal averages removed and smoothed 1-2-1 in time: NMC 30-10 mb thickness (dotted); SSU channel 26X centered at approximately 20 mb (solid); and SSU channel 25 centered at approximately 15 mb (three short dashes and a long dash) for (a) Northern Hemisphere average, (b) Southern Hemisphere average, (c) global average, and (d) 30°S-30°N average. Tick marks on the abscissa correspond to the D-J-F seasons.

2.4.4 Influence of Solar Activity

Since the OTP report, a statistical relationship has been established between the temperature, the 11-year solar cycle, and the equatorial QBO (Labitzke, 1987; Labitzke and Van Loon, 1988). The relationship has first been observed in Arctic polar temperatures, when the temperatures are classified between years according to the west and east phases of the QBO. During the west phase, the polar temperatures are correlated with the solar cycle, while in the east phase, the polar temperatures are anti-correlated. The amplitude of this 11-year polar temperature cycle is approximately 10–15 K for either phase of the QBO. The relationship is illustrated in Figure 2.4-4 for the North Pole (from Labitzke and Van Loon, 1988). It has been since extended to other latitudes and altitudes (Labitzke and Chanin, 1988), and to the Southern Hemisphere. At present, no physical mechanism has been found to explain this relationship.
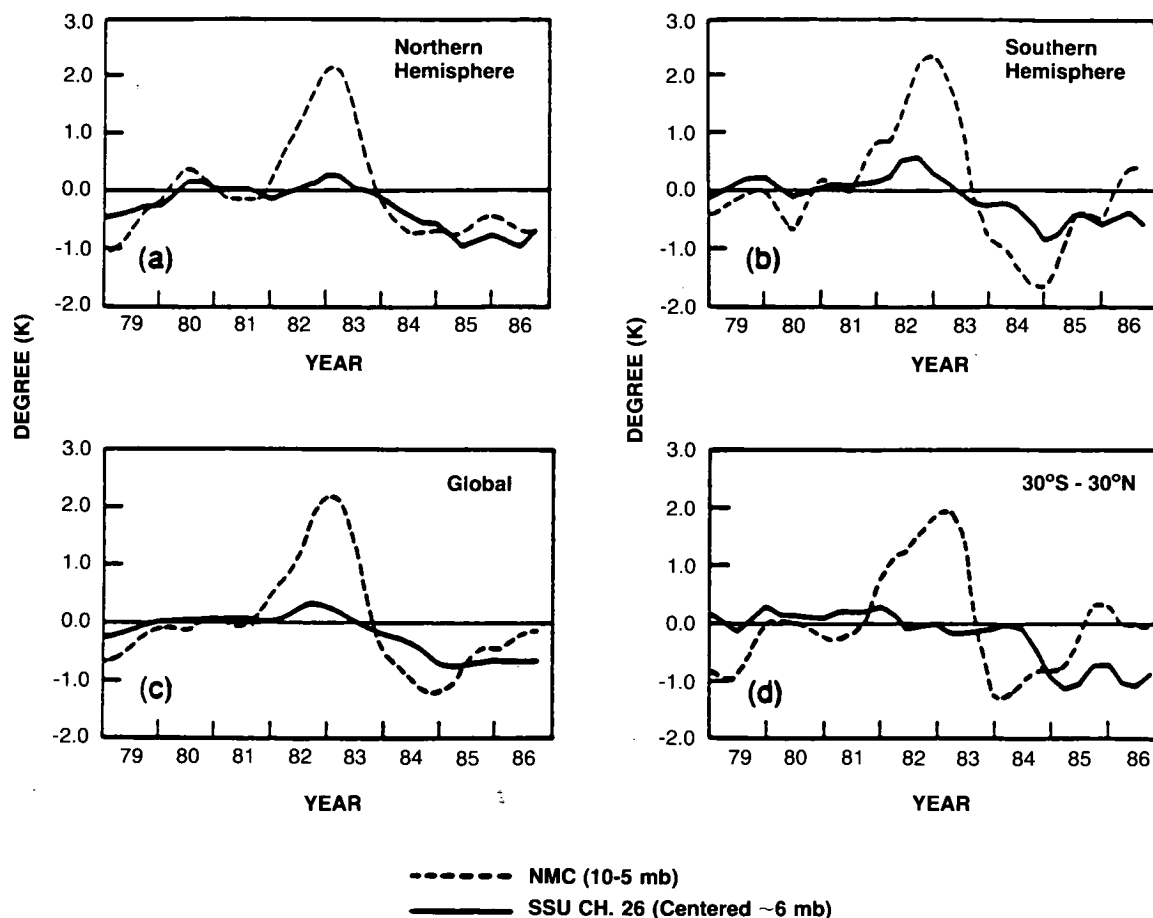
Figure 2.4-1c. Seasonal temperatures with the long-term seasonal averages removed and smoothed 1-2-1 in time: NMC 10-5 mb thickness (dotted); and SSU channel 26 centered at approximately 6 mb (solid), for (a) Northern Hemisphere average, (b) Southern Hemisphere average, (c) global average, and (d) 30°S-30°N average. Tick marks on the abscissa correspond to the D-J-F seasons.

The main consequence of the QBO-solar cycle relationship relevant to the present analysis is that it may be a source of long-term interannual variability. In addition, this relationship is variable with season, latitude, longitude, and height and generally, local data show a significantly larger QBO-solar cycle signal than zonal mean data. One should then be cautious when using local or regional data, unless the record length is large enough to allow the separation of trend and solar induced effects.

2.4.5 Updating of Previously Used Data Sets

Updates of global stratospheric temperature trends have been performed from radiosondes data by Angell (1988) and Labitzke (1989, private communication). Updates of the rocketsonde data have also been provided by Kokin et al. (1989) for the USSR stations of Heiss Island, Volgograd, Thumba, and Molod-ezhnaya and by the Japan Meteorological Agency for the Ryori station.
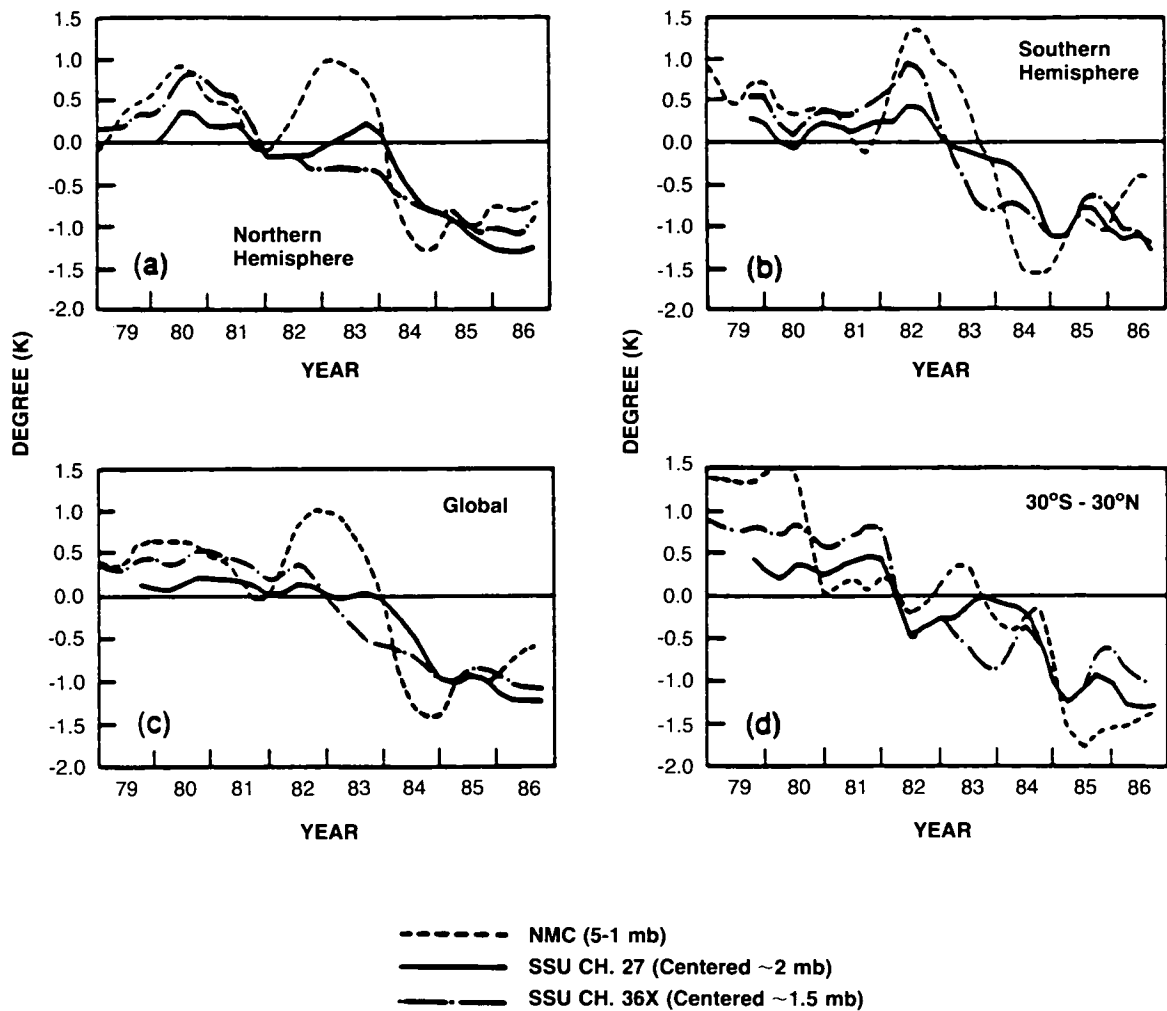
Figure 2.4-1d. Seasonal temperatures with the long-term seasonal averages removed and smoothed 1-2-1 in time: NMC 5-1 mb thickness (dotted); SSU channel 27 centered at approximately 1.5 mb (solid dot) for (a) Northern Hemisphere average, (b) Southern Hemisphere average, (c) global average, and (d) 30°S-30°N average. Tick marks on the abscissa correspond to the D-J-F seasons.

Angell (1988) derives a global cooling of −0.62 K/decade in the 100–50 hPa layer over the period 1973–1987, which mostly results from a strong cooling (−2 K in the Antarctic region). Both Labitzke (1989, private communication) and Angell (1988) conclude on a barely significant warming in the temperate Northern Hemisphere (0.2 K/decade at 50–60°N from Labitzke) at the same altitude level.

At lower latitudes (10–30°N) at the 30 hPa pressure level, Labitzke (1989, private communication) reported no trend in the summer between 1961 and 1981 (excluding the periods during which volcanic aerosols may have warmed the lower stratosphere following the eruptions of Agung [1963] and El Chichon [1982]). Angell (1988) found a 0.4-K trend for the Western Hemisphere tropics. On the other hand, a mean decrease in temperature of 0.4 K is reported by Labitzke (1989, private communication) at 50–60°N, and a large decrease of 2 K at the polar stations is reported by Kokin et al. (1989) for the last 20 years.
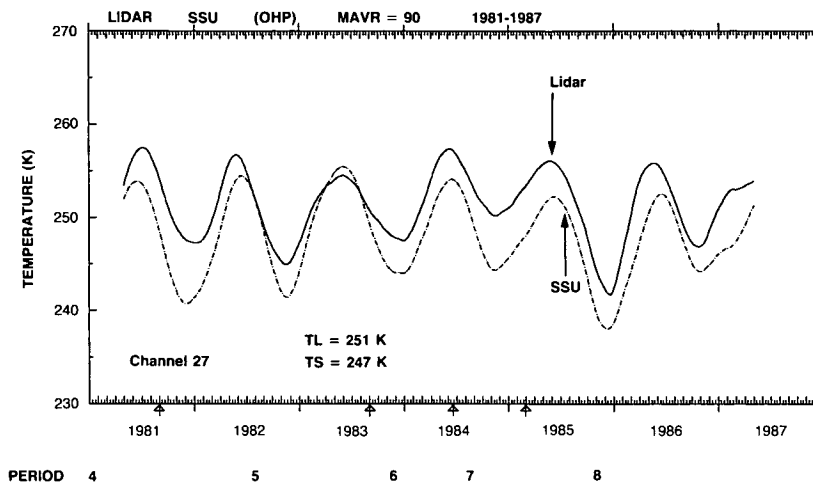
Figure 2.4.2. Lidar temperature and SSU channel 27 brightness temperature from 1981 to 1987 (with a running mean of 90 days).
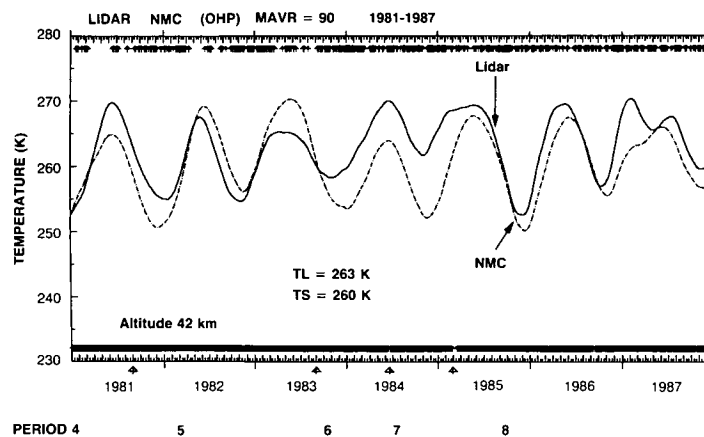

Figure 2.4-3. Lidar and NMC temperature at 42 km (with a running mean of 90 days). The periods corresponding to different NMC analyses are indicated at the bottom.

At the 10-hPa (30 km) pressure level, Labitzke (1989, private communication) reported a -0.5 K/ decade trend for the latitude region between 20–50°N over the period 1964–1987. Over the same period, Angell (1988) reported a trend of -0.2 K/decade based on radiosonde data. At the same altitude level, the updated rocket data of USSR and Japan led both to a larger trend of -1.5 K/ decade, although with a large spatial variability. Using also rocketsonde data, Angell (1988) calculated a trend of -0.8 K/decade at 10 hPa in the Western Hemisphere tropics (1973–1987), and -1 K/decade in the upper stratosphere (5–0.5 hPa). Although the difference between the 10 hPa pressure level radiosonde and the rocketsonde-based trends is within a ± 2 σ confidence intervals (Angell, 1988), the OTP reported serious disagreements between edited (see OTP Section 6.2.3) and unedited rocketsonde data. Since the Angell (1988), USSR, and Japan results are from unedited rocketsonde data, caution should be exercised when comparing those data to the rocketsonde data of the OTP. Furthermore, trends at these individual stations might be mainly representative of local evolution.
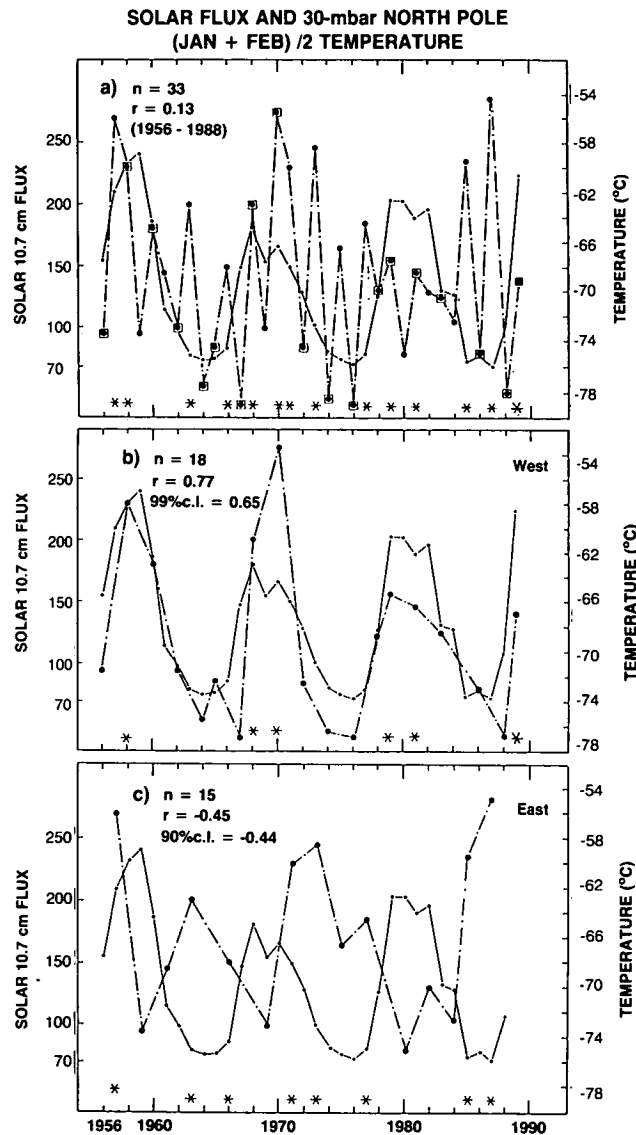
242

SOLAR FLUX AND 30-mbar NORTH POLE
(JAN + FEB) /2 TEMPERATURE

Figure 2.4-4. Comparison of the 10.7 cm solar flux, in 10^{-22}W/(m²Hz) (solid line) and the 30 mb temperature, in degrees Centigrade, at the North Pole, averaged for January and February for (a) all winters, (b) winters in the West phase of the quasi-biennial oscillation (QBO), (c) winters in the East phase of the QBO. Asterisks denote major mid-winter stratospheric warmings (from Labitzke and van Loon, 1988).

As a common conclusion, these studies give some evidence of a generally negative trend, with large spatial variability. The upper limit of the zonally averaged trend is between −0.6 and −0.8 K/decade between the 100 hPa and 10 hPa pressure levels (16–30 km) respectively, with the exception of the Antarctic region. These values are much lower than the local trends derived from rocketsonde data.

2.4.6 Comparison with Trends in Ozone Distribution

The reported SAGE I/SAGE II changes between the 1979–1981 and 1984–1988 periods, in the 20–50 degree latitude bands lead to a maximum decrease of 3% ±2% in ozone concentration at 40 km and a

decrease of -5% at 50 km in the tropics (see Section 2-3-2). These values are very similar to those already reported in the OTP.where the SAGE data used were the zonal mean profiles for the latitude band 15°S to 15°N which gave an ozone concentration decrease of -5% peaking at 50 km. Because the predicted temperature change is sensitive to the ozone change above 50 km, two cases were considered: (1) no ozone change outside the 26–50 km altitude range were SAGE measurements are available, (2) a -5% ozone change above 50 km and a -2% change below 26 km. The radiative response showed a temperature decrease of 1K to 1.4 K at 50 km. An additional 0.8-K cooling will occur at the same altitude due to the decrease in the solar flux during the declining phase of the solar cycle. Thus, the expected 50 km temperature was estimated to be of 1.8 to 2.2 K in the tropics. With the updated value of the tropical ozone decrease of 4%, the 50 km change should be 1.4 to 1.8 K.

Changes on global and equatorial temperatures over the period from 1979–1980 to 1984–1985 are shown in Figures 2.4-5 and 2.4-6, reproduced from OTP Figures 6.3.2.1 and 6.3.2.2. The decrease in equatorial temperatures at 48 km from satellite and rocket data over the same period is about 1.75 K $\pm$ 1 K. Global temperatures show a smaller decrease of 1.5 K $\pm$1 K. The SAGE ozone changes and the observed equatorial temperature changes appear to be in satisfactory agreement within the $\pm 2\,\sigma$ confidence interval of the analyses.

2.5 TRENDS IN TROPOSPHERIC GASES AND OZONE

2.5.1 Introduction

The Ozone Trends Panel (OTP) Report presented information on the global trends of a number of tropospheric trace gases that interact with stratospheric ozone, either chemically, as sources of nitrogen,

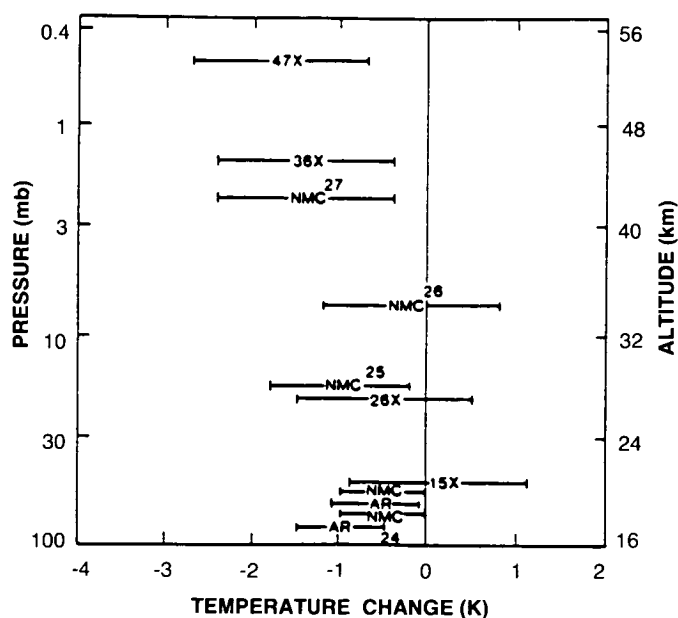**Figure 2.4-5.** Summary of global stratospheric temperature differences (1985 and 1986 minus the average of 1979 and 1980). Symbols denote Angell's radiosonde data (AR), NMC data (NMC), and satellite data (channel numbers, see Figure 6.2.2.1 of the OTP Report). Error bars denote uncertainties (see text). Nash and Forrester (1988) estimate their satellite errors as 0.2 K rms (1 K rms for synthesized channels).
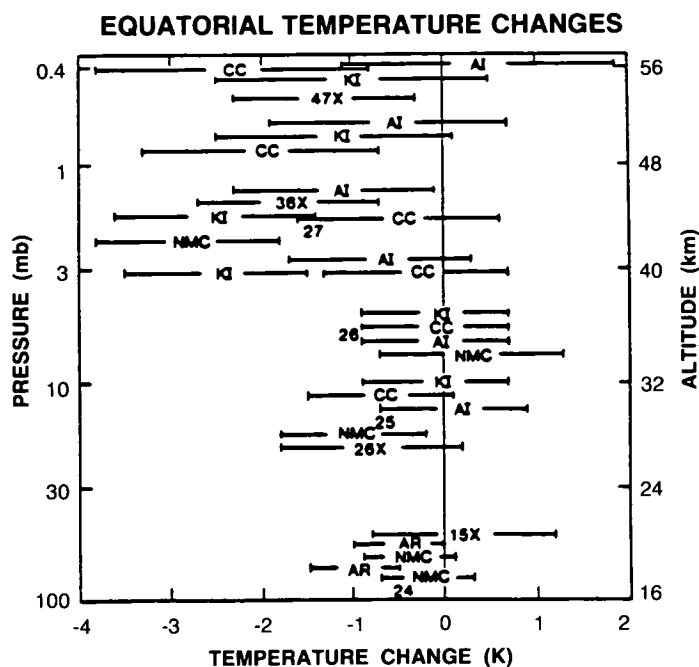
244

EQUATORIAL TEMPERATURE CHANGES

Figure 2.4-6. As in Figure 2.4-4, except for tropics and including rocket stations. Kwajalein Island (KI; 9°N, 168°E), Ascension Island (AI; 9°S, 14°W), and Cape Canaveral (CC; 28°N, 81°W).

hydrogen and halogen catalysts that substantially control ozone destruction, or indirectly by influencing stratospheric temperatures. The OTP Report reviewed available data up to the end of 1986. The purpose of this section is to update the OTP Report with data, where possible, from 1987 and 1988. Section 2.5.2 describes the trends in halocarbons and reviews the progress in the area of trace gas calibration. As shown in the OTP Report, the calibration uncertainties associated with several trace gases are significant, particularly methyl chloroform (CH_3CCl_3), carbon tetrachloride (CCl_4), CFC-113 (CCl_2FCClF_2), and carbon monoxide (CO). Sections 2.5.3, 2.5.4, and 2.5.5 review the trends observed in atmospheric nitrous oxide (N_2O), methane (CH_4), and carbon monoxide (CO), as these species are of particular importance in determining future stratospheric ozone levels. It would appear in particular that the current rate of CH_4 increase is not constant and this is examined in the available data sets. Also, historical CH_4 data from ice core studies suggest a connection between CH_4 levels and climate. Carbon dioxide (CO_2), a radiatively important trace gas, was not considered in significant detail in the OTP Report. The Section 2.5.6 examines the global rate of increase of CO_2 over the last decade, which shows considerable variability. Finally, the data available on surface and free tropospheric ozone measurements at a number of locations are reviewed in Section 2.5.7 in the light of recent suggestions of large-scale tropospheric increases in the Northern Hemisphere. As an overview, the current trends, concentrations, and lifetimes of trace gases are summarized in Table 2.5-1.

2.5.2 Halocarbons

A variety of anthropogenic and natural halocarbons are present in the global atmosphere. The abundance, sources, and sinks of this group of chemicals have been recently discussed in Gammon et al. (1986) and in the OTP Report (Ehhalt et al., 1989).

Table 2.5-1. Concentrations and global trends of tropospheric gases for 1987. Lifetimes are given, where available (adapted from Ehhalt et al., 1989)

Source Gas	Mixing Ratio pptv	Rate of Increase pptv/yr	Rate of Increase %/yr	Lifetime yr
CCl_3F[a]	240[h]	9.5	4.0	110
CCl_2F_2[a]	415[h]	16.5	4.0	75
CH_3CCl_3[a]	150[h]	6.0	4.0	7
CCl_4[b]	140[h]	2.0	1.5	40
CCl_2FCClF_2[b]	45[i]	4–5	10	90
$CHClF_2$[c]	100[h]	7	7	20
CH_3Cl[d]	600			1.5
$CHCl_3$[e]	30[h]			0.7
CH_2Cl_2[e]	35[j]			0.6
CCl_2CCl_2[e]	30[h,j]			0.6
CH_2ClCH_2Cl[e]	35[j]			0.6
$CClF_2CClF_2$[c]	15[j]			180
$CHClCCl_2$[e]	10[h,j]			0.1
$CClF_2CF_3$[e]	5[h]			380
$CClF_3$[e]	5[h]			400
$CBrClF_2$[d]	1.7[h]	0.2	12	25
$CBrF_3$d	2.0[h]	0.3	15	110
CH_3Br[d]	10–15			1.5
$CHBr_3$[e]	2–3			0.4
CH_3Br_3[e]	2–3			0.5
CH_3CH_3Br[e]	2–3			
CH_3BrCl[e]	1–2			
$CHBr_3Cl$[e]	1			0.6
CH_3BrCH_3Br[e]	1			0.6
$CHBrCl_3$[e]	1			0.6
N_2O[f]	307[k,n]	0.6–0.7[k,m,n]	0.2	150
CH_4	1680[i,n]	12[f,g,n]	0.7	10
	1680[q,n]	16[q,n]	1.0	
CO[g]	90[i,n]		≈1 (NH)	0.2
			≈0 (SH)	
CO_2[f]	348[f,l,p]	1.6–1.9[f,p]	0.45–0.55[f]	
O_3	≈20[n]		≈1 (NH)	
			≈0 (SH)	

[a] GMCC-GAGE data
[b] 1987 GAGE data (Cape Grim) and 1986 global distribution (Ehhalt et al., 1989)
[c] OGC data at Cape Grim and observed global distribution (Rasmussen and Khalil, 1982)
[d] 1986 data (Ehhalt et al., 1989)
[e] Gammon et al., 1986
[f] GMCC
[g] CSIRO

[h] OGC calibration
[i] NBS calibration
[j] SRI calibration (Singh et al., 1979)
[k] GMCC calibration
[l] WMO calibration
[m] SIO data, calibration
[n] ppbv
[p] ppmv
[q] UC data

C-4

The halocarbons are the most rapidly increasing species on a percentage basis in the global atmosphere over the last several decades. There is concern about this class of compound because they are sources of stratospheric halogen-free radicals, which catalytically destroy ozone (Rowland and Molina, 1975) and because they absorb in otherwise low opacity infrared wavelength regions of the atmospheric absorption spectrum and thus contribute significantly to the greenhouse effect (Ramanathan et al., 1985). For halo-carbons, whose tropospheric lifetimes are much longer than global circulation times, the trends measured at ground level, at sites remote from halocarbon sources, can provide a reasonably accurate determination of global atmospheric trends (Prinn et al., 1983). The global rate of accumulation of halocarbons in the background atmosphere have been recently reviewed (Prinn, 1988a; Ehhalt et al., 1989).

2.5.2.1 CCl_3F, CCl_2F_2, CH_3CCl_3, CCl_4

The global rates of increase of these compounds in 1987 (Table 2.5-1) are similar to those given in the OTP Report. Sources of new observations up to the end of 1987 are the GMCC (Geophysical Monitoring for Climatic Change) program with stations at Barrow, Alaska (71°N); Niwot Ridge, Colorado (40°N); Mauna Loa, Hawaii (20°N); Cape Matatula, Samoa (14°S), and at the South Pole (CCl_3F, CCl_2F_2: Bodhaine and Rosson, 1988). An update of the observations at Cape Point, South Africa (34°S) (CCl_3F, CCl_4: Scheel et al., 1989) and Hokkaido, Japan (45°N) (CCl_3F, CCl_2F_2, CH_3CCl_3 and CCl_4: Makide et al., 1987) is also included.

Global data, additional to that presented in the OTP Report (up to mid-1986), are not available from the GAGE (Global Atmospheric Gases Experiment) program due to an ongoing calibration re-evaluation. Possible revisions to previously presented data (post mid-1985) (Ehhalt et al., 1989) are believed to be small (Prinn, 1989, private communication). The GAGE data collected at Cape Grim, Tasmania, up to the end of 1987 are shown in Figure 2.5-1.

The rate of increase of CH_3CCl_3 at Hokkaido (3.7 ± 0.8 pptv per year [± 2 σ as for all confidence intervals given hereafter]; Makide et al., 1987) is significantly lower than the global rate of 6.2 ± 0.2 pptv per year deduced from the GAGE program (Prinn et al., 1987). If the low CH_3CCl_3 growth rate measured at Hokkaido is representative of a large area of the Northern Hemisphere, then this implies that the lifetime of CH_3CCl_3 is shorter than that shown in Table 2.5-1. The observed calibration difference of about 20% between the two data sets cannot account for this discrepancy between the observed trends.

As stated in the OTP Report there are considerable uncertainties associated with the absolute cali-bration of CH_3CCl_3 and CCl_4. For example, the concentrations observed on Hokkaido for these two species are approximately 20% lower than observations reported from the GAGE program for similar latitudes. Analysis of GAGE CCl_4 data suggests that the Makide CCl_4 calibration (Yokata et al., 1985) is consistent with the calculated industrial CCl_4 emissions and an atmospheric lifetime of about 40 years (Simmonds et al., 1988). These calibration uncertanties remain and need to be resolved, as they introduce considerable uncertainty into the deduction of atmospheric lifetimes for these species.

2.5.2.2   Other Chlorocarbons

CCl_2FCClF_2 (CFC-113)

Observations of global background mixing ratios of CCl_2FCClF_2 were summarized in the OTP Report and found to be increasing at about 11% per year in 1986. Further observations at Cape Grim (1984–87) show mean concentrations and increases in 1987 of 33 pptv and 3.4 (± 0.5) pptv per year (Figure 2.5-1).
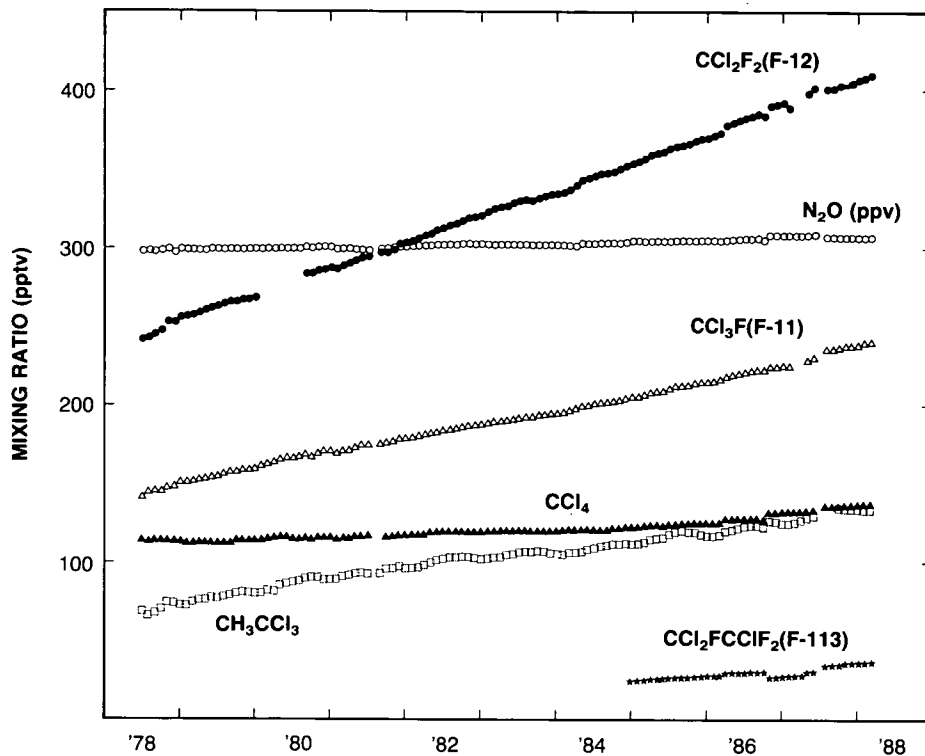
247

Figure 2.5.1. Halocarbon (pptv) and nitrous oxide (ppbv) observations at Cape Grim, Tasmania, as part of the GAGE program (Fraser and Derek, 1989).

Based on the observed Northern Hemispheric-Southern Hemispheric concentration ratio (Ehhalt et al., 1989), and converting the OGC (Oregon Graduate Center) scale to the NBS scale (NBS/OGC = 1.31, Rasmussen, 1989, private communication), an approximate global mean mixing ratio (45 pptv) and growth rate (10% per year) can be derived. This change in the OGC calibration of CCl_2FCClF_2, if substantiated, will essentially remove the differences between the GAGE measurements in the Northern Hemisphere and those made on Hokkaido, Japan (for discussion, see OTP Report).

$CHClF_2$ (HCFC-22)

Recent observations of global background mixing ratios of $CHClF_2$ have been reviewed (Ehhalt et al., 1989) and found to be increasing at about 7% per year. Further observations at Cape Grim (1984–87) show a mean concentration and increase in 1987 of 91 pptv and 6.5 (± 0.3) pptv per year (Figure 2.5-2). Based on the previously observed global distribution (Rasmussen and Khalil, 1982) an approximate global average mixing ratio (100 pptv) can be derived (Table 2.5-1).

CH_3Cl

Methyl chloride (CH_3Cl) is the most abundant halocarbon in the atmosphere, and is thought to be largely of natural origin. Observations of global background mixing ratios of CH_3Cl have been reviewed (Ehhalt et al., 1989), suggesting a global background level of 600 pptv. Further observations at Cape Grim (1984–1987) show a 1987 mean level of around 570 pptv and a clear annual cycle (Figure 2.5-3), which has
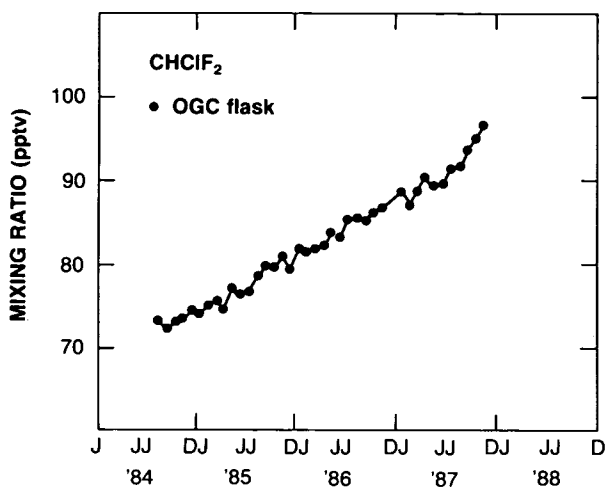
Figure 2.5-2. CHClF$_2$ (pptv) observations at Cape Grim, Tasmania, from the Oregon Graduate Center flask sampling program (Fraser et al., 1989).
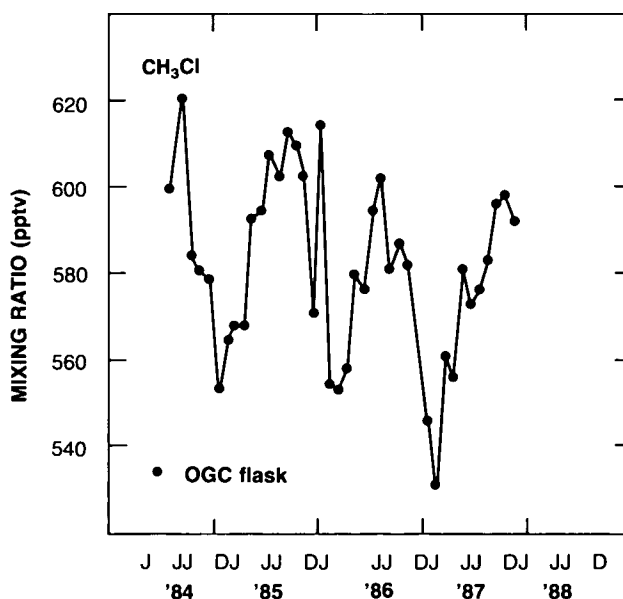
Figure 2.5-3. CH$_3$Cl (pptv) observations at Cape Grim, Tasmania, from the Oregon Graduate Center flask sampling program (Fraser et al., 1989).

been attributed to seasonal variations in the magnitude of the CH$_3$Cl-OH radical sink (Ehhalt et al., 1989). Cape Grim record is too short to deduce whether there exists a long-term regional trend in CH$_3$Cl.

CHCl$_3$

Global background observations of CHCl$_3$ from the OGC flask-sampling network have been published (Khalil et al., 1983), suggesting a global average mixing ratio of approximately 30 pptv. Further observations

at Cape Grim (1984–87) show a large interannual variability. There is also a suggestion of an annual cycle. The mean level at Cape Grim was about 10 pptv (Fraser et al., 1989; Figure 2.5-4).

2.5.2.3 Bromocarbons

Bromine species are relatively minor components of the stratosphere compared to chlorine species, but are nevertheless important because bromine radicals can very efficiently catalyze ozone destruction (McElroy et al., 1986).

The major sources of stratospheric bromine are the naturally occurring organobromine species such as methyl bromide (CH_3Br), methylene dibromide (CH_2Br_2) and bromoform ($CHBr_3$), produced by oceanic algae (Rasmussen and Khahil, 1984; Penkett et al., 1985; Khalil and Rasmussen, 1985; Khalil et al., 1987; Cicerone et al., 1988; Class and Ballschmiter, 1988) and the anthropogenic organobromine species, bromodifluoromethane ($CBrClF_2$, halon-1211) and bromotrifluoromethane ($CBrF_3$, halon-1301), used exclusively as fire fighting agents, and ethylenedibromide (CH_2BrCH_2Br), a gasoline additive.

The concentrations of the halons have been growing rapidly in recent years (Lal et al., 1985), and there could be a substantial anthropogenic contribution to the methyl bromide observed in the atmosphere. Penkett et al. (1985) measured average concentrations of 15.4 ± 1.9 pptv and 10.6 ± 0.9 pptv for CH_3 Br in the Northern and Southern Hemisphere, respectively, on ship voyages down the Atlantic Ocean from Southampton to Antarctica in 1982 and 1983. They estimated a total source strength of approximately 10^5 tons per year to account for the data, of which 75% could be of anthropogenic origin (Wofsy et al., 1975).

The significance of the growing halon concentrations and a potentially large anthropogenic component in the measured methyl bromide is that these are the predominant forms in which bromine is transferred to the stratosphere, prior to breakdown into Br atoms and BrO radicals.

2.5.3 Nitrous Oxide

Nitrous oxide (N_2O) is an important component of the background atmosphere, being a climatically significant species (Ramanathan et al., 1985), as well as a source of nitrogen oxides in the stratosphere,

Figure 2.5-4. $CHCl_3$ (pptv) observations at Cape Grim, Tasmania, from the Oregon Graduate Center flask sampling program (Fraser et al., 1989).
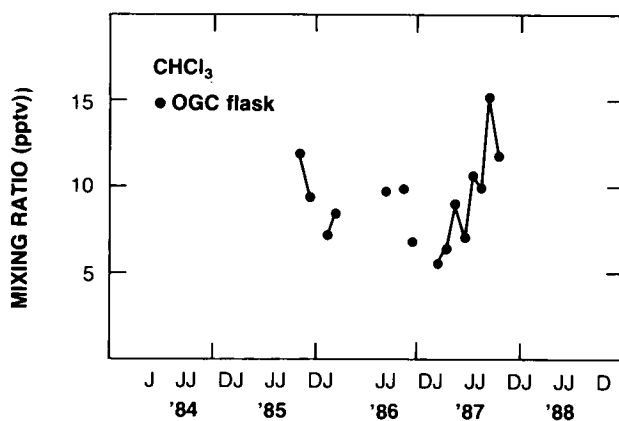
which play a major role in regulating stratospheric ozone levels (Crutzen, 1970). Natural sources of N_2O include microbiological processes on the continents and in the oceans, and anthropogenic sources arise from the combustion of fossil fuels (Weiss and Craig, 1976), biomass burning (Crutzen et al., 1979), and the use of nitrogenous fertilizers (Crutzen and Ehhalt, 1977).

There are several long-term N_2O measurement programs on the background atmosphere at various locations around the globe. Data from the SIO (Scripps Institute for Oceanography) network showed that the global rate of increase in 1986 was 0.63 (± 0.07) ppbv per year (Ehhalt et al., 1989). The Northern Hemispheric data from this program are shown in Figure 2.5-5 (Weiss, 1989), which show an average increase of 0.60 (± 0.06) ppbv per year (Table 2.5-2).

N_2O measurements have been made on air samples collected at the GMCC (Geophysical Monitoring for Climatic Change) sites (Barrow, Niwot Ridge, Mauna Loa, Samoa, and South Pole) since 1977 (Bodhaine and Rosson, 1988). The global average mixing ratio in 1987 was 306.7 ppbv, increasing at 0.73 (± 0.05) ppbv per year (Table 2.5-2). The globally averaged data are also shown in Figure 2.5-5.

A long-term N_2O data record has been collected at Cape Point, South Africa, by scientists from the Fraunhofer Institute for Atmospheric Environmental Research (FIAER), FRG, and CSIR, South Africa, using an *in situ* gas chromatograph (Figure 2.5-5). The 1987 average mixing ratio was 301.2 ppbv, increasing at 0.6 (± 0.2) ppbv per year (Table 2.5-2; Scheel et al., 1988).

A combined OGC-GAGE data analysis showed a global increase of 0.8 ± 0.1 ppbv per year (Ehhalt et al., 1989). Further analysis of the GAGE N_2O data has been delayed by the GAGE calibration re-evaluation. However, the preliminary GAGE N_2O data from Cape Grim in 1987 (Fraser and Derek, 1989) have been analyzed and show an average mixing ratio of 307.8 ppbv increasing at 0.95 (± 0.06) ppbv per year (Table 2.5-2, Figure 2.5-5). The trends deduced from GAGE data are significantly larger than those

Table 2.5-2. N_2O mixing ratios and rates of increase observed in the troposphere

| Site	Laboratory	N_2O (ppbv) 1987	Rate of Increase ppbv/yr ($\pm 2\,\sigma$)	%/yr	Reference
Global Average	GMCC	306.7	0.73 (± 0.05)	0.24	Bodhaine and Rosson (1988)
NH Average	SIO	305.1[a]	0.60 (± 0.06)		Weiss (1989)
Global Average	SIO	305.1[a]	0.63 (± 0.07)		Ehhalt et al. (1989)
Cape Point S. Africa	FIAER-CSIR	301.2	0.62 (± 0.20)	0.21	Scheel et al. (1989)
Global Average	OGC	308.2[b]	0.83 (± 0.05)	0.27	Ehhalt et al. (1989)
Cape Grim Tasmania	CSIRO	307.8	0.95 (± 0.06)	0.31	Fraser and Derek (1989)

[a]1986 data
[b]1985 data
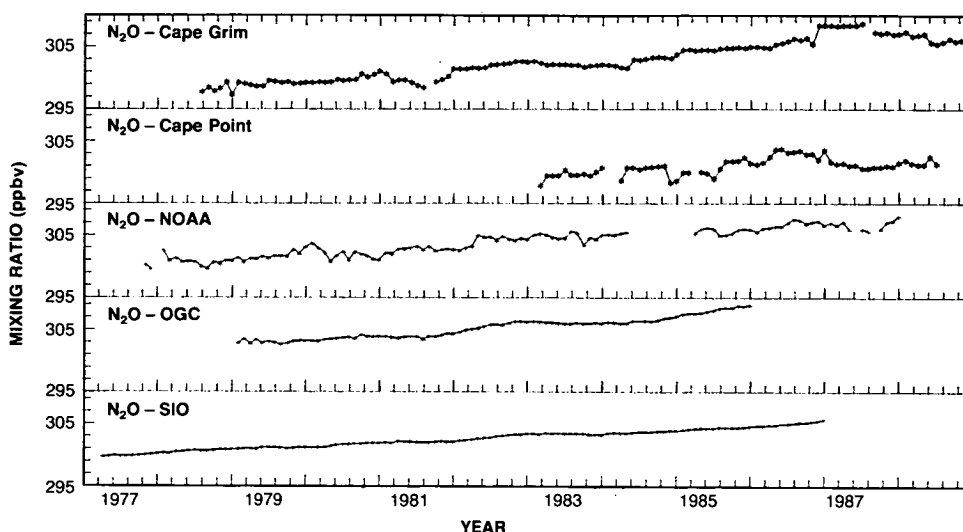
Figure 2.5-5. Long-term trends of N_2O from the GMCC program (average of data from Barrow, Niwot Ridge, Mauna Loa, and Samoa), the SIO program, the OGC-ALE program (average of data from Barrow, Adrigole, Cape Meares, Mauna Loa, Barbados, Samoa and Cape Grim), the FIAER-CSIR program (Cape Point, South Africa) and CSIRO-GAGE data (Cape Grim, Tasmania) (Bodhaine and Rosson, 1988; Weiss, 1989; Ehhalt et al., 1989; Scheel et al., 1988; Fraser and Derek, 1989).

from SIO, GMCC or FIAER-CSIR data (Table 2.5-2), but the significance of these differences cannot be fully assessed until the GAGE re-calibration is completed. The GAGE calibration scale is also significantly higher than those of GMCC and SIO, but this cannot account for the trend differences observed. The globally averaged trends (Table 2.5-1) are based on SIO and GMCC data.

In the OTP Report data were shown on ice core studies of N_2O which, despite a noisy record, showed that N_2O concentrations prior to 1800 were about 280-290 ppbv. Further data have been published (Khalil and Rasmussen, 1988a), that confirm this result with more precise data which show that N_2O levels have risen by about 8% during the last century.

2.5.4 Methane

Methane is an important trace gas because it absorbs infrared radiation, and thus impacts on climate. It affects tropospheric chemistry via hydroxyl radical and ozone budgets, and it impacts on stratospheric chemistry as a source of hydrogen and water vapor and as a sink for stratospheric chlorine.

Recent data from three laboratories making global measurements (GMCC, CSIRO, and UC (University of California)) are summarized in Table 2.5-3. The GMCC and CSIRO programs show significantly lower rates of increase (≈ 12 ppbv per year) than the UC program (16 ppbv per yr). From the GMCC (Steele et al., 1989) and CSIRO (Fraser et al., 1989) programs it would appear that the global rate of CH_4 increase has slowed in recent years. Figure 2.5-6 shows the data from the CSIRO program as well as data collected at Cape Point, South Africa (Scheel et al., 1988), which also show a current low rate of increase (10 ppbv per year). The cause of the recent slowing of the CH_4 increase is not known. Clearly longer data records are necessary to properly define long-term CH_4 variability.

252

Table 2.5-3. Global average methane mixing ratios and rates of increase observed in the troposphere by various laboratories

Laboratory	Mixing Ratio ppbv	Rate of Increase ppbv/yr ($\pm 2\,\sigma$)	%/yr	Reference
GMCC	1674[a]	12.1[a]	0.7	Steele et al., 1987, 1989
UC	1680[b]	16 ± 1	1.0	Blake and Rowland, 1988
CSIRO	1682[c]	12 ± 2	0.7	Fraser et al., 1986b, 1989
FIAER-CSIR	1612[d]	10.3 ± 0.4	0.6	Scheel et al., 1988

[a] 1988 data, OGC calibration
[b] 1987 data, UC calibration
[c] 1987 data, NBS calibration
[d] 1987 data, FIAER calibration

The zonally averaged distribution of methane in the remote marine boundary layer is shown in Figure 2.5-7, from 5 years of data from the GMCC sampling network, comprising 26 globally distributed sites (Steele et al., 1987). The seasonality in the Southern Hemisphere is very repeatable, as is the average latitudinal gradient.

New data have become available on past CH_4 levels. Using infrared solar spectra recorded at the Jungfraujoch Station, Switzerland, in 1951-52 and 1984-87 it has been shown that the total vertical column abundance of CH_4 increased by $0.7(\pm 0.2)\%$ per year during this period (Zander et al., 1989a). Ice core studies of historic CH_4 levels were reviewed in the OTP Report, which showed that over the past 300 years CH_4 levels have more than doubled. Further studies have been published which extend the CH_4 record back more than 100,000 years. Stauffer et al. (1988) show that the concentration of CH_4 was about 500 ppbv 100,000 years ago and fell to around 350 ppbv near the peak of the last ice age, 18,000 years ago, before rising to a typical Holocene value of about 650 ppbv. Raynaud et al. (1988) have extended the CH_4 record back to 160,000 years before present, and have shown that CH_4 was similarly low at the end of the preceding ice age. These results suggest a relationship between CH_4 levels and climate that may provide further clues in understanding modern CH_4 variability.

2.5.5 Carbon Monoxide

Carbon monoxide is an important trace gas in the troposphere because it plays significant roles in controlling the chemistry of ozone production and hydroxyl radical destruction in the lower atmosphere. It directly affects the oxidizing capacity of the lower atmosphere and can thus influence the concentrations of climatically important gases such as methane, for which oxidation by hydroxyl radical is a major sink.

Because of its short atmospheric residence time (2–3 months) the determination of a secular trend in CO mixing ratio is difficult. Increases are expected because significant CO sources are under human control, such as fossil fuel use, and have been growing (Cicerone, 1988). The available global CO data have
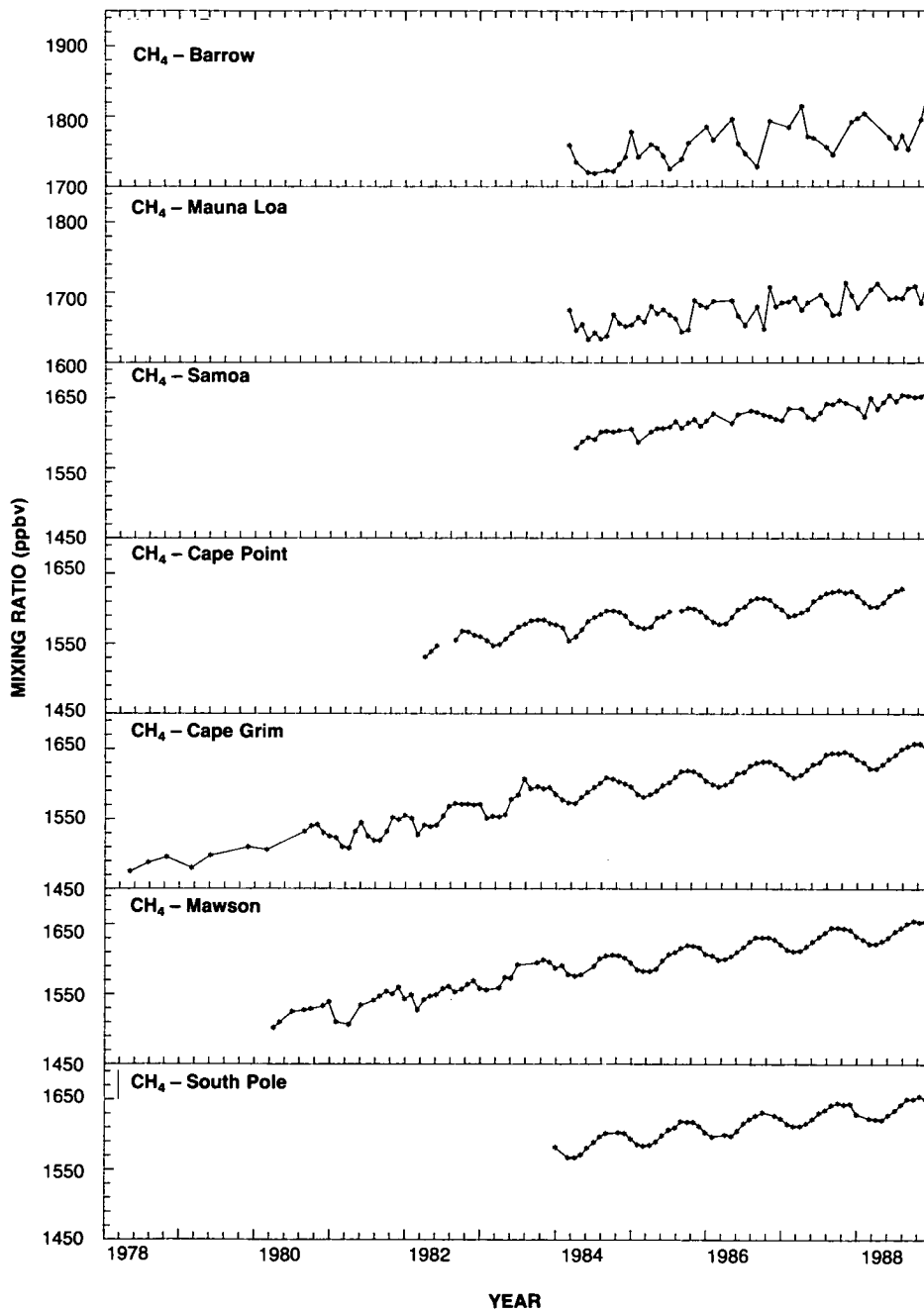
Figure 2.5-6. Long-term trends of CH_4 from the CSIRO global program (Fraser et al., 1986a, 1989) and the FIAER-CSIR program at Cape Point, South Africa (Scheel et al., 1988).

been reviewed (Cicerone, 1988; Ehhalt et al., 1989) suggesting that CO has increased in the Northern Hemisphere over the past 15–30 years, but data from the Southern Hemisphere show no significant or uniform trends. The data have been updated in Table 2.5-4 to include observations from the OGC and CSIRO sampling networks, as well as from Cape Point, South Africa. The CSIRO and FIAER-CSIR data are shown in Fig. 2.5-8.

Figure 2.5-7. The global distribution, seasonality, and trend of CH_4 from the GMCC network (Steele et al., 1987 and unpublished data).
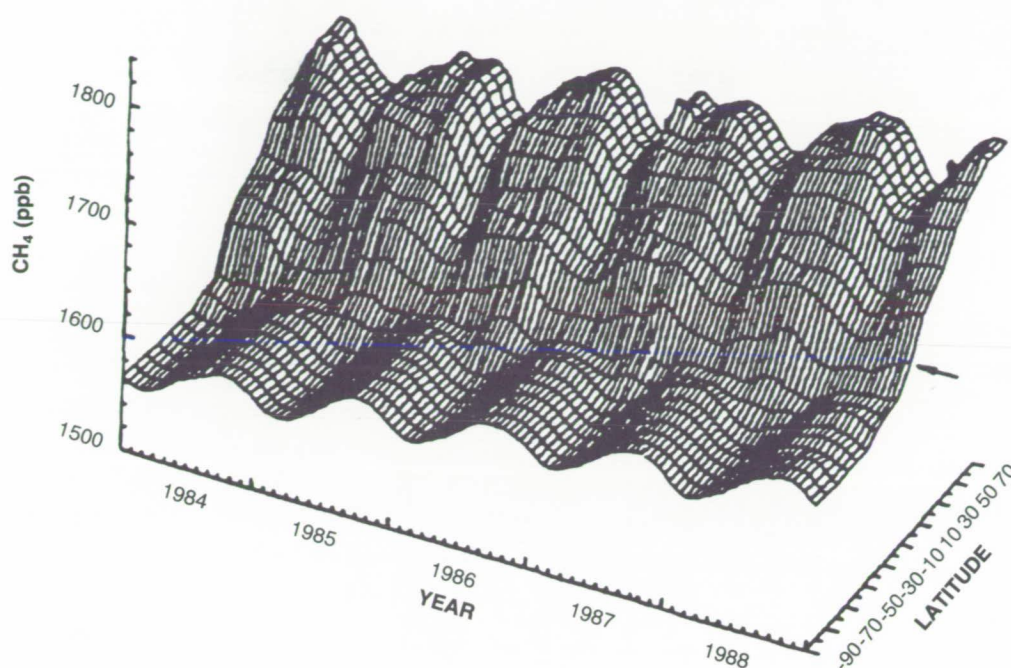
All data sets show statistically significant positive CO trends in the Northern Hemisphere of about 1% per year, except the relatively short records collected by CSIRO at Barrow and Mauna Loa, which do not show significant trends. The Southern Hemispheric data do not show consistent trends. The data collected by OGC (Khalil and Rasmussen, 1988b), over the period 1980–87, and CSIRO (1984–88) show a significant, positive trend at Samoa, but not at Cape Grim (CSIRO:1978–88). The relatively long records at Cape Point (1978–88) (Scheel et al., 1988) and Mawson (1980–88) do not show significant trends, whereas the relatively short CSIRO record at the South Pole shows a significant, positive trend. The mid-to-high latitude data from the Southern Hemisphere show remarkably uniform (amplitude and phase) seasonal variations (late summer minimum, winter maximum), which are probably in response to the hydroxyl radical sink (Fraser et al., 1986a,b; Ehhalt et al., 1989).

The secular increase of the total vertical column abundance of CO over Europe has been derived from sets of infrared solar spectra recorded at Jungfraujoch Station, Switzerland, in 1950–51 and in 1985–87. The mean cumulative rate of increase of the total column abundance of CO over this 35-year period was found to be 0.85 (± 0.2)% per year (Zander et al., 1989b). As Cicerone (1988) has pointed out, the detection of sustained temporal trends in atmospheric CO is very challenging. Atmospheric CO concentrations are strongly influenced by sources and sinks that vary greatly with season, latitude, and longitude. A successful trend-detection strategy must account for this variability and be capable of dealing with differences between continental and marine regions and between the planetary boundary layer and the free troposphere.

255

Table 2.5-4. Surface carbon monoxide concentrations and trends

Site	Lat.	Period	Conc. ppbv 1987	Trend %/yr ($\pm 2\,\sigma$)	Reference
Moscow	56°N	1952,53–1970,76		1	Dianov-Klokov & Yurganov, 1981
Northern Hemisphere		1970–82		1.5	Dvoryashina et al., 1984
Jungfraujoch	46°N	1950,51–1985–87		0.85(± 0.2)	Zander et al., 1989b
New Jersey	40°N	1968–77		positive	Graedel & McRae, 1980
OGC network[a]		1980–87			Khalil &
Northern Hemisphere			105	0.9(± 0.5)	Rasmussen, 1988b
Southern Hemisphere			50	1.9(± 0.8)	
Cape Point[b]	34°S	1978–88	60	0.1(± 0.2)	Scheel et al., 1988
CSIRO network[c]					
Barrow	71°N	1984–88	155	−1.5(± 2.3)	Fraser et al.,
Mauna Loa	20°N	1984–88	90	0.2(± 2.9)	1986a,b
Samoa	14°S	1984–88	65	3.4(± 2.0)	Fraser, 1989
Cape Grim	41°S	1978–88	60	−0.1(± 0.7)	
Mawson	68°S	1980–88	60	0.2(± 0.9)	
South Pole	90°S	1984–88	55	2.5(± 1.8)	

[a]OGC scale
[b]FIAER scale
[c]NBS scale

2.5.6 Carbon Dioxide

Carbon dioxide (CO_2) is the major greenhouse gas in the atmosphere whose abundance is changing in response to human activities. CO_2 plays a significant role in regulating the temperature of the stratosphere, which in turn influences stratospheric ozone chemistry and abundance. Precise atmospheric measurements of CO_2 have been made since the late 1950s, initially in Antarctica and at Mauna Loa, Hawaii, and presently by an international network of more than 40 sites. The increase of CO_2 in the background atmosphere over the past 15 years has been well documented.

Carbon dioxide data for 1987 from *in situ* analyzers are available from the GMCC network (Bodhaine and Rosson, 1988) and from Cape Grim, Tasmania (Beardsmore and Pearman, 1989). The global average mixing ratio in 1987 deduced from these sites is 348.1 ppmv, with a global average increase of 1.6 ppmv from 1986 to 1987. The long-term trends of CO_2 (1973–1987) from the GMCC sites are shown in Figure 2.5-9. On average, the global increase over this period has remained steady at about 1.5 ppmv per year, but at certain times and sites increases as large 3 ppmv per year and as small 0 ppmv per year have been observed. There are strong correlations between the rates of increase observed at these widely distributed sites.
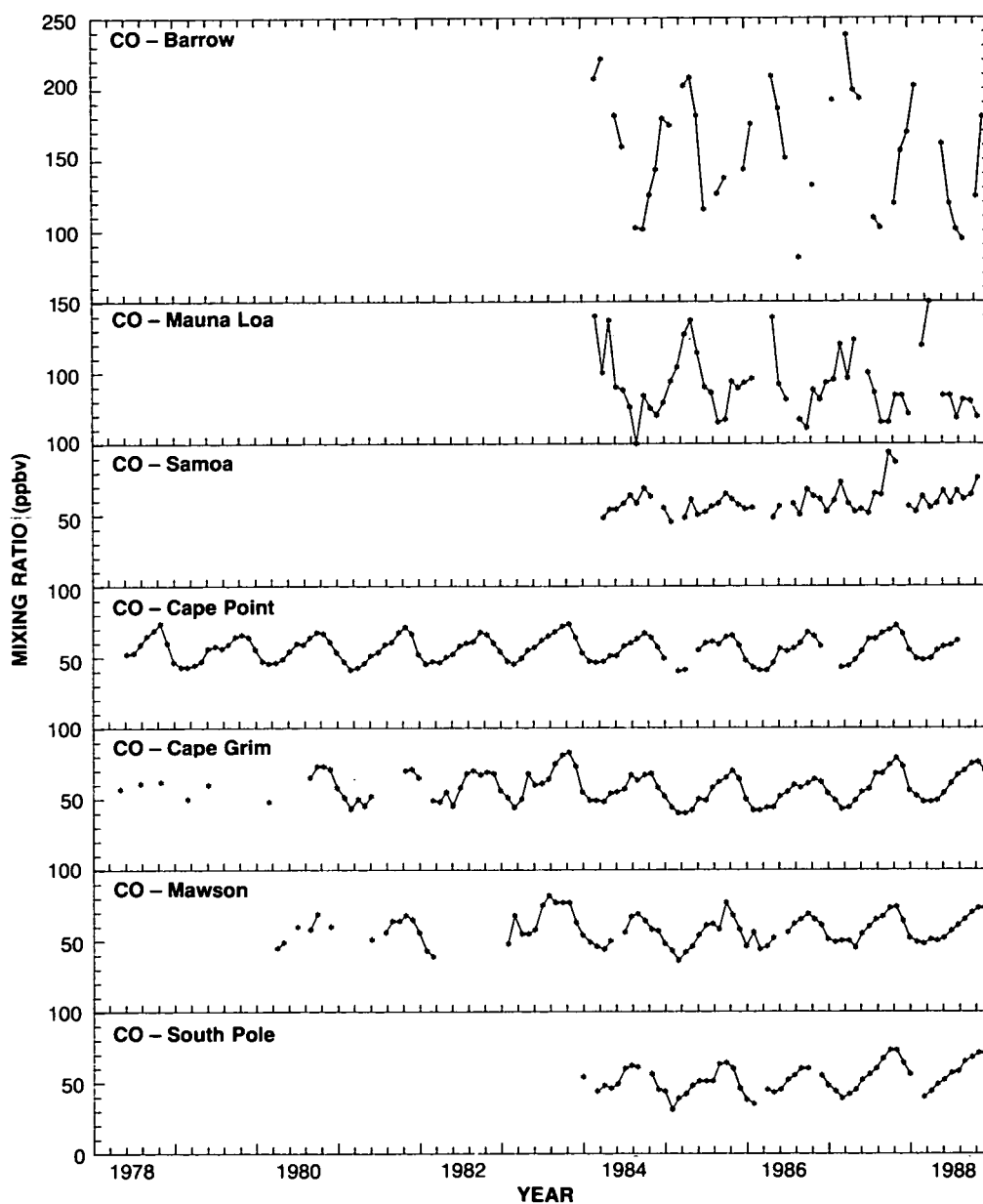
Figure 2.5-8. Long-term trends of CO from the CSIRO network and from Cape Point, South Africa (Fraser et al., 1986a,b, 1988; Fraser and Coram, 1988; Scheel et al., 1988).

Measurements of the global distribution of CO_2 from a network of 26 flask sampling sites (Conway et al., 1988) continued in 1987 (Bodhaine and Rosson, 1988). The global average concentration in 1987 from this network was 348.3 ppmv, and the global average CO_2 increase (1986 to 1987) was 1.9 ppmv.

2.5.7 Tropospheric Ozone

Tropospheric ozone impacts in several important ways on the tropospheric levels of source gases (Levy, 1971). Most notably, it is essential for the photochemical production of the hydroxyl radical, OH,
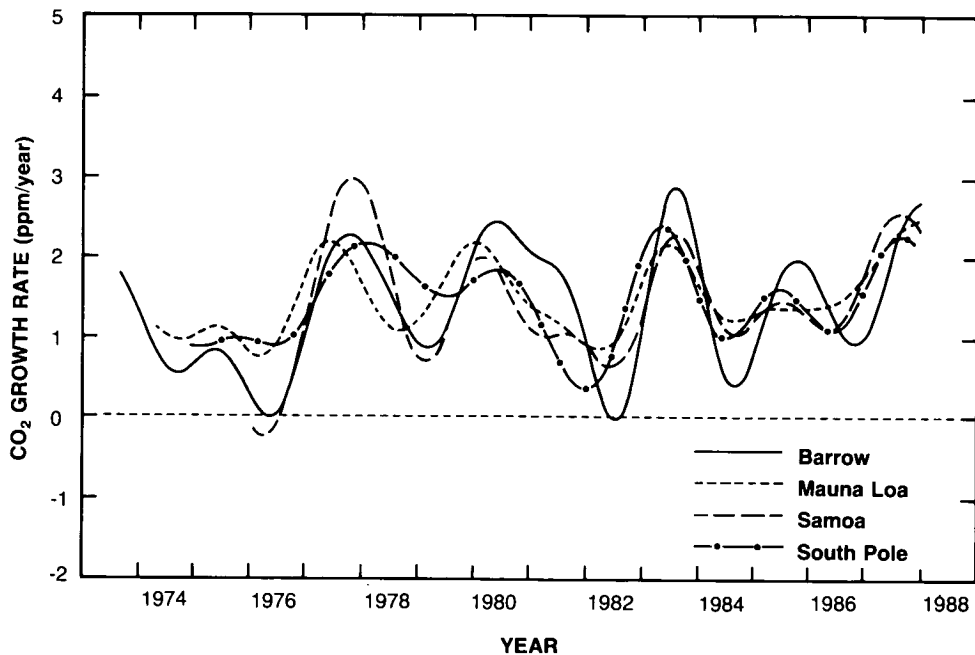
Figure 2.5-9. The temporal behavior of the CO_2 trends observed at the GMCC stations (Bodhaine and Rosson, 1988).

which determines the lifetime of many tropospheric trace gases, and thus also in part determines the ozone depletion potential of the hydrogen-containing source gases. In addition, tropospheric ozone makes a contribution of about 10% to the total ozone column in the atmosphere. Thus, a trend in tropospheric ozone has important consequences for stratospheric ozone concentrations and the detection of stratospheric ozone trends. Tropospheric ozone is also a significant greenhouse gas (Ramanathan et al., 1985).

In fact, a trend in tropospheric ozone, particularly in the Northern Hemisphere, is not unexpected. Ozone is produced photochemically in the troposphere and its precursors, nitrogen oxides, CO, CH_4, and non-methane hydrocarbons are known to have increased, mainly due to anthropogenic emissions (Gammon et al., 1986; Ehhalt et al., 1989).

The evidence for increases in tropospheric ozone has been reviewed (Logan, 1985; Bojkov, 1986, 1988; Penkett, 1988). The available observations on current trends in ozone at or near the Earth's surface are summarized in Table 2.5-5. They seem to support the expected positive trend in regions of the Northern Hemisphere. All seven European sites show statistically significant positive trends. However, all four Canadian sites show negative trends, of which only one is significant. All three Japanese sites show positive trends; two are significant. The Southern Hemispheric sites do not show statistically significant trends, except for the South Pole, which shows a significant negative trend. The central European trends reach as high as 3% per year. It should be noted that these trends fluctuate in time and that some of the European stations have exhibited a slowing down of the positive trends and even a decrease of ozone in recent years.

Only a few of the stations listed in Table 2.5-5 are clean air sites, making semi-continuous surface measurements (at least daily), namely Barrow and Mauna Loa in the Northern Hemisphere and Samoa, Cape Point, Cape Grim (Galbally et al., 1986) and the South Pole in the Southern Hemisphere. These stations are sited to represent large regional air masses. Data from these stations are shown in Figure 2.5-10. Both stations in the Northern Hemisphere show significant positive trends of 0.8% per year, indicating

Table 2.5-5. Surface ozone concentrations and trends deduced from ground based and balloon borne instruments

Site	Latitude	Period	Average Mixing Ratio (ppbv)	Trend %/yr ($\pm 2\,\sigma$)
Northern Hemisphere				
Resolute[a]	75°N	1966–85		−0.1(±0.1)
Barrow	71°N	1973–87	26[b,c]	0.8(±0.4)
Churchill[a]	59°N	1974–85		−0.7(±1.3)
Arkona	55°N	1956–84	19[d]	1.4(±0.8)
Edmonton[a]	54°N	1973–85		−0.1(±1.4)
Goose[a]	53°N			−1.1(±1.0)
Dresden	51°N	1952–84	10[d]	2.6(±1.6)
Kaltennordheim	51°N	1955–83	16[d]	3.1(±2.1)
Gr.Inselberg	51°N	1972–83	21[d]	3.1(±2.4)
Fichtelberg	50°N	1954–84	23[d]	1.1(±2.0)
Hohenpeissenberg	48°N	1974–86	31[b,d]	1.1(±0.3)
Hohenpeissenberg[a]	48°N	1969–86		2.3(±0.5)
Payerne[a]	47°N	1968–86		2.4(±0.8)
Sapporo[a]	43°N	1969–86		0.9(±1.1)
Tateno[a]	36°N	1969–86		1.3(±0.6)
Kagoshima[a]	32°N	1969–86		2.5(±1.0)
Mauna Loa	20°N	1973–87	27[b,c]	0.8(±0.4)
Southern Hemisphere				
Samoa	14°S	1976–87	14[b,c]	−0.3(±0.7)
Cape Point	34°S	1982–88	20[e]	0.3(±2.0)
Cape Grim	41°S	1982–86	24[f]	0.6(±0.7)
South Pole	90°S	1975–87	20[b,c]	−0.5(±0.4)

[a]sonde data
[b]nbar
[c]Oltmans and Komhyr, 1986; Bodhaine and Rosson, 1988
[d]Feister and Warmbt, 1987
[e]Scheel et al., 1988
[f]Galbally et al., 1986; Elsworth et al., 1988

that tropospheric ozone increases can be observed in sites remote from industrial emissions (Oltmans and Komhyr, 1986; Bodhaine and Rosson, 1988).

There are nine stations, two in Europe, three in Japan, and four in Canada which provide measurements of ozone in the free troposphere using balloon-borne ozonesondes. The data have been reviewed in Section 2.3-3 and are listed in Table 2.3-4. As indicated above, all European and Japanese stations exhibit positive trends and all Canadian stations exhibit negative trends. The Canadian data might be affected by an instrument change that occurred at all stations in the early 1980s (Bojkov, 1988). A previous analysis of these data (Tiao et al., 1986) showed some evidence for a positive trend of 0.8% per year in the lower troposphere. Averaging over all nine stations the current analysis shows a significant trend in the first three kilometers of 0.8(±0.5)% per year. Average trends in the troposphere above this altitude were not significant.
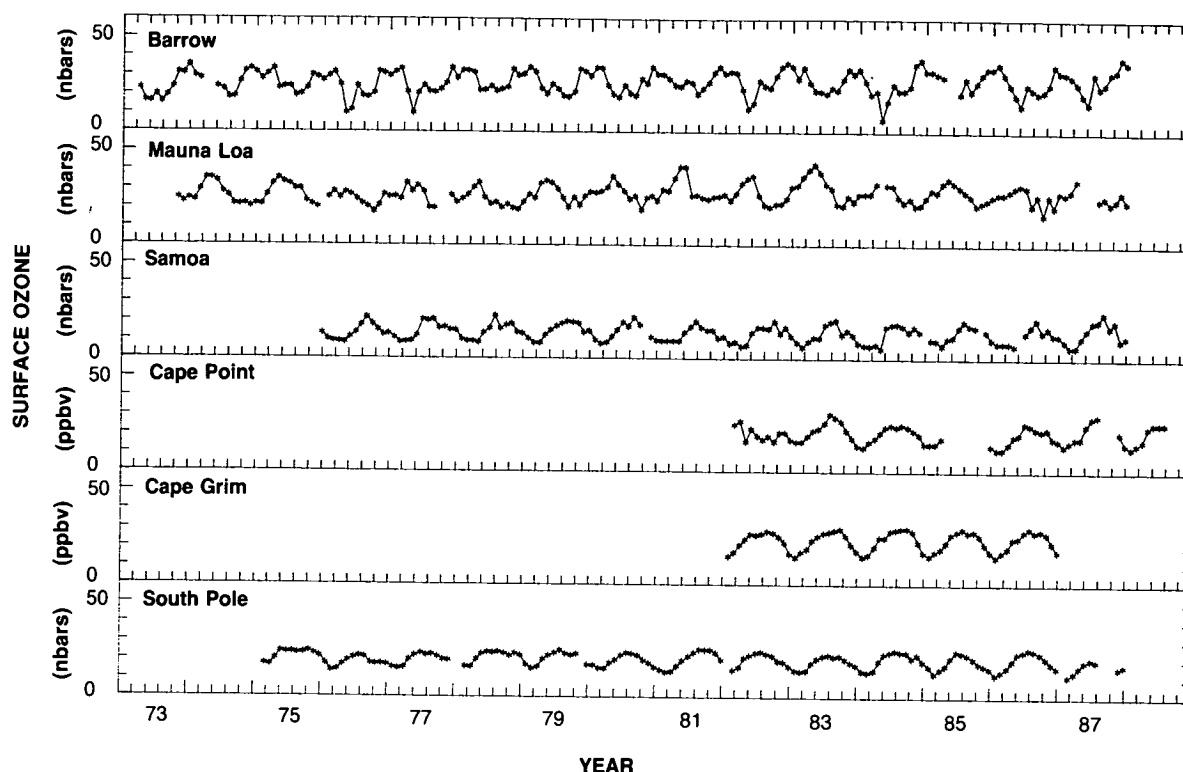
Figure 2.5-10. Surface ozone measurements at the GMCC stations (Olmans and Komhyr, 1986; Bodhaine and Rosson, 1988), at Cape Point, South Africa (Scheel et al., 1988), and at Cape Grim, Tasmania (Galbally et al., 1986; Elsworth et al., 1988).

In addition to the recent tropospheric ozone measurements, there are a few historic records of surface ozone measurements. The most important is a complete series of daily means collected at the Montsouris Observatory in Paris between the years 1876 and 1905. These data were re-analyzed by Bojkov (1986) and Volz and Kley (1988). The annual averages were shown to vary between 5 and 15 ppbv, about a factor of two lower than present ozone levels in a comparable environment.

None of the various pieces of evidence obtained so far and reviewed above provide convincing proof that ozone is increasing on more than a regional scale. When combined, however, they do suggest that ozone has been increasing over a wide scale in the Northern Hemisphere. On the other hand, the few measurements existing in the Southern Hemisphere indicate more or less constant ozone levels, which is not unexpected due to the low levels of ozone precursors observed in the Southern Hemisphere.

It has been suggested that typical tropospheric ozone variability means that the current ozonesonde network, and presumably the network of surface ozone measurement sites, are insufficient to detect a global trend in tropospheric ozone of about 1% per year at the 2 σ confidence level, even at stations with records a decade in length (Prinn, 1988b). To detect an ozone trend of 1% per year on a decadal time frame, daily measurements of ozone are required from approximately 40 sites, chosen to represent continental and marine, tropical, temperate, and polar air masses in both hemispheres (Prinn, 1988b). This will require a doubling of the current network. Measurements are particularly lacking from Africa, South America, and Asia. It would appear that similar requirements may be necessary for a suitable global CO network.

2.6 TRENDS IN STRATOSPHERIC AEROSOLS

2.6.1 Introduction

Chapter 10 of the Ozone Trends Panel Report (OTP) presented a detailed description of stratospheric aerosols, their properties, and their possible effects on ozone and ozone observations. The specific objectives of the chapter were: (1) to define the fundamental characteristics of stratospheric aerosols, particularly their morphological, radiative, and chemical properties; (2) to analyze long-term aerosol data bases for possible trends that might influence the identification or interpretation of long-term ozone trends; (3) to assess the transient impacts of volcanically generated aerosols on remote sensing observations such as Umkehr and SBUV measurements over the last two decades, and to consider possible schemes for correcting aerosol errors in these baseline ozone data records; and, (4) to describe polar stratospheric clouds (PSCs) in terms of their frequency, spatial extent duration, and physicochemical properties, on the basis of observational and theoretical studies.

The purpose of this section of the present assessment is to review the findings of the OTP Report, and bring the reader up to date regarding any new or extended aerosol data. Chapter 1 of this assessment on polar ozone described in detail the climatology of PSCs in both polar regions, their physical properties, and heterogeneous phase chemistry involving PSCs. Thus, this section will not include any discussion of PSCs.

2.6.2 Stratospheric Aerosols

With the data available at the time of the OTP Report, no significant trends were detected in the properties of the global background stratospheric aerosol layer. Figure 1.2-30 in Chapter 1 of this document plots the SAM II stratospheric optical depth at a wavelength of 1 μm for the period November 1978 through February 1988 for the Arctic and Antarctic regions. Figure 10.7 in the OTP Report showed the SAM II data record through only 1986. Evident from these figures is the rapid impact of volcanic eruptions and their subsequent slow decay. Over this time period, the strongest impacts were experienced in the Arctic but for the case of El Chichon (17.3°, 93.2°W), which erupted in April 1982, both hemispheres were strongly perturbed.

These enhanced aerosol levels from volcanic eruptions can dramatically and deleteriously impact remote sensors. For example, after the eruption of El Chichon, sea surface temperature retrievals from AVHRR were adversely impacted by as much as a few degrees (Strong, 1984). Similarly, the retrieval of ozone profiles from Umkehr and SBUV measurements were affected, complicating the interpretation of these remote sensing data, especially when used to determine long-term changes or trends. Obviously, as Figure 1.2-30 shows, the El Chichon eruption caused the largest perturbation to stratospheric aerosols experienced over this last decade, but even the impact of smaller eruptions must be understood in order to remove their effects from various data sets. The problem is to determine when the aerosol loading is low enough not to adversely affect the interpretation of the particular sensor's data. The last eruption thought to have caused a level of perturbation similar to that experienced after the eruption of El Chichon was the March 1963 eruption of Agung (8.3°S, 115.5°E).

Routine balloon and lidar aerosol measurements of the stratosphere began in the late 1960s and early 1970s. These long-term measurements have been obtained primarily in the Northern Hemisphere with some short-term data records in the Southern Hemisphere. All these measurements have shown the period of 1978 to 1979 to be lowest on recent record. Therefore, this period has been referred to by most

investigators as a background period for stratospheric aerosols. In the strictest sense, however, with a data record of only 20 years, no one can definitively claim this to be a true background period.

As of this writing, mid-1989, the SAM II record and the lidar record from the NASA Langley Research Center shown in Figure 2.6.1, as well as other similar records, show values that have gradually approached, albeit not yet reached, the values measured in 1978–1979. Since the El Chichon eruption, the only other eruption to significantly perturb the global stratospheric aerosol was the eruption of Ruiz ($4.9°N$, $75.4°W$) in November 1985. The Ruiz enhancement was similar to the enhancement caused by the Mount St. Helens ($46.2°N$, $122.2°W$) eruption of May 1982 and, therefore, most likely has delayed somewhat the recovery from the El Chichon eruption. For example, the present value at Langley for peak backscatter ratio at a laser wavelength of 694 nm, is about 1.2, which represents a 20% enhancement over molecular scattering. In early 1979, this ratio was 1.08 for an 8% enhancement. These are to be compared to the peak backscatter value in late 1982 of 24, which was caused primarily by El Chichon. Integrated backscatter over the stratosphere is also used to describe lidar results. It provides a measure of stratospheric total column loading versus time over the lidar site. Values in 1989 have fallen to $0.8 \ 10^{-4}sr^{-1}$ from peak values in early 1983 of $27 \ 10^{-4}sr^{-1}$. Values in early 1979 were only $0.4 \ 10^{-4}sr^{-1}$. The SAM II results are similar, with lowest Antarctic optical depths measured in October 1979 of $0.5 \ 10^{-3}$ compared to $1.7 \ 10^{-3}$ in October 1988, and lowest Arctic optical depths of $1.2 \ 10^{-3}$ in February 1979 compared to $1.7 \ 10^{-3}$ in February 1989. Although the 1978–1979 aerosol minimum values have not yet been reached, there is no hard evidence that they will not be reached again, and therefore, there is no evidence that an upward trend in "background" stratospheric aerosols has occurred.

2.6.3   Global Heterogeneous Effects

Recently, Hofmann and Solomon (1989) suggested that stratospheric aerosols, especially during periods enhanced by volcanic eruptions, could possibly cause an ozone depletion through heterogeneous chemistry similar to that occurring on PSCs. They reached this conclusion because recent laboratory studies suggest that the same reactions that occur on PSCs in the cold Antarctic stratosphere, can also
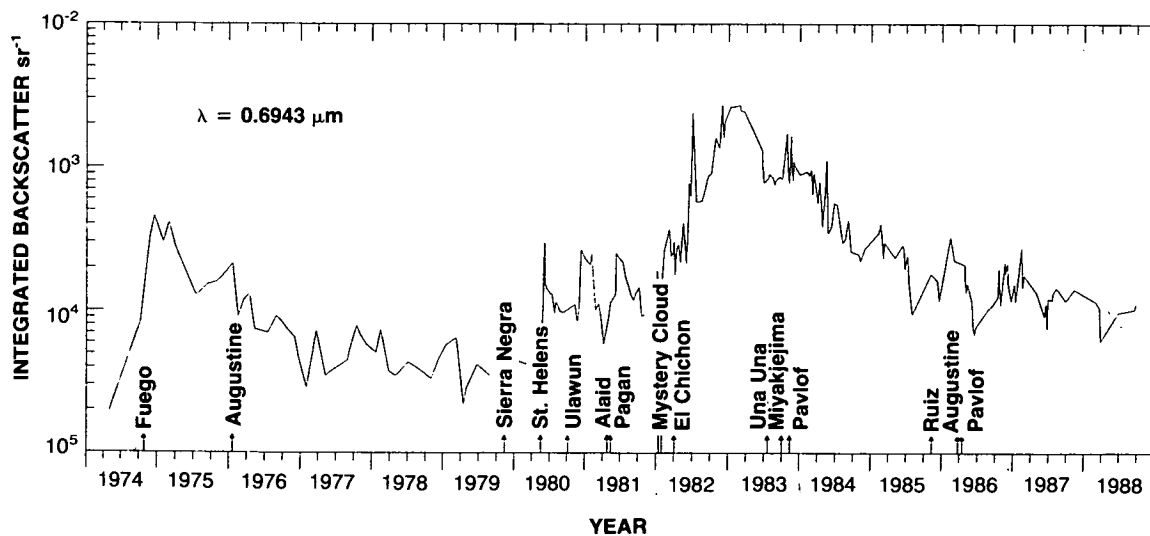

Figure 2.6-1. Aerosol integrated backscatter coefficient over the period 1974-1988 as observed by the NASA Langley Research Center lidar.

262

take place on sulfuric acid particles present at all latitudes (although at lower rates), and because all the reduction in stratospheric ozone observed at northern mid-latitudes in late 1982 and most of 1983 following the El Chichon eruption cannot be accounted for by considering other known mechanisms. Their model calculations indicate that these reactions will be of greatest potential importance in the middle-to-high latitudes in winter, where the reported total ozone trends (see Section 2.2) are largest and the ozonosonde measurements show record lows after El Chichon. Their results also predict substantial decreases in NO_2 abundances following El Chichon, particularly at middle latitudes in winter. Recall from Chapter 1 that decreases in total odd nitrogen are predicted to be an essential element in Antarctic heterogeneous ozone loss. At Boulder, Colorado (40°N) total column NO_2 measurements showed a pronounced decrease, coincident with the poleward movement of the El Chichon cloud in late 1982. The results from Hofmann and Solomon also show high HNO_3 abundances at mid-to-high latitudes in winter, in agreement with the 1978–79 LIMS HNO_3 measurements but not with current "non-heterogeneous" models.

The possibility of this heterogeneous chemistry extending to the global stratospheric aerosol, especially after a large volcanic eruption, makes it even more urgent that scientists understand these heterogeneous reactions as they apply to ozone depletion.

2.7 SURFACE ULTRAVIOLET RADIATION

2.7.1 Predicted Trends Related To Column Ozone, 1970–1986

Several processes act to attenuate solar ultraviolet radiation as it propagates through the atmosphere. The most important of these is absorption by ozone located in the stratosphere and troposphere. However, scattering by molecules, aerosols, and especially by clouds is significant, while absorption by gaseous air pollutants in the troposphere (NO_2, SO_2) should be considered at some locations. A long-term change in the abundances of any of the absorbers or scatterers as well as in the surface albedo will lead to a trend in ultraviolet irradiance at the Earth's surface.

The total downward irradiance at any wavelength is the sum of direct and diffuse components, where the latter consists of photons which have been scattered one or more times. The direct irradiance depends on the total column ozone along the path from the sun to the ground and is readily computed from Beer's Law. Calculation of the diffuse component of irradiance requires solution of the radiative transfer equation and must consider the relative importance of scattering and absorption at each altitude. In general, absorption by ozone reduces the surface irradiance to negligible levels at wavelengths shorter than 295 to 300 nm. Backscattering of sunlight to space by clouds reduces the surface irradiance by roughly a constant factor at all wavelengths. To a first approximation the surface ultraviolet irradiance varies linearly with fractional cloud cover, and typical values under a completely cloud covered sky are less than 50% of those for clear skies (Mo and Green, 1974; Ilyas, 1987).

Figure 2.7-1 presents the solar spectral irradiance at the Earth's surface for January and July at latitudes 34.5, 46.0, and 58.5 degrees North computed from the model of Frederick and Lubin (1988). The latitudes correspond to the centers of the bands used by the Ozone Trends Panel (OTP), being 30–39, 40–52, and 53–64 degrees North. All values in Figure 2.7-1 refer to local noon and clear sky conditions. The natural ultraviolet radiation environment at the Earth's surface is characterized by large variations with month and latitude. The sharp decrease in irradiance at wavelengths shorter than 330 nm results from absorption by ozone, and spectral structure between 310 and 330 nm arises from the Huggins bands.
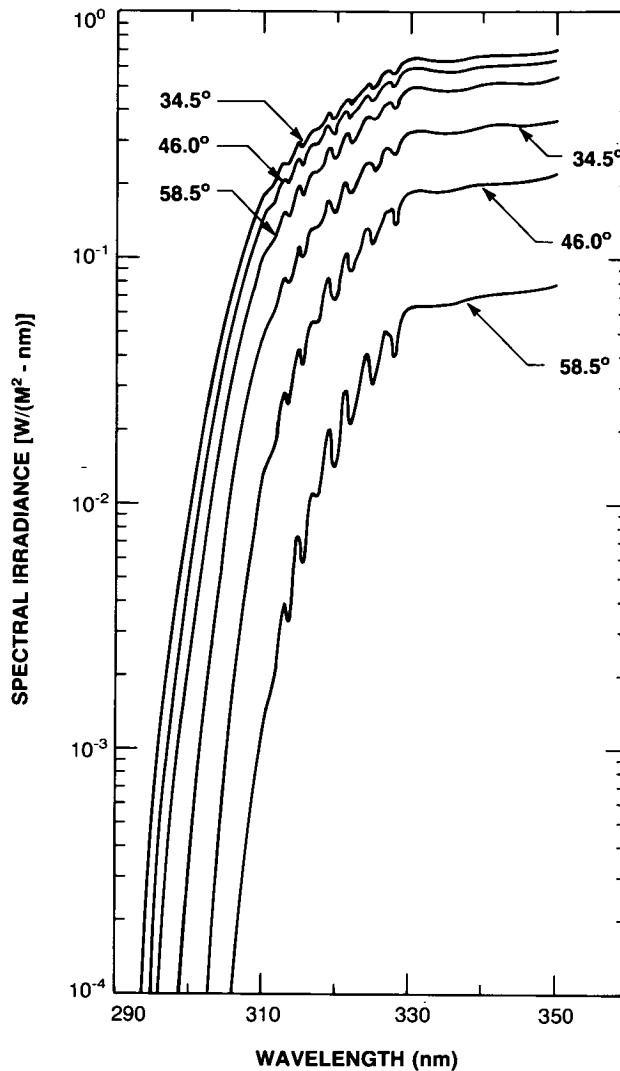
263

Figure 2.7-1. Solar spectral irradiance incident on the Earth's surface computed for January and July at latitudes 34.5°, 46.0°, and 58.5°N. Calculations refer to clear skies, local noon, and serve as baseline cases appropriate to the year 1970. The top three curves refer to July and the bottom three refer to January.

The Ozone Trends Panel reported a percent change in column ozone for each month of the year over the period 1970 through 1986 in the latitude zones defined above. Table 2.7-1 lists these for the three latitudes represented in Figure 2.7-1 during the months of January, March, and July. Imposed on the long-term trend are variations related to the solar cycle, the QBO, and a random interannual variability. The calculations reported below include only the linear trend component.

Figure 2.7-2 presents the percent changes in noontime surface irradiance attributable to the trend in total ozone between 1970 and 1986. These calculations refer to clear skies, include only the decrease in column ozone, and neglect changes in the profile shape. All curves in Figure 2.7-2 show the expected

264

Table 2.7-1. Percent Changes in Total Column Ozone, 1970–1986, Used in the Radiative Transfer Calculations*

| | Latitude Band | | |
Month	30–39°N (%)	40–52°N (%)	53–64°N (%)
January	−2.2	−2.6	−8.3
March	−3.5	−5.6	−4.0
July	−1.3	−2.2	0.0

*Values from NASA (1988)

increase in percent change as wavelength decreases. In addition, a given percent change in ozone has an increasing impact on surface irradiance as the sun nears the horizon. In general, the largest percent changes occur at wavelengths where the absolute irradiances are small. At wavelengths longer than 330 nm, a trend in total ozone has negligible influence on the surface irradiance.

When the sun is high in the sky, as in summer, it is possible to experience a decrease in ultraviolet irradiance at the ground even with a decline in column ozone. This would arise from a change in the shape of the ozone profile, not included in Figure 2.7-2, and requires an increase in tropospheric ozone, which only partially offsets a reduction in the column at higher altitudes (Bruhl and Crutzen, 1989). The presence of aerosols and clouds leads to efficient scattering of the direct solar beam. This increases the effective path length taken by radiation through the lower atmosphere and consequently enhances absorption by tropospheric ozone (Frederick and Lubin, 1988).

2.7.2 Observed Trends in Surface Ultraviolet Radiation

Scotto et al. (1988) performed a trend analysis of ultraviolet irradiance data collected by a network of eight Robertson-Berger (RB) meters located over the United States from latitudes 30.4 to 46.8 degrees North. The time period covered was 1974 through 1985. The RB meter responds to broadband radiation convolved with an instrument response function which covers the spectral region from the ozone cutoff near 295 nm to approximately 340 nm. The RB data base indicates no increase in irradiance over the 12-year period, and decreases statistically significant to the ±2 σ confidence level or higher occurred at five of the stations. The discussion below assumes that the derived trend in irradiance is a real atmospheric phenomenon. However, a thorough evaluation of the long-term stability of the RB meter network would be of value.

The numerical analysis of Scotto et al. (1988) was based on the annually integrated RB meter response at each station. The large annual cycle evident in Figure 2.7-1 implies that the annually integrated value receives its greatest contribution from the summer months. This is the season in which Dobson data show little change in total ozone over North America between 1970 and 1988 (see Table 2.2-5). However, Scotto et al. (1988) also examined RB readings by individual months and still found decreases in surface irradiance. The output of the RB meter includes substantial contributions from solar irradiance at wavelengths where absorption by ozone is weak. The meter is therefore not a sensitive indicator of small changes in atmospheric ozone content. With the RB meter response function from Caldwell et al. (1986), the 2.2% decrease in ozone for 40–52 degrees North during July between 1970 and 1986 implies a 1.5–1.6% increase in RB meter response. The 5.6% decrease in ozone during March would appear as a 4.7–4.8% increase in RB output.
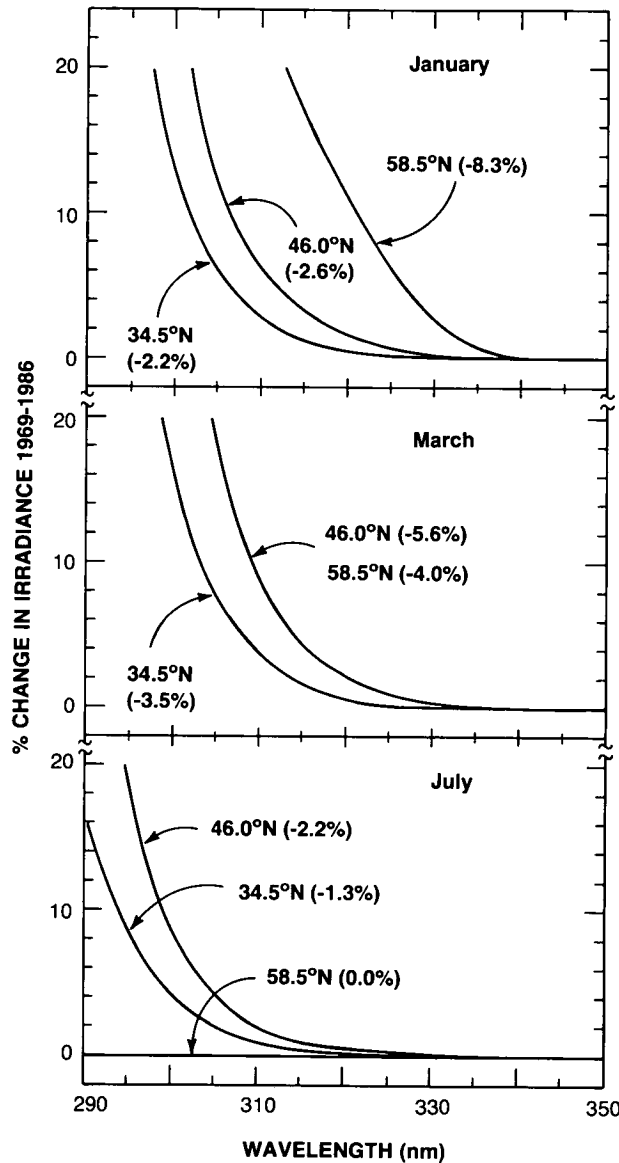
Figure 2.7-2. Percent changes in solar spectral irradiance between 1970 and 1986 computed for January, March, and July at latitudes 34.5°, 46.0°, and 58.5°N. Calculations include only the linear trend in ozone for a given month between 1970 and 1986. The percentage changes in ozone appear in parentheses. Curves for 46.0°N and 58.5°N in March are indistinguishable.

Given that cloud cover, aerosols, localized sources of air pollution, and likely increases in tropospheric ozone influence ground-based radiation measurements, it is not surprising that the RB meter network did not observe an increase in irradiance related to the downward trend in total ozone. The RB results are nonetheless very significant. In particular, they show that a trend in total ozone need not appear as an obvious trend in surface ultraviolet irradiance. The role of cloudiness and other factors that influence the transmission of the troposphere must be considered as well. The major conclusion here is that the results of the RB meters do not contradict the observed downward trend in ozone presented in Section 2.2.

2.8. OUTSTANDING ISSUES

Although a large amount of data has been collected over many years by instruments whose characteristics are reasonably well known, few of these instruments were made for the purpose of determining trends or long-term changes. Taking into account the deficiencies of the present observation system and looking to the future, priority should be given to a system approach based on the complementarity of ground-based and satellite observations. Both total column and vertical distribution satellite measurements of ozone should be checked for instrumental drifts by comparison with a network of carefully calibrated ground-based instruments based on both passive—Dobson, UV, IR, and microwave spectrophotometers—and active-lidar systems. The implementation of such a Network for Detection of Stratospheric Changes requires an internationally coordinated effort with a long-term commitment for scientifically driven operation of the stations. Special attention should be paid to the present dramatic lack of measurements outside of the band from 30 to 60 degrees in the Northern Hemisphere as reflected in particular in the absence of trend determination in the tropical regions. It is therefore of prime importance to establish new sites with an appropriate geographical distribution that takes into account the latitudinal and regional patterns already revealed by the present data analyses. Furthermore, the measurements should not be limited to stratospheric ozone. Data on the vertical distribution of ozone in the troposphere are, for example, required to take into account a possible trend in this atmospheric region. Additional atmospheric variables such as temperature or aerosols have been shown in this report to be of direct influence on the ozone trend. Their measurements will also be complemented by those of selected stratospheric trace gases that are required to quantitatively relate the observed ozone trend to anthropogenic influence. This can be illustrated by the present difficulty in interpreting for example the observed variations of hydrogen chloride (HCl), over the past 15 years.

Based on observed annual changes in CFCs and chemical partitioning arguments, it is expected that HCl should be increasing in the stratosphere at an annual rate of about 3.5%. Insufficient data exist, however, to confirm this important prediction. The longest data records have been collected from aircraft over the period 1978 to 1982 by Mankin and Coffey (1983) and from the Jungfraujoch station over the period 1976 to 1985 by Zander et al. (1987a). Both sets of observations were taken in the solar absorption mode using a high-resolution Fourier transform spectrometer and grating spectrometer, respectively. The Mankin and Coffey (1983) results give an indicated annual increase of 5% in column amount, but the estimated uncertainty in using the data to determine long-term change is 9% (2 σ) per year when factors such as frequency of observations, length of data record, and long-term stability of absolute and relative calibration procedures are considered (Prinn, 1988a). The uncertainty estimate is probably conservative. Zander (1989, private communication) reports that the largest increase that can be derived from the ground-based results is 1.5% per year after seasonal effects are removed from his data spanning the 1976 to 1985 time interval. Prinn (1988a) estimates the uncertainty in using these data for detection of long-term changes to ±2% per year (2 σ). Similar Jungraujoch data covering the period 1985 to 1989 indicate a significantly larger trend than the one mentioned above (Zander, 1989, private communication). Tropospheric HCl could make some contribution to the measured total column but, since the Jungfraujoch station is at a 3.5 km altitude, this effect should be relatively small. Both the aircraft and ground-based data sets show an HCl increase with time over the period of their respective data records which is greater than the individual measurements error bars, but they each imply different rates of increase, and their use in quantifying yearly changes leads to uncertainties that preclude verification of the expected annual HCl increase. A much broader space and time sample, combined with the investigations of sporadic potential natural sources of HCl (e.g., volcanic eruptions), is required to address this question. A less definitive, but useful, test of anthropogenic contributions to the stratospheric halogen budget is provided by contemporary measurements of the HCl/HF ratio. Since substantially all of the HF in the present-day stratosphere is of anthro-

267

pogenic origin, while part of the HCl input is natural, the HCl/HF ratio at any time gives an indication of the anthropogenic input. Measurements covering the period 1977 to 1985 indicate mid-latitude values for this ratio of about 4 to 6 (Zander et al., 1987b), in satisfactory agreement with models and indirectly, therefore, supporting the predicted 3.5% annual change in HCl.

Finally, if technology advances and improvements to old techniques will lead to the implementation of newer and better observing systems, these often require 10 to 15 years before homogeneous data series of at least a decade can be available for trend analyses. It is therefore critically essential that existing measurement programs be maintained and their homogeneity in time be improved. In addition, efforts must be expended to develop a full understanding of the differences between data series from the old and new instruments so that a full-length homogeneous data record can be established to facilitate trend analyses as the newer systems take over from the old ones to provide the mainline data record.

APPENDIX 2.A

2.A.1   Seasonal Trends Model (Total Ozone)

The full statistical model for a monthly ozone series, y_t, , $t = 1,2,\ldots, T$, for the multiple trends case is given by:

$$y_t = \sum_{i=1}^{12} \mu_i I_{i,t} + \sum \beta_i I_{i,t} R_t + \gamma_1 Z_{1;t} + \gamma_2 Z_{2;t-k} + \gamma_3 Z_{3;t} + \gamma_4 Z_{4;t} + N_t \qquad (A1)$$

where:

μ_i = ozone mean in month i, i = 1...12,

$I_{i;t}$ = indicator series for the ith month of the year,
= 1 if month t corresponds to month i of the year
  0 otherwise

β_i = trend in Dobson units per year after 12/69 in month i of the year,

R_t = linear ramp function beginning in 12/69,
  $(t - t_o)/12$ if $t > t_o$, where t_o corresponds to 12/69
  0 if $t < t_o$

$Z_{i;t}$ = solar series minus 120 flux units (minus 120 so that percentage trends will be based on ozone at mid solar cycle),

$Z_{2;t-k}$ = QBO series lagged k months

$Z_{3;t}$ = nuclear weapons series

$Z_{4;t}$ = intervention for calibration shift (some stations, when using the original published data),
  1 after the shift
=
  0 before the shift

γ_t = coefficients to be derived for each Z term , i = 1, 2, 3, 4

N_t = residual noise series

There is a month-to-month correlation in ozone values, even after the seasonal and other effects in equation (A1) have been removed, i.e., in the N_t series. This is modeled by allowing N_t to be an autoregressive series of order 1:

268

$$N_t = \phi \, N_{t-1} + e_t \tag{A2}$$

where e_t is an uncorrelated series (See Box and Jenkins, 1976; Tsay, 1984).

The noise series N_t is much more variable in winter than in summer. This is accounted for in the statistical model by fitting the above equation with individual months weighted inversely proportional to the monthly variances of the N_t; for example, all Januarys get the same weight (the UW&C model uses weights applied to the e_t series rather than the N_t series).

Estimated changes in ozone reported in Table 2.2-1 are given as cumulative percent changes over the 17-year period 1970-1986 inclusive, to be comparable to results reported in the OTP summary:

$$
\begin{aligned}
\omega_i &= \text{17-year change in month i in percent} \\
&= \frac{17 \times \beta_i}{\mu_i} \times 100\%
\end{aligned}
\tag{A3}
$$

Percent changes for the winter months (December through March), the summer months (May through August), or the whole year are the average of the percent changes in the corresponding months.

In other tables, trends are given in percent per decade, with 17 years replaced by 10 years in equation (A3).

2.A.2 Uniform Trends Model (Total Ozone)

The uniform trends model is similar to equation (1), except that the coefficient β of the ramp function is the same for all months of the year:

$$y_t = \sum_{i=1}^{12} \mu_i I_{i;t} + \beta R_t + \gamma_1 Z_{1;t} + \gamma_2 Z_{2;t-k} + \gamma_3 Z_{3;t} + \gamma_4 Z_{4;t} + N_t \tag{A4}$$

The percent change over the 17-year period for the uniform model is given by:

$$
\begin{aligned}
\omega &= \text{17-year change in percent (uniform model)} \\
&= \frac{17 \times \beta}{\text{Ave}_i\{\mu_i\}}
\end{aligned}
\tag{A5}
$$

Trends expressed as percent per decade replace 17 years with 10 years in equation (5).

Monthly weighting is done as described in the previous section.

2.A.3 Regional Models (Total Ozone)

The individual station trend results may be combined within regions (North America, Europe, Japan) to give estimates of regional trends. The methodology, given in Reinsel et al. (1987), calculates the regional trend as a weighted average of the individual station trends. The station weights are functions of the trend uncertainties at each station and the spread among the station trends, with stations with less precisely measured trends (e.g., from shorter records or more variable data) receiving less weight.

269

The ozone trends in each of the regions are expressed as a random effects model

$$\omega_j = \omega + \theta_j + \epsilon_j \tag{A6}$$

where ω_j is the trend estimate of the jth station (either year-round or by season), θ_j is a random term accounting for station-to-station differences, and ϵ_j represents statistical variation in the trend due to within-station noise.

2.A.4 Regional/Latitudinal Models (Total Ozone)

The regional differences in the trends can be assessed simultaneously with a latitudinal dependence by using the model

$$\omega_{ij} = \delta_o + \delta_1 \, (L\text{-}45°N) + \alpha_i + \theta_{ij} + \epsilon_{ij} \tag{A7}$$

where ω_{ij} is the trend estimate at the jth station in the ith region, L is latitude, α_i is a random term representing region-to-region variation in the trends, θ_{ij} is a random term representing station-to-station variation in the trends, and $\delta_o + \delta_1$ (L-45°N) provides for a linear relationship between the trend estimates and latitude (L) where δ_o and δ_1 are the intercept and slope, respectively. Also, ϵ_{ij} is the statistical error in the jth station trend estimate within the ith region.

2.A.5 Empirical Aerosol-Adjustment Model (Umkehr)

In the empirical aerosol-adjustment approach, the models for the Umkehr data are of the following form:

$$y_t = \mu + S_t + \omega \, x_t + \gamma_1 \, z_t + \gamma_2 \, \mu_{t\text{-}l} + N_t \tag{A8}$$

where y_t, t = 1, ..., T denote the monthly averages of Umkehr profile ozone data at a particular layer and a particular station, $\mu_t = e^{-\tau_t} - 1 \approx -\tau_t$ is a transformation of the composite optical thickness series τ_t and is similar to atmospheric transmission values (see Figure 2.3-5). The value l in (A8) is a time shift in the monthly transmission (optical thickness) series over the period; for the period of study, the values of l used were $l = 1$ month for the station Belsk, $l = 0$ for Arosa, Edmonton, and Boulder, $l = -1$ for Lisbon, Sapporo, Tateno, and Kagoshima, and $l = -6$ for New Delhi and Poona. The other terms in the model are S_t, which represents the seasonal annual and semi-annual sinusoidal components, x_t, which represents the $F_{10.7}$ solar flux series, and z_t, which is the hypothesized deterministic linear trend through the period 1977–1987. Thus, this model allows for a linear relation between the Umkehr data and the composite transmission (optical thickness) data during the period 1977–1987 involving the El Chichon volcano to account for errors in the Umkehr data due to volcanic aerosols. For the station Kagoshima, a simple intervention level shift term, starting in January 1986, was also included in the model to account for a possible change in mean level associated with a change of instrument at that time. (The data for Boulder also suggest a possibility of a mean level shift around the early part of 1982, possibly related to a change to the automated Dobson No. 61 instrument at the beginning of 1982. But such an effect has not been considered in the analysis because there is no definite confirmation of such a possible effect). Also, for the station Lisbon, data were not used prior to 1978 because of a level shift in the data before that time due to a calibration change. As there were a substantial number of missing months in the Umkehr data series for most stations, for convenience an autoregressive process only of order one was considered for the noise term N_t,

$$N_t = \phi \, N_{t-1} + \epsilon_t,$$ (A9)

where the ϵ_t are independent with mean 0 and constant variance σ_t^2.

2.A.6 Theoretical Aerosol-Adjustment Model (Umkehr)

In the theoretical model approach, the monthly average Umkehr data y_t were first corrected for aerosol errors using the error correction factors supplied by DeLuisi et al. (1989a), which resulted in the corrected Umkehr data series denoted as y_t^*. It is noted that the error correction factors were applied to data at the various stations with the same time shift l as the value used in model (A1). For the corrected data, models of a similar form to (A8), but without the empirical aerosol error adjustment factor $\gamma_2\mu_{t-l}$, were considered:

$$y_t^* = \mu + S_t + \omega x_t + \gamma_1 z_t + N_t$$ (A10)

2.A.7 Trends Model Applied to Ozonesonde Data

For each of the 15 layers at each of the 9 stations the following regression model has been used:

$$y_t = \mu + S_t + \omega x_t + \delta u_t + N_t$$ (A11)

where y_t is the average of ozone for month t, m is a constant term, S_t is a seasonal component consisting of annual and semi-annual sinusoidal terms, ωx_t is a trend term, δu_t is a level shift term and N_t is a noise term. The trend term ωx_t is such that $x_t = 0$, $t < T_o$ and $x_t = (t - T_o)/12$ for $t > T_o$, where T_o is December, 1969; thus ω is a parameter representing annual rate of change since 1970. The level shift term δu_t, where $u_t = 0$ for $t < T_l$ and $u_t = 1$ for $t > T_l$ with T_l signifying the time and δ representing the magnitude of the level shift, is used for all layers at the four Canadian stations to account for possible systematic changes in ozone readings due to changes of the sonde instrument from BM to ECC. It is also used for layers 1A–1D at Payerne with $T_l \approx$ April 1977 for possible effects due to the change of ozonesonde release time. Finally, the errors N_t's are assumed to be normally and independently distributed with zero means but having different variances for the 12 months of the year.

REFERENCES

Aimedieu, P., W. A. Matthews, W. Attmanspacher, R. Hartmannsgruber, J. Cisneros, W. Komhyr, and D. E. Robins, Comparison of in situ stratospheric ozone measurements obtained during the MAP/GLOBUS 1983 campaign, *Planet. Space Sci., 35*, 563-568, 1987.

Ancellet, G., A. Papayannis, J. Pelon, and G. Megie, Tropospheric ozone lidar measurements, in *NATO Workshop on Tropospheric Ozone,* Lillehammer, Norway, 1987, edited by I. S. Isaksen, D. Reidel, Holland, 1988.

Angell, J. K., Variations and trends in tropospheric and stratospheric global temperatures, 1958-87, *J. Climate, 1*, 1296-1313, 1988.

Angell, J. K., and J. Korshover, Global temperature variations in the troposphere and stratosphere, *Mon. Wea. Rev., 11*, 901-921, 1983.

Barnes, R. A., Changes in SBUV ozone profiles near Natal, Brazil, from 1979 to 1985, *J. Geophys. Res., 93*, 1704-1717, 1988.

Barnes, R. A., and P. G. Simeth, Design of a rocket-borne radiometer for stratospheric ozone measurements, *Rev. Sci. Instrum., 57*, 544-550, 1986.

Barnes, R. A., A. R. Bandy, and A. L. Torres, Electrochemical concentration cell ozonesonde accuracy and precision, *J. Geophys. Res., 90*, 7881-7887, 1985.

Barnes, R. A., A. C. Holland, and H. S. Lee, An improved rocket ozonesonde (ROCOZ-A) 2. Preparation of stratospheric ozone profiles, *J. Geophys. Res., 91*, 14521-14531, 1986.

Barnes, R. A., A. C. Holland, and V. W. J. Kirchhoff, Equatorial ozone profiles from the ground to 52 km during the Southern Hemisphere autumn, *J. Geophys. Res., 92*, 5573-5583, 1987a.

Barnes, R. A., D. W. Rusch, and C. L. Parson, A comparison of northern mid-latitude ozone measurements from SME and ROCOZ-A from 1983 to 1985, Paper presented at the fall AGU Meeting, San Francisco, CA, 1987b.

Barnes, R. A., M. A. Chamberlain, C. L. Parson, and A.C. Holland, An improved rocket ozonesonde (ROCOZ-A) 3. Northern mid-latitude ozone measurements from 1983 to 1985, *J. Geophys. Res., 94*, 2239-2254, 1989.

Barnett, J. J., and M. Corney, Temperature comparisons between Nimbus 7 SAMS, rocket/radiosondes and the NOAA-6 SSU, *J. Geophys. Res., 89*, 5294-5302, 1984.

Bass, A. M., and R. J. Paur, The ultraviolet cross-sections of ozone: 1. The measurements, in *Atmospheric Ozone, Proceedings of the Quadrennial Ozone Symposium*, Halkidiki, Greece, edited by C. S. Zerefos and A. Ghazi, pp. 606-610, D. Reidel, Dordrecht, Holland, 1985.

Beardsmore, D. J., and G. I. Pearman, Baseline carbon dioxide concentrations, in *Baseline 87*, edited by B. W. Forgan, Bureau of Meteorology/CSIRO, in press, 1989.

Bevilacqua, R. M., and J. J. Olivero, Vertical resolution of middle atmospheric measurements by ground-based microwave radiometry, *J. Geophys. Res., 93*, No. D8, 9463, 1988.

Bhartia, P. K., S. Taylor, and A. J. Fleig, Estimation of errors in the long term change of ozone reported by the SBUV-TOMS instruments—a new way of looking at old data, *Proceedings of the Quadrennial Ozone Symposium 1988*, Gottingen, F.R.G., edited by R. D. Bojkov and P. Fabian, Deepak Publications, Hampton, VA, 1989.

Blake, D. R., and F. S. Rowland, Continuing worldwide increase in tropospheric methane, 1978 to 1987, *Science, 239*, 1129-1131, 1988.

Bloomfield, P., G. Oehbert, M. L. Thompson, and S. Zeger, A frequency domain analysis of trends in Dobson total ozone, *J. Geophys. Res. 88*, 8512-8522, 1983.

Bodhaine, B. A., and R. M. Rosson (Eds.), *Geophysical Monitoring for Climatic Change, Summary Report, 1987*, NOAA Air Resources Laboratory, Boulder, Colorado, 1988.

Bojkov, R. D., Some characteristics of the total ozone deduced from Dobson spectrophotometer and filter-ozone-meter data and their application to a determination of the effectiveness of the ozone network, *Ann. Geophys., 25*, 293-299, 1969.

Bojkov, R. D., Surface ozone during the second half of the nineteenth century, *J. Climate and Applied Meteorology, 25*, 343-52, 1986.

Bojkov, R. D., Ozone changes at the surface and in the free troposphere, in *NATO Workshop on Tropospheric Ozone*, Lillehammer Norway, 1987, edited by I. S. Isaksen, Reidel, Holland, 1988.

Bojkov, R. D., C. L. Mateer, and A. L. Hansson, Comparison of ground-based and total ozone mapping spectrometer measurement, used in assessing the performance of the global ozone observing system, *J. Geophys. Res., 93*, 9525-9533, 1988.

Bojkov, R. D., R. L. Bishop, W. G. Hill, G. C. Reinsel, and G. C. Tiao, Statistical trend analysis of revised Dobson total ozone data over the northern hemisphere, submitted to *J. Geophys. Res.*, 1989.

Bowman, K. P., and A. J. Krueger, A global climatology of total ozone from the Nimbus-7 Total Ozone Mapping Spectrometer, *J. Geophys. Res., 90*, 7967-7976, 1985.

Box, G. E. P. and G. M. Jenkins, *Time Series Analysis: Forecasting and Control*, Holden-Day, San Francisco, 1976.

Brewer, A. W., A replacement for the Dobson spectrophotometer?, *Pure Appl. Geophys., 106-108,* 919-927, 1973.

Brewer, A. W., and J. R. Milford, The Oxford-Kew ozonesonde, *Proc. Roy. Soc. London,* A, 256, No. 1287, 470-495, 1960.

Brezgin, N. I., A. F. Chizhov, G. I. Kuznetsov, and O. V. Shtirkov, Rocket observation of atmospheric ozone and aerosol, *Proc. Joint Symposium of Atmospheric Ozone, Berlin, 2,* 47-52, 1977.

Bruhl, C., and P. J. Crutzen, On the disproportionate role of tropospheric ozone as a filter against solar UV-B radiation, *Geophys. Res. Lett.,* in press, 1989.

Caldwell, M. M., L. B. Camp, C. W. Warner, and S. D. Flint, Action spectra and their key role in assessing biological consequences of solar UV-B radiation change, in *Stratospheric Ozone Reduction, Solar Ultraviolet Radiation and Plant Life,* edited by R. C. Worrest and M. M. Caldwell, Springer-Verlag, Berlin, pp. 87-111, 1986.

Cebula, R. P., H. Park, and D. F. Heath, Characterization of the Nimbus-7 SBUV radiometer for the long term monitoring of stratospheric ozone, *J. Atmos. Oceanic Technol., 5,* 215-227, 1988.

Chanin, M. L, and A. Hauchecorne, Lidar studies of temperature and density using Rayleigh scattering, *MAP Handbook 13,* 87-99, 1984.

Chu, W. P., Inversion of SAGE II measurements, *Proceedings of the Sixth Conference on Atmospheric Radiation,* Williamsburg, VA, May 13-16, 1986.

Chu, W. P., and M. P. McCormick, Inversion of stratospheric aerosol and gaseous constituents from spacecraft solar extinction data in the 0.38-1.0μm wavelength region, *Appl. Opt., 18,* 1404-1413, 1979.

Cicerone, R. J., How has the atmospheric concentration of CO changed?, in *The Changing Atmosphere,* edited by F. S. Rowland and I. S. A. Isaksen, Wiley-Interscience, New York, pp. 49-61, 1988.

Cicerone, R. J., L. E. Heidt, and W. H. Pollock, Measurements of atmospheric methyl bromide and bromoform, *J. Geophys. Res. 93,* 3745-49, 1988.

Class, Th., and K. Ballschmiter, Chemistry of organic traces in air. VIII: Sources and distribution of bromo- and bromochloromethanes in marine air and surface water of the Atlantic ocean, *J. Atmos. Chem. 6,* 35-46, 1988.

Connor, B. J., J. W. Barrett, A. Parrish, P. M. Solomon, R. L. De Zafra, and M. Jaramillo, Ozone over McMurdo station, Antarctica, austral spring 1986, Altitude profiles for the middle and upper stratosphere, *J. Geophys. Res., 92,* 13221-13230, 1987.

Conway, T. J., P. P. Tans, L. S. Waterman, K. W. Thoning, K. A. Masarie, and R. H. Gammon, Atmospheric carbon dioxide measurements in the remote global troposphere, 1981-1984, *Tellus, 40 B,* 81-115, 1988.

Crutzen, P. J., The influence of nitrogen oxides on the atmospheric ozone content, *J. Roy. Met. Soc., 96,* 320-325, 1970.

Crutzen, P. J., and D. H. Ehhalt, Effects of nitrogen fertilizers and combustion on the stratospheric ozone layer, *Ambio, 6,* 112-117, 1977.

Crutzen, P. J., L. E. Heidt, J. P. Krasnec, W. H. Pollock, and W. Seiler, Biomass burning as a source of atmospheric gases CO, H_2, N_2O, NO, CH_3Cl and COS, *Nature, 282,* 253-256, 1979.

Cunnold, D. M., F. N. Alyea, and R. G. Prinn, Preliminary calculations concerning the maintenance of the zonal mean ozone distributions in the northern hemisphere, *Pure Appl. Geophys., 118,* 229-354, 1980.

Cunnold, D. M., W. P. Chu, R. A. Barnes, M. P. McCormick, and R. Veiga, Validation of SAGE II ozone measurements, *J. Geophys. Res. 94,* 8447-8460, 1989.

Dave, J. V., J. J. DeLuisi, and C. L. Mateer, Results of a comprehensive theoretical examination of the optical effects of aerosols on the Umkehr measurements, *Spec. Environ. Rep. 14,* 15-22, World Meteorological Organization, Geneva, 1979.

De la Noe, J., J. Lenoble, and T. Ogawa, Comparison of remote ground-based and satellite ozone profiles at strato-mesospheric altitudes, *Proceedings Int'l Radiation Symposium,* Lille, France, 1988.

DeLuisi, J. J., Umkehr vertical ozone profiles errors caused by the presence of stratospheric aerosols, *J. Geophys. Res., 84,* 1766-1770, 1979.

DeLuisi, J. J., D. U. Longenecker, C. L. Mateer, and D. J. Wuebbles, An analysis of northern middle-latitude Umkehr measurements corrected for stratospheric aerosols for the years 1979-1986, *J. Geophys. Res.,* in press, 1989a.

DeLuisi, J. J., D. U. Longenecker, P. K. Bhartia, S. Taylor, and C. L. Mateer, Ozone profiles by Umkehr, SBUV, and ozonesondes: A comparison including the inversion algorithms for Umkehr and SBUV-TOMS instruments—a new way of looking at old data, *Proceedings of the Quadriennial Ozone Symposium 1988,* edited by R. D. Bojkov and P. Fabian, Gottingen, F.R.G., Deepak Publications, Hampton, VA, 1989b.

DeMore, W. B., and M. Patapoff, Comparison of ozone determinations by ultraviolet photometry and gas-phase titration, *Environ. Sci. Technol., 10,* 897-899, 1976.

Dianov-Klokov, V. I., and L. N. Yurganov, A spectroscopic study of the global spacetime distribution of atmospheric CO, *Tellus, 33,* 262-273, 1981.

Dobson, G. M. B., Observers handbook for the ozone spectrophotometer, *Annals of the International Geophysical Year V, Part I,* pp. 46-89, Pergamon Press, New York, 1957.

Dobson, G. M. B., and C. W. B. Normand, Determination of the constants sets used in the calculation of the amount of ozone from spectrophotometer measurements and of the accuracy of the results, *Annals of the International Geophysical Year XVI, Part II,* pp.161-191, Pergamon Press, New York, 1962.

Dvoryashina, E. V., V. I. Diavov-Klokov, and L. N. Yurganov, Variations of the content of carbon monoxide in the atmosphere in the period from 1970 to 1982, *Izvestya, Academii Nauk. Phys. Atm. Okeana, 20,* 27-33, 1984.

Ehhalt, D. H., P. J. Fraser, D. Albritton, Y. Makide, R. J. Cicerone, F. S. Rowland, M. A. K. Khalil, L. P. Steele, M. Legrand, and R. Zander, Trends in source gases, in *Report of the International Ozone Trends Panel - 1988,* WMO Report Number 18, WMO, Geneva, 1989.

Elsworth, C. M., I. E. Galbally, and R. Paterson, Ozone in near surface air, in *Baseline 86,* edited by B. W. Forgan and P. J. Fraser, Bureau of Meteorology, CSIRO, 1988.

Evans, W. F. J. and J. B. Kerr, A comparison of satellite data with Brewer ozone data, *Proceedings of the Quadrennial Ozone Symposium 1988,* Gottingen, F.R.G, edited by R. D. Bojkov and P. Fabian, Deepak Publications, Hampton, VA, 1989.

Feister, U., and W. Warmbt, Long-term measurements of surface ozone in the German Democratic Republic, *J. Atmos. Chem. 5,* 1-21, 1987.

Fisletov, V. E., The total ozone trend in the northern hemisphere, *Meteorologia i Gidzologia,* in press, (in Russian), 1989.

Fleig, A. J., P. K. Bhartia, and D. S. Silberstein, An assessment of the long term drift in SBUV total ozone data, based on comparison with the Dobson network, *Geophys. Res. Lett., 13,* 1359-1362, 1986.

Fleig, A. J., D. S. Silberstein, C. G. Wellemeyer, P. K. Bhartia, and J. J. DeLuisi, An assessment of the SBUV/TOMS Ozone data quality, based on comparison with external data, *Proceedings of the Quadrennial Ozone Symposium 1988,* Gottingen, F.R.G., edited by R. D. Bojkov and P. Fabian, Deepak Publications, Hampton, VA, 1989a.

Fleig, A. J., D. S. Silberstein, C. G. Wellemeyer, R. P. Cebula, and P. K. Bhartia, An assessment of the long-term drift in TOMS total ozone data, based on comparison with the Dobson network, *Proceedings of the Quadrennial Ozone Symposium 1988,* Gottingen, F.R.G., edited by R. D. Bojkov and P. Fabian, Deepak Publications, Hampton, VA, 1989b.

Fraser, P. J., and S. Coram, Atmospheric methane, carbon monoxide and carbon dioxide, 1986, in *Baseline 86,* edited by B.W Forgan and P.J. Fraser, Bureau of Meteorology/CSIRO, 65-66, 1988.

Fraser, P. J., and N. Derek, Atmospheric halocarbons, nitrous oxide and methane - the GAGE program, 1987, in *Baseline 87,* edited by B. W. Forgan and G. Ayers, Bureau of Meteorology/CSIRO, in press, 1989.

Fraser, P. J., P. Hyson, R. A. Rasmussen, A. J. Crawford, and M. A. K. Khalil, Methane, carbon monoxide and methylchloroform in the southern hemisphere, *J. Atmos. Chem. 4,* 3-42, 1986a.

Fraser, P. J., P. Hyson, S. Coram, R. A. Rasmussen, A. J. Crawford and M. A. K. Khalil, Carbon monoxide in the southern hemisphere, *Proc. of the 7th World Clean Air Congress, 2,* 341-52, Sydney, Australia, August 1986b.

Fraser, P. J., R. J. Francey, J. Mansbridge, and I. E. Enting, The CSIRO global methane program. Presented at the Second Conference on the Scientific Application of Baseline Observations of Atmospheric Composition (SABOAC II), CSIRO, Aspendale, Victoria, Australia, November 14-17, 1988, submitted to *J. Atmos. Chem.,* 1989.

Frederick, J. E., and D. Lubin, The budget of biologically active ultraviolet radiation in the earth-atmosphere system, *J. Geophys. Res., 93,* 3825-3832, 1988.

Galbally, I. E., A. J. Miller, R. D. Hoy, S. Ahmet, R. C. Joynt, and D. Attwood, Surface ozone at rural sites in the Latrobe Valley and Cape Grim, Australia, *Atmos. Environ. 20,* 2403-2422, 1986.

Gammon, R., S. C. Wofsy, R. J. Cicerone, A. C. Delany, R. T. Harriss, M. A. K. Khalil, J. A. Logan, P. Midgley, and M. Prather, Tropospheric trace species, in *Atmospheric Ozone 1985, 1,* pp. 57-116, WMO Global Ozone Research and Monitoring Project, Report Number 16, 1986.

Gelman, M. E., A. J. Miller, K. W. Johnson, and R. M. Nagatani, Detection of long-term trends in global stratospheric temperatures from NMC analyses derived from NOAA satellite data, *Adv. Space Res., 6,* 17-26, 1988.

Gille, J. C., and J. M. Russell, III, The limb infrared monitor of the stratosphere: Experiment description, performance, and results, *J. Geophys. Res., 89,* 5125-5140, 1984.

Godin, S., G. Megie, and J. Pelon, Systematic lidar measurements of the stratospheric ozone vertical distribution, *Geophy. Res. Lett.,* in press, 1989.

Graedel, T. E., and J. E. McRae, On the possible increase of the atmospheric methane and carbon monoxide concentrations during the last decade, *Geophys. Res. Lett. 7,* 977-979, 1980.

Griggs, M., Studies of atmospheric ozone, Ph.D. Thesis, University of Oxford, Clarendon Laboratory, Oxford, 1961.

Gustin, G. P., Universal ozonometer, *Proc. Main Geophys. Obs. Leningrad, 141,* 83-98, 1963.

Gustin, G. P., On the methodology of total ozone measurements in the global network, *Proc. Main Geophys. Obs. Leningrad, 406,* 63-75, 1978.

Gustin G. P., and S. A. Sokolenko, Design of optical and electric systems of ozonometer 124, *Proc. Main Geophys. Obs. Leningrad, 487,* 30-36, 1985.

Hauchecorne, A., and M. L. Chanin, Density and temperature profiles obtained by lidar between 30 and 70 km, *Geophys. Res. Lett., 7,* 564-568, 1981.

Heath D. F., A. J. Krueger, H. A. Roeder, and B. H. Henderson, The Solar Backscatter Ultraviolet and Total Ozone Mapping Spectrometer (SBUV/TOMS) for Nimbus G, *Opt. Eng., 14,* 323-331, 1975.

Hill, W. G., G. W. Oehlert, and G. C. Reinsel, Trend analysis sensitivity studies of Dobson total ozone data through 1984, *J. Geophys. Res., 91,* 14515-14520, 1986

Hilsenrath, E., W. Attmanspacher, A. Bass, W. Evans, R. Hagemeter, R. A. Barnes, W. Komhyr, K. Maursberger, J. Mentall, M. Proffitt, D. Robins, S. Taylor, A. Torres, and E. Weinstock, Results from the balloon ozone intercomparison campaign (BOIC), *J. Geophys. Res., 91,* 13137-13152, 1986.

Hofmann, D. J., and S. Solomon, Ozone destruction through heterogenous chemistry following the eruption of El Chichon, *J. Geophys. Res., 94,* 5029-5041, 1989.

Holland, A. A. C., R. A. Barnes, and H. S. Lee, Improved rocket ozonesonde (ROCOZ-A) 1. Demonstration of precision, *Appl. Opt., 24,* 3286-3295, 1985.

Ilyas, M., Effect of cloudiness on solar ultraviolet radiation reaching the surface, *Atmos. Environ. 21*, 1483-1484, 1987.

Kerr, J. B., C. T. McElroy, D. I. Wardle, R. A. Olafson, and W. F. J. Evans, The automated Brewer spectrophotometer, in *Atmospheric Ozone, Proceedings of the Quadrennial Ozone Symposium*, Halkidiki, Greece, edited by C. S. Zerefos and A. Ghazi, pp. 396-410, D. Reidel, Dordrecht, Holland, 1985.

Kerr, J. B., I. A. Asbridge, and W. F. J. Evans, Intercomparison of total ozone measured by the Brewer and Dobson spectrophotometers at Toronto, *J. Geophys. Res., 93*, 11129-11140, 1988.

Kerr, J. B., C. L. Mateer, C. T. McElroy, and W. F. J. Evans, Umkehr measurements made with the Brewer Ozone Spectrophotometer, *Proceedings of the Quadrennial Ozone Symposium 1988*, Gottingen, F.R.G., edited by R. D. Bojkov and P. Fabian, Deepak Publications, Hampton, VA, 1989a.

Kerr, J. B., I. A. Asbridge, and W. F. J. Evans, Long-term intercomparison between the Brewer and Dobson spectrophotometers at Edmonton, *Proceedings of the Quadrennial Ozone Symposium 1988*, Gottingen F.R.G, edited by R. D. Bojkov and P. Fabian, Deepak Publications, Hampton, VA, 1989b.

Khalil, M. A. K., and R. A. Rasmussen, The trend of bromochlorodifluoromethane and other bromine containing gases at the South Pole, *Antarctic J. United States, 19*, 206-207, 1985.

Khalil, M. A. K., and R. A. Rasmussen, Nitrous oxide: Trends and global mass balance over the last 3,000 years, *Ann. Glac., 10*, 73-79, 1988a.

Khalil, M. A. K., and R. A. Rasmussen, Carbon monoxide in the Earth's atmosphere: Indications of a global increase, *Nature, 332*, 242-245, 1988b.

Khalil, M. A. K., R. A. Rasmussen, and R. Gunawardena, Atmospheric bromine in the polar regions, in *Geophysical Monitoring for Climatic Change, Summary Report 1986*, edited by R. S. Schnell and R. M. Rosson, pp. 123-125, 1987.

Khalil, M. A. K., R. A. Rasmussen, and S. D. Hoyt, Atmospheric chloroform ($CHCl_3$): Ocean-air exchange and global mass balance, *Tellus, 35B*, 266-274, 1983.

Kokin, G. A., E. V. Lysenko, and S. Kh. Rosenfeld, Temperature variations in the stratosphere and mesosphere in 1964 to 1988 based on rocket sounding data, *Izvestia Akademii Nauk, Phys. Atm. Okeana*, in press, 1989.

Komhyr, W. D., A carbon-iodine ozone sensor for atmospheric soundings, *Proceedings of the Ozone Symposium*, W.M.O., Albuquerque, NM, 1964.

Komhyr, W. D., Electrochemical concentration cells for gas analysis, *Ann. Geophys., 25*, 203-210, 1969.

Komhyr, W. D., R. D. Grass, R. D. Evans, R. K. Leonard, and G. M. Semeniuk, Umkehr observations with automated Dobson spectrophotometers, in *Atmospheric Ozone, Proceedings of the Quadrennial Ozone Symposium*, Halkidiki, Greece, pp. 371-375, D. Reidel, Dordrecht, Holland, 1985.

Komhyr, W. D., R. D. Grass, and R. K. Leonard, Dobson spectrophotometer No. 83: A standard for total ozone measurements, 1962-1987, *Proceedings of the Quadrennial Ozone Symposium 1988*, Gottingen, F.R.G., edited by R.D. Bojkov and P. Fabian, Deepak Publications, Hampton, VA, 1989.

Konkov V. I., and S. P. Perov, Some preliminary results of chemiluminescent measurements of atmospheric ozone by meteorological rocket, *Proc. of the Joint Symposium on Atmospheric Ozone, 11*, 43-46, 1976.

Krueger, A. J., and W. R. McBride, Rocket ozonesonde (ROCOZ) design and development, *Navy Weapons Cent. Tech. Publ. 4512*, Navy Weapons Cent., China Lake, Calif., 1968a.

Krueger, A. J., and W. R. McBride, Sounding rocket -OGO-IV satellite ozone experiment, Rocket ozonesonde measurements, *Navy Weapons Cent. Tech. Publ. 4667*, Navy. Weapons Cent., China Lake, Calif., 1968b.

Kunzi, K. F., and G. Rubin, The use of microwave sensors in a global ozone monitoring network, Paper presented at Intl. Rad. Symp., Lille, France, Aug. 18-24, 1988.

Labitzke, K., Sunspots, the QBO and the stratospheric temperature in the north polar region, *Geophys. Res. Lett., 14*, 535-537, 1987.

Labitzke, K, J. J. Barnett, and B. Edwards, Draft of a new reference middle atmosphere, *Handbook for MAP, 16*, SCOSTEP Secretariat, Univ. of Illinois, Urbana, 1985.

Labitzke, K., and M. L. Chanin, Changes in the middle atmosphere in winter related to the 11-year solar cycle, *Ann. Geophys., 6*, 643-644, 1988.

Labitzke, K., and H. Van Loon, Association between the 11-year solar cycle, the QBO, and the atmosphere. Part I: The troposphere and stratosphere in the Northern Hemisphere in winter, *J. Atmos. Terr. Phys., 50*, 197-206, 1988.

Lal S., R. Borchers, P. Fabian, and B.C. Kruger, Increasing abundance of CF_2 BrCl in the atmosphere, *Nature, 316*, 135-136, 1985.

Levy II, H., Normal atmosphere: Large radical and formaldehyde concentrations predicted. *Science, 173*, 141-143, 1971.

Lobsiger, E., Ground-based microwave radiometry to determine stratospheric and mesospheric ozone profiles, *J. Atmos. Terr. Phys., 49*, 493, 1987.

Logan, J. A., Tropospheric ozone: Seasonal behavior, trends and anthropogenic influence, *J. Geophys. Res. 90*, 10463-10482, 1985.

Makide, Y., A. Yokohara, Y. Kubo, and T. Tominaga, Atmospheric concentration of halocarbons in Japan 1979-1986, *Bull. Chem. Soc. Japan, 60*, 571-574, 1987.

Mankin, W.G., and M.T. Coffey, Latitudinal distribution and temporal changes of stratosphere HCl and HF, *J. Geophys. Res, 88*, 10776-10784, 1983.

Mateer, C. L., and H. U. Deutsch, Uniform evaluation of Umkehr observations from the World Ozone Network, Part. I. Proposed standard Umkehr evaluation technique. Technical Report, National Center for Atmospheric Research, Boulder, CO, 1964.

Mateer, C. L., and J. J. DeLuisi, A comparison of ozone profiles derived from Standard Umkehr and Short Umkehr measurements from 15 stations, in *Atmospheric Ozone, Proceedings of the Quadrennial Ozone Symposium*, Halkidiki, Greece, edited by C. S. Zerefos and A. Ghazi, pp. 290-294, Reidel, Dordrecht, Holland, 1985.

Mateer, C. L., J. B. Kerr, and W. F. J. Evans, Ozone profiles derived from Umkehr observations obtained from the Brewer Ozone Spectrophotometer, in *Atmospheric Ozone, Proceedings of the Quadrennial Ozone Symposium*, Halkidiki, Greece, edited by C. S. Zerefos and A. Ghazi, pp. 407-411, Reidel, Dordrecht, Holland, 1985.

Mauldin, L. E., III, and W. P. Chu, Optical degradation due to contamination on the SAGE/SAGE II spaceflight instruments, *Proceedings of the Society of Photo-optical Instrumentation Engineers*, 1982.

Mauldin, L. E., III, N. H. Zuan, M. P. McCormick, J. H. Guy, and W. R. Vaughan, Stratospheric Aerosol and Gas Experiment II instrument: A functional description, *Opt. Eng., 24*, 307-312, 1985a.

Mauldin, L. E., III, M. P. McCormick, L. R. McMaster, and W. R. Vaughan, The Stratospheric Aerosol and Gas Experiment II (SAGE II) design and in-orbit performance, *Proceedings of the Society of Photo-optical Instrumentation Engineers, Vol. 589, Instrumentation for Remote Sensing from Space*, pp. 104-111, 1985b.

McCormick, M. P., P. Hamill, T. J. Pepin, W. P. Chu, T. J. Swissler, and L. R. McMaster, Satellite studies of the Stratospheric Aerosol, and Gas Experiment (SAGE II), *Bull. Am. Met. Soc., 60*, 1038-1046, 1979.

McDermid, I. S., and S. Godin, Ground-based laser DIAL system for long-term measurement, *Applied Optics*, in press, 1990.

McElroy, C. T., C. L. Mateer, J. B. Kerr, and D. I. Wardle, Umkehr observations made with the Brewer ozone spectrophotometer, *Proceedings of the Quadrennial Ozone Symposium 1988*, Gottingen, F.R.G, edited by R. D. Bojkov and P. Fabian, Deepak Publications, Hampton, VA, 1989.

277

McElroy, M. B., R. J. Salawitch, S. L. Wofsy, and J. A. Logan, Reductions in Antarctic ozone due to synergistic interactions of chlorine and bromine, *Nature, 321*, 756-762, 1986.

McKenzie, R. L., and P. V. Johnston, Seasonal variations in stratospheric NO$_2$ at 45 S, *Geophys. Res. Lett., 9*, 1255, 1982.

McPeters, R. D., and W. D. Komhyr, Long-term changes in SBUV-TOMS relative to the world primary standard Dobson instrument, *Proceedings of the Quadrennial Ozone Symposium 1988*, Gottingen, F.R.G, edited by R. D. Bojkov and P. Fabian, Deepak Publications, Hampton, VA, 1989.

Mégie, G., J. Y. Allain, M. L. Chanin, J. E. Blamont, Vertical profile of stratospheric ozone by lidar sounding from the ground, *Nature, 270*, 5635, 1977.

Mo, T., and A. E. S. Green, A climatology of solar erythema dose, *Photochem. Photobiol., 20*, 483-496, 1974.

Mount, G. H., R. W. Sanders, A. L. Schmeltekopf, and S. Solomon, Visible spectroscopy at McMurdo Station, Antarctica, 1. Overview and daily variations of NO$_2$ and O$_3$ austral spring, 1986, *J. Geophys. Res., 92*, 8320, 1987.

Nagatani, R. M., A. J. Miller, K. W. Johnson, and M. E. Gelman, *An Eight Year Climatology of Meteorological and SBUV Ozone Data*, NOAA Technical Report NWS 40, 1988

NASA, *Present State of Knowledge of the Upper Atmosphere: An Assessment Report*, NASA Reference Publication 1208, August 1988.

Nash, J., and G. F. Forrester, Long-term monitoring of stratospheric temperature trends using radiance measurements obtained by the TIROS-N series of NOAA spacecraft, *Adv. Space. Res., 6*, 37-43, 1986.

Nash, J., Extension of explicit radiance observations by the Stratospheric Sounding Unit into the lower stratosphere and lower mesosphere, *Quart. J. Roy. Met. Soc., 114*, 1153-1171, 1988.

Newchurch, M. J., G. W. Grams, D. M. Cunnold, and J. J. DeLuisi, A comparison of SAGE I, SBUV and Umkehr ozone profiles including a search for Umkehr aerosol effects, *J. Geophys. Res., 92*, 8382-8390, 1987.

Noxon, J. F., E. C. Whipple, Jr., and R. S. Hyde, Stratospheric NO$_2$ 1. Observational method and behavior at mid-latitude, *J. Geophys. Res., 84*, 5047, 1979.

Oltmans, S. J., and W. D. Komhyr, Surface ozone distributions and variations from 1973-1984 measurements at the NOAA Geophysical Monitoring for Climatic Change Baseline Observatories, *J. Geophys. Res., 91*, 5229-5236, 1986.

Ozone Trends Panel Report-1988, Global ozone research and monitoring project, Report Number 18, edited by R. T. Watson, World Meteorological Organization, Geneva, in press, 1989.

Pelon, J., and G. Megie, Ozone monitoring in the troposphere and lower stratosphere: Evaluation and operation of a ground-based lidar station, *J. Geophys. Res., 87*, 4947, 1982.

Pelon, J., S. Godin, and G. Megie, Upper stratospheric (30-50 km) lidar observations of the ozone vertical distribution, *J. Geophys. Res., 91*, 8667, 1986.

Penkett, S. A., Indications and causes of ozone increase in the troposphere, in *The Changing Atmosphere*, edited by F. S. Rowland and I. S. A. Isaksen pp. 91-103, Wiley-Interscience, New York, 1988.

Penkett, S. A., B. M. R. Jones, M. J. Rycroft, and D. A. Simmons, An interhemispheric comparison of the concentration of bromine compounds in the atmosphere, *Nature, 318*, (6046), 550-553, 1985.

Perov, S. P., and A. Khrgian, Sovremennie problemy atmosphernogo ozona *L. Hydrometeoizdat*, 1980.

Perov, S. P., and S. V. Tishin, A rocket gas chemiluminescent technique for measurement of atomic oxygen and ozone concentration in the 15-95 km region, in *Atmospheric ozone, Proceedings of the Quadrennial Ozone Symposium*, Halkidiki, Greece, edited by C. S. Zerefos and A. Ghazi, D. Reidel, Dordrecht, Holland, pp. 527-531, 1985.

Pommereau, J. P., and F. Goutail, O$_3$ and NO$_2$ ground-based measurements by visible spectrometry during Artic winter and spring 1988, *Geophys. Res. Lett., 15*, 891, 1988a.

Pommereau, J. P., and F. Goutail, Stratospheric O₃ and NO₂ observations at the Southern Polar Circle in summer and fall 1988, *Geophys. Res. Lett. 15*, 895, 1988b.

Prinn, R. G., How have the atmospheric concentrations of the halocarbons changed?, in *The Changing Atmosphere*, edited by F. S. Rowland and I. S. A. Isaksen, pp. 33-48, Wiley-Interscience, New York, 1988a.

Prinn, R. G., Toward an improved global network for determination of tropospheric ozone climatology and trends, *J. Atmos. Chem.*, *6*, 281-298, 1988b.

Prinn, R. G., P. G. Simmonds, R. A. Rasmussen, R. D. Rosen, F. N. Alyea, C. A. Cardelino, A. J. Crawford, D. M. Cunnold, R. Fraser, and J. E. Lovelock, The Atmospheric Lifetime Experiment: 1. Introduction, instrumentation and overview, *J. Geophys. Res. 88*, 8853-8867, 1983.

Prinn, R., D. Cunnold, R. Rasmussen, P. Simmonds, F. Alyea, A. Crawford, P. Fraser, and R. Rosen, Atmospheric trends in methylchloroform and the global average for the hydroxyl radical, *Science*, *238*, 945-950, 1987.

Ramanathan, V., R. Cicerone, H. Singh, and J. Kiehl, Trace gas trends and their potential role in climatic change, *J. Geophys. Res.*, *90*, 5547-5566, 1985.

Rasmussen, R. A., and M. A. K. Khalil, Latitudinal distributions of trace gases in and above the boundary layer, *Chemosphere*, *11*, 227-235, 1982.

Rasmussen, R. A., and M. A. K. Khalil, Gaseous bromine in the Arctic and Arctic haze, *Geophys. Res. Letts. 11*, 433-436, 1984.

Raynaud D., J. Chappellaz, J. M. Barnola, Y. S. Korotkevich, and C. Lorius, Climatic and CH₄ cycle implications of glacial-interglacial CH₄ changes in the Vostok ice core, *Nature, 333*, 655, 1988.

Regener, V. H., On a sensitive method for the recording of atmospheric ozone, *J. Geophys. Res.*, *65*, 3975-3977, 1960.

Regener, V. H., Measurement of atmospheric ozone with the chemiluminescent method, *J. Geophys. Res.*, *69*, 3795-3800, 1964.

Reinsel, G. C., and G. C. Tiao, Impact of chlorofluoromethanes on stratospheric ozone: A statistical analysis of ozone data for trends, *J. Amer. Stat. Assoc.*, *82*, 20-30, 1987.

Reinsel, G. C., G. C. Tiao, J. J. DeLuisi, C. L. Mateer, A. J. Miller, and J. E. Frederick, An analysis of upper stratospheric Umkehr ozone profile data for trends and the effects of stratospheric aerosols, *J. Geophys. Res.*, *93*, 1689-1703, 1984.

Reinsel, G. C., G. C. Tiao, A. G. Miller, D. J. Wuebble, P. S. Connell, C. L. Mateer and G. G. DeLuisi, Statistical analyses of total ozone and stratospheric Umkehr data for trends and solar cycle relationship, *J. Geophys. Res.*, *92*, 2201-2209, 1987.

Reinsel, G. C., G. C. Tiao, S. K. Ahn, M. Pugh, S. Basu, J. J. DeLuisi, C. L. Mateer, A. J. Miller, P. S. Connell, and D. J. Wuebbles, An analysis of the 7-year record of SBUV satellite ozone data: Global profile features and trends in total ozone, *J. Geophys. Res.*, *93*, 1689-1703, 1988.

Reinsel, G. C., G. C. Tiao, J. J. DeLuisi, S. Basu, and K. Carriere, Trend analysis of aerosol corrected Umkehr profile ozone data through 1987, *J. Geophys. Res.*, in press, 1989.

Rowland, F. S., and M. Molina, Chlorofluoromethanes in the environment, *Rev. Geophys. Space Phys.*, *13*, 1-35, 1975.

Rusch, D. W., G. H. Mount, C. A. Barth, R. J. Thomas, and M. T. Callan, Solar mesospheric explorer ultraviolet spectrometer: Measurements in the 1.0 to 0.1-mbar region, *J. Geophys. Res.*, *89*, 11677-11687, 1984.

Scheel, H. E., E. G. Brunke, and W. Seiler, Trace gas measurements at the monitoring station Cape Point, South Africa, between 1978 and 1988. (Presented at the Second Conference on the Scientific Application of Baseline Observations of Atmospheric Composition (SABOAC II), CSIRO, Aspendale, Victoria, Australia, November 14-17, 1988). *J. Atmos. Chem,* 1988.

Schoeberl, M. R., A. J. Krueger, and P. A. Newman, The morphology of Antarctic total ozone as seen by TOMS, *Geophys. Res. Lett., 13,* 1217-1220, 1986.

Scotto, J., G. Cotton, F. Urbach, D. Berger, and T. Fears, Biologically effective ultraviolet radiation: Surface measurements in the United States, 1974-1985, *Science, 239,* 762-764, 1988.

Simmonds, P. G., D. M. Cunnold, F. N. Alyea, C. A. Cardelino, A. J. Crawford, R. G. Prinn, P. J. Fraser, R. A. Rasmussen, and R. D. Rosen, Carbon tetrachloride lifetimes and emissions determined from daily global measurements during 1978-1985, *J. Atmos. Chem., 7,* 35-58, 1988.

Singer, S. F., and R. C. Wentworth, A method for the determination of the vertical ozone distribution from a satellite, *J. Geophys. Res., 62,* 299-308, 1957.

Singh, H. B., L. J. Salas, H. Shigeishi, and E. Sciber, Atmospheric halocarbons, hydrocarbons and sulfur hexafluoride: Global distributions, sources and sinks, *Science, 203,* 899-903, 1979.

Somayajulu, Y. V., K. S. Zalpuri, and S. Sampath, Rocket measurement of ozone density distribution in the equatorial stratosphere and mesosphere, *Indian J. Radio Space Phys., 10,* 197-200, 1981.

St. John, D. S., S. P. Bailey, W. H. Fellner, G. M. Minor, and R. D. Snee, Time series search for trend in total ozone measurements, *J. Geophys. Res., 86,* 7299-7311, 1981.

Stauffer, B., E. Lochbronner, H. Oeschgern, and J. Schwander, Methane concentration in the glacial atmosphere was only half of the pre-industrial Holocene, *Nature, 332,* 812, 1988.

Steele, L. P., P. J. Fraser, R. A. Rasmussen, M. A. K. Khalil, T. J. Conway, A. J. Crawford, R. H. Gammon, K. A. Masarie, and K. W. Thoning, The global distribution of methane in the troposphere, *J. Atmos. Chem., 5,* 125-171, 1987.

Steele, L. P., P. M. Lang, and R. C. Martin, Atmospheric methane in Antarctica, submitted to *Antarctic J. United States,* 1989.

Stolarski, R. S., A. J., Krueger, and M. R. Schoerberl, Total ozone trends from TOMS data, *Proceedings of the Quadrennial Ozone Symposium 1988,* Gottingen, F.R.G, edited by R. D. Bojkov and P. Fabian, Deepak Publications, Hampton, VA, 1989.

Strong, A. E., Monitoring El Chichon aerosol distribution using NOAA-7 satellite AVHRR sea surface temperature, *Geof. Int., 23-2,* 129-142, 1984.

Subbaraya, B. H., and S. Lal, Rocket measurements of ozone concentrations in the stratosphere and mesosphere over Thumba, *Proc. Indian Acad. Sci. (Earth Planet. Sci.), 90,* 173-187, 1981.

Tiao, G. C., G. C. Reinsel, J. H. Pedrick, G. M. Allenby, C. L. Mateer, A. J. Miller, and J.J. DeLuisi, A statistical trend analysis of ozonesonde data, *J. Geophys. Res., 91,* 13121-13136, 1986.

Tiao, G. E., G. C. Reinsel, D. Xu, X. D. Zhu, A. J. Miller, J. J. DeLuisi, C. C. Mateer, and D. J. Wuebbles, Effects of autocorrelation and temporal sampling schemes on estimates of trend and spatial correlation, *J. Geophys. Res.,* in press, 1989.

Torres, A. L., and A. R. Bandy, Performance characteristic of the electrochemical concentration cell ozonesonde, *J. Geophys. Res., 83,* 5501-5504, 1978.

Tsay, R. S., Regression analysis with time series errors, *J. Am. Stat. Assoc., 79,* 118-124, 1984.

Uchino, O., M. Maeda, J. Kohno, T. Shibata, C. Nagasawa, and M. Hirono, Observation of stratospheric ozone layer by XeCl laser radar, *Appl. Phys. Lett.,* 1978.

Volz, A., and D. Kley, Ozone measurements in the 19th century: An evaluation of the Mountsouris series, *Nature, 332,* 240, 1988.

Wang, P. H., M. P. McCormick, L. R. McMaster, S. Schaffner, and G. E. Woodbury, Time-periodic variations in stratospheric ozone from satellite observations, *Proceedings of the Quadrennial Ozone Symposium 1988,* Gottingen, F.R.G. edited by R. D. Bojkov and P. Fabian, Deepak Publications, Hampton, VA, 1989.

Wardle, D. I., C. D. Walshaw, and T. W. Wormell, A new instrument for atmospheric ozone, *Nature, 199,* 1177-1178, 1963.

Weiss, R. F., Global warming, *Chemical and Engineering News,* March 13, 25-44, 1989.

Weiss, R. F., and H. Craig, Production of atmospheric nitrous oxide by combustion, *Geophys. Res. Lett. 3,* 751-753, 1976.

Werner, J., K. W. Rothe, and H. Walther, Monitoring of the stratospheric ozone layer by laser radar, *Appl. Phys. B., 32,* 113, 1983.

WMO, World Meteorological Organization, Report of the WMO Meeting of Experts on Assessments of Performance Characteristics of Various Ozone Measuring Systems, *Global Ozone Research and Monitoring Project,* Report 9, WMO, Geneva, 1980.

WMO, The stratosphere-1981:Theory and measurements, *Global Ozone Research and Monitoring Project, Report 11,* WMO, Geneva, 1981.

WMO, Sources of errors in detection of ozone trends, *Global Ozone Research and Monitoring Project, Report 12,* WMO, Geneva, 1982.

WMO, Review of the Dobson spectrophotometer and its accuracy, *Global Ozone Research and Monitoring Project, Report 13,* WMO, Geneva, 1983.

WMO, Atmospheric ozone 1985: Assessment of our understanding of the processes controlling its present distribution and change, Global Ozone Research and Monitoring Project, *WMO, Report 16,* sponsored by WMO NASA, NOAA, FAA, UNEP, CEC, and BMFT, Washington, DC, 1986.

WMO, Report of the NASA/WMO ozone trends panel, 1989, *Global Ozone Research and Monitoring Project, Report 18,* WMO, Geneva, 1989 (cited in text as OTP).

Wofsy, S. C., M. B., McElroy and Y. L. Yung, The chemistry of atmospheric bromine, *Geophys. Res. Lett., 2,* 215-218, 1975.

Wuebbles, D. J., and D. E. Kinnison, A two-dimensional study of past trends in global ozone, *Proceedings of the Quadrennial Ozone Symposium 1988,* Gottingen, F.R.G., edited by R. D. Bojkov and P. Fabian, Deepak Publications, Hampton, VA, 1989.

Yokata, A., Y. Makide, and T. Tominaga, A new calibration method for the measurement of CCl_4 concentration at 10^{-10} v/v level and the behavior of CCl_4 in the atmosphere, *Bull. Chem. Soc. Japan, 58,* 1308-1314, 1985.

Zander, R., G. Roland, L. Delbouille, A. Savuel, C. B. Farmer, and R. H. Norton, Column abundance and long-term trend of hydrogen chloride (HCl) above the Jungfraujoch station, *J. Atmos. Chem, 5,* 395-404, 1987a.

Zander, R., G. Roland, L. Delbouille, A. Savuel, C. B. Farmer, and R. H. Norton, Monitoring of the integrated column of hydrogen fluoride above the Jungfraujoch station since 1977. The HF/HCl column ratio, *J. Atmos. Chem., 5,* 385-394, 1987b.

Zander, R., Ph. Demoulin, D. H. Ehhalt, and U. Schmidt, 1989a, Secular increase of the vertical abundance of methane derived from IR solar spectra recorded at the Jungfraujoch Station, *J. Geophys. Res.,* in press, 1989a.

Zander, R., Ph. Demoulin, D. H. Ehhalt, U. Schmidt, and C. P. Rinsland, Secular increase of the total vertical abundance of carbon monoxide above central Europe since 1950, *J. Geophys. Res.,* in press, 1989b.

Zommerfeld, W., and K. F. Kunzi, Operational ground based ozone sensor (OGOS), *Proceedings of the Quadrennial Ozone Symposium 1988,* Gottingen, F.R.G., edited by R. D. Bojkov and Fabian, Deepak Publications, Hampton, VA, 1989.